# NOVEL METHODS TO CHARACTERISE TEXTURE CHANGES DURING FOOD BREAKDOWN

**A thesis presented in partial fulfilment of the requirements for the degree of**

**Doctor of Philosophy in Food Technology**

**at Massey University, New Zealand**

**Ng Cui Fang, Grace**

**2018**

# Abstract

The purpose of the mastication process is to break down food for bolus formation so that it can be swallowed safely. Although light has been shed on the criterion for a swallow safe bolus, quantifying these in terms of the bolus properties is not fully understood. There is a lack of suitable measurement techniques to quantify these identified bolus properties. Thus, the purpose of this work was to develop novel techniques that would be useful in in-vitro studies of food breakdown for the characterisation of bolus properties.

A mastication robot (MR) had been previously developed to enable the reproducible mastication of food so that masticatory efficiency and food breakdown dynamics can be assessed quantitatively. To evaluate if the MR could be a controllable and reproducible alternative to subjects for food break down studies, a series of experiments involving the mastication of peanuts using a range of machine parameters was conducted. The bolus particle size distributions were used to characterise the breakdown of the peanuts. There were significant differences in the average particle size of the particles chewed by the different chewing trajectories during the initial chews. The performance of the mastication robot was validated against human subjects (n=5) by comparing the particle size distribution (PSD) of peanut boluses collected from subjects and the MR. Although the MR was unable to achieve similar breakdown capability as that for the human subjects, the MR proved to have good reproducibility in bolus preparation.

Two novel techniques were developed to characterise bolus properties. The slip extrusion test was developed to characterise two determinant properties for safe swallowing, the bolus deformation and slippage properties. The test measures the force needed to extrude a bolus through a test bag imitating the swallowing action of a bolus. The multiple pin penetrometer was previously developed to measure the spatial distribution of texture in foods exhibiting heterogenous structures. The forces experienced by each pin is measured independently as they pushed through the food, providing a pressure distribution for each food. This allowed the characterisation of fibrous (non-fracturable) foods in a similar way to PSD analysis, offering a method to characterise boluses that do not form discrete particles. The variability in the structure of the boluses was also characterised using the grey level co-occurrence matrix through the image textural features: contrast, energy and homogeneity.

Finally, these developed novel techniques were applied to five real foods with varying textures to show how the MR and these techniques may be used to characterise the changes in bolus properties

across the mastication stages. Subjects (n=5) were asked to masticate the foods to determine their chewing behaviour and the bolus properties (deformation and slip properties) at swallow point. The chewing parameters from the median subject (subject A) was used to establish the parameters for the mastication robot's set up for the factorial design of experiments. The developed models from the factorial study were used to optimize the conditions needed for the MR to achieve boluses with similar DR and SR properties as subject A. The five foods were then broken down using the MR configured in this way, and bolus properties were evaluated at various stages of the mastication process through the application of the slip extrusion test, textural mapping using the multiple pin penetrometer, and the back-extrusion test. Factor analysis was applied to the various data collected, which showed that the properties related to the hardness, swallowability and homogeneity attributes were best at describing the changes in the boluses as they were masticated to swallow point.

In conclusion, the mastication robot could be used to replicate human chewing trajectories to consistently produce boluses in a controlled trajectory with controlled "simulated saliva" rates throughout the various stages of mastication. Thus, it is relevant as a tool to produce boluses for comparative analysis especially for studies investigating the properties of boluses collected from various stages of the mastication process. In addition, the developed characterisation techniques could be used to track the dynamic changes in the bolus properties for most of the mastication stages from initial chews to the swallow point and beyond that.

# Acknowledgements

I would like to thank my supervisors, Professor John Bronlund, Professor Nigel Grigg and Mr Marco Morgenstern for their advice and encouragement throughout this project. I cannot forget Dr Eli Gray-Stuart for his input and time given for the numerous meetings. The discussions with all of you were never dull, and I enjoyed the film and music “homework” given! To all of you, a big thank you for always helping me feel positive about the project especially at times when my battery needed recharging. I would like to express my deepest gratitude to John for providing this opportunity and funding this research.

Special thanks to Anne-Marie Jackson, Garry Radford, John Edwards, Michelle Tamehana, Steve Glasgow, Warwick Johnson for all their help in the lab and to Dr Gonzalo Martinez for his patience and help with Matlab coding. Thank you to Nayoko Marou and Theliana for their assistance and to all my dear subjects for being my “chompsters”. I would like to acknowledge my mastication robot for being a cooperative companion in the last days of my labwork.

Thanks to all my friends and church mates, especially members of the Awesome Club and my neighbour on the 2nd floor, without you guys, my memories and experience in NZ would be incomplete. Every road trip and weekend hang out was awesome with y’all! Thanks to my XYZ girls for keeping me close and providing me with lots of laughter. To my bestie, thanks for all the entertainment, purple-shirt moments and even the hard conversations. To my partner who supported and took care of me amidst the challenges he faced with his own project, I could never have survived this without him. Thank you for loving me in my worst moments and I’m sure you have it in you to take up this challenge for life. To my dearest family back home in Singapore, thank you for always supporting me through prayers and daily conversation so I feel like home is not too far away. Dad, Mum and Mei, thanks for all your love and accommodation. Above all, thank you Abba Father for His providence and blessings throughout this journey. Thank you all of you for your love and I am indeed very blessed.

And since my mentor says that Singlish is the new English, I would like to declare that, "I completed my thesis already lo! Wah, It feels damn shiok! Thanks to my very zai and garang supervisors for all your time and God for pulling me through whenever I felt like I CMI. This chewing journey has been awesome, if you like to learn more about it, you can start by reading my thesis. Don’t say I bojio!"

# List of Publications and Presentations

**Published papers:**

Ng, G. C. F., Gray-Stuart, E. M., Morgenstern, M. P., Jones, J. R., Grigg, N. P., & Bronlund, J. E. (2017). The slip extrusion test: A novel method to characterise bolus properties. *Journal of Texture Studies, 48*(4), 294-301. doi:10.1111/jtxs.12254

**Conference presentations and posters:**

Ng, G.C.F., Gray-Stuart, E., Morgenstern, M.P., Jones, J.R, Bronlund, J.E.(2016). Evaluating the Slip Extrusion Test Using Three Model Food Systems. Flash presentation, 4th International Conference on Food Oral Processing, Lausanne, Switzerland, 3-6 July 2016.

Ng, G.C.F., Gray-Stuart, E., Morgenstern, M.P., Bronlund, J.E.(2014). Evaluating Particle Breakage in a Chewing Robot. Poster presentation, 3rd International Conference on Food Oral Processing, Wageningen, The Netherlands, 29 June-2 July 2014.

# Table of Contents

# List of Figures

# List of Tables

# Chapter One Project Overview

## 1.1. Introduction

Food oral processing is a developing research field. Knowledge of how food properties such as structure, hardness or rheological behaviour and how individual masticatory variations such as saliva flow, dentition and eating behaviour affect breakdown is useful for food design. The objectives for food design may be to achieve enhanced sensory experience or to create products targeted to specific groups for example, elderly with reduced muscle strength and dentition.

Bolus particle size distribution is  often used as the key parameter to study food structure breakdown. Peyron, M. A. et al. (2004) measured the particle size distribution of six natural foods to study the inter-individual variability in the particle sizes of food boluses at the end of the chewing process. Jalabert-Malbos et al. (2007) found that the particle size distributions of the boluses collected at swallow point were different for different foods but were similar across the subjects for the same food. Chen, J. et al. (2013) studied the particle size distributions of boluses formed from food of varying hardness to understand the influence of food properties on bolus formation and swallowing. These studies were usually conducted on foods such as peanuts, carrots, gherkins, jellies, peach and nuts which formed discrete particles during mastication. The problem is that there are no methods to evaluate foods that are not particulate or fracturable such as meat, bread, and fruit. For fibrous and cohesive foods, researchers have studied the food bolus properties at the swallow point by adapting methods to suit a single system. For example, Mioche's group used the double bladed shear cell to measure the mechanical properties of meat boluses (Mioche, Laurence et al., 2002; Yven, C et al., 2005), and Loret et al. (2011a) characterised the cereal boluses by measuring the rheological properties such as viscosity. Although these methods could characterise some aspect of food structure, they are relevant only for a narrow range of food systems and are not appropriate to follow the changes in structure from food ingestion to swallow point.

The dynamic changes in the bolus properties that occur during mastication results in a bolus that is safe for swallowing. A few conceptual models describing the criterion for a safe swallow have been proposed (Hawthornthwaite et al., 2015; Hutchings & Lillford, 1988; Prinz & Lucas, 1997). Peyron et al. (2011) reported that particle size and hardness were not the only decisive factors to trigger a safe swallow. Gray-Stuart et al. (2017) proposed a conceptual model based on a hazard and operability study (HAZOP) that identified the food properties that needed to be avoided for a safe swallow. The conceptual model consists of six criteria evaluating four bolus properties, which are the bolus

volume, adhesion, bolus consistency, and bolus deformability, however, it was concluded that more work was needed to test the validity of the criteria in the proposed model and to define the thresholds for these criteria. To do so, the identified bolus properties need to be quantifiable through some form of measurement. Hence, it is of interest to find or develop techniques that would be suitable for the measurement of such properties. During mastication, humans use one set of equipment to characterise food breakdown from the first chew to the swallow point. However, there is currently no technique that can characterise food breakdown like what the mouth does. Ideally, a novel technique should be developed to characterise food breakdown that is suitable for all food systems across all stages of mastication.

Having established the need to characterise food structure from ingestion to swallow, we need methods to do this. Lewis and Sun developed a mastication robot (Lewis, D., 2006; Sun, 2012b; Sun, C. et al., 2014; Xu et al., 2008) with the aim of simulating human chewing behaviours for the purpose of objective measurements of food texture changes during chewing and preparation of food bolus. This device can measure the forces applied on the molars during chewing in three dimensions in real time and the trajectory of motion can be controlled to mimic different human chewing behaviours. It has the potential to simulate human chewing in-vitro and use the measured forces to characterise the food structure breakdown. However, work has not been done to validate the mastication robot's ability to simulate human chewing trajectories. Thus, the first objective of this thesis was to test if it can simulate human chewing trajectories and be used as a controllable and reproducible alternative to subjects for food break down studies. Although light has been shed on the criterion for a swallow safe bolus, quantifying these in terms of the bolus properties is not fully understood. Thus, the second area to be explored in the thesis is the development of suitable techniques that can be used to characterise the dynamic changes in bolus properties throughout the mastication stages. Al-Battashi et al. (2015) developed a multiple pin penetrometer to measure the spatial distribution of texture in foods exhibiting heterogeneous structures. A two dimensional array of 1mm probes are pushed into the food/bolus and the forces on each pin are independently measured. This technique could potentially be used to understand the texture variability in the structure of boluses for a range of different foods at different stages of chewing. Additionally, one target of bolus formation is to allow a safe swallow, so a method could be developed considering the properties of the bolus that might trigger a swallow. The third objective was to then demonstrate the application of these novel techniques to real foods and show how they may be used to characterise the changes in bolus properties for foods during oral processing.

## 1.2. Research objectives

As identified above, there is currently no single technique that can quantitatively characterise food breakdown for all food systems across all stages of mastication. In response to this shortfall, the purpose of this work was to develop novel techniques that would be useful in the in-vitro studies of food breakdown for the characterisation of bolus properties. Figure 1-1 shows the research objectives to be achieved for each stage of the research work. The goal for the development of the mastication robot (MR) was to prepare bolus in a reproducible way and to provide information on the breakdown forces exerted during the mastication. However, the use of the MR is only relevant if it can simulate human chewing well. Thus, chapters 3 and 4 are focused on the evaluation of the MR's operation and validation of its chewing performance against human subjects. The initial evaluation of the MR's mechanical chewing functionality are evaluated through the breakdown of peanuts and methods of quantifying the breakdown are explored (chapter 3). Based on the observations noted during the experiments, improvements were then made to the MR. Chapter 4 then looks at the performance of the improved MR by comparing the breakdown of optosil and peanuts with human subjects.

The development and establishment of two novel techniques to characterise the food bolus throughout chewing of a range of foods are explored in Chapter 5; the multiple pin penetrometer test (MPP) and the slip extrusion test (SET). The development of the methodology for the MPP was done by demonstrating its use with four foods and the grey level co-occurrence matrix (GLCM) as a method to analyse the data. The design and development of the SET is discussed, and two experiments are carried out to evaluate this test and its applications.

The remaining chapters show how the MR and developed techniques can be applied to five selected foods presenting different initial texture properties. Chapter 6 focuses on understanding the chewing parameters used by human subjects in the mastication of these five foods and using this knowledge to simulate the chewing process in the MR. A factorial design was used to optimise the chewing parameters to be used in the MR for each of the foods based on the bolus properties measured by the SET.

Chapter 7 shows how the MR and the developed characterisation techniques may be used in an in-vitro study. The chewing trials consisted of the collection of boluses across the different stages of mastication which were then characterised by using the developed techniques to track the dynamic

changes in the bolus properties. Chapter 8 provides a summary of the conclusions and recommendations for future work.

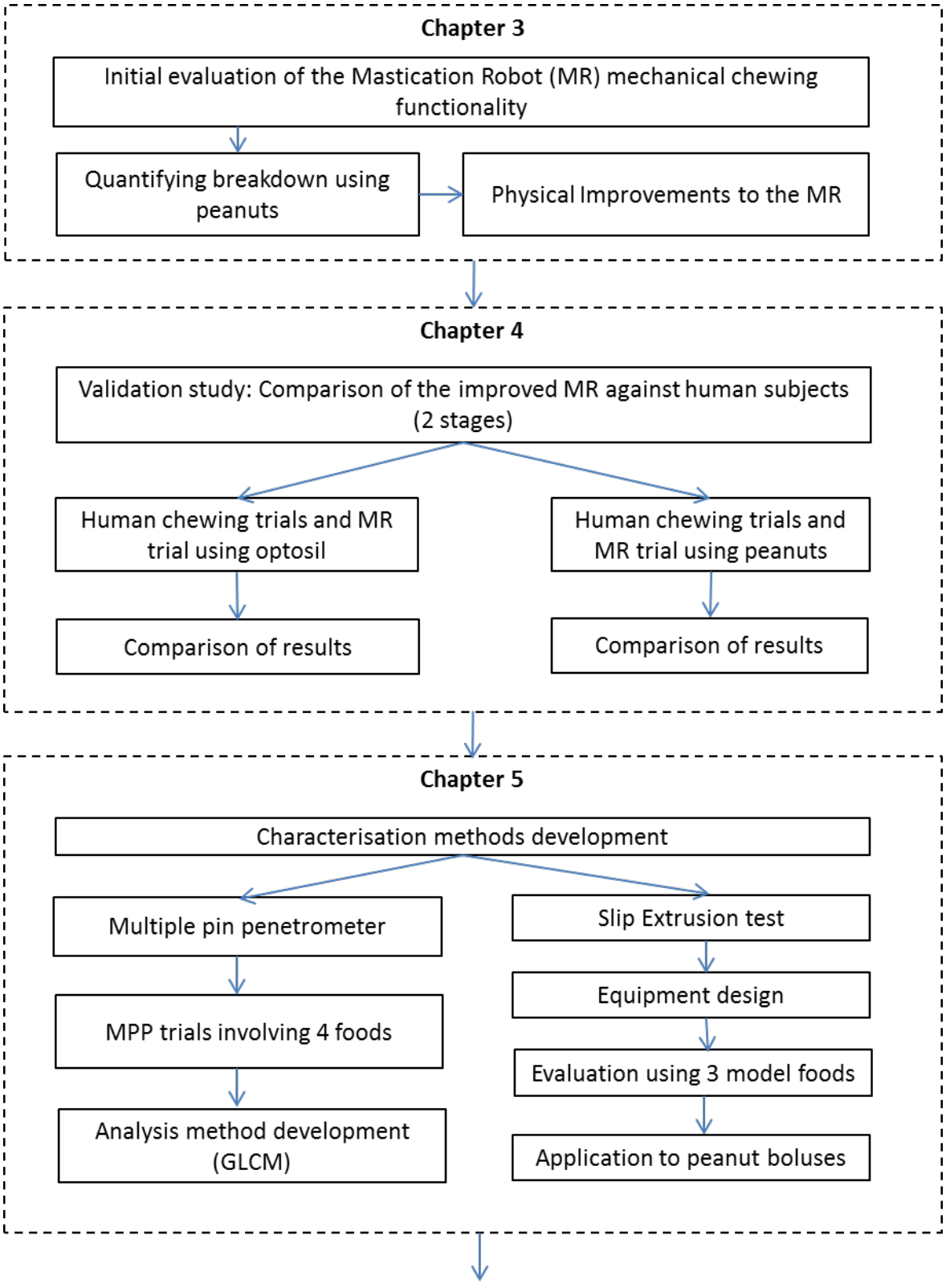

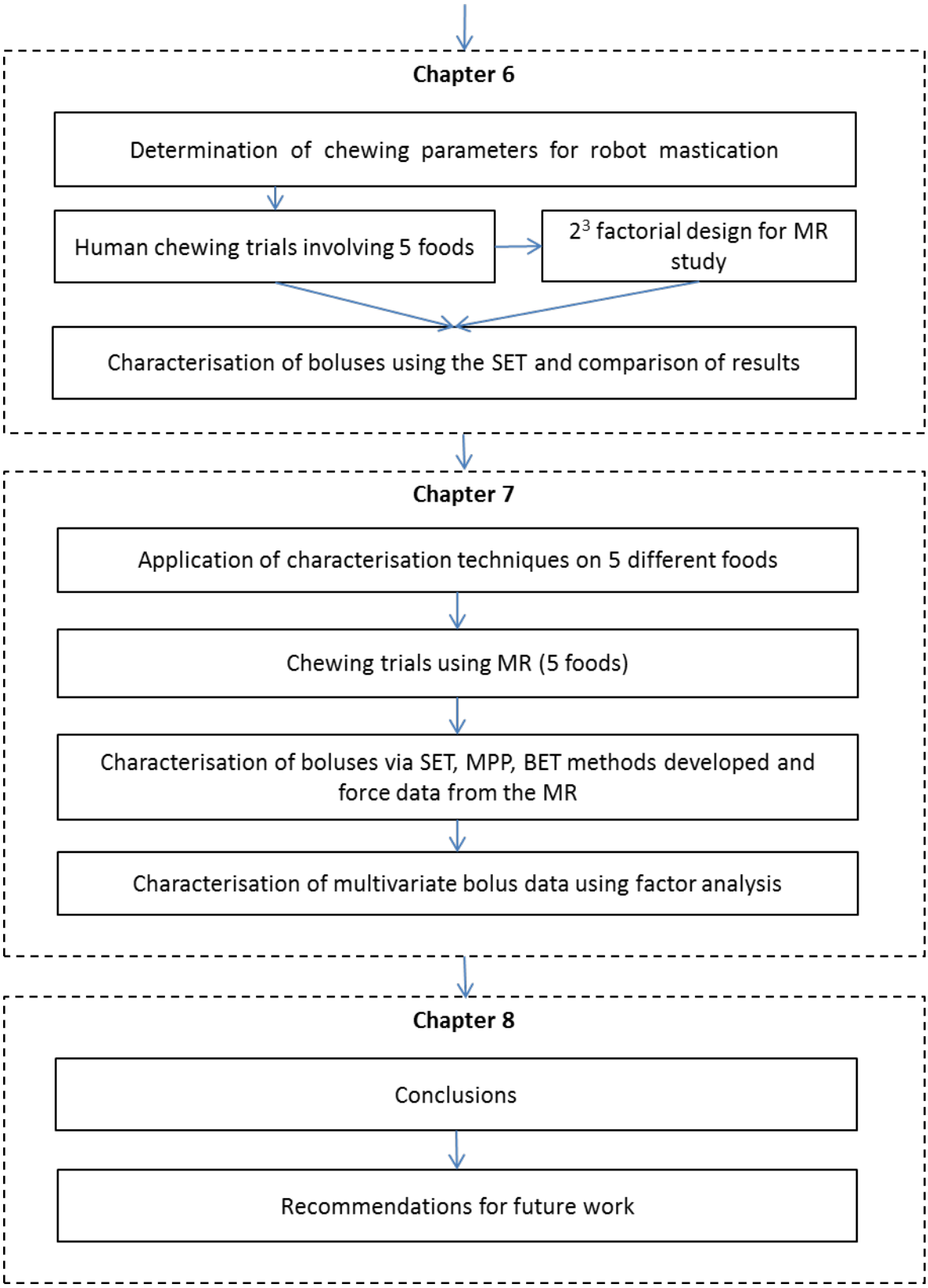


*Figure 1-1: Flow diagram showing the flow of the research done and what is the objective that each chapter sets out to achieve.*

The primary objectives of this project were to:

1. verify if the MR was reliable in producing reproducible food structure breakdown and determine whether the MR was able to mimic human chewing trajectories with similar breakdown properties in comparison with human subjects chewing model foods.
2. develop and establish novel characterisation methods that may be employed to track the bolus properties throughout different stages of mastication.
3. develop an experimental methodology that could be used for the in-vitro study of food break down and demonstrate the application of the MR and the developed novel techniques to different foods.

# Chapter Two Literature Review

## 2.1. Introduction

Food takes a breakdown pathway during the mastication process, thus it is essential to understand how the properties of food affect the breakdown pathways taken. This study involves the development of quantitative techniques that can quantify textural properties of foods dynamically to allow understanding of the breakdown strategies adopted during mastication of different types of food. These techniques could then be applied in future work, for example, towards the understanding of how food structure relates to how perceived food texture changes during oral processing.

Texture attributes of food have been commonly evaluated by sensory or instrumental analysis. Much work has been done to correlate the mechanical properties of food to perceived texture in sensory evaluation. However, the texture may not be quantified in a meaningful way as the physical properties of the food are changed during chewing and the process of texture perception is dynamic. Much of the research aimed to examine the mastication process during which texture assessments are made and the changes in the mastication process as the physical properties of food changes. This led to the development of mastication measurement techniques to study the breakdown process of food. The literature review will review the current texture measurement techniques and their limitations in evaluating the texture attributes of food. A summary of the human masticatory system follows to give an understanding of the process during which textural properties of the food are being perceived and how the dynamics of the mastication process affect it. Suggested theories of food breakdown models to determine the end point of mastication prior to swallowing are discussed. A summary of the mastication robots used in oral processing studies and will be introduced.

## 2.2. The Importance of Texture

Texture is a cognitive response to visual, tactile and auditory stimuli which contributes to the consumers' perception of a food. It is a key quality attribute that determines the overall acceptability of food (Bourne, M. C., 2002). As foods changes during storage, the perception of quality is highly linked with the textural property of food (Bruhn et al, 1991).

In a study which required respondents to supply the first three word associations they thought of when a food product was mentioned, Szczesniak (1971) found that the difference between the frequency of flavour and texture associations was small. This indicates that these two sensory characteristics are equally important. In a subsequent study to understand the consumers' awareness and attitudes to food texture, Szczesniak and Kahn (1971) found that texture awareness is taken more or less for granted. However, when the textural aspects did not meet expectations, there was a sharp increase in the awareness of the texture and resulted in criticism of its quality.

## 2.3. Traditional Methods and Limitations

The textural properties of foods are mainly divided into three classes, mechanical, geometrical and other characteristics (Szczesniak, 1963). The classification of textural properties led to the development of the Texture Profile Analysis (TPA) used with sensory and instrumental analysis. Instrumental analyses study the food's structure before or at the start of consumption while sensory evaluation focuses on the perceived texture after starting consumption of a food. Sensory and instrumental measurements are commonly used to evaluate attributes at the start of consumption or during the first-chew. However, attributes determined during mastication or after some degree of mastication have been difficult to predict based on the current knowledge of structures and mechanical properties. This is probably because of the involvement of saliva, surface interactions, and the bolus formation process in evaluating these terms. Mastication measurements study the oral process during eating of a food to understand how the dynamics relate to physical properties of food structure and food structure breakdown (Wilkinson et al., 2000).

### 2.3.1. Sensory Measurement

Sensory evaluation provides valuable information whether a food has desirable textural properties based on what is perceived by the human senses. Since humans are able to perceive and register all these details best as compared to a machine, this technique is still employed although it is more time consuming, expensive and the judgement has greater variability. A sensory texture profile analysis is usually conducted with a trained panel where panellists evaluate the food in the following sequence as in Figure 2-1 to provide descriptive and quantitative sensory data on the textural characteristics of food.

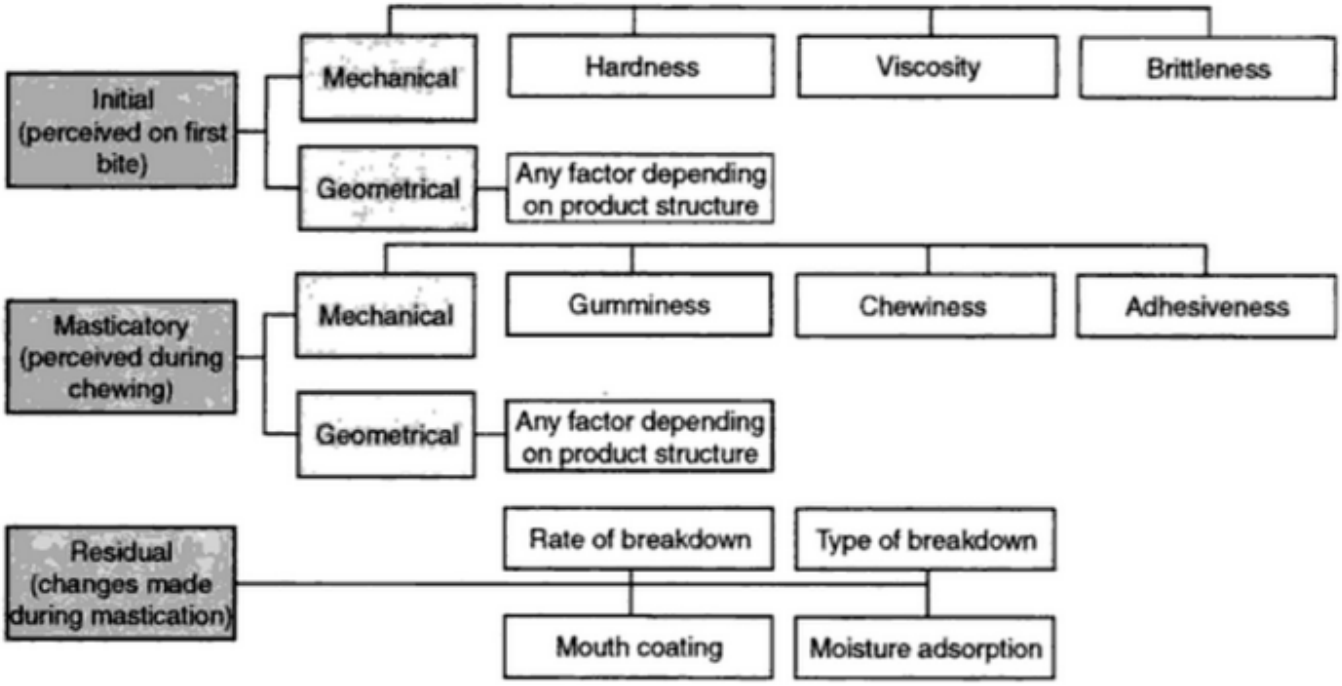


*Figure 2-1.The procedure for evaluating food texture as defined by (Brandt et al., 1963).*

Time resolved sensory methods such as the temporal dominance of sensations (TDS) and the temporal check-all-that-apply (TCATA) have recently been used to determine the dynamic textures perceived during mastication (Devezeaux de Lavergne, et al., 2017). In the TDS method, the dominant sensations perceived over time and their intensity are scored by the subject (Pineau et al., 2003). The dominant sensory sensations change throughout the whole mastication process as a result of the changes in the structure of the food and lubrication with saliva during mastication. This technique allows for the dominant dynamic changes in texture perception to be captured during the breakdown of the food. TDS has been applied to a number of food items such as biscuits (Cheong et al., 2014; Young et al., 2013), breakfast cereals (Lenfant et al., 2009), peanuts (Rosenthal & Share, 2014), cheese (Saint-Eve et al., 2015) and gels (Devezeaux de Lavergne, et al., 2015). The TDS methodology proved to be a suitable technique for untrained subjects. Oral processing parameters and food bolus assessment were correlated, and the results of the TDS technique and the dominant texture perceived could be explained by the change in bolus properties as the structure of the food was transformed over the different stages of mastication (Fiszman & Tarrega, 2018).

In the TCATA method, the subjects select all the terms applicable to the sensations they perceive throughout each moment of the evaluation process. Ares et al. (2015) found that the TCATA allowed a more detailed description of the dynamics of sensations perceived and better discrimination of the

attributes that were simultaneously perceived as compared to TDS. In another study, both TCATA and TDS were employed to examine the effect of hydrocolloid addition on sensory properties of pureed carrots and both tests captured similar attributes in the samples (Sharma & Duizer, 2019).

### 2.3.2. Instrumental Measurement

Texture analysis by instrumental measurement evaluates the mechanical characteristics of a food through subjecting it to a controlled force from which a deformation curve is generated. Alternatively, a food may be deformed to a fixed distance and the force required for deformation to occur is obtained. Although test results do not directly relate to product texture, results have been shown to have good statistical correlation to textural attributes assessed through sensory evaluation (Szczesniak et al., 1963).

The puncture test and compression test are the most common methods used to measure food texture properties. For both tests, the force required to push a probe into a food is measured. The depth of penetration or compression is usually held constant and the test generally causes irreversible crushing of the food. The tests are rapid, mechanically simple and are suitable for many different kinds of foods (Bourne, 2002). However, they may not be suitable for brittle foods as they get scattered after the initial breakage, thus making it difficult to obtain force-strain curves (Takahashi et al., 2009). The Warner–Bratzler Shear Force test is the most widely used instrumental measure for meat and meat products. It measures the maximum force encountered to cut fibrous food giving an indication of tenderness. Mioche, et al. (2002) employed the shear cutting test to study the bolus properties of beef throughout the duration of chewing. One of the mostly widely used imitative methods is the texture profile analysis (TPA) which is a test that compresses a bite-size piece of food twice in a reciprocation motion that simulates the chewing action of the jaw. The food texture properties such as hardness, springiness, cohesiveness, adhesiveness, resiliency, fracturability and gumminess are analysed from different positions of the force-time curves. The TPA is suitable for solid food measurement but it cannot be used for measuring boluses due to the loss of structure and inability to stand on its own. A modified TPA protocol consisting of two consecutive thrusts of the piston to compress the bolus in a cup was used by (James et al., 2011a; Peyron, & Gierczynski, 2009) to test biscuit boluses.

In addition to the tests mentioned above, several methods have been used to characterise the properties of boluses in food oral processing studies. For example, oscillatory rheological characterisation was carried out on breakfast cereal boluses (Loret et al., 2011b), and back extrusion

was carried out on biscuit boluses (James et al., 2011a) and bread boluses (Gao et al., 2015). It is difficult to apply the same test for a food over the range of mastication or have one test that can be compared across a range of foods. For example, the compression test may be used to assess the bread during initial stage of chewing but it would not be suitable for assessing a paste-like bolus formed in the later stage of chewing. Thus, current methods are not adequate for characterising the texture of foods during mastication.

Most instrumental measurements of food texture often focus on a single one-dimensional large deformation that provides information on initial food properties only. Some textural parameters are felt when the food is first placed in the mouth, although most are perceived when food is deformed during mastication, getting transferred around by the tongue and when mixed with saliva. Even as the food is being masticated, the texture of foods changes, thus the subsequent bites also contribute to the texture of the food. In addition, current methods are not able to simulate the complex crushing movements during mastication, and are without saliva-like lubrication. Most test machines compress food at a uniform speed (10-100 mm/min) that is slower than the rapid and non-uniform compression (800-1200 mm/min) during a chewing cycle, which causes larger errors in characterising foods that are strain rate sensitive (Bourne, 2002; Brown, 1995).

Traditional texture measurement techniques provide an average measurement which is useful in characterising homogenous textures. Characterising heterogeneous foods like the kiwifruit would involve multiple measurements at various locations within the food. Even so, limited information of the foods' textural properties can be inferred as there is no measurement of the spatial distribution of the texture. The 'Multiple Puncture Probe' is a novel test rig developed by Stable Micro Systems (Smewing, 2015) to measure the firmness of non-homogenous samples via a compression test. However, the force measured is the resultant of the forces exerted on the probes in the rig. This test rig had been adapted and a multiple pins penetrometer was developed by Al-Battashi et al. (2015) to measure the spatial distribution of texture in foods exhibiting heterogeneous structures (Figure 2-2).

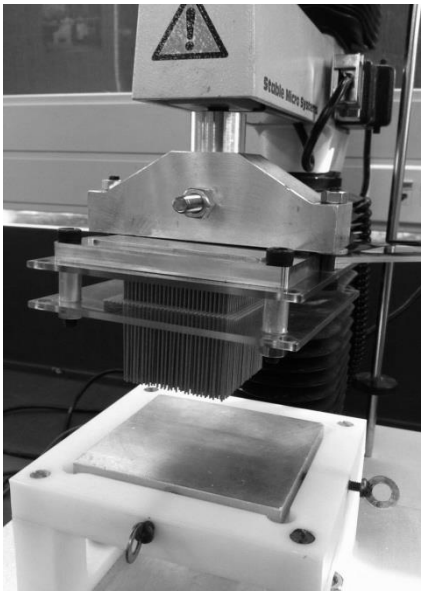

*Figure 2-2. Experimental set up of the multiple pins penetrometer attached to the TA.XT2 Texture Analyser.*

The multiple pins penetrometer attachment consists of 1024 flat end cylindrical pins (1 mm diameter) and is mounted on a TA-XT plus texture analyser (Stable Micro Systems Ltd, UK). A sensing device measures the forces experienced by each pin independently as they travel through the food. The TA.XT2 Texture Analyser has a force capacity of 50-500N and crosshead speeds of 6-2400mm $min^{-1}$. Information on the force-time and force-deformation history is recorded during each test.

Testing was conducted on kiwi fruit, cake and cheese to demonstrate the device's ability to measure the varying texture at different locations within the food. However, no systematic experiment was done to evaluate if there were any effects on measurement due to interactions between pins and protocol developed for data analysis so that the data collected across a plane can provide useful information about the spatial distribution of texture across the food. If this methodology provides robust and repeatable results, it could be used to characterise changes in the texture distribution of food boluses during mastication.

### 2.3.3. Mastication Measurement

The study of mastication patterns is to assist in describing breakdown paths for different foods, and highlight differences in the way individuals' break down foods in relation to their different perceptions of texture. Bite measurement using a multiple-point sheet sensor; electromyography (EMG) measurement of muscle activity; electromagnetic articulography (EMA) studying 3-D movements of the tongue and jaw during mastication are methods of mastication measurement collecting real time data during chewing.

Mastication patterns revealed by EMG and EMA records have been shown to be reproducible for individuals, but exhibit differences both between individuals and between food types (Brown, et al., 1994; Jemt & HedegÅRd, 1982). In a study conducted by Takahashi et al. (2009), subjects were asked to chew a food sample attached to a multiple point sheet sensor using their molar teeth twice and the bite force was measured. The 11 food samples were divided into four classes based on the bite curve shape and bite force magnitude. Brittle food such as the cookies had a strong bite force and a zigzag pattern in the early stages, while fibrous foods such as meat had a strong bite force and one peak. The high correlation between ease of chewing based on sensory evaluation and impulse of the first bite suggests that subjects assess it as work done during biting. Thus, the human bite parameters have been well correlated to the mechanical properties of food and to sensory-determined ease of chewing of food.

Since mastication is a dynamic process, it is thus essential to understand the relationships between the mechanics of mastication and the texture of food beyond the first bite. Increasing hardness in the food resulted in increased EMG activity, sequence duration and number of chewing cycles (Anderson, et al., 2002; Hiiemae, et al., 1996; Koç et al., 2014; Peyron, et al., 2002; Woda et al., 2006). Woda et al. (2006) found that the variables related to the chewing trajectories such as the vertical amplitude, lateral amplitude and closing velocity were affected by the rheological properties of the food and this was demonstrated using food models displaying elastic and plastic behaviour (jellied confectioneries and hard caramel confectioneries respectively). As the initial properties of the food shifted from elastic to plastic behaviour, the amplitudes of the chewing movements and closing velocity increased.

## 2.4. The Human Masticatory System

The main objective of mastication is to reduce food size and produce a food bolus suitable for swallowing. For brittle foods, this is done through fracturing of food particles which exposes more food surface area to allow increased release of taste and aroma substances and the rate at which digestive enzymes act on food. Oral manipulation and mixing with saliva softens and prepares a cohesive bolus for swallowing. Identifying the mechanisms occurring during mastication will give a better understanding of texture perception of foods.

### 2.4.1. The Muscles Controlling the Jaw

The human masticatory system consists of teeth located on an upper (maxilla) and lower (mandible) jaw, working together with the tongue, cheek and saliva to enable efficient mastication of food. The upper jaw is fused with the skull and the lower jaw is attached to the skull by muscles. These muscles are responsible for chewing and belong to five main muscle groups (Lucas, 2004a):

1) Temporalis muscles are attached from the side of the skull to the top of the lower jaw. They help the mouth close and move the lower jaw forward and backward.
2) Masseter muscles are attached between the cheek and lower rear section of the lower jaw. They help the mouth close and move the lower jaw laterally from side to side.
3) Medial Pterygoid muscles are attached on the inside of the skull and the lower jaw. They are used to move the jaw laterally from side to side and help the mouth close.
4) Lateral Pterygoid muscles are attached between the skull and the lower jaw. They are used to move the lower jaw forward and backward.
5) The Digastric muscle is attached between the chin and the bottom of the skull. It is used to open the mouth.

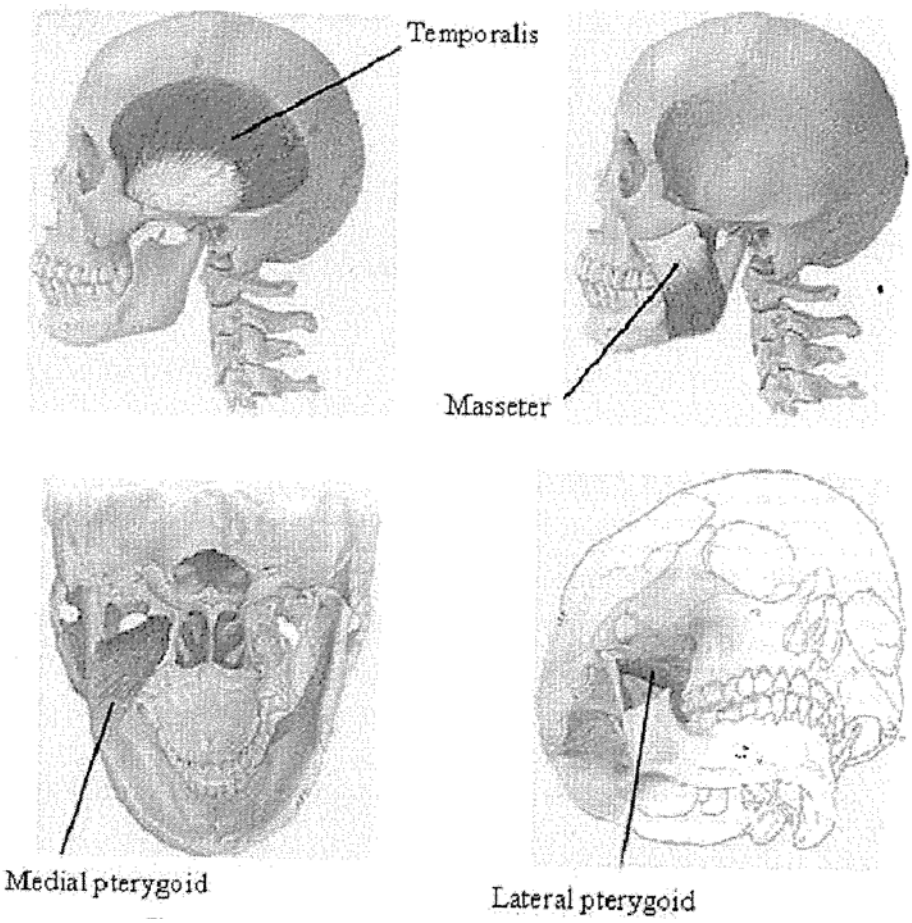


*Figure 2-3. The locations of the chewing muscle groups (Hannam, 1997)*

Using these muscle groups in different ways allows the lower jaw to move with six degrees of freedom (Koolstra & van Eijden, 1999), thus producing complex motions.

### 2.4.2. Teeth

The function of the teeth is to fracture foods into smaller particles during mastication. There are a number of various teeth shapes which perform different functions. The incisors and canine teeth are wedge-shaped and have a very sharp blade like edge for cutting foods, usually in the first bite. They are located at the front of the mouth and thus are known as the anterior teeth. The posterior teeth or postcanine teeth which are located behind consist of premolars and molars. The premolars are used to tear and break food while the molars are used to fracture and grind food into smaller particles.

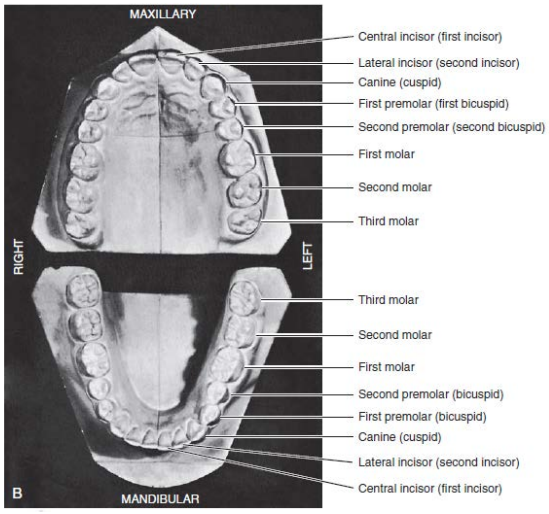


*Figure 2-4. The occlusal view of teeth in the human mouth (Ash & Nelson, 2003).*

The cutting surfaces are formed by incisal edges or cusps on tooth crowns. The crown of a tooth may have an incisal edge as in the central and lateral incisors; a single cusp as in the canines; or two or more cusps as on premolars and molars (Ash & Nelson, 2003). A cusp is a blunt mound that makes an indentation in a food particle when pressed onto it. The resulting force from this indentation would start cracks and fracture the food particle. Sharp cusps are more likely to suppress cracking and plastically deform food particles instead. Hence, the shape of cusps is thought to be spherical (Lucas, 2004c). Figure 2-5 shows how fracturing of a food particle occurs by using a three-point bending principle. The fracture force that results in cracking is proportional to the radius of the spherical cusp (Frank & Lawn, 1967).

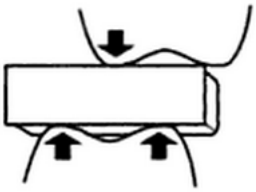

*Figure 2-5. The fracturing of food by three-point bending of a food particle (Lucas, 2004c).*

Since the focus of this study is on the breakdown of food particles and the teeth mainly used in fracturing are the molars, the teeth for the mastication robot was modelled from the first molar. The surfaces of the premolars and molars that come in contact (occlusion) with those in the opposite jaw as the mouth closes during chewing are called occlusal surfaces.

### 2.4.3. The Masticatory Process

The masticatory process consists of three phases, starting with initial ingestion of food where the food is assessed externally by lips and the tip of the tongue and then internally with the first bite by the incisors. At this point, the texture and flavour of food is evaluated to determine if food is to be expectorated or transferred to the occlusal surface of the teeth by the tongue for further processing. This is followed by a series of chewing cycles where food is broken down into particles to form a bolus. The final phase is when the bolus is ready and swallowed (Heath, R. M., 2002; Heath, R. M. & Prinz, 1999).

Chewing Cycle

Each chewing cycle consists of an opening, closing and occlusal phase. Ogawa et al. (2001) have defined the occlusal phase as an area within 0.5 mm from the maximum intercuspation (MI). The MI is the point at which the upper and lower jaw is in maximum contact with each other when the mouth is closed. The opening phase is where the lower jaw leaves the 0.5 mm point from the MI as the mouth opens and closing phase is where the lower jaw returns to the 0.5 mm point from the MI as the mouth closes.

*Figure 2-6. The opening, closing and occlusal phase of a chewing cycle (Ogawa et al., 2001).*

Several studies have measured the chewing trajectories in three-dimensional coordinates for different types of foods. It has been shown that the chewing trajectories were different and thus there is a need to characterise how different food properties affect the chewing trajectories. Anderson, K. et al. (2002) conducted a study to determine the effect of bolus hardness on the masticatory kinetics and found that harder food resulted in an enlarged chewing trajectory although the shape is not changed.

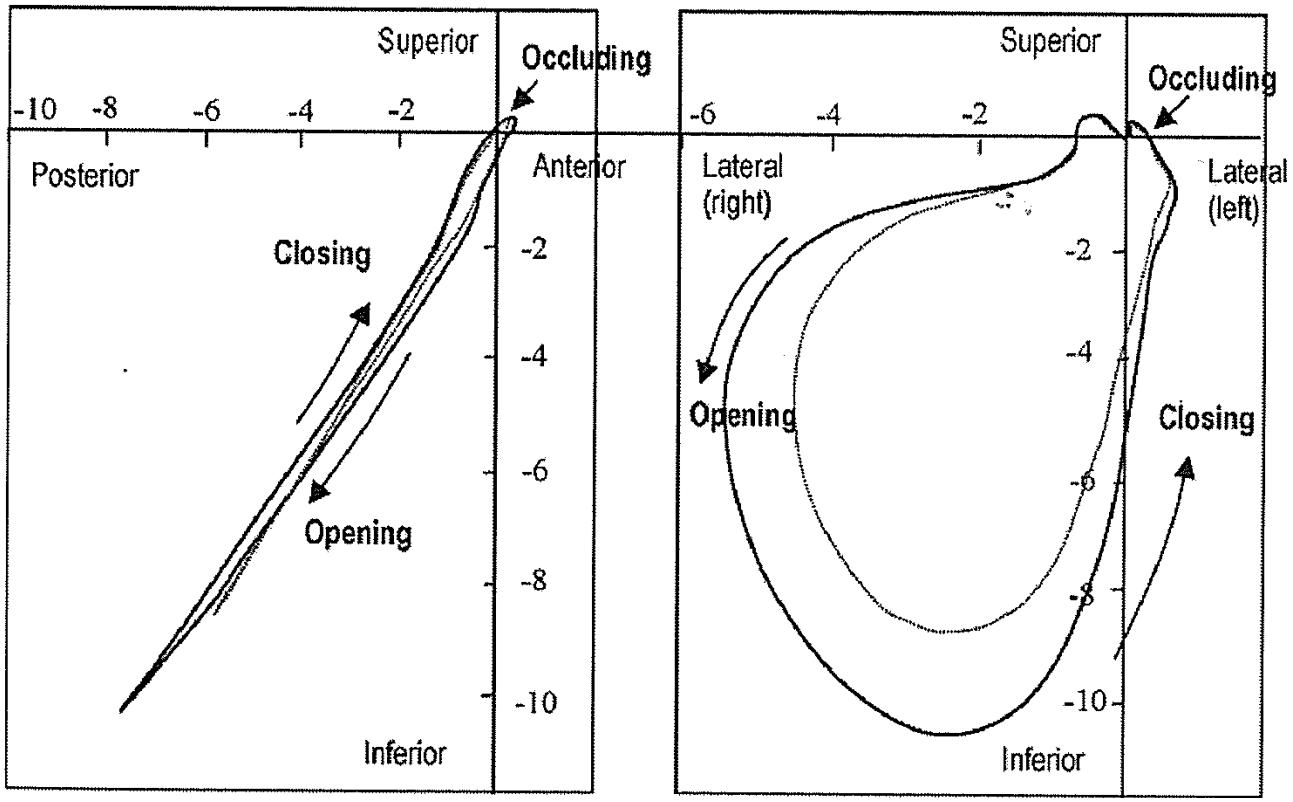


*Figure 2-7. The chewing trajectories in the sagittal and frontal plane (from left to right) for soft (dotted line) and hard chewing gum (solid line), (Anderson, K. et al., 2002). The sagittal plane corresponds to looking at the side of the skull and frontal plane corresponds to looking at the face.*

Trajectories in the sagittal plane show that teeth can come together at a zero degree angle which may vary to a 30 degree angle. Trajectories in the frontal plane also show that teeth may occlude vertically or laterally where the teeth slide across each other horizontally (Anderson, K. et al., 2002).

The shape and texture of the food particles affects the type of chewing trajectory being used. The vertical chewing trajectory results in the teeth cusps fracturing food particles while a more lateral chewing trajectory results in the sharp edges being used to cut food particles (Lucas, 2004c). Figure *2-8* demonstrates how the food properties and dental features lead to the decision as to how the teeth is to be used, which will affect the chewing trajectory used. The teeth are used as sharp

blades to cut up food if the particles are thin sheets or rods, whereas the texture of thick blocks of food will be assessed from the $(R/E)^{0.5}$ value. R is defined as the food toughness and E is the Young's modulus of elasticity. Blunt cusps are used on foods of low $(R/E)^{0.5}$ while the sharp blades are used on foods of high $(R/E)^{0.5}$. The application of this model implies that foods which are not tough and have a relatively high modulus of elasticity (low $(R/E)^{0.5}$) such as peanuts and biscuits would require fracturing and thus utilise the vertical chewing trajectory. On the other hand, foods such as meats and vegetables require cutting and thus utilise the lateral chewing trajectory.

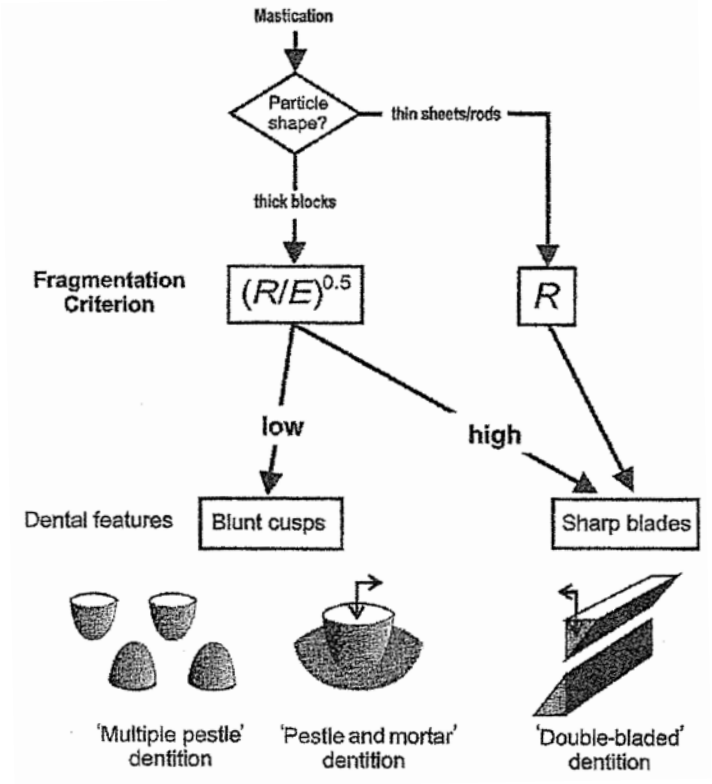


*Figure 2-8. An evaluation of how the shape and texture of food affects the type of dental features used for chewing. The texture is evaluated from the $(R/E)^{0.5}$ value where R is the food toughness and E is the Young's modulus of elasticity (Lucas, 2004c).*

The difference in the mandible movements for the vertical and lateral chewing trajectories of the incisors in the frontal plane was studied by Ogawa et al. (2001) as shown in Table 2-1. These are the parameters that should be followed closely to achieve both vertical and lateral trajectories in the mastication robot, so as to simulate human chewing.

*Table 2-1. Movement variables for the vertical and lateral chewing trajectories (Ogawa et al., 2001).*

| | Lateral chewing | Vertical chewing |
|---|---|---|
| Closing angle (°) | 46.6 | 72.5 |
| Opening angle (°) | 113.1 | 78 |
| Total angle (°) | 66.5 | 5.5 |
| Vertical opening (mm) | 14.6 | 15.1 |
| Lateral displacement in opening (mm) | 1.1 | 0.4 |
| Lateral displacement in closing (mm) | 4 | 3.1 |
| Cycle time (s) | 0.77 | 0.7 |
| Occlusal time (s) | 0.12 | 0.16 |
| Opening/closing time (s) | 0.65 | 0.54 |

In a study of the swallowing thresholds of peanuts, cheese and carrots in 87 dentate subjects, results showed that the number of chewing cycles required before swallowing the food linearly increased with the food volume (Fontijn-Tekamp et al., 2004). Thus, the portion size is one of the factors influencing the masticatory performance.

Chewing Forces

Several studies conducted; have studied the forces during chewing by using transducers positioned on the cusp, bridges and crowns of teeth. The chewing forces applied on the teeth vary with the different types of food being chewed. Anderson, D. J. (1956) found that the chewing force on a single molar tooth range between 70 and 150 N during the chewing of biscuits, carrots and cooked meat. Gibbs et al. (1981) found that the chewing force on all the contacting teeth range between 190 and 260 N during the chewing of cheese, raisins, bread, beef, carrots and gum. Kohyama, Hatakeyama, Sasaki, Dan, et al. (2004) found that the food hardness and thickness have an effect on the human chewing force by measuring the chewing force on a silicone rubber as a food model. The chewing forces of the silicone rubber at varying degrees of hardness and thickness were measured. The chewing force increased as the sample hardness increased (Figure 2-9). The maximum chewing force was at a food thickness of 2 mm and decreased as the sample thickness increased (Figure 2-10). It was suggested that the narrower jaw opening in the posterior position resulted in decreasing bite force.

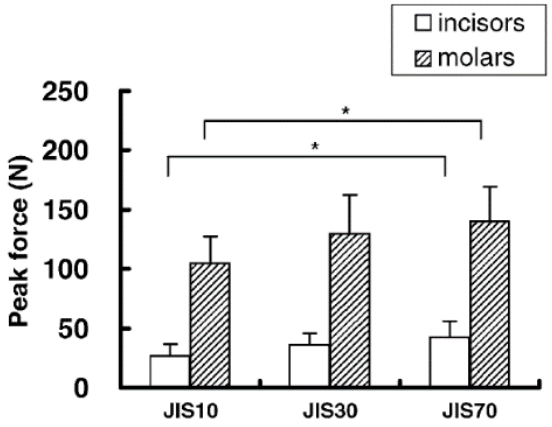


*Figure 2-9. Peak force measured for silicone rubber samples of three hardness where JIS10 is the softest and JIS70 is the hardest (Kohyama, Hatakeyama, Sasaki, Dan, et al., 2004).*

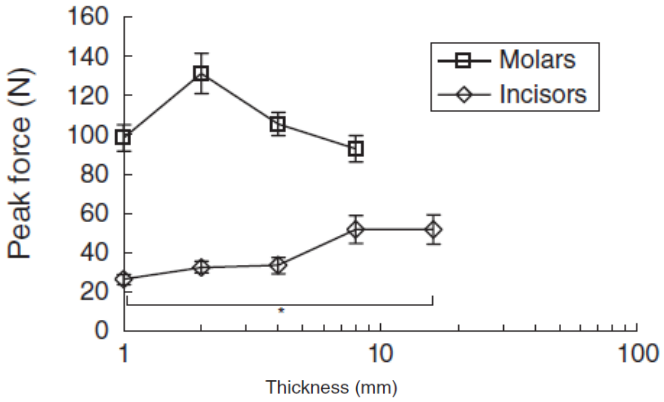


*Figure 2-10. Peak force measured for silicone rubber samples of different thickness (Kohyama, Hatakeyama, Sasaki, Azuma, et al., 2004).*

It can be concluded that the properties of food will influence the chewing force exerted by humans as well as the number and type of chewing cycles needed to prepare the food for swallowing.

Characterising Masticatory Performance

The breakdown of brittle foods involves two processes, selection and breakage. The selection and breakage functions are used to characterise mastication efficiency through the study of particle size in food boli. The selection function describes the possibility of the food making contact with the teeth while the breakage function describes the degree of size reduction, size and number of fragments when the selected particles break. The selection of particles is determined by the particle size and the tendency of particles to clump together to form a bolus. Selection is also related to subjects' manipulation ability of food. Breakage is associated with the mechanical properties of food and mechanical action applied. Tooth shape, food characteristics, and coordination of jaw-muscle activity affect the breakage process (Lucas & Luke, 1983; Van der Bilt, A.  et al., 1987).

### 2.4.4. Function of the Tongue and Saliva during Mastication

The function of the tongue is to collect food particles, transfer food particles from the incisors to the postcanines, mix particles with saliva in bolus formation and for deglutition. The tongue is in a trough-like formation to collect particles in the early jaw opening stage. It then twists over on one side to throw the particles laterally towards the teeth during the late jaw opening stage. This deposits the food particles onto the occlusal surfaces of the lower postcanines for the next cycle of chewing. The tongue also mixes the particles with saliva by pressing them against the hard palate. Upon the tongue's release of pressure on the particles, food particles will fall apart and the chewing cycle is repeated until the food particles are sufficiently crushed and mixed with saliva. The bolus is ready for deglutition when the particles remain clumped together. The tongue exerts pressure on the bolus against the palate, forcing it to move backwards towards the pharynx and swallowing occurs (Abd-El-Malek, 1955; Okada et al., 2007).

As the tongue manipulates the food particles, surface attributes of the foods are being evaluated. The mechanical properties of the food particles are evaluated during fracture. These are sources of sensory feedback to the brain which results in a corresponding motor response (Lucas, 2004b).

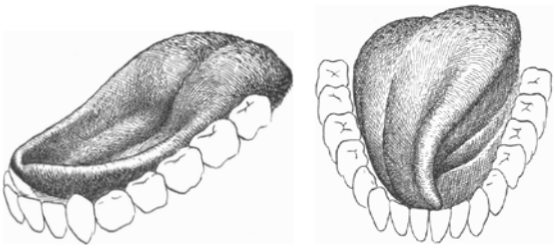

*Figure 2-11.The positions of the tongue during early and late jaw opening (Abd-El-Malek, 1955).*

The function of saliva is to lubricate the food bolus for swallowing, soften dry foods for breakdown, flush away small food particles, dissolve and release food taste and odour chemicals for normal taste perception, and deglutition (Mandel, 1987). Studies showed that the masticatory efficiency had significantly decreased as the number of chewing strokes and time in the mouth before swallowing significantly increased after experimentally induced oral dryness (Ishijima et al., 2004; Liedberg & Owall, 1991). Another study showed that more saliva was required for oral manipulation of powdered crisp bread than for pieces of crisp bread as the larger surface area of the powder required more saliva for lubrication and cohesive binding in preparation for deglutition (Pangborn & Lundgren, 1977). Mioche et al. (2003) found that more saliva was incorporated into a bolus of tough

meat as compared to a bolus of tender meat based on boluses collected at the point when swallowing would normally have been triggered.

Masticatory performance can be evaluated in terms of the capacity to reduce the size of food particles (Dahlberg, 1942) as well as the number of chews necessary to render food ready for swallowing (Chauncey et al., 1984). Thus, the incorporation of saliva to achieve bolus formation is required.

### 2.4.5. Theories of Swallowing

The physical characteristics of the bolus that initiate swallowing are not completely known.

*Figure 2-12. The breakdown path (Hutchings, J. B. & Lillford, 1988).*

Hutchings & Lillford suggest that each food's texture influences the breakdown strategy that it takes during mastication. The model proposes that the degree of structure and lubrication which changes with time and more chews are the factors that determine when a bolus is ready for swallowing (Hutchings, J. B. & Lillford, 1988). Thus, studying the effect of mechanical breakdown and lubrication on bolus formation is essential to understand what makes a bolus swallowable.

The change in degree of structure during mastication has often been analysed in terms of particle size (Hutchings, S. C. et al., 2011; Jalabert-Malbos et al., 2007; Lucas & Luke, 1983; Olthoff et al., 1984; Van der Bilt, A. et al., 1987). The particle size distributions formed during chewing may be variably skewed as the number of chewing cycles increase, thus the median particle size is the best indicator of the degree of the particle size breakdown (van der Bilt, A. et al., 1993). The Rosin-Rammler equation is commonly used to characterise the particle size distributions which provide the median particle size ($d_{50}$) and the spread of the distribution (Olthoff et al., 1984). The pre-swallow food particle size distribution is often used to characterise a food bolus.

However, particle size reduction is not the only factor affecting the degree of structure during mastication especially for foods that agglomerate to form a strongly cohesive bolus such as in cookies. Studies suggest that the purpose of extended chewing, once the desired particle size is achieved, is to wet and lubricate the fractured particles to form a bolus (Lillford, 2011; Rodrigues et al., 2014). Lubrication is affected by the water or fat content in the food as well as the saliva present.

Another theory suggested by Prinz and Lucas (1997) is that swallowing is triggered when an optimum cohesive force binding the food particles is achieved, forming an adherent food mass. This ensures bolus transport through the pharynx is safe by minimising the chance for food particles to stray away into the airway. The volume of saliva present is the key factor affecting the viscous forces that hold the bolus together.

In a study conducted by Mishellany et al. (2006) , it was suggested that subjects used different strategies for mastication to obtain food boli of a similar degree of comminution and the distribution of the size of particles collected after mastication depended on the food properties. The study concluded that a swallowing threshold probably existed in terms of particle size but highlighted that it did not take into account other determinants for triggering deglutition such as optimal lubrication or the perception of cohesive forces unifying the bolus.

Additionally, Young et al. (2013) found that cohesiveness was not a swallowing trigger for the swallow point of biscuit boluses. Biscuits of varying initial hardness were used to test if the resulting boluses at swallow point would have similar cohesiveness. The results suggested that there was no swallowing trigger in terms of the cohesiveness threshold as there were significant differences in the cohesiveness of the biscuit boluses at swallow point. Loret et al. (2011a) found that the perception of fluidity which was related to the moisture content of the bolus at swallow point could not be

differentiated across the cereals of differing initial rheological and water content properties, thus hypothesizing that a fluidity threshold to trigger swallowing may exist for each general category of food.

There is much importance in knowing what determines the end point in a chewing process so that we can study these features of the chewing sequence and understand how these features influence the assessment of particular textural characteristics of food. Taking into consideration the suggested models, it is essential to understand the physical ways in which foods break down and how these change with breakdown conditions, as well as to understand the dynamics of saliva in terms of lubricating and forming the bolus. Currently, measurement of particle size distributions and mechanical properties of the chewed food are commonly used to characterise the breakdown. However, current methods for measurement of lubrication and cohesiveness may not be adequate.

### 2.4.6. Artificial Masticators

The WY-5 (Waseda-Yamanashi) is a parallel mechanism robot with 6-DOF which was first used to manipulate a patient's jaw as part of the training to help patients to control their jaw movement (Takanobu et al., 2003). This was then modified for food texture measurement and WWT-1 (Waseda Wayo Texturobot) was developed in 2004 (http://www.takanishi.mech.waseda.ac.jp). This food texture measurement robot had a 6-DOF force sensor that was able to detect a minimum force of 0.001 N.

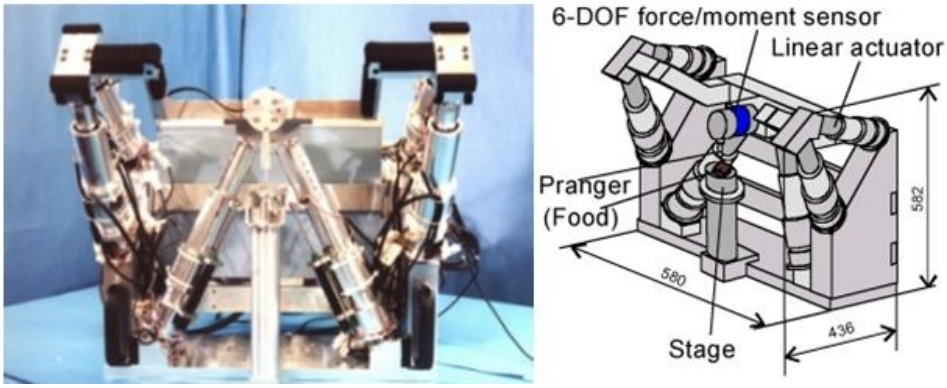


*Figure 2-13. The food texture measurement robot WWT-1 (taken from [http://www.takanishi.mech.waseda.ac.jp](http://www.takanishi.mech.waseda.ac.jp)).*

The Artificial Mouth developed by Salles et al. (2007) was used for the in-vitro study of flavour release during the mastication of foods (Figure 2-14). The mouth consisted of an actuated lower mandible, an actuated tongue and a fixed upper mandible. The lower mandible could move vertically and rotate, producing shear and compression strengths comparable to that of human mastication.

The mechanical performance of the device was validated using peanuts via the comparison of mastication efficiencies with *in-vivo* tests.

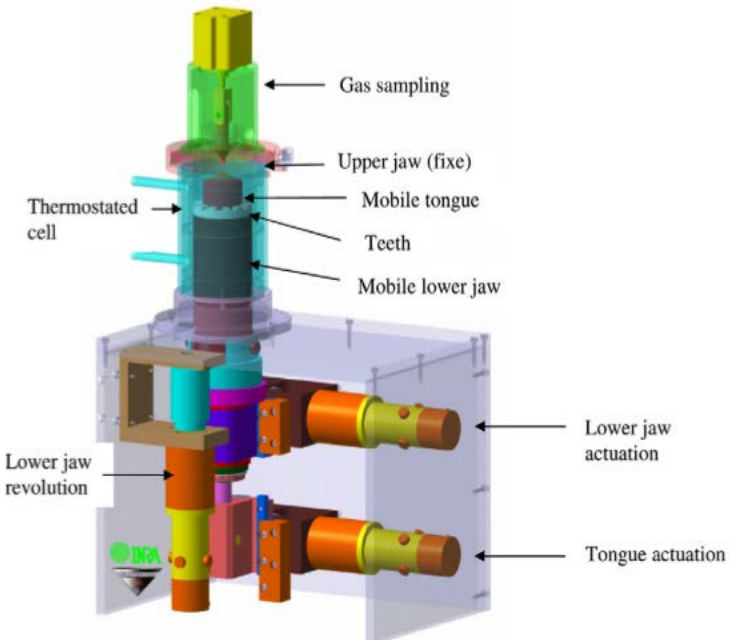


*Figure 2-14. The Artificial Mouth developed by Salles et al. (2007).*

The Artificial Masticatory Advanced Machine (AM2) developed by researchers from the University of Auvergne (Monique et al., 2007). Parameters such as the number of mastication cycles, the cycle duration, the force range applied to the food, the mastication chamber temperature and the quantity of artificial saliva could be controlled in this artificial masticator. The mastication chamber is a cylindrical chamber formed by a stationary "maxillary disc" and a moving "mandibular disk". Food gets "masticated" by the action of the moving disc that moves back and forth towards the stationary disc, and also rotates around the central axis of the cylinder. Woda et al. (2010) demonstrated that the AM2 could produce boluses with similar food particle size distribution to those collected from human subjects.

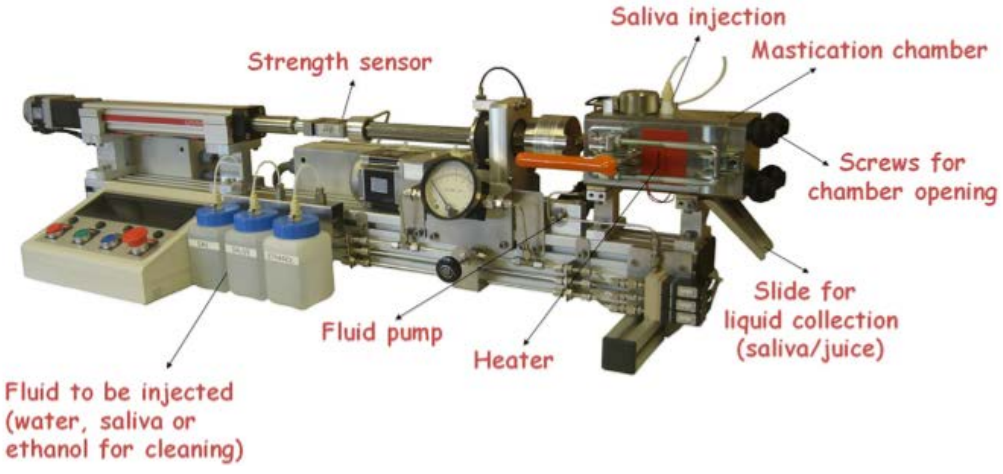


*Figure 2-15.The AM2 developed by researchers from the University of Auvergne (Monique et al., 2007).*

## 2.5. Novel Techniques

### 2.5.1. Mastication Robot

The contact surfaces in current imitative tests are not representative of teeth, such as the use of flat plates in compression tests. In reality, the chewing movement is three dimensional but current test methods are mostly one-dimensional large deformations. A mastication robot (Figure 2-16) was developed to simulate human chewing behaviour in terms of kinematics requirements and bite forces (Lewis, Darren, 2006; Sun, 2012a). A brief introduction is presented in the literature review with more details discussed in chapter 3.

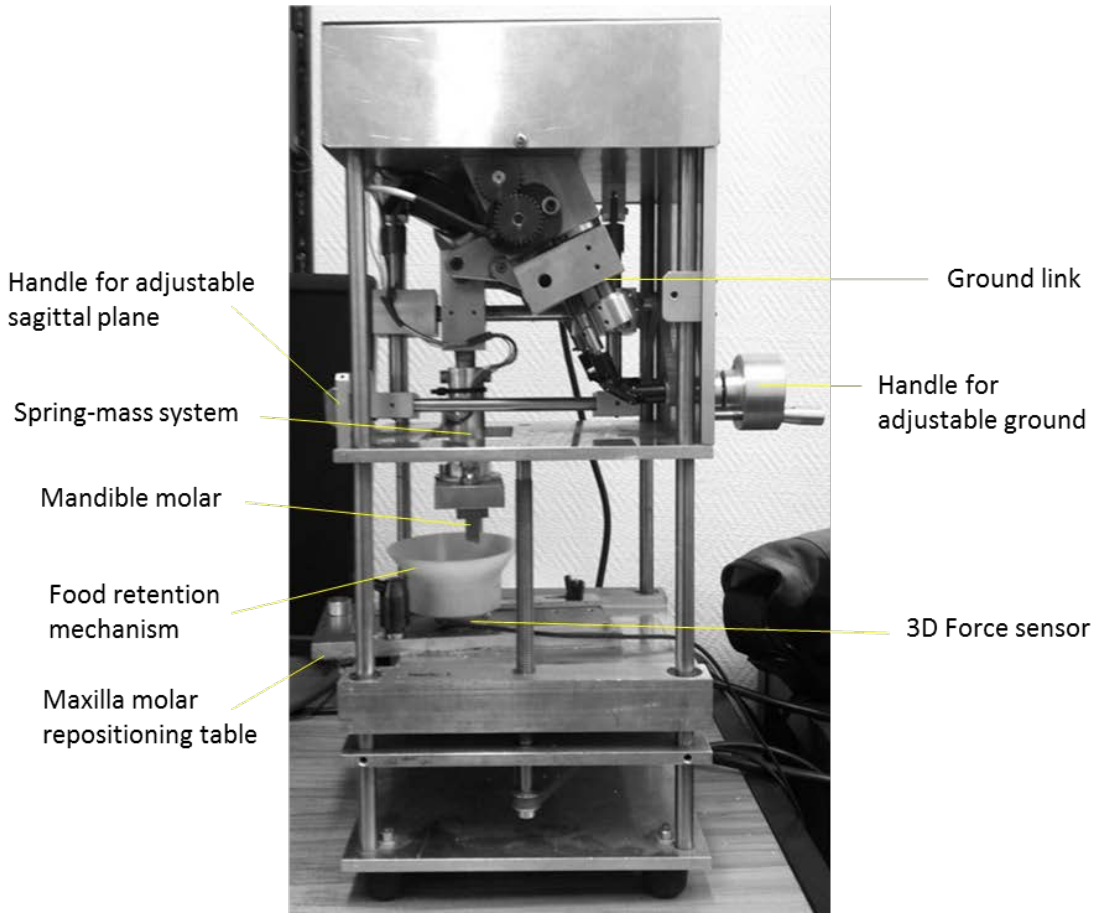


*Figure 2-16. The mastication robot developed by Lewis, Darren (2006), and Sun (2012a).*

The inverted design where the upper teeth is the mandible teeth and lower teeth is the maxillary teeth is so that gravity can ensure that the food may be retained on teeth by using a bowl like system to guide the food back onto the teeth embedded in it. As such the bottom jaw needs to be in a fixed position which meant that the maxillary teeth need to be at the bottom (Figure 2-17).

*Figure 2-17. The lower teeth in the food retention system.*

The set of upper and lower teeth in the mastication robot was modelled after 3D scans of the first human molars and is made out of brass (Figure 2-18). The teeth only have the occlusal surface area of the molars and not the whole teeth shape. The upper and lower teeth are aligned in one straight line such that they can occlude perfectly to ensure an efficient fracturing and grinding effect as in human jaws.

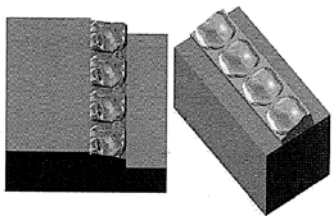

*Figure 2-18. The lower (maxillary) and upper (mandible) molar teeth of the mastication robot (Sun, 2012a).*

The mastication robot was built to reproduce the chewing trajectory of the first molar in 2D space since fracturing of particles is mostly done using the molar teeth. The mastication robot is able to reproduce any trajectory between the lateral and vertical trajectories in the frontal plane as defined in Table 2-1. Other than the chewing trajectory, the bite force, chewing efficiency and salivary flow rate will contribute to the breakdown of food particles which ultimately results in a food bolus that is ready for swallowing. Sun (2012) demonstrated the use of a pretightening plate to adjust the initial spring compression displacement to provide different initial force depending on the desirable force profile during occlusion required for the different foods. A 3D force sensor is installed under the lower jaw to collect real time force data during the chewing cycle.

The application of the mastication robot to chew foods had been limited to the chewing of a few foods such as peanuts to get an output of the measurements that could be collected from the robot. However, no systematic experiment has been conducted to demonstrate the robot's ability to chew food in different trajectories and to validate its chewing efficiency against that of human subjects.

## 2.6. Conclusion

The current methods used in characterising breakdown during mastication has been largely limited to particle size measurement. The problem is that there are no methods to evaluate foods that are not particulate or fracturable such as meat, bread, and fruit. For fibrous and cohesive foods, researchers have studied the food bolus properties at the swallow point by adapting methods to suit a single system. However, the limitations of these tests are that the methods can only be used to study the boluses collected at the end of the chewing process; or that the volume needed for the test is much larger than the usual volume of the bolus expectorated for a single portion. All the methods are not very useful due to the nature of the bolus which changes significantly from the initial stages of mastication till the swallow point. Although the modified TPA method was not designed for measuring initial properties of food, this is the only method that is physically possible to be used for all the stages as the boluses at the end stages can be confined in a container for the analysis.

Two novel devices, the mastication robot and the multiple pins penetrometer, were developed but had not been implemented in systematic study for food breakdown or characterisation purposes. The mastication robot was developed to simulate human chewing behaviour and measure the forces exerted during mastication. The multiple pins penetrometer was developed such that the forces exerted by the individual pins in contact with the food is measured and a spatial distribution of the force profile is measured. These two devices have been applied to some foods and could potentially be used for measuring bolus properties during food breakdown. However, the operation of both devices to characterise food was not developed and no systematic study had been done to validate the mastication robot.

The research in the current work will contribute to the development of techniques that could be used to characterise the textural changes during food breakdown. Thus, the technique should be able to measure a food's initial properties as well as the bolus properties.

# Chapter Three  Evaluation of the mastication robot

A mastication robot (MR) was previously developed (Xu et al., 2008) to enable the reproducible mastication of food so that masticatory efficiency and food breakdown dynamics can be assessed quantitatively. This device was developed to achieve three purposes; 1) To mimic human chewing (trajectory, forces, dentition shape etc.), 2) To collect dynamic data on the changes in food properties (e.g. forces) in real time during chewing, and 3) To allow reproducible preparation of boluses for subsequent characterisation (e.g. texture, cohesiveness etc.). Such a device could be a useful tool for the study of food oral processing and in this work. Although the machine is well documented in terms of design (Sun, 2012a; Sun, Cheng et al., 2014), little systematic analysis on its application to characterise food texture has been carried out. For this reason, a characterisation of the chewing robot was required:

- To understand its operation such as determining which machine parameters can be changed and in what range, and how sensitive the break down of the food is to these changes in operation parameters.
- To identify any key problems with its design and implement modifications if necessary.
- To collect data from the MR and develop methodologies to analyse these data.
- To characterise the reproducibility of bolus preparation using the MR.

The objective of this work was to carry out this characterisation before validation of the device against human chewing was carried out. There is a need to ensure that the MR is reliable in producing reproducible breakdown and that the MR can chew in different trajectories as planned. Then, it will be justifiable to carry out further work involving human subjects for the validation of its chewing performance. In this chapter, peanuts were used as a model food system as this is a commonly studied brittle food system for which breakdown during oral processing can be followed easily by measuring changes in the bolus particle size distribution (Hiiemae, M. K. & Palmer, 1999; Mishellany-Dutour et al., 2011; Pereira et al., 2006; van der Bilt, A. & Abbink, 2017).

## 3.1. Overview of the mastication robot

The MR consists of a six-bar linkage system that was attached to a set of upper molar teeth with a spring-mass system to ensure maximum occlusion during chewing, a lower molar teeth repositioning table, and a simple food retention mechanism that collects chewed food particles. A 3D force sensor is installed under the lower teeth to collect real time force data during the chewing cycle.

The MR has an inverted design where the upper teeth are the mandible teeth and lower teeth are the maxillary teeth, so that gravity can ensure that the food may be retained on teeth by using a bowl like system to guide the food back onto the teeth embedded in it (Figure 2-17). As such the bottom jaw needs to be in a fixed position which meant that the maxillary teeth need to be at the bottom (Figure 2-16). The set of upper and lower teeth in the mastication robot was modelled after 3D scans of the first human molars and is made out of brass. The teeth only have the occlusal surface area of the molars and not the whole teeth shape. The upper and lower teeth are aligned in one straight line such that they can occlude perfectly to ensure an efficient fracturing and grinding effect as in human jaws. The occlusal surface in the MR simulates one sided chewing in human subjects.

The mastication robot was built to reproduce the chewing trajectory of the first molar in 2D space since fracturing of particles is mostly done using the molar teeth. The mastication robot is able to reproduce any trajectory between the lateral and vertical trajectories in the frontal plane to evaluate different foods. The mastication robot has an adjustable ground length (Figure 3-1) to achieve vertical (ground length=38 mm) and lateral (ground length=50 mm) chewing trajectories. The base of the six-bar linkage can be tilted so that the chewing trajectory in the sagittal plane could be set an angle ranging between 0° and 30° to the horizontal plane when required to match that in human.

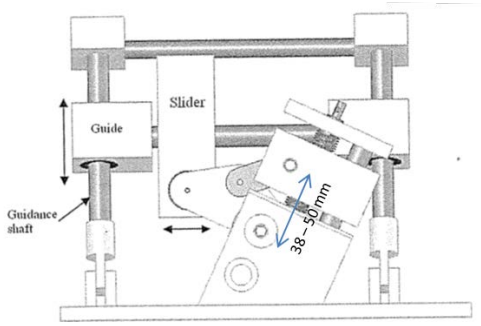


*Figure 3-1: An adjustable ground length was used to achieve the different chewing trajectories.*

Although the data is based on the trajectories of incisors, Lewis (2006) found that the trajectories of the first molar were vertically compressed versions of the incisor trajectories and that the entry and exit angle to and from occlusion was similar. Trajectory measurement in the frontal plane showed that the trajectories produced by the mastication robot were close to the human chewing trajectories (Figure 3-2 and Figure 3-3).

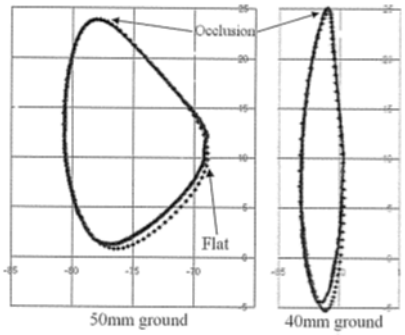


*Figure 3-2: The lateral and vertical trajectories that the mastication robot can achieve and the desired human chewing trajectories indicated by the solid and dotted lines respectively (Lewis, Darren, 2006).*

| | Lateral chewing | | Vertical chewing | |
|---|---|---|---|---|
| | Human | Linkage | Human | Linkage |
| Closing angle (°) | 46.6 | 45 | 72.5 | 99 |
| Opening angle (°) | 113.1 | 112 | 78 | 105 |
| Total angle (°) | 66.5 | 67 | 5.5 | 6 |
| Vertical opening (mm) | 14.6 | 23 | 15.1 | 34 |
| Lateral displacement in opening (mm) | 1.1 | 3 | 0.4 | 3 |
| Lateral displacement in closing (mm) | 4.0 | 9 | 3.1 | 0 |

*Figure 3-3. A tooth trajectory and its defining parameters (Xu et al., 2008).*

The Labview program (National Instruments ™ LabVIEW), written by Xu et al. (2008), to operate the robot allows for control of three parameters to produce different velocity profiles (Figure 3-4). The control parameters are: 1) Occlusal time which is the time needed for an occlusal phase; 2) Opening/closing time which is the time needed to return to the start of the next occlusal phase; 3) Occlusal angle which specifies the point at which the occlusal phase starts and ends. The control of the chewing trajectory and velocity profile allows for simulation of different jaw movements observed in human subjects.

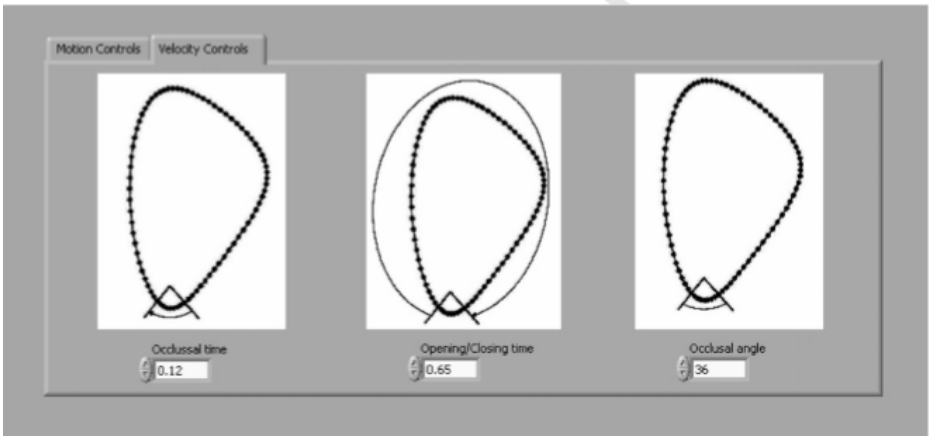


*Figure 3-4: The parameters that can be adjusted to control the velocity profile during the chewing cycle.*

The mastication robot (MR) was developed so that it could potentially be used in the following ways: (i) to prepare boluses in a reproducible way, (ii) to mimic real human chewing behaviour but is more controlled and reproducible as compared to human subjects, (iii) where it is not possible to ask human subjects to chew food unnaturally, it can be controlled to follow an unnatural trajectory (E.g. to explore how food breakdown is affected by different trajectories), and (iv) to measure the magnitude and the direction of the forces that are applied dynamically during each chew. In order to use the MR purposefully, work needs to be done to understand the operation of the MR, and how the data collected could be used to characterise breakdown during a chewing sequence.

## 3.2. Preliminary investigation

A preliminary investigation was conducted to obtain the optimised experimental and robot parameters to be used in the analysis. The variables that could be adjusted were: 1) the chewing trajectory which could be changed by adjusting the ground link; 2) the sagittal plane angle which could be adjusted by tilting the base of the six-bar linkage; 3) the baseline force which could be adjusted by changing the maxilla molar repositioning table (termed as stage height for easy reference); 4) the chewing velocity which was adjusted by changing the occlusal time, the time taken for one chewing cycle, and the occlusal angle.

Five half peanuts (2.1 ± 0.1 g) were chewed using the robot for 10 and 20 cycles without any reloading of food onto the occlusal surface. The settings were extreme lateral and vertical chewing trajectory (ground link of 50 and 38mm) with 0 degrees at sagittal plane. The stage height was set at 9.9 mm for lateral and 12.95 mm for vertical trajectory. The stage heights were adjusted to achieve the same baseline forces, i.e. the vertical force exerted by the upper teeth upon occlusion without the presence of food sample. The chewing velocity of the robot was adjusted to match the velocity profile from human measurements (Xu, Lewis, Bronlund, & Morgenstern, 2008). The opening/closing time was set to 0.65 s, occlusal time was set to 0.12 s and occlusal angle set as 36° to follow the human movement closely as observed by Ogawa et al. (2001). The 3D force profile during breakdown was recorded.

The chewed particles were collected using a vacuum device (Figure 3-5) and placed in petri dishes (ø: 150 mm) for image analysis using a protocol from Hutchings, Scott C. et al. (2012) . The vacuum device consisted of a vacuum cleaner attached to a Schott bottle which had two openings, one for the vacuum to be delivered (outlet) and other for the particles to be sucked into the bottle (inlet). Filter paper was used to cover the opening of the outlet to prevent particles from being sucked into

the vacuum cleaner. After each collection, the particles were emptied out of the bottle using a brush.

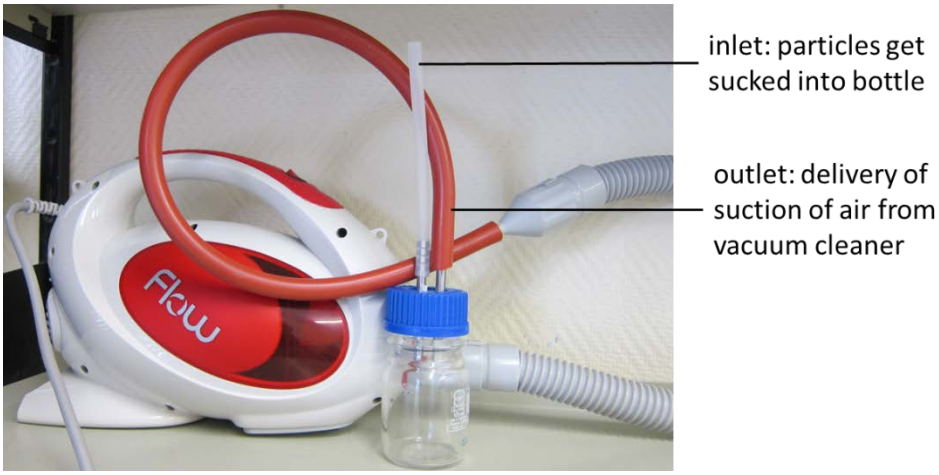


*Figure 3-5: The vacuum device used to collect chewed particles had an outlet tube providing the air suction from the vacuum cleaner. The outlet was covered by filter paper which allowed the particles to be trapped in the bottle.*

The particles were separated using a plastic spatula and by gently shaking the petri dish horizontally on a flat surface. Digital photographs of the particles were taken at 800 dpi using a flat bed scanner (Epson Perfection, 3490, Photo) and processed using ImageJ®. The colour images were converted to greyscale before a black and white threshold was applied to convert the greyscale images into binary images. The number and size (area) of the particles were determined using the <Analyse Particles> command. The output from the ImageJ program (area for each counted particle) was used to create particle size distributions (PSD) based on volume. Each particle size diameter was calculated by assuming that the particles were circular to obtain the projected area diameter. The volume of particles was calculated by assuming the particles were cylindrical where the height of the cylinder was 25% of the particle diameter. The calculated volume was ± 15% of the actual volume of the peanut.

(a) (b)

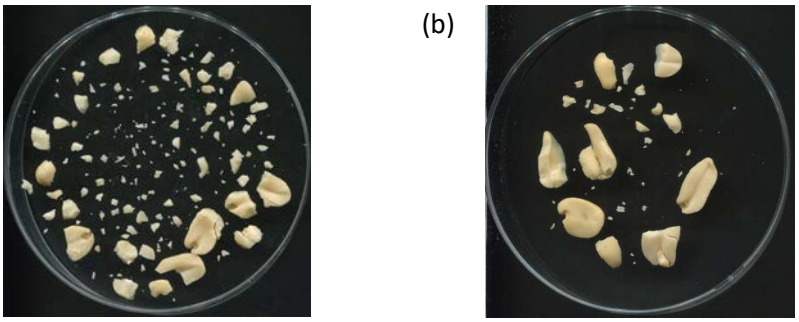

*Figure 3-6. Particles after ten lateral chewing cycles (a); and particles after ten vertical chewing cycles (b) (from left to right).*

The peanuts after 10 chews in the lateral trajectory were broken down more compared to those chewed with the vertical trajectory. This is likely to be due to the lateral shear in the lateral trajectory which makes contact with a larger area of the particles in each occlusal cycle and contributes to a higher resultant force. Some particles were not fragmented at all after ten cycles of chewing in both trajectories. It was noted that particles were pushed away from the occlusal surface after the first and second chews. Without the reloading of particles onto the occlusal surface, the particles were no longer being broken down effectively after the second chew. Only the particles that remained on the occlusal surface were continuously broken down after each cycle of chewing which accounts for the small fragments. The particles after 20 chews in the vertical trajectory (Figure 3-7a) were broken down more compared to the particles after 10 chews (Figure 3-6). In order to have more homogenous chewing of particles, the particles needed to be reloaded onto the occlusal surface between cycles, a function performed in humans by the tongue (Lucas, 2004). Mioche, L. et al. (2002) described one of the key functions of the tongue is to reposition food on the occlusal surface by pushing food laterally before each cycle of chewing.

(a)  (b) 

*Figure 3-7. Particles after 20 vertical chewing cycles without (a) and with (b) reloading onto occlusal surface (from left to right).*

In additional experiments, particles were reloaded using a spatula to push the particles back onto the occlusal surface, between every two cycles. Five half peanuts were chewed for 20 cycles with the food reloaded onto the occlusal surface after every two chews (Figure 3-7b). Figure 3-8 show that the $d_{50}$ of the chewed particles with reloading during chewing is approximately half the size of the chewed particles with no reloading. The $d_{50}$ is the theoretical sieve size (mm) through which 50% of the total projected area of the particles will pass. Thus, the efficiency of mastication significantly increased when particles were reloaded back onto the occlusal surface.

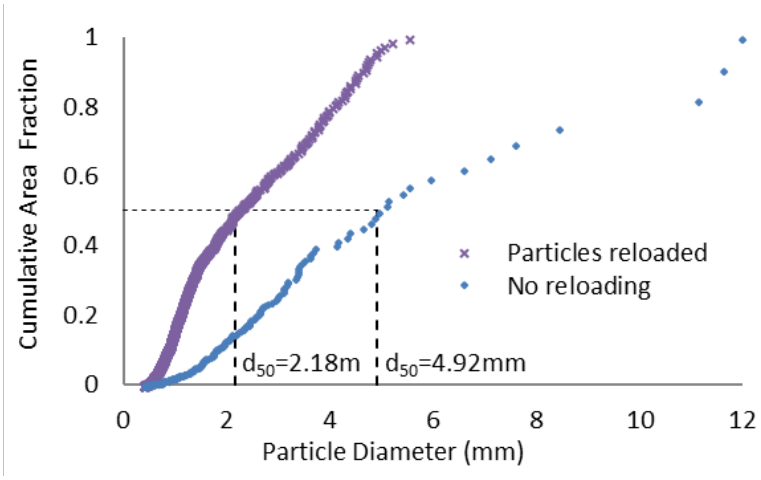


*Figure 3-8. The particle area distribution of five peanuts after 20 chewing cycles with and without reloading onto the occlusal surface. The particle diameter is the area equivalent sphere diameter.*

Figure 3-9 shows an example of the forces applied (vertical direction) during a series of 20 cycles. The first four peaks are the measurement of the baseline force (i.e. the force measured during chewing without the presence of any food particles), the fifth peak is the first chewing cycle after the peanuts were loaded. The force measured is highest at this point and reduces with increasing chews as the peanuts are broken down. As the large particles broke down in the first six chewing cycles, the force measured decreased due to the reduced compression in the spring. The decrease became more gradual as the particles broke down to a uniform and smaller particle size.

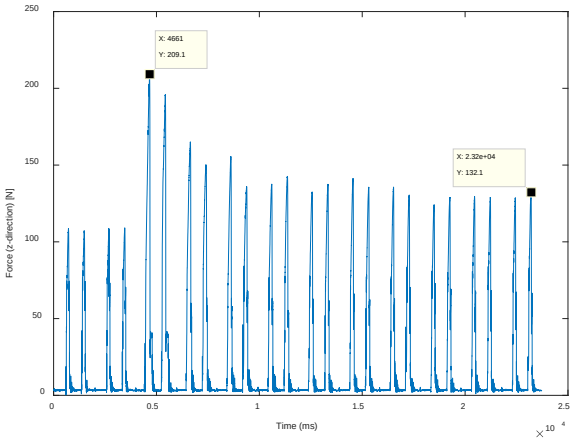


*Figure 3-9. The vertical force measured as exerted by 5 half peanuts during 20 cycles of chewing with a vertical trajectory and reloading onto occlusal surface.*

From the preliminary investigations, it was decided that the particles should be reloaded onto the occlusal surface before the next chew as most of the particles fell off the occlusal surface after one chew. The real time force measurements collected was able to track the changes in the forces needed as the peanuts were broken down, thus it could potentially be used as a method to characterise breakdown in food. The force data showed that after five chewing cycles, the changes in the force measurements were small. This suggests that much of the breakdown occurs in the initial chews, thus the PSDs of the particles should be determined at closer intervals in the initial stage of mastication, i.e. to collect samples at one, five, ten and fifteen chews instead.

## 3.3. Quantifying the rate of breakdown of peanuts using particle size analysis

Since the MR was designed to be able to chew in different chewing trajectories, one of its function would be to control the trajectory to change the particle breakdown rate. Thus, it is essential to determine if the different trajectories do influence breakdown. Single half or quarter peanuts were chewed and the 3D force profile during breakdown was recorded. The particle size distribution (PSD) of the chewed peanuts was measured by image analysis. The PSD of a chewed peanut after one cycle was used to determine the breakage function which is a measure of the fragmentation of particles into smaller size classes. Breakage and selection functions (Van der Bilt, A. et al., 1987) and the chewing efficiency (Van der Bilt, A. et al., 1992) were applied to quantify breakdown differences between the lateral and vertical chewing trajectories.

### 3.3.1. Materials and methods

In order to characterise how much the trajectory influences food breakdown, three experiments were carried out: 1) Measurement of the breakage function; 2) Vertical versus lateral chewing of single quarter nuts; and 3) Vertical versus lateral chewing of a mouthful of nuts. Similar operation parameters from the preliminary experiment were used. The length of the ground link was varied from 38 mm (vertical chewing) to 50 mm (lateral chewing) to achieve two different chewing trajectories and the sagittal plane was set such that the chewing trajectories in the sagittal plane were at an angle of 0 degrees to the horizontal plane. The opening/closing time was set to 0.65 s and the occlusal time was set to 0.12 s. Food reloading was manually done after every two chewing cycles when applicable. The 3D force profile during breakdown was recorded. Four replicates were done for each of the three chewing experiments described below.

### Experiment one:

Single half (0.45 ± 0.05 g) or quarter peanuts (0.23 ± 0.02 g) were chewed once in the lateral and vertical chewing trajectories. The stage height was set at 9.9mm and 12.95mm for the lateral and vertical trajectory, respectively.

### Experiment two:

Single quarter peanuts were chewed with lateral and vertical trajectories for 1, 5, 10, 15 and 30 cycles by the robot jaw. The stage height was set at 9.9 mm and 12.95 mm for the lateral and vertical trajectory, respectively.

### Experiment three:

Five quarter (1.1 ± 0.1 g) peanuts were chewed in lateral and vertical trajectories for 1, 5, 10 and 15 cycles by the robot jaw. The stage height was set at 9.9 mm for lateral and 12.95mm for vertical trajectory, respectively. This was repeated with chewing in the vertical trajectory at a stage height of 16.95 mm to allow similar final forces to be obtained (i.e. the vertical force exerted by the upper teeth upon occlusion with the presence of food sample).

### Data Analysis

Experimental particle size distributions can be described through fitted distribution. One such distribution commonly used for fractured particles and comminuted food is the Rosin-Rammler distribution function as in Olthoff, Vanderbilt et al. (1984), which is given by:

$$Q = 1 - exp\left[-\left(\frac{x}{x_{50}}\right)^{b} . ln2\right] \qquad \text{Eq. (3-1)}$$

where $x$ is the sieve size of a particle (mm), $Q$ is the area fraction of particles with a smaller diameter than $x$, $x_{50}$ is the median diameter taken as the sieve size through which 50% of the particle area will fall (mm), and $b$ is the slope of the cumulative area distribution curve which describes the broadness of the distribution.

A cumulative size volume was plotted against a normalised particle size ($x/x_0$) for the results obtained in experiment one where by single half or quarter peanuts were chewed once in the vertical or lateral trajectory. In the subsequent analysis of the next two experiments, the cumulative area instead of volume was used as it was discovered that the total particle volume became overestimated as the particles broke down further with increasing chews. Thus, the cumulative size

distribution of cumulative area ($mm^2$) was plotted against the particle size diameter (mm) and each distribution was fitted to a Rosin-Rammler function as shown in Equation (3-1). The $x_{50}$ and b values obtained were used to compare the distributions from the different multiple chewing cycles.

One of the main objectives was to investigate the effect of trajectory change on the particle breakdown rate. Data from the PSD of particles collected after one chew (experiment one) was used to explain the breakage. The breakdown of food is dependent on the selection and breakage process of food particles. A comminution model using the selection and breakage functions in a matrix algebra has been used to model the particle size distribution of particles after various number of chewing cycles (Van der Bilt, A. et al., 1987). The comminution matrix is built from a selection and breakage matrix which is constructed from the variables of the selection and breakage functions (Equation 3-2 and 3-3).

The selection chance for breakage of a food particle is dependent on its size and is described by a power-law relationship (Lucas & Luke, 1983; Van der Glas et al., 1987):

$$S(x) = vx^w \qquad \text{Eq. (3-2)}$$

where *S(x)* is the fraction of particles of size $x$ that are selected, $v$ is the chance of selecting a particle with a size of $x$ *mm* and $w$ determines how strongly the selection chance depends upon particle size.

The fraction of fragments of the selected food particle that are formed by breakage is described by a cumulative distribution function (Van der Glas et al., 1987):

$$B(x) = 1\ (1 + r\frac{x}{x_0})(1 - \frac{x}{x_0})^r \qquad \text{Eq. (3-3)}$$

where *B(x)* is the fraction of particles produced below size $x$, $x_0$ is the original particle size, and $r$ is the degree of fragmentation. A larger $r$ indicates better fragmentation.

The breakage function was determined from particle size distributions obtained from experiment one. A cumulative size volume was plotted against a normalised particle size ($x/x_0$). Each distribution was fitted to a breakage function as shown in Equation (3-2). The particle size distributions of the chewed particles after multiple chews were used to determine the selection function (Equation 3-2). The selection function was obtained by finding the $v$ and $w$ values which gave the best fit (minimum residuals) for the particle size distributions using Solver in Excel. The average selection and breakage fractions were used in the comminution model.

Another approach for describing the breakdown is using the chewing efficiency. Van der Bilt, A. et al. (1992) characterised chewing efficiency by the number of chewing cycles needed to reduce the original particle size by half, $N_{1/2\text{-}Xo}$. This was done by fitting a 2nd order polynomial function to the non-linear initial part of the *log(x50)-log(N)* relationship and interpolating the value of $N_{1/2\text{-}Xo}$. The $x_{50}$ were obtained from the Rosin-rammler fits for the PSD of the particles collected from the chewing cycles (N=1, 5, 10, 15) for each chewing trajectory (experiment three).

### 3.3.2. Results and Discussion

Figure 3-10 shows the cumulative volume fraction after one chew cycles for peanuts. The lateral chewing produced a higher volume fraction of particles smaller than half their original size after the first chew. The $x_{50}$ of the PSD after one chew in the vertical trajectory is about 23% larger than that of the one in the lateral trajectory for the half peanut and 17% larger for the quarter peanut. The distribution for the half peanuts chewed in the vertical trajectory was smaller (larger b value) than that for the lateral trajectory, indicating that there was a broader spread in the distribution of small and large particles chewed using the lateral trajectory (Table 3-1).

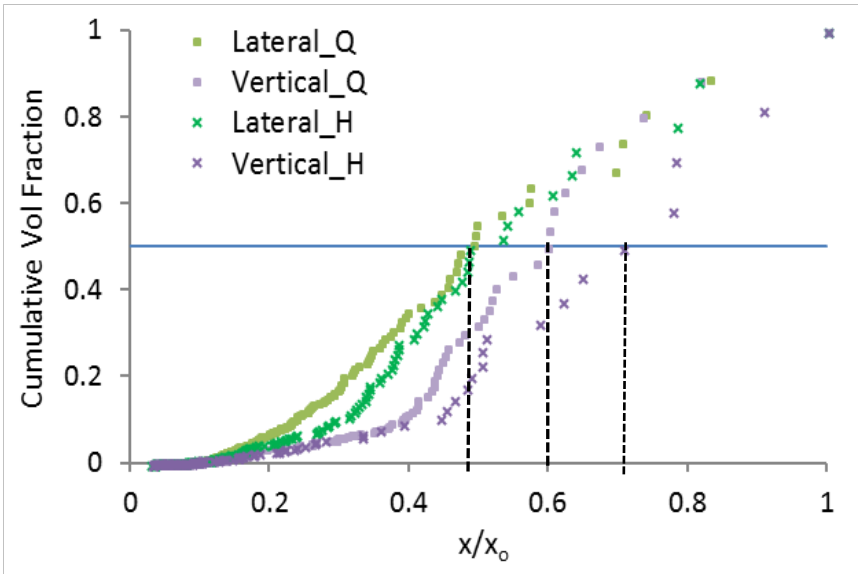


*Figure 3-10. Cumulative volume fraction of selected particles that break down into particles smaller than size $x$ where $x_0$ is the initial size.*

*Table 3-1.The $b$ and $x_{50}$ obtained from the Rosin Rammler fit, after one chew of a single peanut for different initial peanut sizes and chewing trajectories.*

| Chewing Trajectory | Initial Peanut Size | $b$ (broadness of distribution) | $x_{50}$ (mm) |
|---|---|---|---|
| Lateral | Quarter | 2.12 ± 0.11 | 3.30 ± 0.18 |
| Vertical | Quarter | 2.15 ± 0.11 | 4.01 ± 0.17 |
| Lateral | Half | 2.23 ± 0.22 | 5.12 ± 0.18 |
| Vertical | Half | 3.04 ± 0.83 | 7.04 ± 0.26 |

A two-way ANOVA was used to examine the significance of the differences in the $x_{50}$ between different trajectories and different initial particle sizes. The differences in the $x_{50}$ were significant ($P < 0.05$) for both the trajectory and the initial peanut particle size (Table 3-2), indicating that the lateral trajectory was more effective in breaking down the peanuts. There was a significant interaction between the effects of chewing trajectory and initial peanut size. The effect of the trajectory on the $x_{50}$ is more evident when the initial peanut size used is the half peanut. This suggests that as the peanut size gets smaller, the difference in particle breakdown due to the different trajectories is reduced.

*Table 3-2.* Two-way ANOVA results used to assess the significance of the differences in the $x_{50}$ between the chewing trajectories, the initial peanut size and the interactions between the two.

| Source of Variation | SS | DF | MS | F-value | P-value |
|---|---|---|---|---|---|
| Trajectory | 6.970 | 1 | 6.969 | 38.07 | 0.000 |
| Initial size | 23.471 | 1 | 23.471 | 128.19 | 0.000 |
| Trajectory*Initial size | 1.474 | 1 | 1.474 | 8.05 | 0.015 |
| | | | | | |
| Within | 2.197 | 12 | 0.183 | | |
| Total | 34.112 | 15 | | | |

Figure 3-11a shows that the $x_{50}$ of the quarter and half peanuts for both trajectories converge as the particles breakdown with increasing chews. The vertical trajectory had better breakdown efficiency in the first 10 chews as compared to the lateral trajectory. One-way ANOVA (Table 3-3) was used to assess the significance of the differences in the $x_{50}$ between different trajectories. There was a significant difference ($P < 0.05$) between the $d_{50}$ of peanuts chewed in lateral and vertical trajectories after 1, 10 and 15 chewing cycles. The difference between the lateral and vertical trajectories after 5 chewing cycles was not significant due to the large standard deviation within the $x_{50}$ of the peanuts chewed in the vertical trajectory. After 30 chews, there was no significant difference ($P > 0.05$) between the $x_{50}$ of peanuts chewed in lateral and vertical trajectories, which indicates that after the particles have broken down to a certain size, the different trajectories no

longer have an effect on the rate of breakdown. There is significant difference ($P < 0.05$) between the $x_{50}$ of the half and quarter peanuts after 30 chews which indicate that a larger initial particle size has a faster rate of breakdown. Although the $x_{50}$ of the half peanuts were much larger than the quarter peanuts after the first chewing cycle, it was almost the same after 30 chewing cycles. Thus, the rate of break down is higher with the larger particles, which indicates that there is a higher selection frequency for particles and results in more efficient break down.

The variable $b$ is a Rosin Rammler equation parameter that indicates the broadness of the distribution of particle sizes. Figure 3-11b shows the broadness depends on the number of chewing cycles. The broadness of the distributions after one chew is similar for both trajectories. Although the b value increased significantly with the number of chews for both trajectories, the distributions generated by lateral chewing had a smaller spread in particle size.

(a)

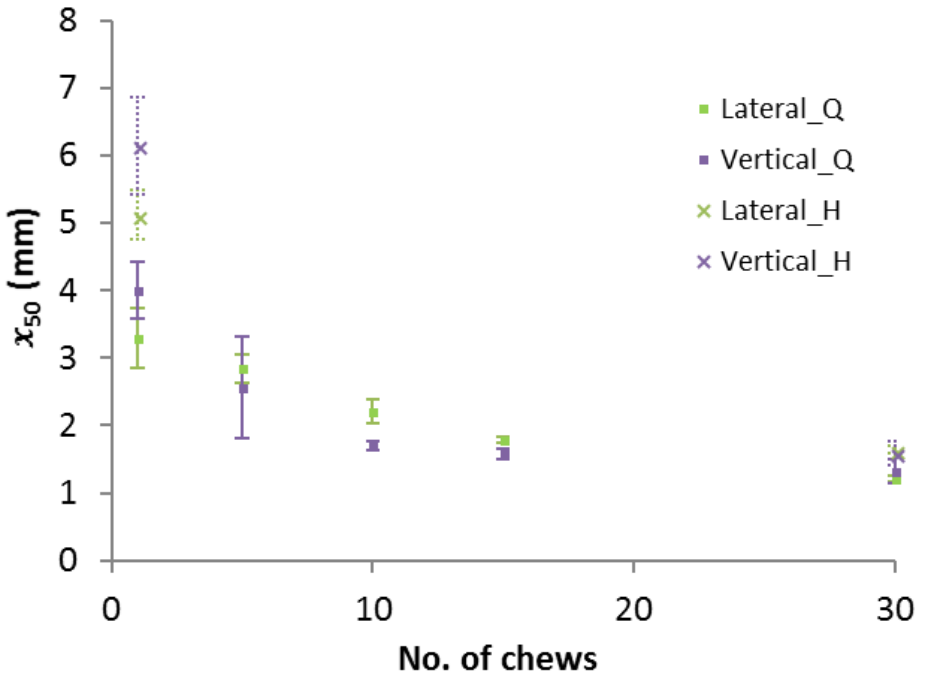


(b)

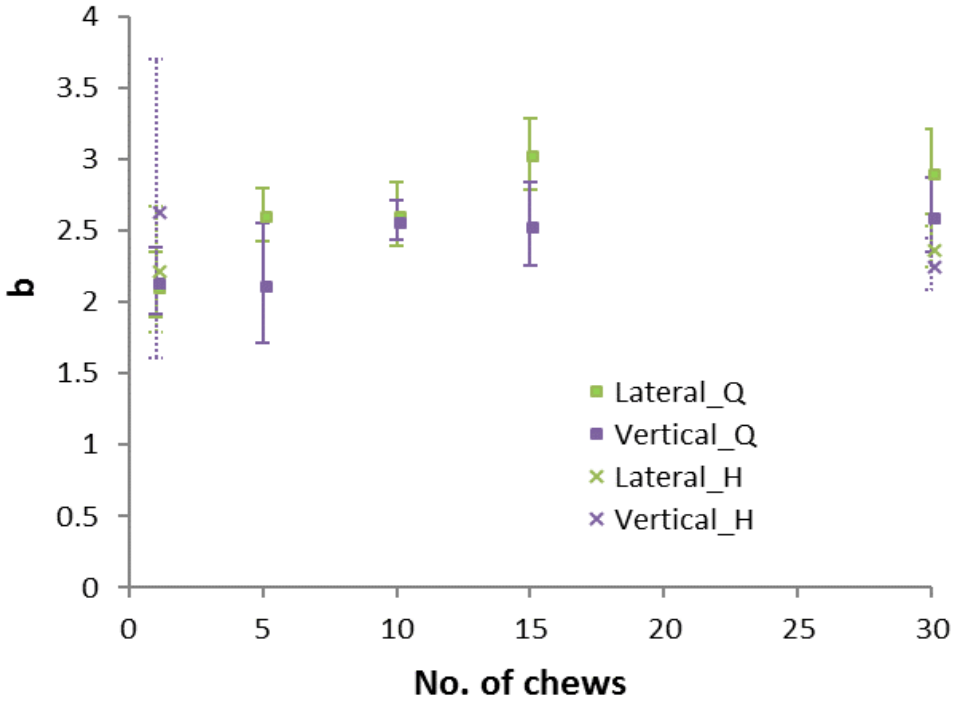


*Figure 3-11. The $x_{50}$ and $b$ values from the Rosin-rammler fits of the peanut particles after different number of chewing cycles for single quarter peanuts and half peanuts in the lateral and vertical chewing trajectories. The error bars represent the standard deviation.*

*Table 3-3: One-way ANOVA results used to assess the significance of the differences in the $x_{50}$ between the lateral and vertical chewing trajectories after 1, 5, 10, 15 and 30 chewing cycles.*

| | Source of Variation | SS | DF | MS | F-value | P-value |
|---|---|---|---|---|---|---|
| After 1 chew | Between Groups | 1.016 | 1 | 1.016 | 6.103 | 0.048 |
| | Within Groups | 0.999 | 6 | 0.167 | | |
| | Total | 2.016 | 7 | | | |
| After 5 chews | Between Groups | 0.168 | 1 | 0.168 | 0.415 | 0.544 |
| | Within Groups | 2.426 | 6 | 0.404 | | |
| | Total | 2.593 | 7 | | | |
| After 10 chews | Between Groups | 0.490 | 1 | 0.490 | 20.524 | 0.004 |
| | Within Groups | 0.143 | 6 | 0.024 | | |
| | Total | 0.633 | 7 | | | |
| After 15 chews | Between Groups | 0.087 | 1 | 0.087 | 15.835 | 0.007 |
| | Within Groups | 0.033 | 6 | 0.006 | | |
| | Total | 0.120 | 7 | | | |
| After 30 chews | Between Groups | 0.019 | 1 | 0.019 | 0.824 | 0.399 |
| | Within Groups | 0.137 | 6 | 0.023 | | |
| | Total | 0.156 | 7 | | | |

The differences observed may be due to the breakage and selection function for the different trajectories. The different shapes of the teeth affect the breakage and the different chewing trajectories affect the selection of the particles. We would expect the trajectory to influence the rate of particle breakdown, because of the difference in the forces applied. A shear force is applied in the lateral trajectory while a vertical force is applied in the vertical trajectory. The shape of the teeth serves to trap the particles, and this increases the selection chances. The use of the texture analyser to simulate breakdown would not have all these variations. The MR is able to adjust these parameters and allow study on how these parameters influence the breakdown rate. Thus, these two measures could potentially be used to explain the difference in the particle breakdown. The term '$r$' could be used to describe the degree of fragmentation (Equation 3-3) while '$v$' and '$w$' could be used to quantify the selection chances (Equation 3-2). Table 3-4 shows the degree of fragmentation after one chew of quarter and half peanuts in the lateral and vertical trajectories. The degree of fragmentation '$r$', was larger for lateral chewing than for vertical chewing. The degree of fragmentation also became smaller as the initial particle size increased. The vertical force exerted on the lateral half and lateral quarter were 181 N and 154 N respectively. Although the overall force exerted on the half peanut was larger, the area that force is exerted on in the quarter peanut is smaller. Thus, there is a larger pressure exerted on the quarter peanut. The degree of fragmentation was greater when the pressure exerted was larger.

*Table 3-4: The breakage function after one chew of a single peanut for different initial peanut sizes and chewing trajectories.*

| Chewing Trajectory | Initial Peanut Size | $r$ (degree of fragmentation) | $x_{50}$ (mm) |
|---|---|---|---|
| Lateral | Quarter | 1.74 ± 0.12 | 3.30 ± 0.18 |
| Vertical | Quarter | 1.45 ± 0.18 | 4.01 ± 0.17 |
| Lateral | Half | 1.49 ± 0.25 | 5.12 ± 0.18 |
| Vertical | Half | 0.70 ± 0.27 | 7.04 ± 0.26 |

Van der Bilt et al. (1987) had used a comminution model using the selection and breakage functions to model the particle size distribution of particles after various number of chewing cycles. The original particle size of the quarter peanut (9.5 ± 0.5 mm) was reduced to about 50 % after the first chew (Figure 3-12). The breakdown comminution model was fitted to the data using Solver function (Microsoft Excel) producing Model L and V as the predicted data and the respective breakage functions. The degrees of fragmentation, $r$, were 1.7 and 1.4 and the selection frequencies, $v$, were 0.21 and 0.33 for lateral and vertical chewing respectively and $w$ was 2 for both. The $x_{50}$ was compared between the model and experimental data. Figure 3-12 shows the model gave a good fit. Although the breakage function for the lateral trajectory was more efficient at size reduction, this was offset by a lower selection frequency.

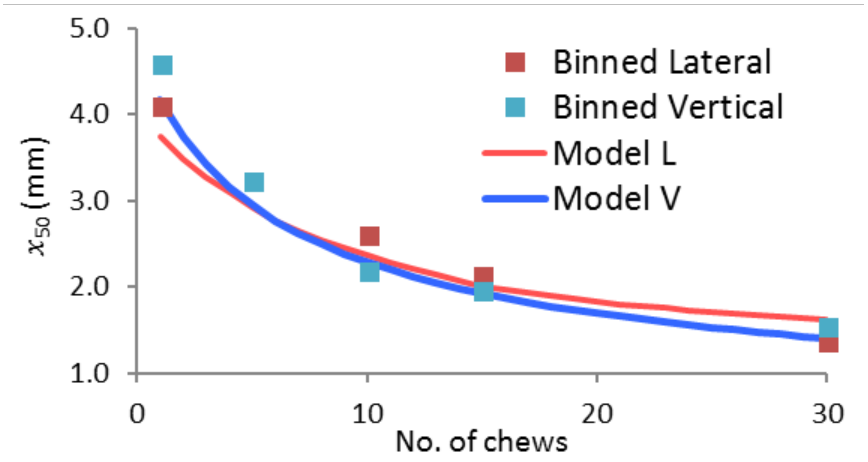


*Figure 3-12. The $x_{50}$ of the particle volume distributions at 1, 5, 10, 15 and 30 chews for quarter sized peanuts.*

Figure 3-13 shows that a larger loading size results in larger particles after one chew. This indicates that there is a limitation on the amount of fragmentation when the entire occlusal surface is occupied with particles. The $x_{50}$ of the chewed single quarter peanut was 3.1 mm while that of the five quarter peanuts was 6.4 mm. The force measured during the breakdown was 144.5 N for the loading of five quarters while that for a single quarter was 131.2 N. The force is larger for the loading

of five peanuts as it has to overcome a greater resistance in order to fracture. However, the force per unit area exerted on the single peanut is larger due to a smaller area as compared to the loading with five peanuts; this explains the greater breakdown of particles in the loading with single peanut. The larger degree of fragmentation (Table *3-5*) in the single loading size is in agreement with the particle size distributions.

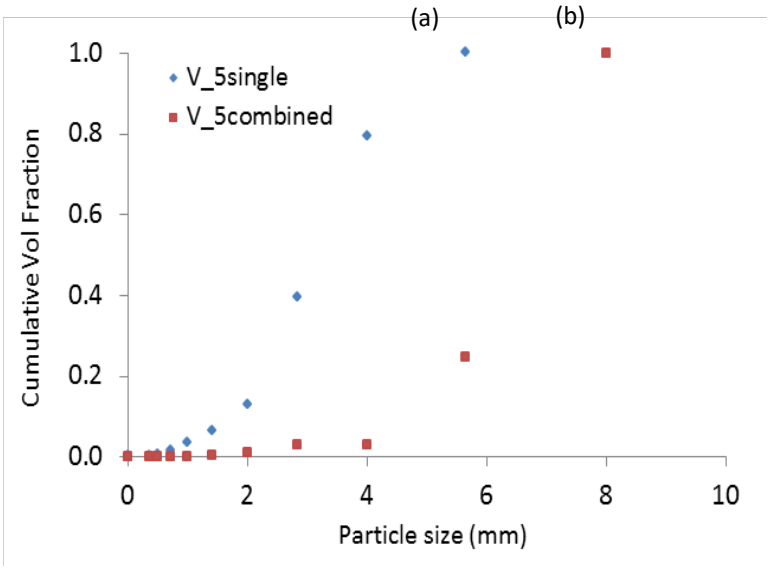


*Figure 3-13. The particle size distribution of two different loading sizes after one chew in the vertical trajectory: (a) five replicates of single quarter peanut and (b) five quarter peanuts chewed simultaneously.*

Table 3-5. The mean breakage function and mean $x_{50}$ of quarter peanuts after one cycle of chewing in the vertical trajectory for the different loading sizes.

| Loading Size | $r$ (degree of fragmentation) | $x_{50}$ (mm) |
|---|---|---|
| Single | 1.5 | 4.01 |
| Five | 0.4 | 6.24 |

Solver was used to determine the following terms by fitting equations (3-2) and (3-1) to the data collected for the breakdown of the five quarter sized peanuts. The degrees of fragmentation, $r$, were 0.7 and 0.4 and the selection frequencies, v, were 0.40 and 0.70 for lateral and vertical chewing respectively and $w$ was 1 for both. The $x_{50}$ of the distribution from the lateral chewing reduced faster as compared to the vertical chewing (Figure 3-14). Although the selection was poorer for the lateral chewing trajectory, the degree of fragmentation seemed to be more important in influencing the breakdown when the loading size was increased.

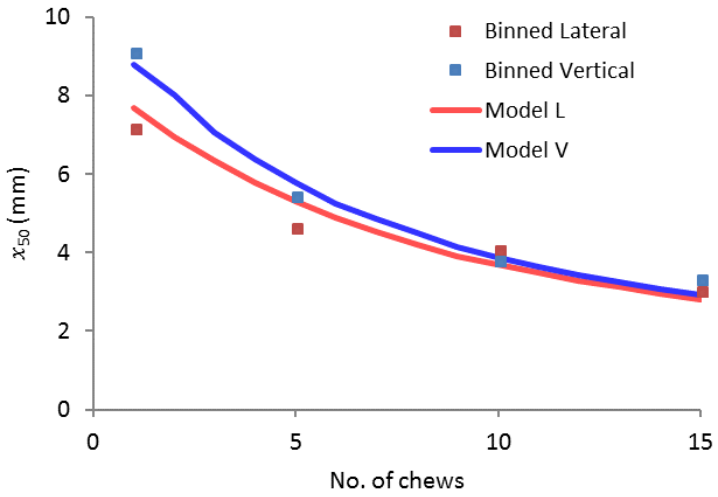


*Figure 3-14. The $x_{50}$ of the particle volume distributions at 1, 5, 10, and 15 chews for five quarter sized peanuts.*

The $x_{50}$ of the distributions for five quarter size peanuts had reduced by 52 % and 60 % after 15 chews as compared to 53 % and 58 % for the single quarter peanut in the lateral and vertical trajectory. Although the degree of fragmentation is lower with a larger loading size, the chance of the particles being selected is decreased as the particles get smaller (Van der Glas et al., 1987). The breakdown of the quarter peanut had plateaued after its particles were small enough such that they were no longer efficiently selected for fragmenting. Thus, after a certain number of chews, the reduction in the $x_{50}$ of the distributions were not statistically different for the two loading sizes.

The degree of fragmentation, $r$ is dependent on the pressure exerted on the peanut particles (Pearson's correlation coefficient, r=0.67). Higher pressure exerted resulted in more fragmentation of the peanuts (Figure 3-15). This result agrees with work done by Engelen et al. (2005) who concluded that higher chewing forces consequently resulted in better chewing efficiency as indicated by the smaller median particle size. The pressure exerted on the single quarter peanut is higher as the force is exerted over a smaller area compared to five peanuts. The five quarter peanuts chewed with a higher stage height (16.5 mm) for the lower jaw had a higher pressure exerted as the spring was compressed more. Thus, increasing the stage height setting achieves a higher biting force and resulted in a distribution with smaller particles.

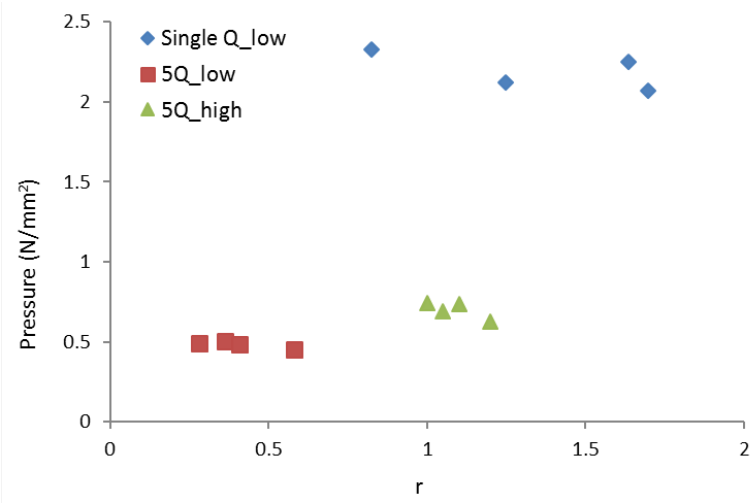


*Figure 3-15. The relationship between the pressure exerted and breakage variable, r for the loading of single and five quarter peanuts after one chew in the vertical trajectory.*

The chewing efficiency as proposed by Van der Bilt, A. et al. (1992) is an alternative method to compare the breakdown between the lateral and vertical chewing trajectories. Since half of the initial particle size is 4.48mm, the number of chewing cycles needed to reduce the original particle size by half, $N_{1/2\text{-}Xo}$ was determined by substituting $y$=log(4.48) for both the equations in Figure 3-16 and solving for $x$. The number of chews needed to reduce the particle size of the peanuts by half was 6.5 and 7.1 chews for lateral and vertical trajectory respectively. Thus, the lateral trajectory was more efficient in the breakdown which agrees with the finding that the lateral trajectory provided better breakage as compared to the vertical trajectory.

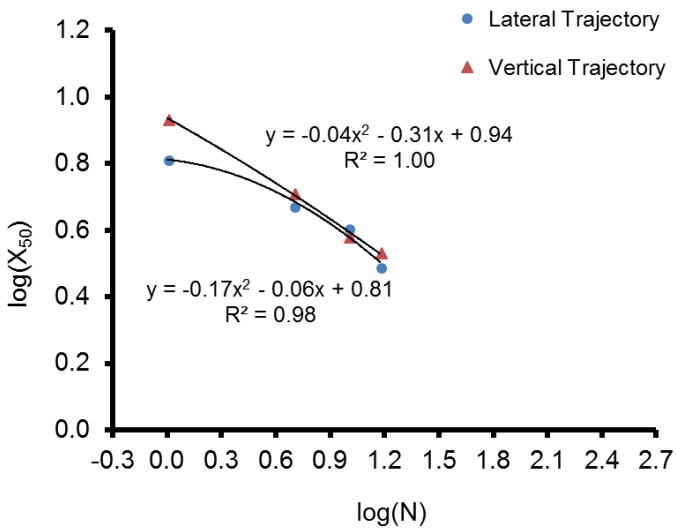


*Figure 3-16: The log($x_{50}$)-log(N) relationship for both the lateral and vertical chewing trajectories.*

From these series of experiments, it was found that both the selection of particles and their breakage are affected by trajectory. This is useful to understand the breakdown in brittle foods where particle size analysis is employed. It was shown that the MR can be used to study how different chewing parameters such as the trajectory can influence particle breakdown since these parameters can be controlled.

Three approaches of describing the breakdown were employed. The $x_{50}$ and $b$ values obtained from the fitting of the Rosin-rammler function to the distribution described the PSD well. The comminution model was good, but it required having to determine the breakage and selection function before input into the model. The chewing efficiency served as a simple way of characterising breakdown by using particle size analysis. It is useful but it may not be suitable for brittle foods that get halved within the first chew.

## 3.4. Force Data as a tool to measure breakdown

Particle size analysis of chewed peanuts has shown that the lateral chewing trajectory resulted in a higher breakage function. Sun (2012a) also demonstrated that lateral chewing (compressive shear) was more effective for the breakdown of peanuts compared to vertical chewing (compression). The 3D force profiles recorded dynamically throughout the breakdown process could provide an insight into how the magnitude of the forces and the directions in which they are applied differ between chewing trajectories.

### 3.4.1. Preliminary Analysis of the Force Data

Figure 3-17 shows an example force vs time cycle occurring during a single chew of peanut particles (the first two cycles are for occlusion of the teeth with no food). The chewing force acting on the food in the X, Y, and Z-axis were the shearing force in the sagittal plane, shearing force in the frontal plane and vertical downward force respectively. The chewing force indicated by the black line is the magnitude of the resultant force. Both trajectories resulted in a large vertical downward force acting on the food, although there is significant shearing force in the frontal plane for the lateral trajectory. Although the maximum vertical force (Z direction) is similar for the baseline forces in both trajectories, it increased more for the lateral trajectory when food is present. This contributes to a larger resultant force which explains why the breakage function of peanuts in the lateral trajectory is higher.

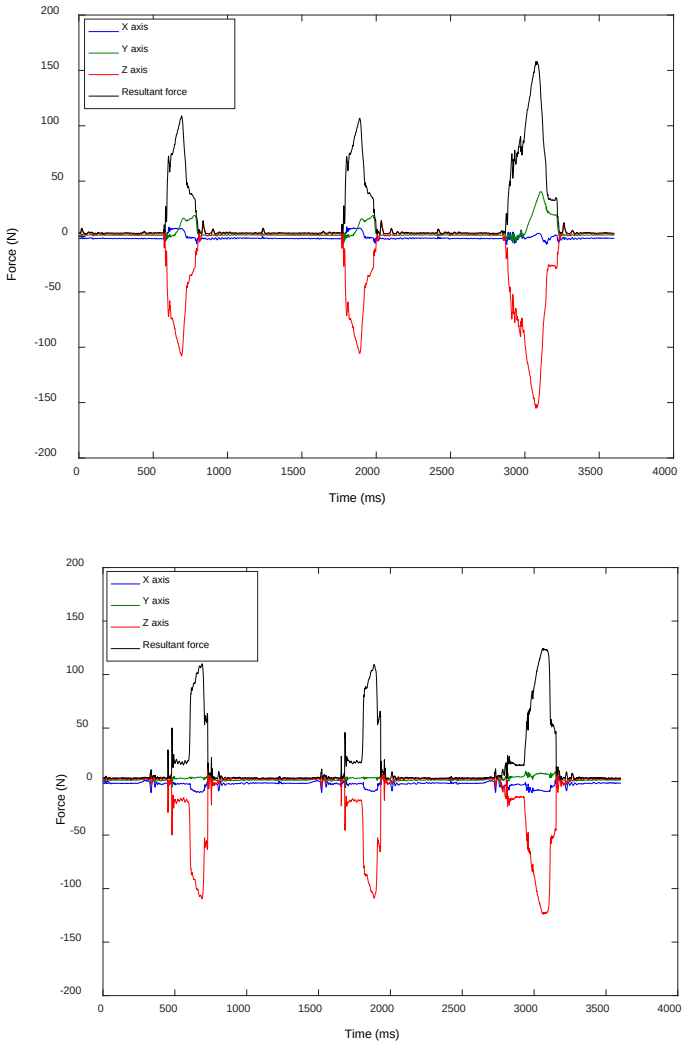


*Figure 3-17.The force profiles of two baseline chews followed by a chew of a single quarter peanut in the lateral and vertical trajectory (from top to bottom).*

The force profile data of one chewing cycle of single quarter peanuts and five quarter peanuts were analysed from the experiment with the vertical trajectory and stage heights of 12.95 mm and 16.95 mm. Before each food sample was loaded onto the occlusal surface, a single chew was done to obtain the baseline force. The force profiles of the two baseline forces for each stage height show a similar pattern in terms of their profile shape (Figure 3-18). The baseline measurements of the chewing cycles in Table 3-9 have little variation (< ± 5%) and thus there is have good repeatability. With increased stage height, the forces increased at an earlier time during the chewing cycle and resulted in a larger baseline force. This is expected as the spring experiences a greater displacement.

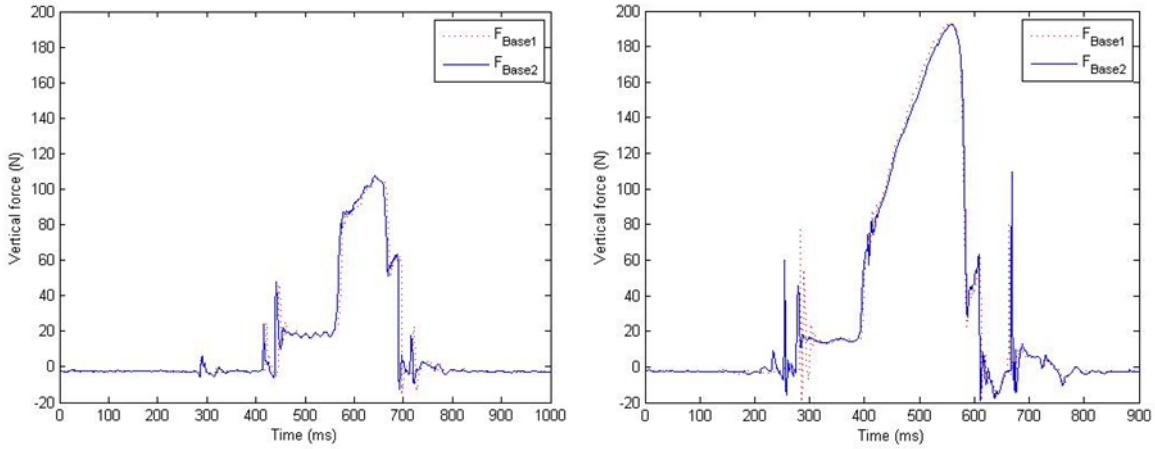


*Figure 3-18. The force profiles of two vertical chews without any food particles (i.e. baseline force) at stage height of 12.95 mm and 16.95 mm (from left to right).*

The increase in the force starts earlier when there is food present as the upper teeth meet resistance earlier in the chewing cycle (Figure 3-19a), further increasing the spring compression. There are multiple small peaks as the force increases indicating that there is some fracturing in the peanut before it reaches a peak force at 123.4 N. The baseline force was subtracted from the force profile of the chew with the peanut to obtain the resistance of the peanut exerted on the force sensor as seen in Figure 3-19b. The increase in force measured due to the peanut was 72.94 N.

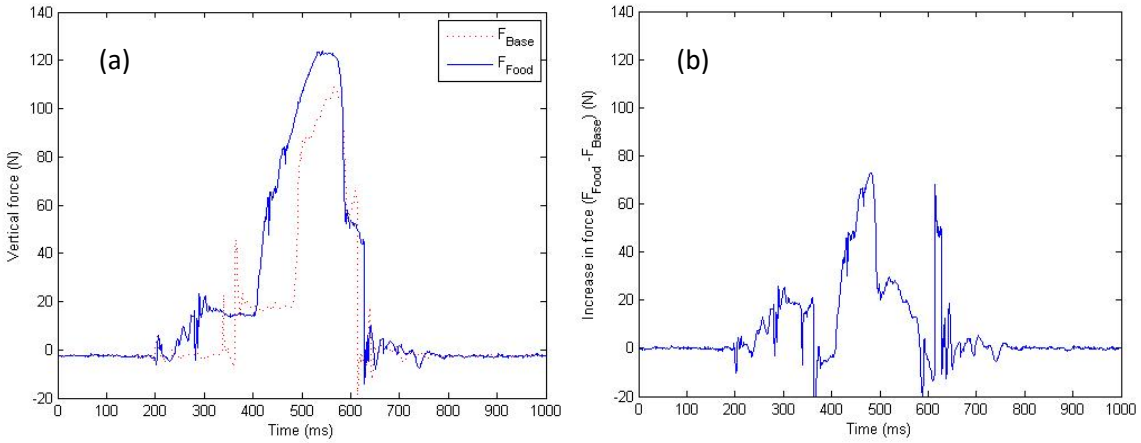


*Figure 3-19. (a) The force profile of the baseline force (red dotted line) and the total force (blue line) measured during a vertical chew of a single quarter peanut. (b) The increase in force measured due to a single quarter peanut during a chewing cycle, i.e. the total force minus the baseline force.*

The mastication robot was developed as a tool to simulate mastication in a more representative manner than traditional food characterisation methods. To demonstrate this, it was essential to compare the breakdown by the mastication robot with a current test method. For example, real chewing movements are three dimensional but current test methods involve mostly one dimensional-large deformations. The Texture Profile Analysis (TPA) (Bourne, M. C., 2002) is a two-

step compression test commonly used to measure the texture of a food by simulating the first two bites taken during chewing of the food. In this study, a single compression was carried out on a single quarter peanut. Four replicates of peanut samples were compressed by a flat cylinder attachment (ø: 50 mm) up to a strain of 95%, at a pre-test and test crosshead speed of 1 mm $s^{-1}$ and a trigger force of 0.1 N using the TA-XT plus texture analyser. Similarly, a single quarter peanut was chewed once by the mastication robot in a vertical trajectory. The forces during breakdown and the $d_{50}$ of the particle size distribution collected from both techniques were compared.

Figure 3-20 shows the force deformation profile of a single quarter compressed to 90% strain. Although the peanut fragmented into smaller pieces initially shown by the multiple fracture peaks, the peanut particles were subsequently flattened instead of being fragmented shown by the smooth increase in force after 50% strain. This required extremely high forces that exceeded 300 N; much higher than the usual bite force applied by humans (Anderson, D. J., 1956; Gibbs et al., 1981). There are multiple fractures along the curve and this is similar to the force profile of the peanut chewed by the mastication robot.

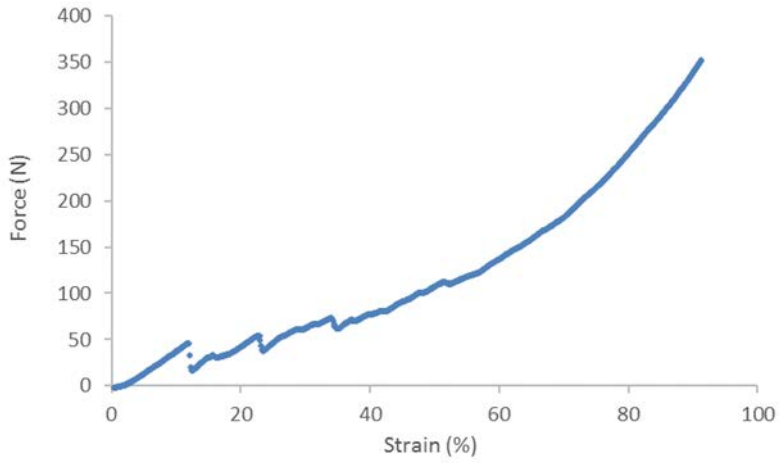


*Figure 3-20. An example of the force deformation profile in which the force measured was plotted against the distance travelled by the probe as it crushed the single quarter peanut.*

The first fracture in the force-time curve for the compression by the texture analyser was at a force of 44.4 N (± 9.77) while the first fracture in the force-time curve at which the teeth were coming into maximum occlusion for the mastication robot was at a force of 53.4 N (± 10.7) (Figure 3-19b). It was noted that there were more fractures in the force profiles of the mastication robot and this was supported by a higher number of particles as compared to the compression by the texture analyser (Table 3-6). The differences in the magnitudes of the forces measured may be due to differences in particle deformation between the two instruments. The deformation in the texture analyser is fixed,

but in the mastication robot, the deformation is changing with response to fracture. The mastication robot had a smaller standard error obtained for the average maximum peak force measured, thus it had better repeatability as compared to the texture analyser. In addition, the particle size distributions of the particles broken down by the mastication robot was smaller than those compressed by the texture analyser (see comparison of the respective $d_{50}$). This may be due to shape of the teeth which allows better efficiency of breaking the food down in the first bite, thus the particles are more homogenous and the maximum forces measured are more similar in the mastication robot.

*Table 3-6. The average maximum force, number of particles and $d_{50}$ (± SE) measured for one chewing cycle or one compression for a single quarter peanut where four replicates were conducted for each.*

| Equipment | Average Force (N) | No. of particles | $d_{50}$ (mm) |
|---|---|---|---|
| Mastication Robot | 131.1 ± 3.64 | 59 ± 3 | 4.01 ± 0.22 |
| TA-XT plus texture analyser | 369.6 ± 58.38 | 35 ± 6 | 5.09 ± 0.11 |

### 3.4.2. Determination of Spring Constant

A spring system had been incorporated on the mandible of the mastication robot to ensure that the upper and lower teeth are able to maintain contact throughout occlusion. The four-bar linkage mechanism prescribes an elliptical motion, ensuring the entry and exit trajectories of an occlusion are correct. The more intricate trajectory during occlusion is dependent on the teeth shape, where the opposing teeth prescribe a glide path where the teeth rub over each other. A spring is used to allow these deviation from the overall elliptical pathway. The force applied by the spring depends on its compression, but this can be adjusted to ensure teeth contact during occlusion. The full deformation of the food to allow true occlusion may not always occur. During chewing, the robot must provide enough force to deform the food such that the set occlusal trajectory may be achieved. Sun (2012) demonstrated the use of a pretightening plate to adjust the initial spring compression displacement to provide different initial force depending on the desirable force profile required during occlusion for different foods. The amount of force exerted during occlusion is dependent on the extent of spring compression. To understand the relationship between the forces exerted and the extent of spring compression, the spring constant was determined.

Static measurements were done by setting the upper teeth to be perfectly occluded with the lower teeth and with 40N of force applied by the upper teeth. This was taken to be the spring displacement reference position (0 mm). The stage on which the lower teeth were mounted on was at a stage height of 8.95mm. The experiment was carried out with the upper and lower teeth fully

occluding throughout. The lower teeth were then by raised from the reference position to a series of defined displacements as shown in Figure 3-21. The Z-direction force measured using the 3-D force sensor was a result of the increase in spring compression. The slope of the plot of force against spring displacement gives the spring constant. The equation of the fitted line was $y = 15.279x + 42.624$, thus the spring displacement was determined to be 15.3 N/mm.

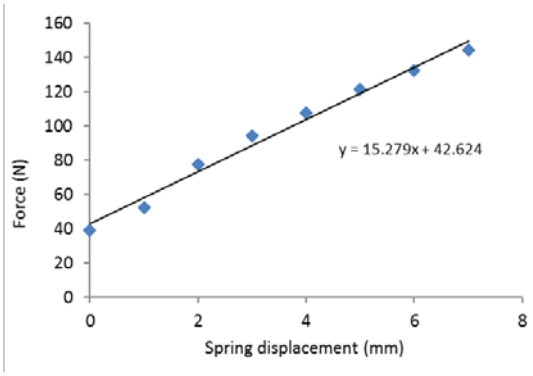


*Figure 3-21. The forces measured as the lower teeth was raised up from 0 to 7 mm.*

A chewing experiment was conducted to measure the displacement of the spring during the first chewing cycle of a single quarter peanut. The stage height with the lower teeth was set to 12.95 mm and a GoPro Hero4 (GoPro, Inc., California, US) camera was used to record the chewing cycle at 60 frames per second. The video was analysed and the frame showing the upper and lower teeth at maximum occlusion before the peanut fragmented was selected for image analysis. ImageJ® (1.48q, National Institutes of Health, USA) was used to measure the distance between the upper and lower teeth. This distance is equivalent to the spring displacement determined by the thickness of the particle being chewed. Four replicates were carried out and the experiment was repeated with half peanuts. Before each sample was loaded, the base force exerted by the upper teeth during occlusion was measured.

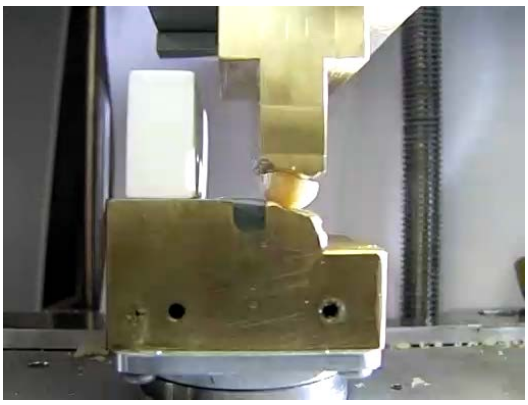

*Figure 3-22: Example of the frame selected for image analysis which shows the upper and lower teeth at maximum occlusion before the peanut was fragmented.*

*Table 3-7. The summary of the average thickness, maximum force, and ΔF (± SE) were collected from the experiment while the predicted thickness of peanut and percentage difference were calculated using the spring constant.*

| Size of Peanut | Average Thickness of Peanut (mm) | Average Maximum Force (N) | Average ΔF (N) | Predicted Thickness of Peanut (mm) | Percentage Difference (%) |
|---|---|---|---|---|---|
| Quarter | 3.30 ± 0.3 | 128.3 ± 4.8 | 86.6 ± 5.2 | 2.88 | 13.1 |
| Half | 3.60± 0.5 | 159.8 ± 3.3 | 106.9 ± 9.1 | 4.21 | 16.8 |

The ΔF was determined by subtracting the baseline force from the force measured during the chew as explained previously in Figure 3-19. From this force, the thickness of the food sample was formed using the spring constant equation and solving for *x.* From the average ΔF in Table 3-7, it is found that the predicted maximum thickness of peanut ((86.6 – 42.624) ÷ 15.279 N/mm) = 2.88 mm) which agrees with the experimental data measured using the video analysis. Thus, the food resistance obtained from the force sensor results from the spring compression during occlusion. This indicates that the spring compression is dependent on the particle thickness. A thicker particle would result in a greater compression in the spring which causes a larger force to be exerted on the particle. The lower teeth and the thickness of the food sample on the occlusal surface may cause the upper teeth to have some deviation from the set trajectory, for example tough foods that do not fracture easily. The determination of the spring constant allows for calculation of the gap between the occlusal surfaces due to the thickness of the food before it breaks down. Information such as the maximum point of occlusion and the exact trajectory of the upper teeth, which is influenced by the properties of the food, during the chew can be determined.

### 3.4.3. The effect of trajectory, initial food loading size and lower teeth table height on the force measurement during the first chew

The force data collected from the chewing experiments was analysed to understand how the forces changed with respect to the chewing trajectory, lower teeth stage height settings, and the initial food loading size. The factors varied are detailed in Table 3-8 and results summarised in Table *3-9*. $F_{peak}$ is the peak force before the first fracture occurred ($F_1$); ΔF is the increase in force due to food obtained by subtracting the base force from the peak force; Impulse is the area under peak

force; ΔImpulse is the increase in impulse due to the food; Δx is the increase in spring displacement due to the food.

*Table 3-8: Summary of factors that were varied to understand their effects on the resulting forces measured.*

| **Factors** | **Variation 1** | **Variation 2** | **Variation 3** |
|---|---|---|---|
| **Chewing trajectory** | lateral (L) | Vertical (V) | |
| **Lower teeth stage height** | similar base force ($V_1$) | similar peak force ($V_2$) | |
| **Initial food loading size** | single quarter ($Food_{1/4}$) | single half ($Food_{1/2}$) | five quarters ($Food_{5/4}$) |

$V_1$Base was the average base force measured for an empty chewing cycle in the vertical trajectory. The lower teeth stage height setting for $V_1$ was such that the magnitude of the base force was similar to that for the lateral trajectory (LBase). The lower teeth stage height setting for $V_2$ was increased such that the magnitude of the peak force (Eg. $V_2Food_{1/4}$) during the chewing cycle with food is similar to that for the lateral trajectory (Eg. $LFood_{1/4}$). $V_2$Base was a much higher force due to a greater compression of the spring during occlusion as the lower teeth are raised higher.

*Table 3-9. Summary of the peak force ($F_{peak}$), force before first fracture occurred ($F_1$), increase in force due to food obtained by subtracting the base force from the peak force (ΔF), area under peak force (Impulse), increase in impulse due to food (ΔImpulse), and increase in spring displacement due to food (Δx) for the various trials where V is the vertical trajectory, L is the lateral trajectory, Base is the base force, $Food_{1/4}$, $Food_{1/2}$,and $Food_{5/4}$ indicates a single quarter peanut, half peanut and five quarter peanuts respectively. The values reported are the mean and standard error of four replicates each.*

| Trial | $F_{peak}$ (N) | $F_1$ (N) | ΔF (N) | Impulse (N.s) | ΔImpulse (N.s) | Δx (mm) |
|---|---|---|---|---|---|---|
| $V_1$Base | 106.1 ± 1.2 | | | 10.8 ± 0.3 | | |
| $V_1Food_{1/4}$ | 131.1 ± 3.6 | 51.4 ± 0.3 | 78.9 ± 2.6 | 20.7 ± 0.7 | 9.2 ± 0.9 | 5.2 ± 0.2 |
| $V_1Food_{1/2}$ | 164.6 ± 1.0 | 53.0 ± 9.7 | 109.9 ± 4.1 | 28.9 ± 0.8 | 18.2 ± 1.4 | 7.2 ± 0.3 |
| $V_1Food_{5/4}$ | 174.6 ± 12.0 | 59.0 ± 4.9 | 116.0 ± 8.2 | 32.5 ± 1.9 | 20.3 ± 2.2 | 7.6 ± 0.5 |
| $V_2$Base | 152.5 ± 8.0 | | | 19.8 ± 1.4 | | |
| $V_2Food_{1/4}$ | 140.3 ± 3.0 | 51.0 ± 1.8 | 76.6 ± 3.2 | 24.6 ± 0.6 | 7.1 ± 0.6 | 5.0 ± 0.2 |
| $V_2Food_{1/2}$ | 182.0 ± 3.5 | 47.3 ± 7.0 | 98.1 ± 9.0 | 31.7 ± 1.0 | 15.8 ± 1.1 | 6.8 ± 0.5 |
| $V_2Food_{5/4}$ | 211.4 ± 5.6 | 57.7 ± 2.7 | 102.4 ± 4.8 | 41.1 ± 1.1 | 14.8 ± 0.8 | 6.7 ± 0.3 |
| LBase | 105 ± 1.1 | | | 10.9 ± 0.3 | | |
| $LFood_{1/4}$ | 155.4 ± 1.7 | 57.7 ± 4.7 | 98.6 ± 2.5 | 25.5 ± 0.3 | 14.6 ± 0.5 | 6.4 ± 0.2 |
| $LFood_{1/2}$ | 181.3 ± 4.6 | 58.0 ± 6.6 | 135.1 ± 7.9 | 33.1 ± 1.1 | 22.8 ± 0.8 | 8.8 ± 0.5 |
| $LFood_{5/4}$ | 213.6 ± 11.4 | 54.4 ± 6.1 | 144.9 ± 8.0 | 36.1 ± 1.6 | 24.8 ± 1.5 | 9.4 ± 0.5 |

As discussed earlier, the peak force for 'Lateral' and 'Vertical 1' are similar in magnitude as expected although the shapes of the peak forces are different (Figure 3-23). The decrease in force is slower for the lateral trajectory due to the lateral shear exerted by the upper teeth. The two base line forces in the vertical chewing trajectory are similar in terms of the shape of the peak forces although the peak force for 'Vertical 2' is larger. This indicates that the magnitude of the base line force changes with different lower teeth stage height settings.

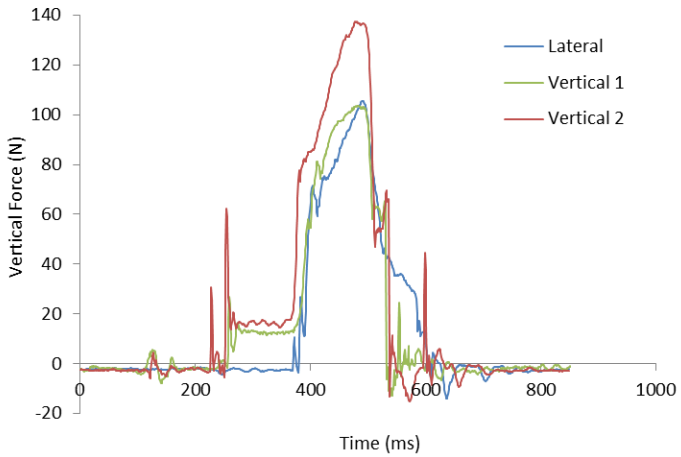


*Figure 3-23. The base line forces measured for the lateral and vertical chewing trajectories, where the lower teeth stage height settings for Vertical 2 is 1.15 mm higher than Vertical 1.*

The peak force for 'Lateral' and 'Vertical 2' are similar in magnitude which is expected as the lower teeth stage height had been raised to achieve this (Figure 3-24). The increase in force started much earlier in 'Vertical 2' as the upper teeth came into contact with the food much earlier in the chewing cycle due to the higher stage height of 4 mm as compared to 'Vertical 1'.

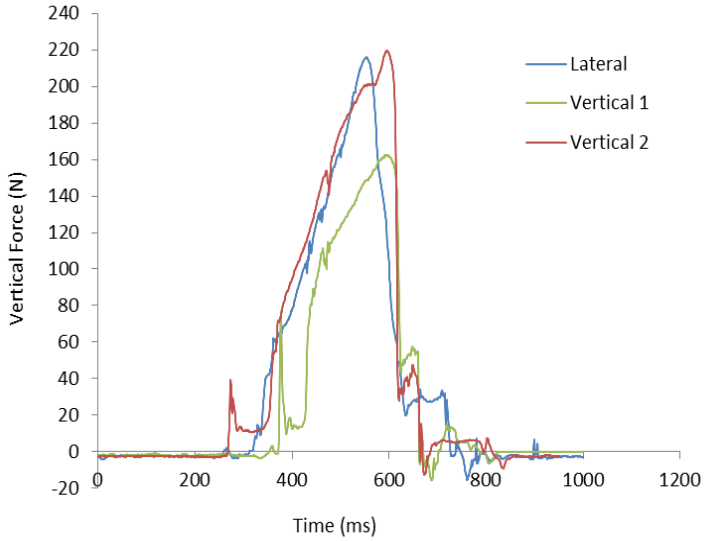


*Figure 3-24. The peak forces measured for the first chewing cycle of five quarter peanuts in the lateral and vertical chewing trajectories, where the lower teeth stage height settings for Vertical 2 is 4 mm higher than Vertical 1.*

Figure 3-25 shows the force profile of the mastication for different loading sizes of peanuts in the lateral chewing trajectory. It shows the peak forces measured for the base line force and first chewing cycle of a single quarter, single half and five quarter peanuts in the lateral chewing trajectory. The shapes of the peak forces are similar as these chewing cycles are all in the lateral trajectory. It can be seen that with increasing amounts of food, the force measured during the

chewing cycle increased. The increase in force is about 150 ms earlier for the chewing cycles with food as compared to the base line force. This is due to the height of the food which caused the upper teeth to come into contact with resistance earlier in the chewing cycle.

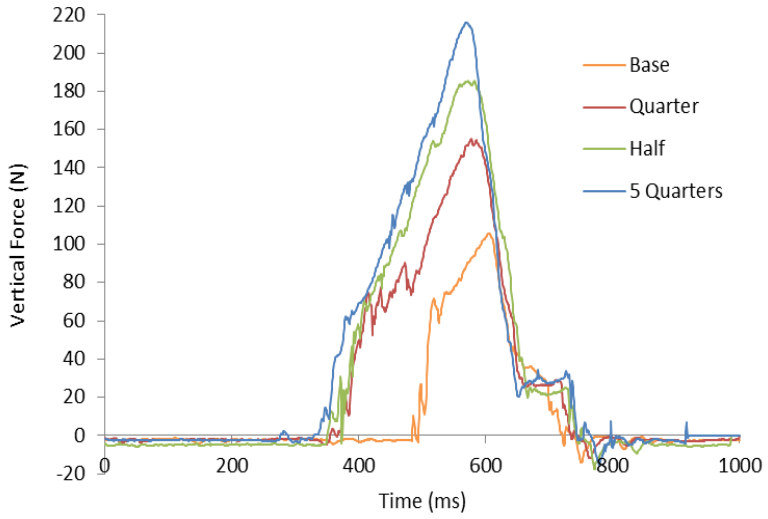


*Figure 3-25. The peak forces measured for the base line force and first chewing cycle of a single quarter, single half and five quarter peanuts in the lateral chewing trajectory.*

The ΔF for the forces measured during chewing in the vertical trajectories at the two different lower teeth stage heights have no significant difference based on the standard error and indicate good repeatability. Thus, ΔF should be used for the comparison of forces measured at different lower teeth stage height settings so that the different base forces are accounted for.

The highest values of $F_{peak}$, ΔF, Impulse, ΔImpulse and Δx were produced by the lateral chewing trajectory. Thus, the lateral trajectory was the most efficient in breaking down the food. This is due to the positive correlation between the force applied and resulting fragmentation on the food. The forces measured at first fracture are around 50 -60 N for all trials. The peak forces increased as the amount of food loaded on the teeth increased. The impulse obtained increased as the peak force increased for all trials. However, the impulse obtained for $V_2Food_{5/4}$ was higher than $LFood_{5/4}$ although the former had a lower peak force. The base force for the vertical chew is much higher as the stage height for the lower teeth was raised 7 mm higher than the setting for the lateral chew (Figure 3-26). With the increased stage height, the upper teeth meets with food resistance earlier in the chewing cycle which accounts for the more rapid increase in force. Thus, the area under the peak force (impulse) for the vertical chew is much higher.

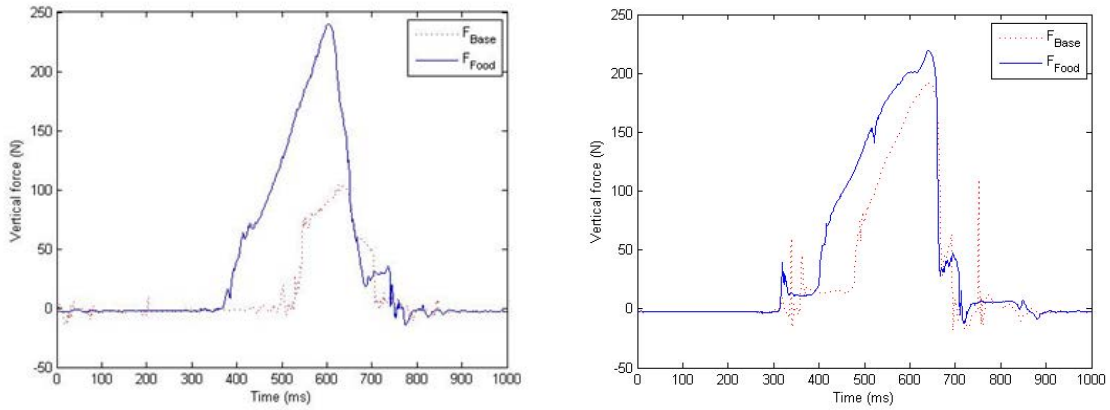


*Figure 3-26. The base force and the force measured for five quarter peanuts in the lateral and vertical chewing trajectories.*

It can be concluded that the force measured is dependent on the amount of spring displacement due to the presence of food particles during occlusion and since the impulse is dependent on the force and time required for each chewing cycle, the $F_{peak}$, ΔF, Impulse, ΔImpulse and Δx can be used to describe the changes associated with increasing number of chews.

The increases in force (ΔF) for single quarter peanut ($V_1Food_{1/4}$), five quarter peanuts with low base force ($V_1Food_{5/4}$) and five quarter peanuts with high base force ($V_2Food_{5/4}$) were plotted against the calculated spring displacement as shown in Figure 3-27. The increase in force measured for the 'five peanuts (high)' was lower than that measured for the 'five peanuts (low)' due to the higher initial base force for the former since the higher stage height caused a greater compression in the spring. However, the difference in the ΔF was not significant ($p>0.05$). The slope obtained is similar to the spring constant of 15.3 N/mm$^2$ that was determined previously. Thus, this suggests that the robot is consistent and behaving as expected.

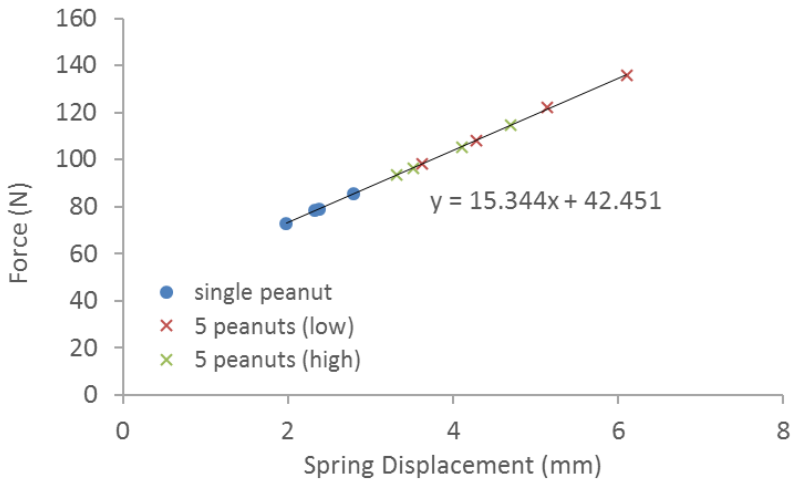


*Figure 3-27. The maximum increase in vertical force exerted during the occlusion of the peanuts plotted against the spring displacement due to the peanuts during a chewing cycle.*

### 3.4.4. Force data collected across multiple chews in the breakdown of peanuts

Figure 3-28 shows the decrease in impulse in the vertical direction with an increasing number of chews for half and quarter peanuts in the lateral trajectory. The impulse decreased the most rapidly in the first five chewing cycles, with the largest decrease between the first and second chew. After the 20th chew, the rate of decrease in impulse had declined for both the half and quarter peanuts. As the particles became smaller with increasing chews, less work was required to fragment the particles. The force exerted reduced as the amount of spring compression reduced when the height of the particles decreased. The impulse in the vertical direction of the 30$^{th}$ chew decreased to a quarter of the initial impulse in the first chew for the half peanuts. The impulse for the quarter peanuts after the 20$^{th}$ chew was about 1 N.s and does not reduce much further, suggesting that the particles have reached a threshold size where they are no longer broken down further. The impulse for the half peanuts was significantly higher than that for the quarter peanuts. This is expected as the half peanuts require more work done to breakdown as they are larger.

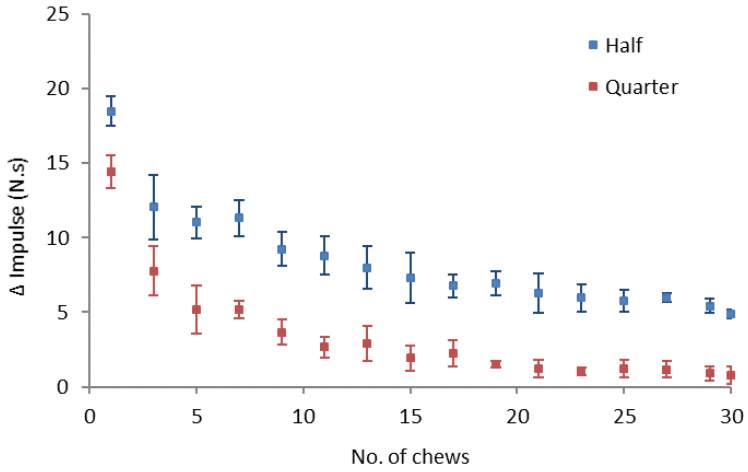


*Figure 3-28.The change in impulse (Z-direction) determined with increasing number of chews in the lateral trajectory for single half and quarter peanuts. The error bars represent the standard deviation of four replicates.*

The impulse in the lateral chewing trajectory was significantly higher than that for the vertical chewing trajectory (Figure 3-29). This is because the forces resulting from the lateral trajectory were higher.

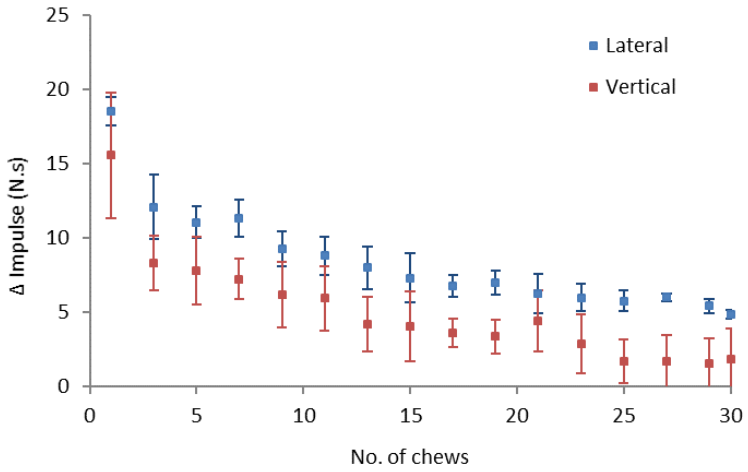


*Figure 3-29. The change in impulse (Z-direction) determined with increasing number of chews for a single half peanut chewed in the lateral and vertical chewing trajectories. The error bars represent the standard deviation of four replicates.*

A larger load of peanuts results in a higher amount of spring compression during chewing, which results in a larger force applied. The time taken for occlusion to occur is longer for a higher load of peanuts which also results in a larger impulse. Figure 3-30 shows the change in impulse with increasing number of chews for a single quarter or five quarter peanuts in the lateral and vertical chewing trajectories. The impulse does not decrease as rapidly for the loading of five quarter peanuts as compared to the single quarter peanuts. The breakdown of a larger load of peanuts is less efficient and thus, the sizes of the particles do not reduce as much. The resulting spring compression during occlusion is dependent on the particle sizes and as such the decrease in the forces applied is much smaller for the five peanuts. It is noted that the impulse decreased after every two chewing cycles for the five quarter peanuts. This is because some particles fall away from the occlusal surfaces after the first chew, leaving the already chewed particles to be chewed again in the second cycle of occlusion. As all the particles are reloaded onto the occlusal surface again after every two cycles, the impulse increased again. Since very little material is left on the occluding surface during the second chew, it is essential to reload the particles onto the occlusal surface after each chew to ensure a better representation of the tongue's function to reload food particles consistently. In the subsequent work in the later chapters, reloading of particles onto the occlusal surface was done after each chew.

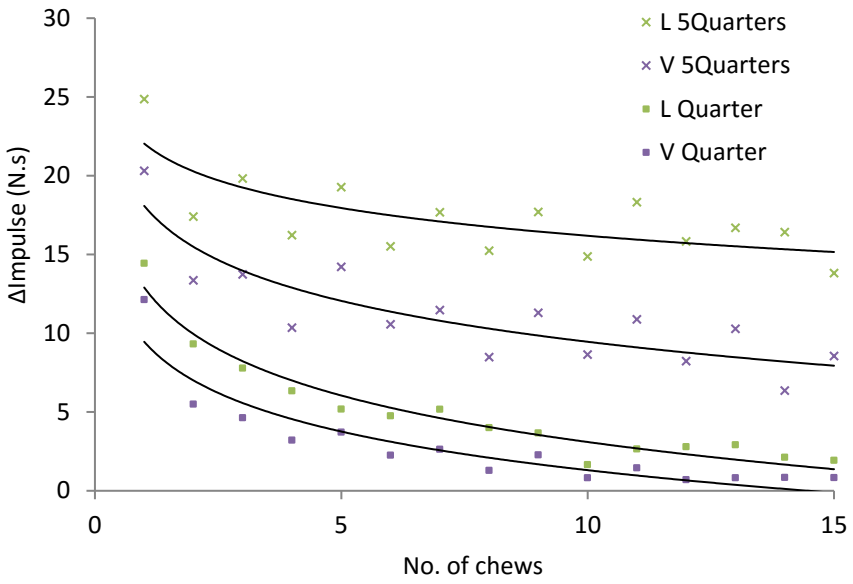


*Figure 3-30. The change in impulse (Z-direction) determined with increasing number of chews for a single quarter or five quarter peanuts in the lateral and vertical chewing trajectories.*

## 3.5. Improvements to the mastication robot

### 3.5.1. Modification of teeth and retention system in MR

Other than the chewing force exerted on the food and the chewing trajectory's effect on the breakdown of food, tooth morphology also plays an important role in the fracture of food particles (van der Bilt et al., 1987). The cusps on teeth facilitate fragmentation during chewing (Lucas et al., 2002) by helping trap particles to increase chances of damage (selection function), and by altering the directions that forces are applied to the food. After observation of the breakdown of the peanuts in the evaluation study, it was decided that the teeth of the MR had to be modified such that the cusps would be more representative of the human molars. The surface of the cusps in the old teeth were flat, thus crack initiation was poor and breaking down of fibrous or tough food like meat would be poor. The new teeth were modelled after denture teeth with accurate morphology (Figure 3-31). In addition, a silicon retention base was fitted into the new teeth for collection of the particles so that it would be easier to return the particles onto the occlusal surface for the next chewing cycle (Figure 3-32). The silicon retention base is like a curved wall that is wide at the top and narrow at the base which serve to keep the food from falling off the occlusal surface completely but yet allowing space for the upper teeth to navigate through its intended trajectory without hitting the sides of the silicon base. However, when particles have been broken down to a certain size, the gap between the occlusal surface and the wall of the base is too large and particles still fall through, thus there is still a need to load particles back onto the occlusal surface after each chew.

*Figure 3-31: Upper and lower teeth (Dental Art, Palmerston North, New Zealand).*

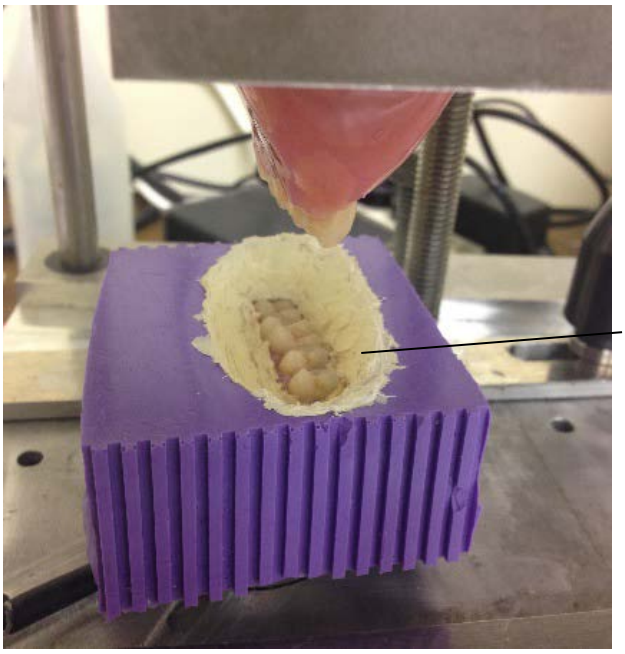


*Figure 3-32: New teeth fitted with a retention system.*

### 3.5.2. Reduction of backlash in the upper teeth

It was discovered that there was backlash in the upper teeth. This is due to wear in the bearings in the four bar linkage mechanism. This slack meant that the upper teeth were not moving in the intended trajectory when it approached occlusion. The forces applied to the teeth surfaces are transferred up through the linkages causing movement, rather than the true occlusal glide trajectory being achieved. The backlash problem was significantly reduced after replacement of the bearings in the robot.

## 3.6. Conclusion

In this chapter, the operation of the mastication robot was explored to determine the effect of chewing trajectory, stage height and the sample loading size on the force measurements and the breakdown efficiency of the robot. The study on the spring constant proved that the chewing forces

applied were due to the spring compression during occlusion as a result of resistance due to the food acting on the spring and that the robot behaved in a consistent manner. The breakage function and $x_{50}$ were used to characterise the particle size distributions of the resulting particles. In this study with peanuts, the initial particle size and loading size had an inversely proportional relationship with the breakage function. A larger initial particle size and loading resulted in smaller breakage functions although it resulted in an increase in the selection frequency. Larger particles increased the chances of selection, and thus made up for the lower breakage. The amount of fragmentation is dependent on the magnitude and direction of forces acting on the food. Higher chewing forces were measured in compressive shear (lateral chewing) as compared to compression (vertical chewing), thus resulting in better breakdown.

The lateral chewing trajectory had a larger breakage function compared to the vertical chewing trajectory. However, it had a smaller selection frequency and this offset the difference in the breakage function. There is a threshold particle size at which the particles are no longer broken down effectively in the mastication robot after a certain number of chews. This is also reflected in the force profiles, where the change in impulse (the area under the measured vertical force vs time graph for a cycle), is about 1 N.s. The implication is that the particles are not large enough to cause the spring to be compressed and thus no force due to the resistance from food is applied. Thus, the $d_{50}$ of the particles chewed by the different chewing trajectories were only significantly different during the initial chews.

As the application of the mastication robot was to simulate mastication in humans, the function of the cusps on the molars and the tongue in manipulating food during breakdown should be closely imitated. The flat cusps on the old molars on the robot could not provide good crack initiation and the poor retention system would cause food to easily fall off the occlusal surface, these factors limit the performance of the robot. Thus, improvements were made to the teeth, retention system and a reduction in the mechanical backlash in the mastication robot. Since improvements were made, the next step was to validate the performance of the mastication robot against human subjects.

# Chapter Four Validation Study: Comparison of the improved mastication robot with human subjects

Chapter 3 discussed limitations of, and improvements made to the mastication robot (MR). This chapter presents further studies to validate the performance of the improved MR through a validation study using two model foods, Optosil and peanuts, and comparing the MR's performance with human performance.

This study was conducted in two stages. The first test food (stage 1) was a non-brittle but fracturable test food known as "Optosil" which had been used in dental and mastication studies (Sierpinska et al., 2008; van den Braber et al., 2001) as a means of measuring chewing efficiency of human subjects. Peanuts are a commonly used natural test food for the determination of mastication performance (Hatch et al., 2001; Kim et al., 2011), thus, they were selected as the second test food (stage 2). Thus, the validation test would be conducted using both a non-brittle and brittle test food. The objective of this stage of the research was to compare the chewing efficiency of the subjects and the MR to evaluate whether the MR could reliably replicate the chewing behaviour of human subjects. The MR was developed so that objective measurement of food breakdown could be efficiently carried out. In light of that, it is important to know whether the MR is able to mimic human chewing with similar breakdown properties and if not, at least an understanding of the limitations of the MR is understood.

## 4.1. Stage 1: Optosil Study

In this study, data were collected from human subjects and the mastication robot, on the breakdown of a test food widely used for dental studies. The test food "Optosil" (Heraeus Kulzer Gmbh., Hanau, Germany) is a silicon rubber that is a widely used dental impression material and test food for masticatory function (Van der Glas et al., 2012; Van der Glas et al., 1987). This data was used to validate the chewing efficiency of the mastication robot.

### 4.1.1. Human Trial Methodology

Five subjects were selected through a screening questionnaire. The subjects selected were male, aged between 18 to 30 years old, had no oral-processing impairment, had complete natural dentition, had no history of orthodontic treatment or jaw injuries, and were currently not on any medication. Subject recruitment was limited to one gender to minimize between subject variations.

Previous work have shown that there is variation in masticatory behavior between males and females. Bite size (Medicis & Hiiemae, 1998), bite force (Palinkas et al., 2010), chewing frequency (Khamnei et al., 2016), chewing cycles, mandibular movements (Youssef et al., 1997) have been shown to be different with males having a more efficient masticatory performance as compared to females. The questionnaire used to select the subjects is included in Appendix A. The study was registered as a low risk notification with the Massey University Ethics Committee. Details of the study were explained to the subjects through an information sheet and subjects gave their consent to participate in the study in a consent form included in Appendix A.

Subjects were instructed to chew four Optosil particles (4.8 x 9.6 x 9.6mm) on their preferred side (i.e. one-sided chewing) and expectorate the bolus into prepared filter paper (20 microns) when instructed to stop. The instructions given to subjects could have caused distraction and resulted in changes in their usual chewing behavior. As such, there was a practice session for each subject to give them time to familiarize themselves with the instructions so that they would be more comfortable with the routine and responding to the instructions would be more intuitive. Samples were collected at a range of different chewing cycles (N=2, 3, 7, 14), washed and dried prior to sieving to obtain the particle size distributions (PSD) of the chewed samples. The sample collection was repeated three times for each chewing trial of N cycles, for each subject, and all trials were randomised. The replicates were pooled together for PSD analysis. Subjects were not informed on the number of chews required, instead, they were watched and told to stop upon achieving the required number of chews. This was to prevent deviation from the natural chewing behaviour as it can differ when the subject is consciously counting the chewing cycles. Video recording was used to track the jaw movement during the chewing sequence. See next section for details.

### 4.1.2. Jaw Movement Tracking

The video recording and tracking method was adopted from the work done by Wilson et al., (2016;2013). Video recording at a resolution of 1920x1080 pixels at 60 frames per second, was done using a GoPro Hero4 (GoPro, Inc., California, US) to track the jaw movement during the chewing sequence. Circular 14mm white adhesive labels with 3mm green centre dots were placed on the subjects' chin. The subject wore head gear with markers as seen in Figure 4-1, such that they formed the corners of a 2D plane that included the chin of the subject. The corners provided a reference plane to track the dot on the chin during image analysis so that any head movement would not affect the tracking.

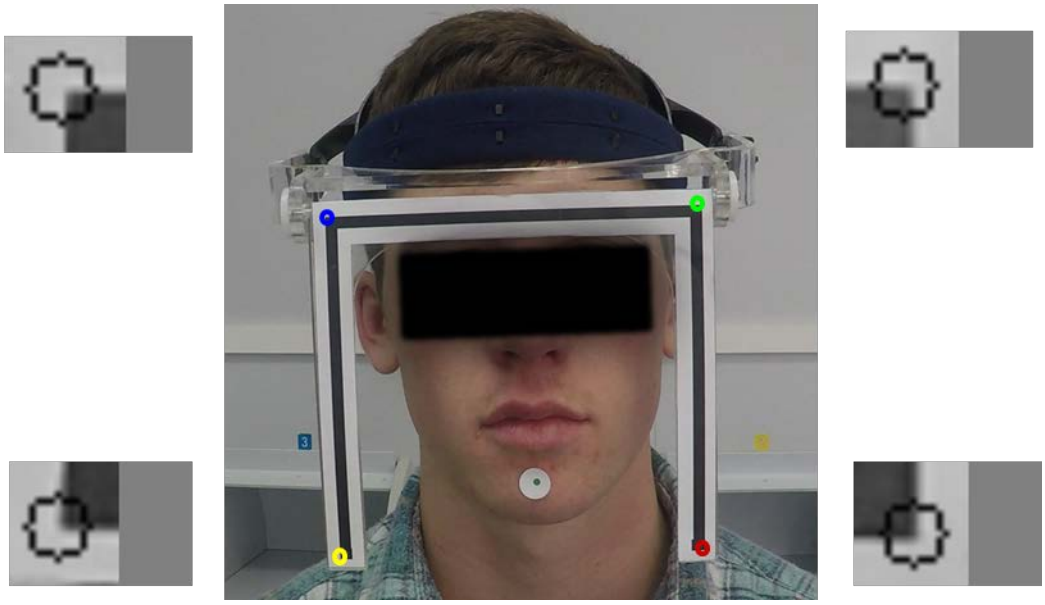

*Figure 4-1: Head gear worn by the subject. The corners indicated by the blue, green, red and yellow rings were used as reference markers for the tracking of the dot on the subject's chin. The black mask over eyes was not actually present and is just placed here to provide subject anonymity.*

The recorded videos were sent to Arran Wilson (Plant & Food Research Limited, New Zealand) and the data analysis of the videos were done using programs he had developed. Homographic transformation was applied to make the image plane perpendicular to the viewer's line of sight and the lateral and vertical (xy) position of the chin dot in each image was saved. The vertical movement in each cycle was divided into three phases: opening, closing and occlusal phases. The start and end of each chewing cycle was defined as the two points of maximum jaw opening. From the data analysis, a summary of the chewing response variables that were obtained are shown in Table 4-1. Of these responses, only the data on the inclination of the closing slope, the lateral and vertical amplitudes were extracted for further discussion. These responses were selected as they provide information on the chewing trajectories which is of interest in this work since this parameter will be controlled in the MR.

*Table 4-1: A summary of some of the chewing response variables that were obtained from the analysis.*

| Variables | Description |
|---|---|
| Chews | Total number of chews |
| Sec per chew | Mean time per chews of all chews (s) |
| Chewing time | Total chewing time (s) |
| Chew cycle time | Chewing time omitting swallowing at end (s) |
| Closing slope | Mean inclination of closing slope (°) |
| Opening slope | Mean inclination of opening slope (°) |
| Chewing frequency | mean inverse of seconds per chew ($s^{-1}$) |
| Closing velocity | mean closing speed (mm/s) |
| Opening velocity | mean opening speed (mm/s) |
| Lateral amplitude | mean width of chew (mm) |
| Vertical amplitude | mean height of chew (mm) |
| Perimeter length | mean distance of chew (mm) |
| Crossed cycle | proportion of crossed chews |
| Crescent cycle | proportion of crescent shaped chews |
| Circular cycle | proportion of circular chews |
| Perimeter distance | sum of all chews perimeter length (mm) |

### 4.1.3. Parameters established from Human Trial

As the particles were broken down to smaller pieces over 10, 20 and 30 cycles, the vertical magnitude of the jaw trajectory increased, indicating that the teeth were not fully occluded at first but became fully occluded after the initial five chews. This explains the increase in the vertical distance over time in the initial few chews (Figure 4-2). However, it is crucial to note that the size of the trajectory is not directly proportional to the occlusion as changes in chewing pattern are also affected by other factors such as the bolus volume and the particle size distribution etc. The peaks (example indicated by the red arrow) before occlusion in Figure 4-2 was due to the subject's habit of moving his chin upwards when occluding. Because the chin is not directly attached to the jaw, these artefacts in the data exist. Thus, these peaks were removed before the data was used to calculate the velocity.

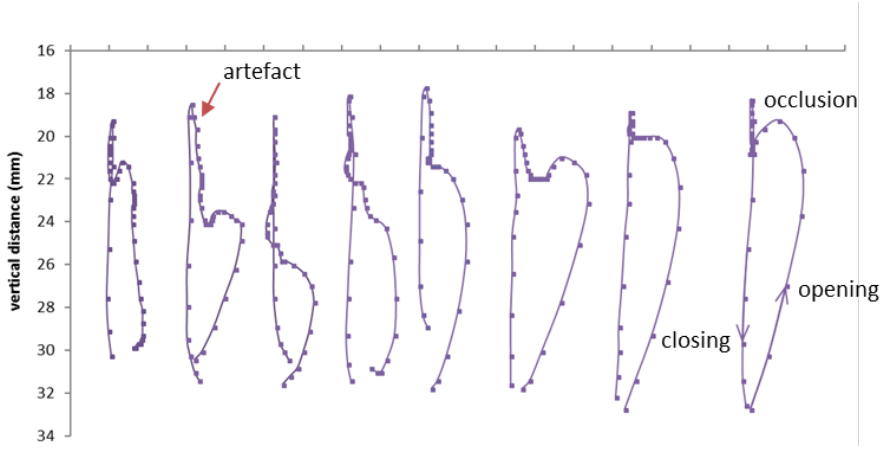


*Figure 4-2: An example of the chewing trajectories of a subject B at various chewing cycles. This is a left sided chewer and the arrows on the last chewing cycle shows the direction of the opening and closing phase.*

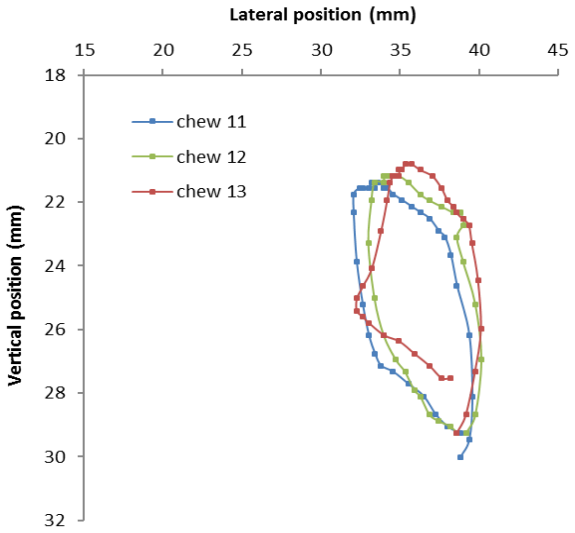


*Figure 4-3: An example of the jaw movement displayed on a 2D plane where x describes the lateral position and y describes the vertical position.*

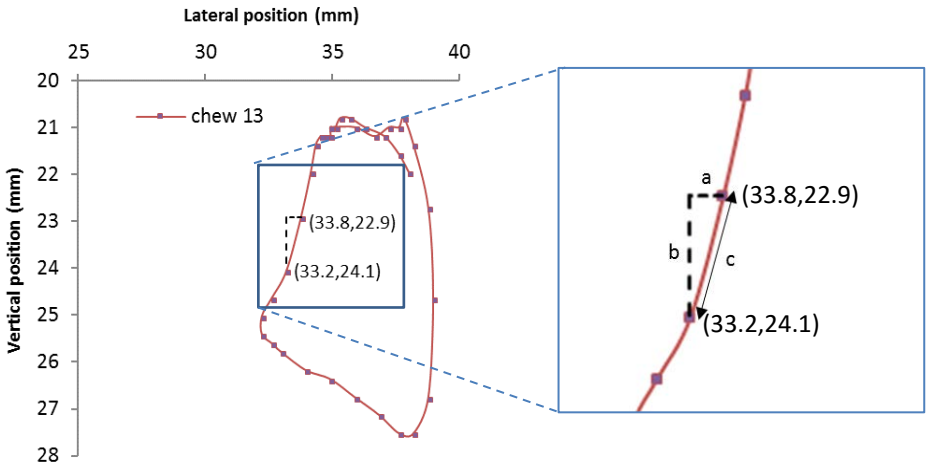


*Figure 4-4: Example to show how the distance travelled during each chew is calculated.*

Pythagoras theorem (Figure 4-4) was used to calculate the distance between one data point to the next by taking the vertical and horizontal distance to calculate the hypotenuse. The distance travelled is calculated by c = $\sqrt{a^2 + b^2}$. For example, $c = \sqrt{(33.8 - 33.2)^2 + (24.1 - 22.9)^2} = 1.3mm$. These distances were summed to obtain the total distance travelled by the lower teeth. To determine the occlusion velocity, the distance travelled, within 2mm of the intercuspal position, was divided by the time needed.

Figure 4-5 shows the average occlusal velocities obtained from three replicates of 14 chewing cycles for each subject. The average occlusal velocity of the subjects was 21.8 mm/s. The larger variation in the occlusal velocity for subject B could be due to the extra distance travelled by the chin movement during occlusion. Figure 4-6 shows the average height obtained from three replicates of 14 chewing cycles for each subject. The maximum jaw opening was between 8-11mm for all subjects except subject B. Again, this was due to the upward movement of the chin during occlusion which has been mistaken as the jaw movement. Subjects B and D use a more lateral trajectory as compared to subjects A, C and E which is seen by the wider width and a gentler closing slope for subjects B and D (Figure 4-7 and Figure 4-8). The variability in chewing parameters amongst subjects agrees with previous findings (Jemt et al., 1979; Lassauzay, Claire et al., 2000).

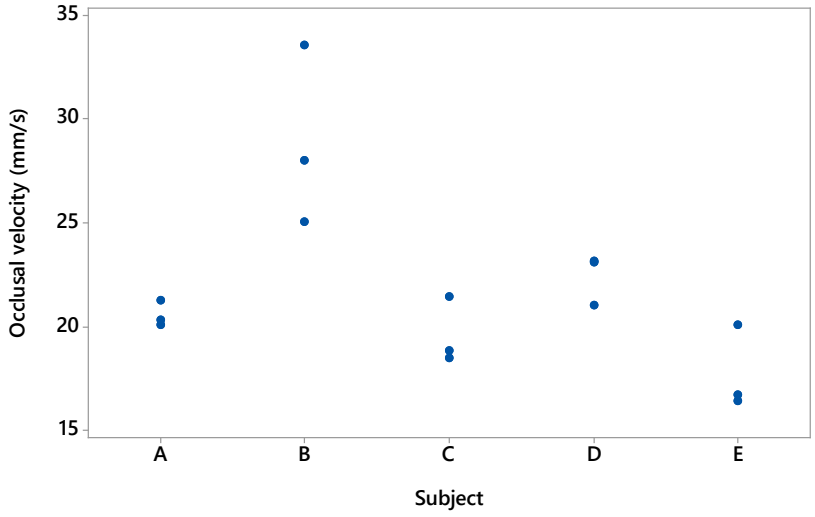


*Figure 4-5: The average occlusal velocity determined from the average of 14 chewing cycles per mastication recording with three recordings for each subject.*

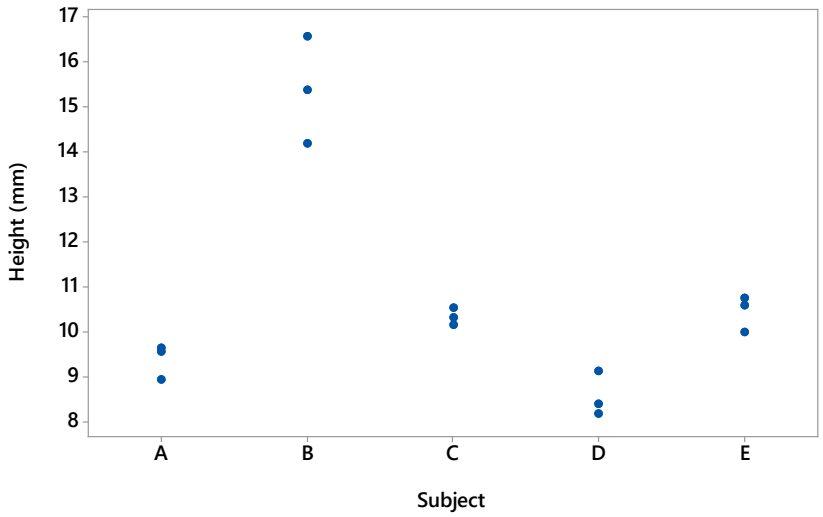


*Figure 4-6: The average height determined from 14 chewing cycles per mastication recording with three recordings for each subject.*

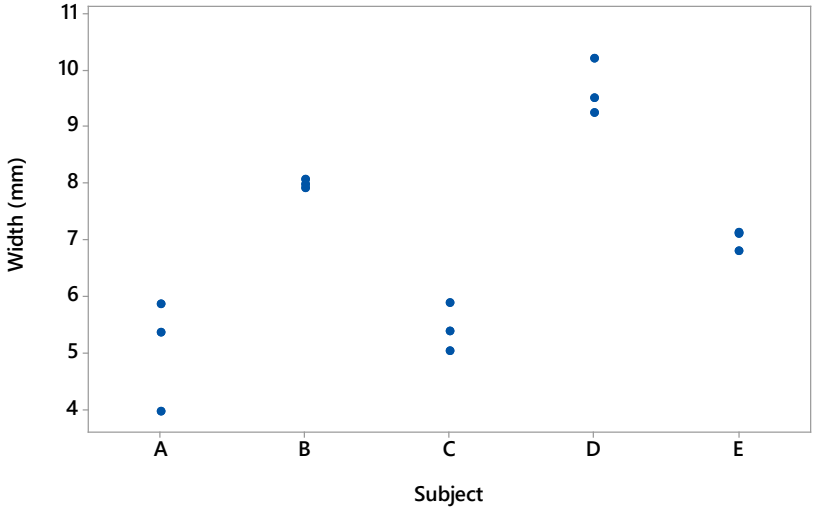


*Figure 4-7: The average width determined from 14 chewing cycles per mastication recording with three recordings for each subject.*

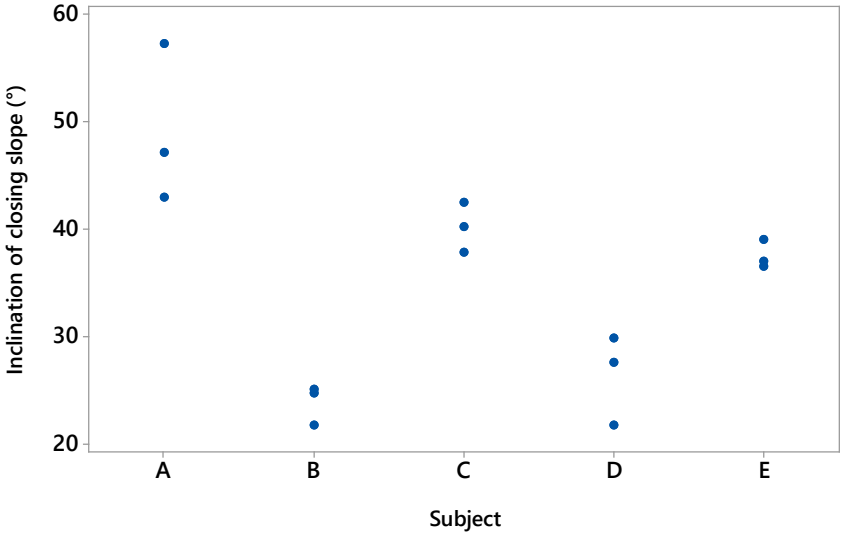


*Figure 4-8: The average angle of the closing slopes in degrees determined from 14 chewing cycles per mastication recording with three recordings for each subject.*

### 4.1.4. MR Trial Methodology

Four Optosil particles were placed on the occlusal surface of the MR for mastication and boluses were collected at different chewing cycles (N=2, 3, 7, 14). The sample collection was repeated three times for each chewing trial of N cycles. As the Optosil particles are hydrophobic, there was no need to add simulated saliva. Particles were repositioned onto the occlusal surface after each chew. Preliminary tests found that the Optosil was too tough to be broken down using the vertical trajectory which only compressed the samples with no resulting breakage. Thus, the ground link was adjusted to 50 mm so that the MR had a lateral trajectory. Figure 4-9 shows the difference between the closing strokes of the lateral and vertical trajectories. There was more horizontal movement as the teeth came into occlusion, thus there is greater shearing action in the lateral trajectory. The MR was set to the configuration (occlusal time= 0.12s, opening/closing time= 0.65s, and occlusal angle= 36°) which gave an estimated occlusal velocity of 21.5 mm/s. To estimate the occlusal velocity, Kinovea (http://www.kinovea.org/) was used to track the marker on the lower jaw and the 2D position (x,y) of the marker was measured in each frame. This data was exported into a spreadsheet for further analysis in Microsoft Excel (2016). Similarly, the distance travelled, within 2mm of the intercuspal position, was divided by the time needed and the average occlusal velocity was determined.

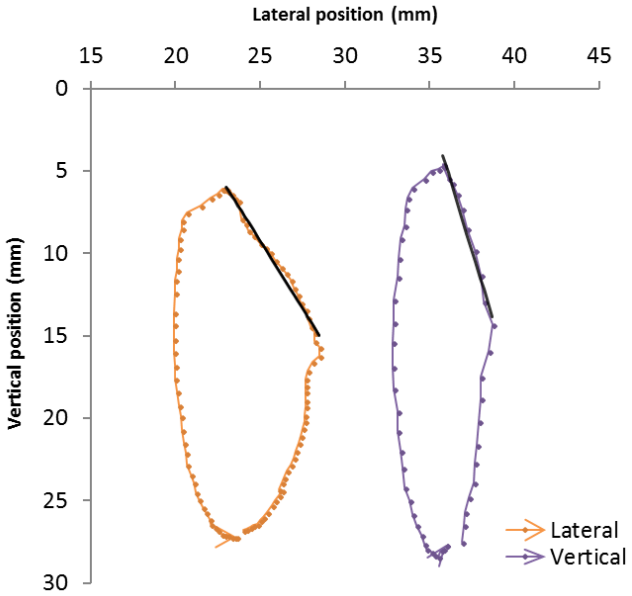


*Figure 4-9: The movement of the upper teeth of the MR displayed on a 2D plane using lateral and vertical chewing trajectory. The black line indicates the pathway of the closing stroke as the upper teeth comes into occlusion.*

### 4.1.5. PSD of the Optosil particles

To prevent the particles from clustering together because of saliva, the collected samples were washed with soap water, rinsed with water and dried in the oven at 80°C overnight. The PSD was determined by sieving the dry particles through a series of 10 sieves (100mm diameter, and 40mm height), with the apertures: 8.00, 5.60, 4.00, 2.80, 2.00, 1.40, 1.00, 0.71, 0.50, 0.25 mm (Endecott, London, UK), which were stacked in a sieve shaker (Octagonal digital shaker, Endecott, London, UK). The sieves were shaken for 10 minutes at amplitude 12. The weight of particles retained on each sieve was measured. The $d_{25}$, $d_{50}$, and $d_{75}$ were the theoretical sieve sizes through which 25%, 50% and 75% of the weight of particles that will pass through respectively.

Figure 4-10 shows the PSD of the optosil particles for the subjects and the MR after two, three, seven and fourteen chews and Table 4-2 shows the $d_{50}$ of the optosil particles for the subjects and the MR after two, three, seven and fourteen chews. The PSD of the particles after the initial two chews for subject E was the smallest amongst the subjects but subject B produced the smallest PSD of the particles after fourteen chews, thus the rate of breakdown for subject E was lower compared to subject B. Although the MR produced particles of smaller PSD than the subjects in the initial three chews, the rate of breakdown reduced drastically after that. The $d_{50}$ of the particles after seven chews had only reduced by 9.2% from the $d_{50}$ after three chews as compared to 26.9% reduction (subject C), which was the poorest reduction amongst the subjects, from the $d_{50}$ after three and seven chews respectively. It is interesting to note that subjects B and D had the smallest $d_{50}$ after 14 chews and both had used a lateral trajectory for mastication.

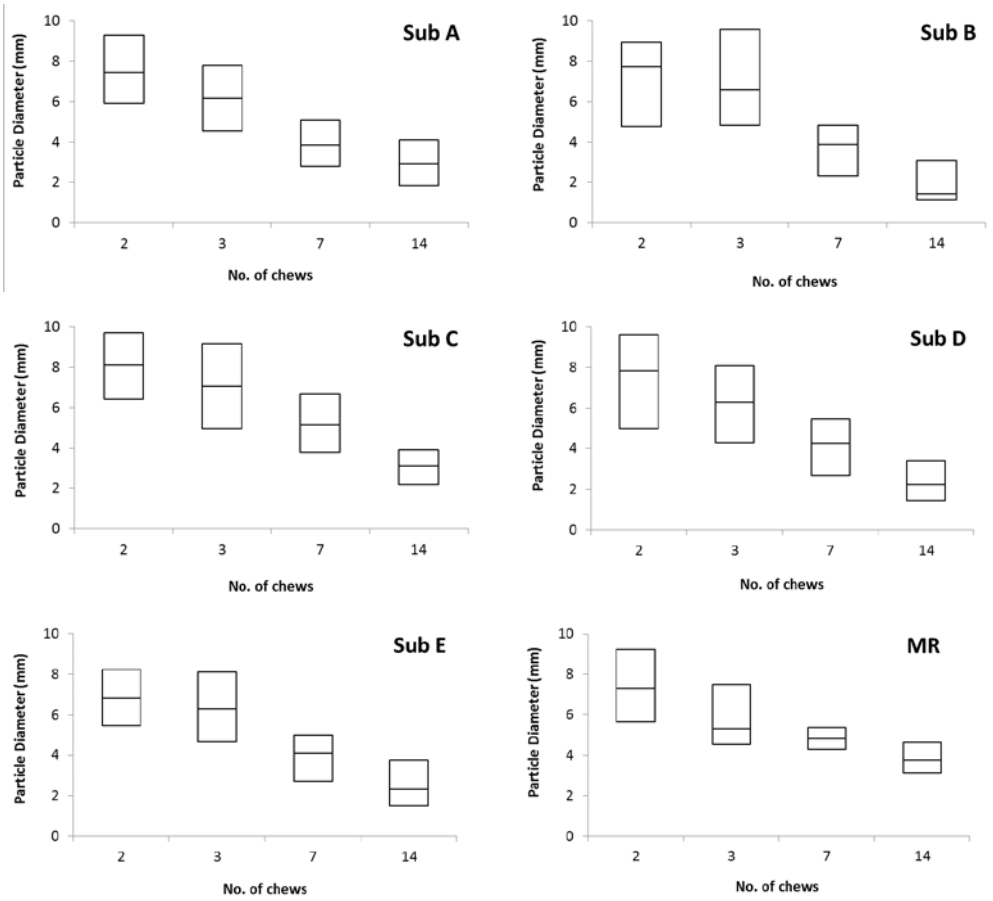


*Figure 4-10: The PSDs of the optosil particles after 2, 3, 7, and 14 chews for the subjects and the MR. The box plots show the $d_{25}$, $d_{50}$, and $d_{75}$ of each PSD.*

*Table 4-2: The $d_{50}$ of the optosil particles after 2, 3, 7 and 14 chews for the subjects and the mastication robot.*

| | 2 chews | 3 chews | 7 chews | 14 chews |
|---|---|---|---|---|
| Subject A | 7.45 | 6.19 | 3.87 | 2.92 |
| Subject B | 7.72 | 6.60 | 3.89 | 1.40 |
| Subject C | 8.11 | 7.06 | 5.16 | 3.10 |
| Subject D | 7.83 | 6.29 | 4.24 | 2.25 |
| Subject E | 6.80 | 6.28 | 4.08 | 2.33 |
| MR | 7.32 | 5.32 | 4.83 | 3.79 |

### 4.1.6. Determination of chewing efficiency from PSD

To characterise the PSD, the Rosin-Rammler distribution function introduced in chapter 3 (Eq. 3-1), $= 1 - exp\,[-\left(\frac{x}{x_{50}}\right)^{b} . ln2]$, was fitted to the cumulative area distribution of each bolus. As the PSD analysis was conducted by sieving, $x$ is the sieve size of a particle (mm), $Q$ is the weight fraction of particles with a smaller diameter than $x$, $x_{50}$ is the theoretical sieve size through which 50% of the weight will pass (mm), and $b$ is the slope of the cumulative area distribution curve which describes the broadness of the distribution, where decreasing values correspond to a broader distribution. The

$x_{50}$ of the boluses collected from the MR was comparable with that of the human subjects in the initial seven chews (Figure 4-11a). The MR could not break down the optosil particles as efficiently after that. The b values for the subjects decreased with increasing number of chews indicating that the broadness of the distributions increased as the optosil particles were broken down (Figure 4-11b). The $b$ values for the MR were high, reflecting a narrow distribution.

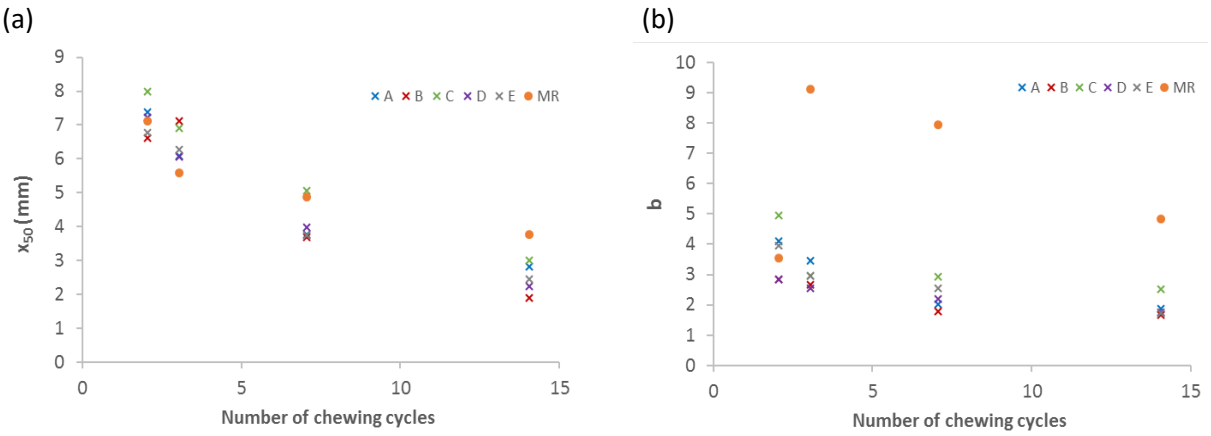


*Figure 4-11: The $x_{50}$ and $b$ values obtained from the Rosin-Rammler function fitted to the PSD of the pooled boluses collected after 2, 3, 7 and 14 chewing cycles for each subject and the MR.*

Van der Bilt et al. (1987; 1992) quantified chewing efficiency by determining the number of chewing cycles needed to halve the initial particle size, $N_{1/2\text{-}Xo}$. This was done by fitting a 2nd order polynomial function to the non-linear initial part of the log($x_{50}$)-log(N) relationship and interpolating the value of $N_{1/2\text{-}Xo}$ for each subject (Figure 4-12). The $x_{50}$ were obtained from the Rosin-rammler fits for the PSD of the boluses from the chewing cycles (N=2, 3, 7, 14). An example of the calculation to determine the $N_{1/2\text{-}Xo}$ is shown below and a summary of the $N_{1/2\text{-}Xo}$ and $x_{50}$ of each bolus distribution after 14 chews is displayed in Table 4-3.

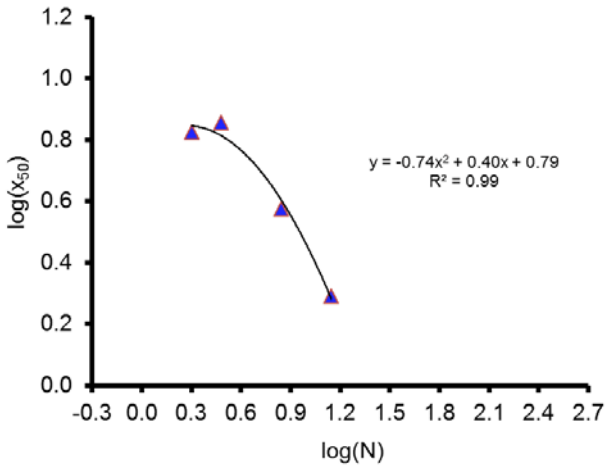


*Figure 4-12: The log($x_{50}$)-log(N) relationship of a subject's chewing is described by a 2nd order polynomial function.*

$N_{1/2\text{-}Xo}$ is solved for by substituting y=log(4.80)=0.68 into the equation in Figure 4-12 as half of the initial particle size is 4.80mm.

Log($N_{1/2\text{-}Xo}$) = $x = \frac{-0.40 \pm \sqrt{0.40^2 - 4(-0.74)(0.79-0.68)}}{2(-0.74)}$ = -0.203 (reject) or 0.743

$N_{1/2\text{-}Xo} = 10^{0.743} = 5.54$

*Table 4-3: The chewing efficiency, $N_{1/2\text{-}Xo}$ (i.e. the number of chewing cycles needed to reduce the initial half-cubes of 9.6mm to a median particle size of 4.8mm), and the $x_{50}$ of each bolus distribution after 14 chews (N=14) for the five subjects and the mastication robot.*

| | $N_{1/2\text{-}Xo}$ | $x_{50}$ | $b$ |
|---|---|---|---|
| **Subject A** | 4.56 | 2.87 | 1.94 |
| **Subject B** | 5.54 | 1.96 | 1.71 |
| **Subject C** | 7.49 | 3.05 | 2.59 |
| **Subject D** | 5.16 | 2.28 | 1.82 |
| **Subject E** | 4.89 | 2.49 | 1.78 |
| **MR** | 6.41 | 3.82 | 4.90 |

This study was conducted to compare the chewing efficiency between human subjects and mastication robot using optosil. A key finding was that the MR was not able to achieve similar chewing efficiency as the subjects (Table 4-3). The PSD of the bolus collected from the MR after 14 chews showed that 80% of the particles were between 2.8mm and 5.6mm. In comparison, the PSD of the boluses collected from the subjects after 14 chews showed that a maximum of 40% of the particles were between 2.8mm and 5.6mm, with the remaining particles well spread along the smaller sieve fractions of the distribution. The Optosil particles did not fragment after they reached a certain size (< 5mm) and were only being compressed during occlusion after this point. This was due to the material's elasticity and fracture toughness which are different from real solid foods. Optosil was found to be more ductile and was penetrated by the cusp before the yield point was reached, thus it does not fracture easily as compared to a brittle material like peanuts (Slagter et al., 1992). Optosil is made of an inert material that allows for particle size characterization and is thus commonly used to evaluate the chewing efficiency in humans. However, the material is unlike an actual food that would be consumed and is rather unpalatable. The flavor and sensory perception of Optosil may result in subjects altering their usual chewing behavior. In previous work, a bite simulator with a 90° cusp form probe required 110N for the Optosil particle to yield during compression. This was much higher than the other test foods like turnip, carrot and peanuts (Olthoff et al., 1986). The Optosil may be better retained between the occlusal surfaces of the teeth in the subjects and the amount of force required to fragment it is higher than what the robot can achieve. In addition, the subjects may use more lateral shearing during occlusion than what the MR can achieve with its current specifications. Thus, it was decided to test a more brittle food.

## 4.2. Stage 2: Peanut Study

### 4.2.1. Human Trial Methodology

The same subjects as used in stage 1 were instructed to chew eight peanut halves (3.0 ± 0.05g) on their preferred side (i.e. one-sided chewing) and expectorate the bolus into prepared filter paper (20 microns) when instructed to stop. Samples were collected at different chewing cycles (N=2, 3, 7, 14), washed and dried prior to sieving to obtain the particle size distributions of the chewed samples. Subjects were also asked to chew until they felt the bolus was ready to swallow and indicate by raising their hand. The number of chews taken to reach swallow point was recorded. The sample collection was repeated 3 times for each chewing trial of N cycles and at swallow point, for each subject, and all trials were randomised. Video recording was done to track the jaw movement during the chewing sequence. For moisture content analysis, five additional boluses were collected after three chewing cycles and at swallow point.

### 4.2.2. Moisture Content Analysis

The moisture content of the foods was determined by measuring the weight loss of a sample dried at 108°C in an air oven overnight for a minimum of 16 h until constant weight was achieved (AACC method 45-30). The boluses were immediately weighed upon collection and then dried in the air oven. The moisture content of the food and bolus was calculated on a wet weight basis (g/g) using Equations 4-2 and 4-3. The values were then used to calculate the moisture content of the bolus and estimate the saliva addition during mastication. The moisture content of the bolus on a dry weight basis and the change in moisture content between the food and bolus were calculated by Equations 4-4 and 4-5.

$$MC_f = \frac{M_f - M_{df}}{M_f} \qquad \text{Eq. (4-2)}$$

Where $MC_f$ is the food moisture content on a wet weight basis (g/g wet wt), $M_f$ is the mass of food before drying (g), and $M_{df}$ is the mass of food after drying (g).

$$MC_b = \frac{M_b - M_{db}}{M_b} \qquad \text{Eq. (4-3)}$$

Where $MC_b$ is the bolus moisture content on a wet weight basis (g/g wet wt), $M_b$ is the mass of the expectorated bolus (g), and $M_{db}$ is the mass of bolus after drying (g).

$$MC_{df} = \frac{MC_f}{(1 - MC_f)} \qquad \text{Eq. (4-4)}$$

Where $MC_{df}$ is the food moisture content on a dry weight basis (g/ g dry solids), and $MC_f$ is the food moisture content on a wet weight basis (g).

$$MC_{db} = \frac{MC_b}{(1-MC_b)} \quad \text{Eq. (4-5)}$$

Where $MC_{db}$ is the bolus moisture content on a dry weight basis (g/ g dry solids), and $MC_b$ is the bolus moisture content on a wet weight basis (g).

$$\Delta MC_{db} = MC_{db} - MC_{df} \quad \text{Eq. (4-6)}$$

Where $\Delta MC_{db}$ is the change in moisture content of the bolus (g/g dry solids). This value was used to calculate the amount of xanthan gum solution to be added to the samples during mastication in the mastication robot.

### 4.2.3. Mastication Robot Trial Methodology

A two-level full factorial design with three factors was conducted to determine the effect of chewing trajectory, occlusal velocity and angle of sagittal plane on the breakdown of the peanut samples as seen in Table 4-4. Modulation of force and jaw movement during mastication is naturally done in response to the textural properties of the food, so that the breakdown is carried out in an efficient way. Thus, the experimental design served to explore some of the factors that can be adjusted in the MR so that optimum breakdown could be achieved.

*Table 4-4: A two-level full factorial design with three factors resulting in eight runs.*

| **Factors** | **Levels** | |
|---|---|---|
| | -1 | +1 |
| **Trajectory** | lateral | Vertical |
| **Sagittal Plane** | 0° | 15° |
| **Occlusal velocity** | 15mm/s | 20mm/s |
| | (0.18, 0.65, 36) | (0.12, 0.65, 36) |

The saliva interactions with the peanut particles play a part in the mastication process, thus there was a need to add simulated saliva during the mastication in the MR. The amount of simulated saliva to be added was estimated from the data collected in the human study (chapter 4.2.1.). The moisture content ($MC_{db}$) of the boluses collected after three chews and at swallow point were plotted against the number of chews. A line was fitted using the least squares method (LINEST

function in Microsoft Excel), to estimate the initial moisture pool added to the bolus at the start of mastication and the rate of saliva addition during chewing were indicated by the intercept and the slope respectively (Table 4-5). To account for the initial uptake of saliva upon the food's contact with the oral mucosa, the difference in moisture content between the peanut sample ($MC_{df}$) and the bolus at the start of mastication (y-intercept) was taken as the amount of saliva to be added at the start of mastication. This was determined for every subject and the average value of the five subjects was used. The amount of the xanthan gum solution to be added, to simulate saliva addition, was calculated on a wet weight basis. Artificial saliva with enzymatic functions was not used in this stage for practical reasons. The enzymatic effects were not the focus in this research and thus would not have been significantly important in the breakdown of the foods selected.

*Table 4-5: A summary of the rate of saliva addition, initial moisture content (MC) of the bolus, and the $R^2$ of the line fitted to five replicates for each subject. The initial saliva is obtained by subtracting the moisture content of the peanuts (0.026 g/g dry solids) from the initial MC.*

| | Rate (g/chew) (slope) | Initial MC (g/g dry wt) (y-intercept) | $R^2$ for fitted line | Initial Saliva (g/g dry wt) |
|---|---|---|---|---|
| Subject A | 0.013 | 0.214 | 0.214 | 0.189 |
| Subject B | 0.013 | 0.162 | 0.162 | 0.137 |
| Subject C | 0.019 | 0.103 | 0.103 | 0.077 |
| Subject D | 0.018 | 0.081 | 0.081 | 0.056 |
| Subject E | 0.014 | 0.195 | 0.195 | 0.170 |
| Average | 0.015 | 0.151 | 0.151 | 0.126 |

Eight peanut halves (3.0 ± 0.05g) were placed on the occlusal surface of the MR and 0.1% xanthan gum (XG) solution was added to simulate saliva addition. 0.3 ml of XG solution was added at the start and 0.036 ml was subsequently added after each mastication cycle, using a syringe pump, (NE-1010, New Era Pump Systems Inc., New York). Samples were collected after different chewing cycles (N=2, 3, 7, 14), washed and dried prior to image analysis to obtain the particle size distributions of the chewed samples. The sample collection was repeated three times for each chewing trial of N cycles for N= 2,3,7 and the boluses were pooled together to obtain the PSD for each trial. Four replicates were done for N=14 and the bolus for each replicate was collected separately for PSD analysis. All trials were randomised.

### 4.2.4. Image Analysis

At the start, the sieving method was used to be consistent with the test method employed by Van der Bilt, A. et al. (1987) in which optosil was used to determine chewing efficiency. However, the MR was unable to break down the optosil, thus the method of analysis will be reverted to the method used in chapter three which is the image analysis technique developed by Hutchings (2011) for study on peanut particle boluses. Each bolus sample was sieved across a 355 μm sieve with warm water for 4 minutes to remove particles smaller than 0.1mm$^2$ before being dried in an oven at 65°C for 1.5h as this dried the particle surfaces sufficiently. The dried peanut particles were placed in petri dishes (140 mm diameter) (Biolab, Auckland, New Zealand) and 60 ml of absolute ethanol (Polychem Marketing Ltd, Auckland, New Zealand) was added to facilitate particle separation. A flat spatula (2mm width) was used to separate the particles before the particles were scanned at 800 dpi (Epson Perfection, 3490, Photo) in colour. The images were processed using Image J® (1.50i, National Institutes of Health, USA). A black and white threshold was applied to obtain binary images and a watershed algorithm was used to separate any abutting particles. The scale measurement was set to 31.5 pixels per mm and the Analyse Particles command was applied to the selected image. A minimum size threshold was set to filter out any remaining <0.1mm$^2$ particles. The data output was exported to Excel and the cumulative particle size distribution in terms of area was obtained for each bolus. All boluses collected from subjects and the boluses collected from the MR after 2, 3, 7 chewing cycles were pooled for PSD analysis. Each replicate bolus collected from the MR after 14 chews was analysed separately to determine if the MR had good reproducibility.

The $d_{25}$, $d_{50}$ and $d_{75}$, which are the theoretical sieve sizes (mm) through which 25%, 50% and 75% of the total projected area of the particles will pass, was determined for each sample's distribution. The factorial design and analysis were performed on the PSD of boluses collected from the MR after 14 chews using Minitab 17 (Minitab Software Inc., USA). The response optimizer function was used to determine the optimum settings for each factor to achieve a minimum $d_{50}$. To characterise the PSD of the boluses, the Rosin-rammler function was fitted to the distributions to obtain the $x_{50}$ and $b$ value.

### 4.2.5. Comparison of breakdown between the MR and subjects

The boluses produced using the MR with a lateral chewing trajectory had a smaller $x_{50}$ than those chewed with the vertical chewing trajectory when the comparison was made after two chews.

However, the differences due to the effect of trajectory were greatly reduced as the number of chewing cycles increased. From the results in *Table 4-6*, it could not be concluded if the different settings for the sagittal plane and occlusal velocity affected the $x_{50}$. To determine if the differences between the results were significant, ANOVA analysis was carried out on the replicate results of the boluses collected after 14 chews. There was good reproducibility for the PSDs of the replicate boluses with the maximum standard deviation smaller than 8%.

*Table 4-6: The results for the factorial design showing the $x_{50}$ for each of the eight settings at 2, 3, 7, and 14 chews. Replicate boluses collected after 2, 3, and 7 chews were pooled for image analysis. The boluses after 14 chews were collected separately for image analysis and the result shown is the mean of four replicates (± SD).*

| Run Code | Trajectory | Coded Factors SP (°) | Coded Factors OV (mm/s) | $x_{50}$ after N chews N=2 | $x_{50}$ after N chews N=3 | $x_{50}$ after N chews N=7 | $x_{50}$ after N chews N=14 |
|---|---|---|---|---|---|---|---|
| R111 | lateral | 0 | 15 | 2.73 | 2.90 | 2.32 | 1.67 ± 0.11 |
| R112 | lateral | 0 | 20 | 3.62 | 2.24 | 1.88 | 1.75 ± 0.12 |
| R121 | lateral | 15 | 15 | 3.46 | 3.46 | 2.28 | 1.61 ± 0.11 |
| R122 | lateral | 15 | 20 | 3.65 | 3.16 | 2.13 | 1.73 ± 0.10 |
| R211 | vertical | 0 | 15 | 5.40 | 4.14 | 2.87 | 2.29 ± 0.08 |
| R212 | vertical | 0 | 20 | 7.20 | 4.95 | 2.93 | 2.14 ± 0.17 |
| R221 | vertical | 15 | 15 | 5.33 | 3.55 | 2.33 | 1.90 ± 0.05 |
| R222 | vertical | 15 | 20 | 4.21 | 4.15 | 2.40 | 1.81 ± 0.06 |

SP: angle in which the sagittal plane is set, OV: occlusal velocity

The trajectory had the greatest effect on the PSD of the boluses, followed by the angle of the sagittal plane (Table 4-7). The interactions between trajectory and angle of sagittal plane and trajectory and occlusal velocity also had significant effects on the PSD of the boluses. The residual plots in Figure 4-13 showed that the residuals were of normal distribution and were stochastic.

*Table 4-7: ANOVA results for the factorial design analysing the $x_{50}$ of replicate boluses after 14 chews.*

| Source of variation | SS | DF | MS | F-Value | P-value |
|---|---|---|---|---|---|
| T | 0.865 | 1 | 0.865 | 79.17 | 0.000 |
| SP | 0.374 | 1 | 0.374 | 34.22 | 0.000 |
| OV | 0.008 | 1 | 0.008 | 0.69 | 0.414 |
| T*SP | 0.162 | 1 | 0.162 | 14.82 | 0.001 |
| T*OV | 0.065 | 1 | 0.065 | 5.95 | 0.022 |
| Residual | 0.284 | 26 | 0.011 | - | - |
| Total | 1.757 | 31 | - | - | - |

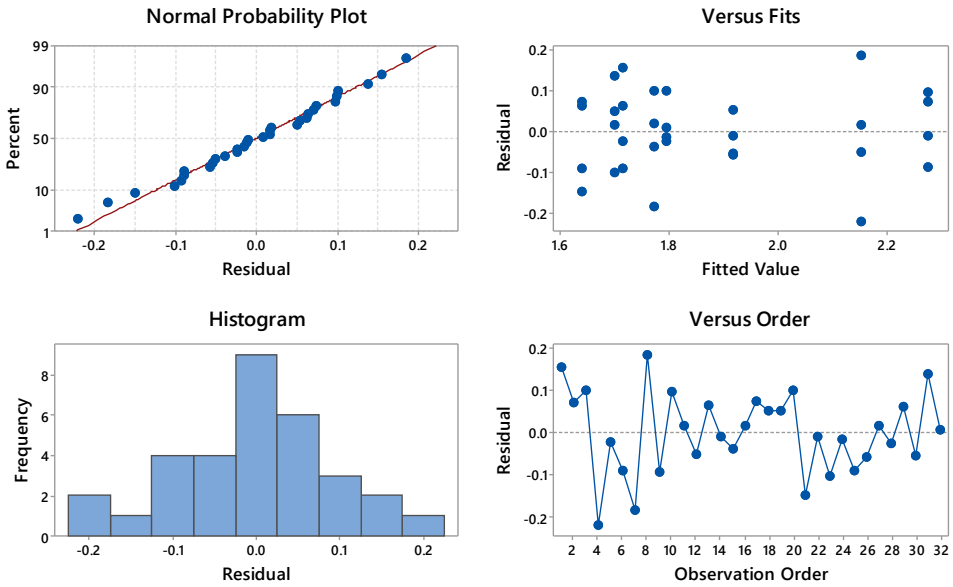


*Figure 4-13: Residual plots for $x_{50}$ of replicate boluses after 14 chews.*

The main effects plot (Figure 4-14) shows that chewing in the lateral trajectory, with the sagittal plane at an angle of 15° and at a higher occlusal velocity resulted in a PSD with a smaller $x_{50}$, although the occlusal velocity's effect was not significant (p=0.414). The interaction plot (Figure 4-15) shows that the effect of the angle of the sagittal plane on reducing the $x_{50}$ was greater with a vertical trajectory. The occlusal velocity affected the $x_{50}$ differently depending on the chewing trajectory, where a lower occlusal velocity resulted in greater reduction of the $x_{50}$. The interaction effects between trajectory and sagittal plane and trajectory and occlusal velocity were significant ($p<0.05$). The optimum settings to obtain a PSD with minimum $x_{50}$ would be to use a lateral chewing trajectory, with the sagittal plane set at an angle of 15° and using a lower occlusal velocity. Thus, the results from run code R121 was used for comparison with the results from the subjects.

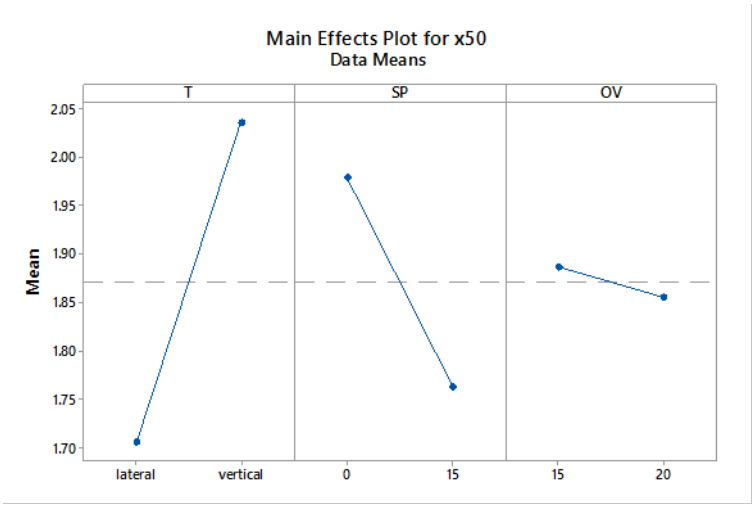


*Figure 4-14: The main effects plot showing the effects of each factor on the data means for $x_{50}$.*

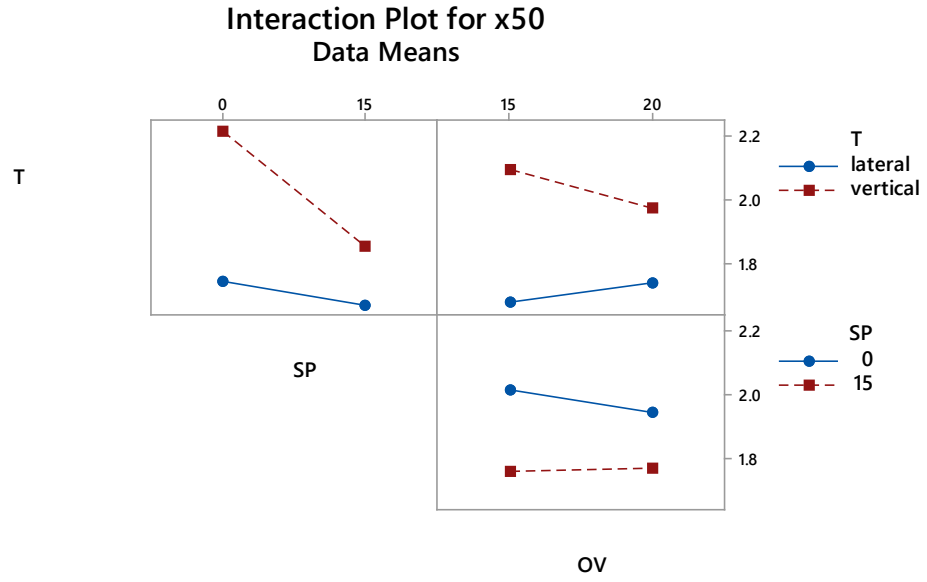


*Figure 4-15: The interaction plot showing interaction effects on the data means for $x_{50}$.*

The subjects are significantly better than the MR at breaking down the food particles (Figure 4-16; Table 4-8). The "swallow point" for the MR was 35 chewing cycles so that the PSD could be compared with the median swallow point from the human subjects (subject A). The boluses collected from run R121, which provided the best breakdown of the peanut samples, used the following parameters: lateral trajectory, 15° sagittal plane, and an occlusal velocity of 15mm/s. Although the subjects have different rates of breakdown and the number of chewing cycles needed for the peanuts to reach the swallow point varied, the PSDs at the swallow point were similar. This agrees with previous work that found that there was small inter-individual variability in the PSD at swallow point of the bolus for a given food type although there was wide inter-individual variability in the physiological parameters such as the number of chewing cycles (Jalabert-Malbos et al., 2007; Mishellany et al., 2006; Peyron et al., 2004).

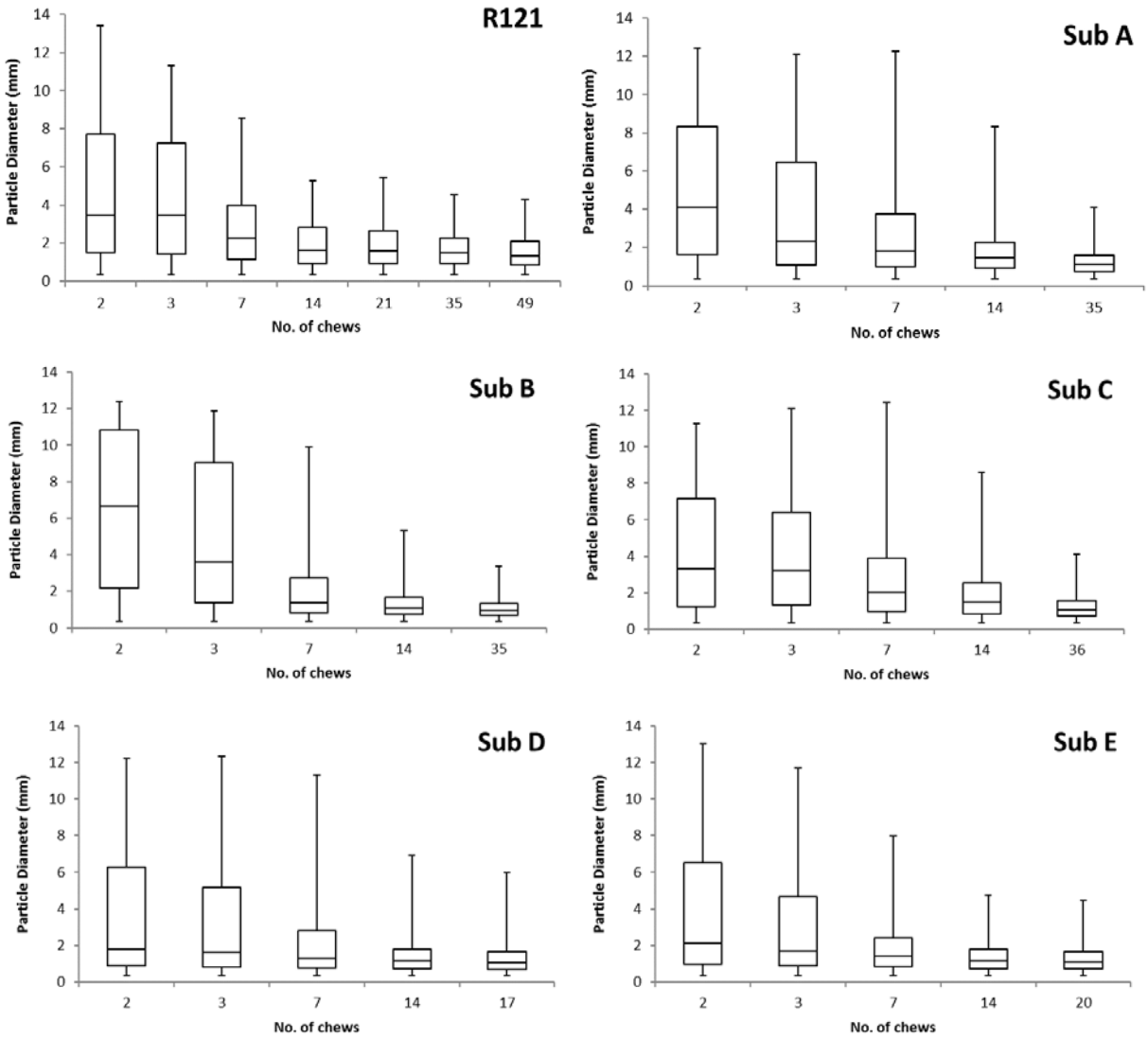


*Figure 4-16: The boxplot shows the PSD of the boluses collected from the MR and subjects after N number of chewing cycles where the 1st, 2nd and 3rd marking represents the $d_{25}$, $d_{50}$ and $d_{75}$ respectively. The error bars represent the diameter of the largest and smallest particle present.*

The $x_{50}$ of the peanut boluses collected from the subjects in the initial chews up to 14 chews was comparable between the MR and the subjects (Figure 4-17a). However, the $x_{50}$ of the boluses collected at swallow point from the subjects was smaller than that for the robot. The broadness of the PSDs was similar between the MR and the subjects except for subject B (Figure 4-17b). The larger b value (subject B) reflects the narrow distribution of the boluses collected after seven chews. This is seen in the cumulative PSD of the boluses collected after 14 chews (Figure 4-18) whereby the slope of the distribution for subject B was the steepest.

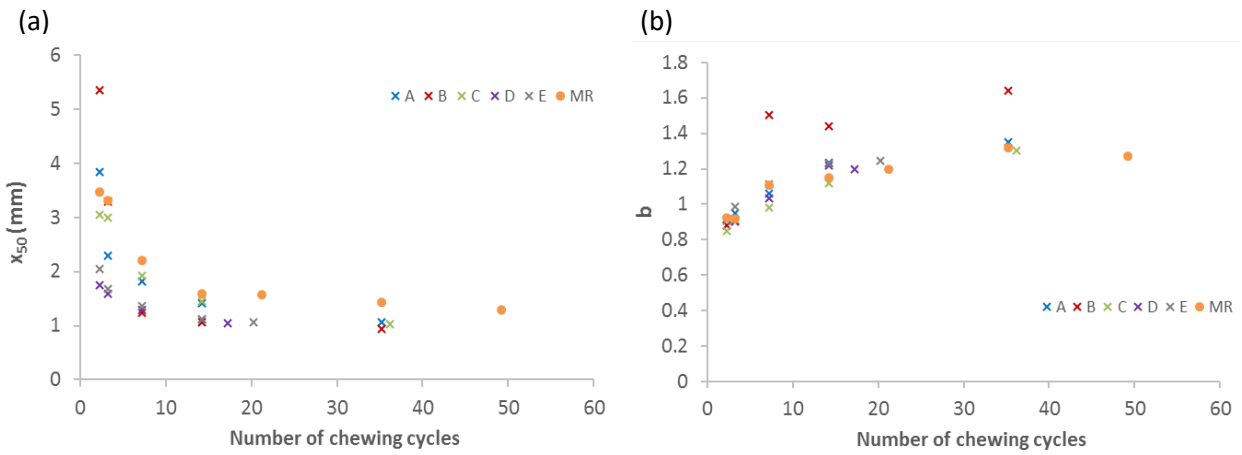


*Figure 4-17: The $x_{50}$ and $b$ values obtained from the Rosin-Rammler function fitted to the PSD of the pooled boluses collected after 2, 3, 7, 14 chewing cycles and at the respective swallow point for each subject and the MR.*

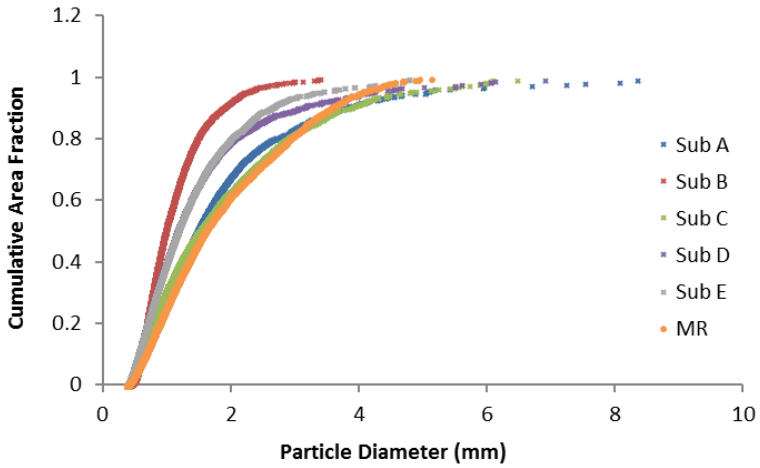


*Figure 4-18: The cumulative particle size distribution of the pooled boluses collected from the subjects and MR after 14 chews.*

The $x_{50}$ of subject A at 14 chews is comparable with that of MR at more than twice the number of chewing cycles at 35 chews (Table 4-8). Although there is still breakdown of particles in the MR after 14 chews, the rate of breakdown had decreased and was plateauing. Poorer breakdown in the MR could be due to the lack of a good sensing system to transfer the larger particles onto the occlusal surface after each chew. In the mouth, the tongue evaluates the geometrical properties of the particles and returns the larger particles to the occlusal surface for breakdown, which is partly a by-product of the natural mixing motion and manipulation by the tongue and cheeks (Mioche, L. et al., 2002). In the MR, the selection of the particles to be placed onto the occlusal surface is a random process which may not be as efficient. Probable reasons would be that the bite forces in the subjects are higher than the MR or the amount of shearing and resulting occlusal contact area in the subjects are higher than in the MR. At this point, no further tests were done to determine the cause of the poorer breakdown in the MR, but future work will be required to improve the MR.

Quantifying the chewing efficiency by determination of the number of chewing cycles needed to halve the initial particle size was not applicable to peanuts as the brittle nature of peanuts resulted in them achieving half the initial particle size within the first chew. Instead, the PSDs of the peanut particles were compared using boxplots as seen in Figure 4-16.

*Table 4-8: The $d_{50}$ determined from the PSD of the boluses after 2, 3, 7, 14 chewing cycles and at swallow point for the five subjects and the MR (R121).*

| Chews | Sub A | Sub B | Sub C | Sub D | Sub E | R121 |
|---|---|---|---|---|---|---|
| **2** | 4.10 | 6.67 | 3.09 | 1.79 | 2.09 | 3.46 |
| **3** | 2.29 | 3.64 | 3.03 | 1.62 | 1.71 | 3.46 |
| **7** | 1.79 | 1.38 | 1.96 | 1.33 | 1.40 | 2.28 |
| **14** | 1.45 | 1.06 | 1.48 | 1.15 | 1.15 | 1.61 |
| **SP** | 1.11 | 0.96 | 1.06 | 1.07 | 1.10 | 1.48 |

Although the MR is unable to achieve the breakdown efficiency similar to that of subjects, it could still be used to understand how the chewing trajectories and occlusal velocities would affect food breakdown. Other factors could be adjusted such that the MR is able to achieve similar PSD as that of subjects. A relationship/model may then be established to relate the breakdown ability of the MR and subjects. Thus, further work was done to explore if the portion size or higher force could be manipulated so that the MR could achieve a similar degree of breakdown as the subjects.

### 4.2.6. Effect of portion size and baseline force on the MR efficiency

An experiment was carried out to investigate the influence of portion size and baseline force on the MR's efficiency. The portion size to be chewed by the MR was reduced, and baseline force was increased as in Table 4-9. The same parameters that provided the best breakdown in the previous section were used: lateral trajectory, 15° sagittal plane, and an occlusal velocity of 15mm/s. There were three replicates for each portion size and baseline force. The boluses collected from the MR after 14 chewing cycles were pooled for PSD analysis.

*Table 4-9: A table of how the parameters of portion size and baseline force were varied for the experiment.*

| | Portion size | Number of half peanuts | Weight (g) |
|---|---|---|---|
| Experiment 1 | 0.25 | 2 | 0.75 |
| | 0.5 | 4 | 1.50 |
| | 0.75 | 6 | 2.25 |
| | 1 | 8 | 3.00 |
| | Baseline force (N) | Stage height (mm) | |
| Experiment 2 | 0 | | |
| | 100 | | |
| | 200 | | |
| | 270 | 5.8 | |

The PSDs of the boluses were reduced when the portion size of the peanut halves was reduced and the baseline force in the MR was increased (Figure 4-19). The $x_{50}$ of the bolus collected from half the portion size and at baseline force of 270N was similar to that of subject A (Table 4-10). Thus, these factors could potentially be used to achieve the chewing efficiency of humans if the MR was required to produce boluses from simulated human chewing.

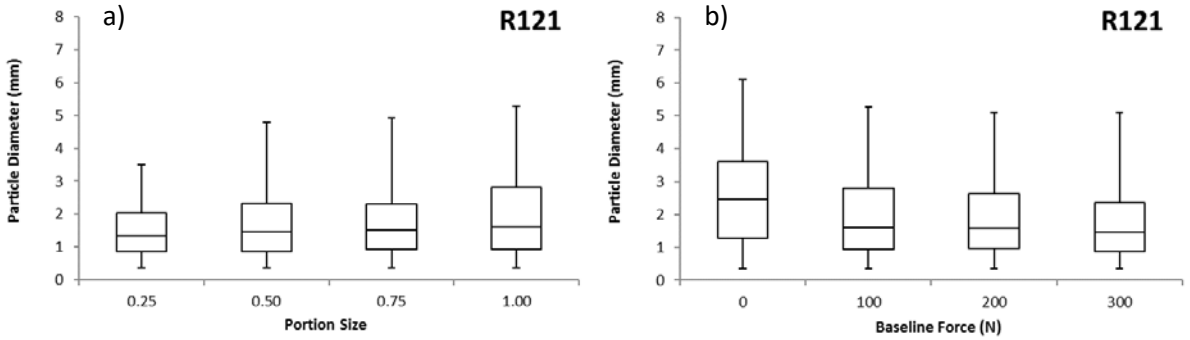


*Figure 4-19: The PSD of the boluses collected from the MR after 14 chewing cycles: (a) The effect of decreasing portion size from 1 to 0.25 of the 8 peanut halves on the PSD of resulting bolus. (b) The effect of increasing baseline force exerted during mastication, of 8 peanut halves, on the PSD of resulting bolus. The 1st, 2nd and 3rd marking of the boxplot represents the $x_{25}$, $x_{50}$ and $x_{75}$ respectively. The error bars represent the diameter of the largest and smallest particle present.*

*Table 4-10: The $x_{25}$, $x_{50}$ and $x_{75}$ determined from the PSD of the boluses collected from the MR and subject A after 14 chewing cycles. The variables were portion size and baseline force in the MR using the same mastication parameters from run R121.*

| **Portion size** | **0.25** | **0.5** | **0.75** | **1** | **Sub A** |
|---|---|---|---|---|---|
| **x50 @ 14C** | 1.35 | 1.46 | 1.50 | 1.61 | 1.45 |
| **x25 @ 14C** | 0.86 | 0.85 | 0.92 | 0.93 | 0.89 |
| **x75 @ 14C** | 2.03 | 2.32 | 2.31 | 2.81 | 2.29 |
| **Baseline Force** | **0N** | **100N** | **200N** | **270N** | **Sub A** |
| **x50 @ 14C** | 2.47 | 1.61 | 1.57 | 1.45 | 1.45 |
| **x25 @ 14C** | 1.29 | 0.93 | 0.97 | 0.87 | 0.89 |
| **x75 @ 14C** | 3.60 | 2.81 | 2.64 | 2.37 | 2.29 |

## 4.3. Conclusion

In this validation study, it was found that Optosil was too tough and unsuitable as a test food for the MR to breakdown once the particles reached a certain size, even though human subjects were able to adapt the chewing pattern to break down the Optosil. A combination of factors such as the subjects ability to: (a) exert a larger bite force, (b) provide more shearing action to crush the small particles, or (c) position the broken-down particles better at the breakage sites such that the sharp cusps could contact the particles at an angle that is more efficient in breaking up the particles. Based on the PSD of the peanut boluses, it can be concluded that the MR has poorer breakdown capability in comparison to the human subjects. Through the $2^3$ factorial design, an optimal combination of parameters was determined, and as a confirmation of the optimal settings, the boluses collected from run R121 provided the best breakdown of the peanut samples and subsequent runs used the following parameters: lateral trajectory, 15° sagittal plane, and at a slower occlusal velocity of 15mm/s. This chapter characterised the limitations of the MR and identified that the reduction of portion size or increased baseline force as a possible solutions if the MR was needed to closely replicate a human subject.

To overcome the limitations of the MR, improvements that could be made to the mastication robot are the inclusion of temperature control in the "oral cavity" and for the saliva added, having a tongue system for repositioning the unchewed particles onto the occlusal surface and mixing of particles with saliva for bolus formation, having a cheek system to keep the particles on the occlusal surface in between chews. The temperature of the oral cavity would be important in sensory perception and the formation of the bolus especially for foods that are creamy or are high fat such as chocolate. The melting of the fat would contribute to the sensations perceived for such food which would affect the chewing dynamics, thus it is ideal to have the temperature controlled such that it is similar to that of the oral cavity. There is no temperature control present in the current robot, which is a limitation if such food type needs to be studied. However, none of the foods selected for the current work are high in fat and thus, temperature control is not significantly important.

Although the MR was unable to achieve similar breakdown capability as that for the human subjects, the MR proved to have good reproducibility in bolus preparation as seen from the standard deviation (<8%) of the $x_{50}$ of the PSDs collected from replicate measurements. Thus, the MR is still relevant as a tool to produce boluses at various stages of mastication in a reproducible manner. In

addition, the MR breakdown capability was comparable to the poorest performing subject which shows that the MR could be used for comparative analysis especially for studies investigating the properties of boluses collected from various stages of the mastication process. In hindset, rather than taking an average, it would have been better to match setting parameters to the median subject as was done in later chapters. The limitation of using the setting parameters based on an average rather than an individual is that the resulting breakdown and mastication efficiency is not usable as a direct comparison with that of an individual subject. From the human study, similar trends in particle breakdown were observed for both Optosil and peanuts. Subjects who could break down the peanuts well had better mastication efficiency.

Although the PSD is one of the factors contributing to bolus formation, it should not be used independently as the determining criterion in triggering a swallow. Other factors related to the rheological properties such as the lubrication of the bolus through the absorption of saliva contribute to the triggering of a swallow (Chen, Jianshe, 2012; Peyron, Marie-Agnès et al., 2011). Through a hazard and operability analysis, Gray-Stuart (2016) had identified that bolus deformation and adhesion (slippage of bolus) were two of the determinant properties for safe swallowing. Thus, these bolus properties should also be studied. The following chapter will focus on two novel techniques developed to characterise some of these bolus properties.

# Chapter Five  Development of novel bolus characterisation methodologies

There has been much interest in understanding how chewing strategies affect the dynamic changes in bolus properties which influences the sensory perception of food during breakdown leading up to a safe-to-swallow bolus. It was thought that the individual size of the bolus particles influenced bolus cohesion, which in turn, was crucial for a safe swallow. Thus, particle size distribution was often used to characterise the boluses (Hutchings, Scott C. et al., 2012; Jalabert-Malbos et al., 2007; Mishellany et al., 2006; Peyron, M. A. et al., 2004). In some studies, the rheological or instrumental textural measurement of boluses were used to understand the dynamic changes in food structure during oral processing (Devezeaux de Lavergne, Marine et al., 2016; Loret et al., 2011a; Panouillé, M. et al., 2014; Young et al., 2013; Yven, C et al., 2005). These methods can be useful but some cannot be applied to non-brittle or non-fracturable materials. Some methods can only be applied to initial foods or after only a few chews, while some methods are only suitable for a well chewed bolus. Ideally, we would like methods that can be applied from the initial bite to swallow point and to all foods.

A novel technique called the multiple pin penetrometer (MPP) built by Al-Battashi et al. (2015), may potentially be used to characterise the variability in structure of boluses – especially lending itself to fibrous meat products that do not form discrete particles. This could provide distribution data, similar to how particle size distribution is used to characterise discrete collections of particles in boluses formed during the chewing of fracturable materials.

The slip extrusion method was also developed in this study to characterise properties related to swallowability that can be applied to all foods at any stage of oral processing. In this chapter, these two novel methodologies are developed and evaluated as tools for characterisation of oral processing.

## 5.1. Multiple Pin Penetrometer

***Overview of the Multiple Pin Penetrometer***

The multiple pin penetrometer attachment consists of 1024 flat end cylindrical pins (1 mm diameter) and was mounted on a TA-XT plus texture analyser (Stable Micro Systems Ltd, UK) to control vertical movement of the device into the food. A Tact Array pressure sensor, (Industrial TactArray 5229,

Pressure Profile Systems Inc, USA), was used to measure the forces experienced by each pin independently as they travelled through the food. The MPP was built to measure the spatial distribution of texture in foods exhibiting heterogenous structures. However, it has not been well established and there has been little work done to validate the approach and demonstrate its application.

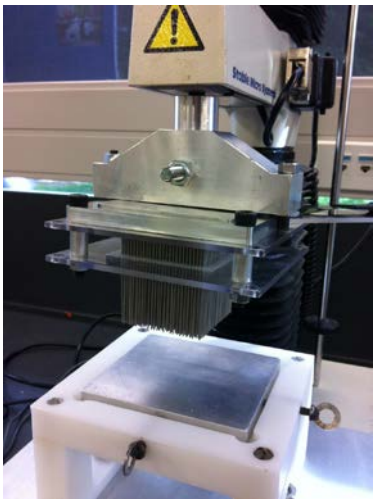

*Figure 5-1:Experimental set up of the multiple pins penetrometer attached to the TA.XT2 Texture Analyser.*

***Methodology***

The pins could be adjusted to different configurations and the MPP attachment was mounted on the texture analyser as seen in Figure 5-2. The test was conducted in compression mode at a crosshead speed of 0.65 mm $s^{-1}$ and set to travel the required distance. The Chameleon TVR software (2012, Pressure Profile Systems Inc, USA), was used to acquire the data and provide real-time visualisation of the force profiles measured by the sensor. The data collected was saved as a csv file for analysis using Microsoft Excel or MATLAB® R2016a.

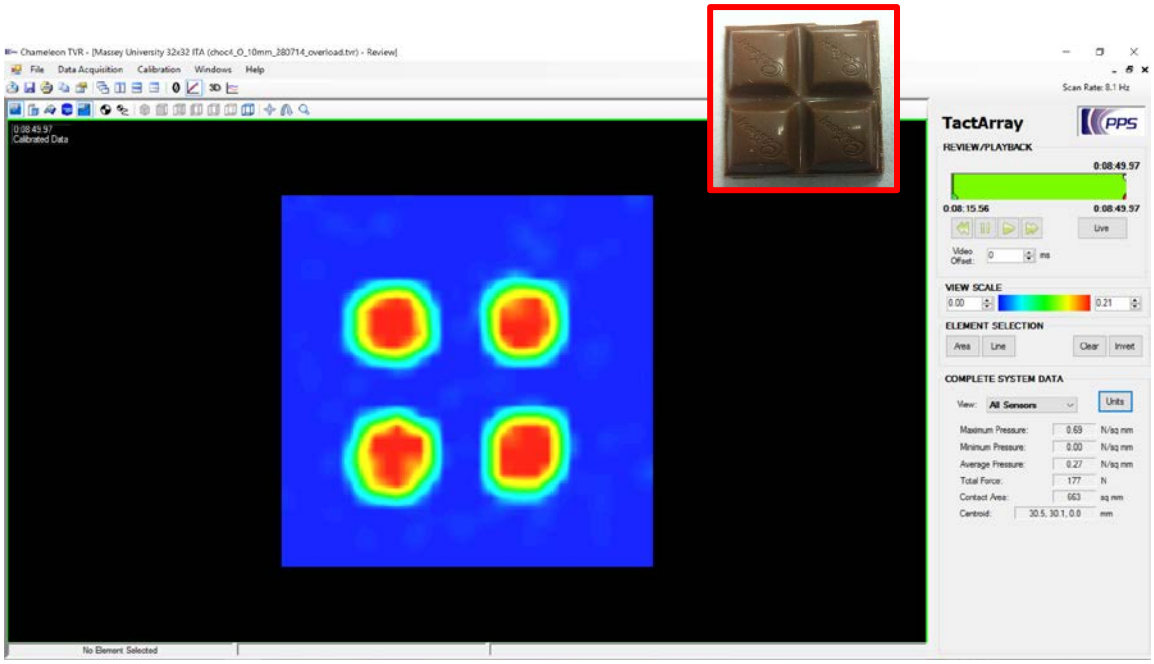


*Figure 5-2: Screenshot of the Chameleon TVR software showing the forces measured as the MPP attachment penetrated a piece of solid chocolate bar (shown on right inset).*

### *Data Analysis*

The data collected was displayed in a table (Table 5-1) and analysed using MATLAB® R2016a. The data was rearranged into a 32 by 32 matrix for each time point and a surface plot was used to present the pressures measured for each pin. A cumulative frequency function was used to describe the pressure distribution measured by the pins. The $P_{50}$ is the median pressure measured by the pins that were in contact with the sample and in many ways is similar to the $d_{50}$ (median particle size) from a PSD in that it represents the median property of a distribution. In a similar way as done for PSD analysis, a measure of variance such as the range or a fitting parameter (like *b* in the Rosin-rammler function) could be also used to characterise the data.

*Table 5-1: A summary of the data collected and exported to a csv file for further data analysis, where the pressures measured by the 1024 pins were indicated by elements 0 to 1023 for each time interval.*

| Time (s) | Average Pressure ($N.mm^{-2}$) | Maximum Pressure ($N.mm^{-2}$) | Minimum Pressure ($N.mm^{-2}$) | Total Force (N) | Contact Area (sq mm) | Elem0 ($N.mm^{-2}$) | Elem1 ($N.mm^{-2}$) | Elem2 ($N.mm^{-2}$) | Elem3 ($N.mm^{-2}$) | … … | Elem1023 ($N.mm^{-2}$) |
|---|---|---|---|---|---|---|---|---|---|---|---|

### 5.1.1. Preliminary Evaluation

Because it was a new method, some questions on its operation needed to be investigated, It was possible that adjacent pins could interfere with each other, and edge effects could exist for the outer pins in the array. To investigate these issues, a preliminary evaluation of the multiple pin penetrometer was done which included exploring how the different orientations of the pins affect the pressure measurements and how the data collected may be analysed.

Texture analysis was conducted on two known homogenous materials (expanded foam rubber and expanded polyurethane foam) as shown in Figure 5-3. The multiple penetrometer attachment was used to puncture the elastic rubber to a depth of 10 mm and stiff foam board to a depth of 4 mm. Three different pin orientations were used for the texture analysis; (a) all pins present, (b) every alternate and diagonal pin removed, and (c) alternate rows of pins removed. The pins were removed in different orientations to check if there were any interactions between pins, such as small forces that were measured in neighbouring spaces even though there were no pins present in those spaces.

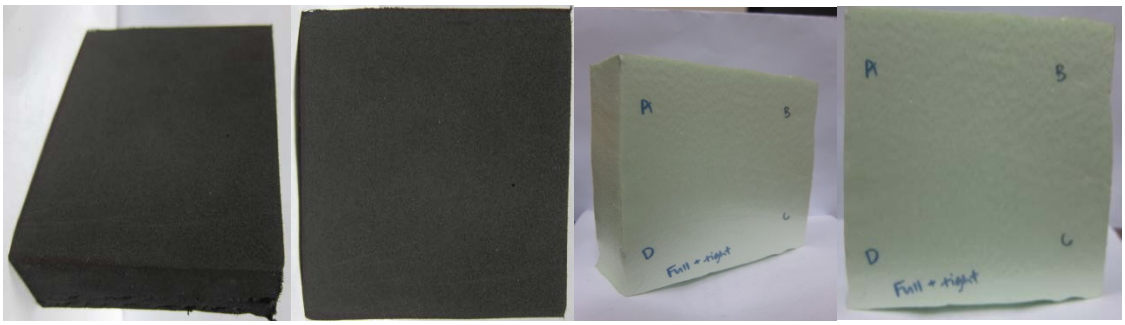


*Figure 5-3. The elastic material and stiff foam board used.*

It was noted that there was some background noise as the probe travelled towards the food even before the pins reached the food (Figure 5-4). The noise consists of pressures of 0.0138 to -0.0207 $N.mm^{-2}$ being measured even though no pins are in contact with the food. To remove the noise, the minimum force measured by each pin before the pins made contact with the food was determined. This minimum force was then subtracted from the subsequent measurements of each respective pin.

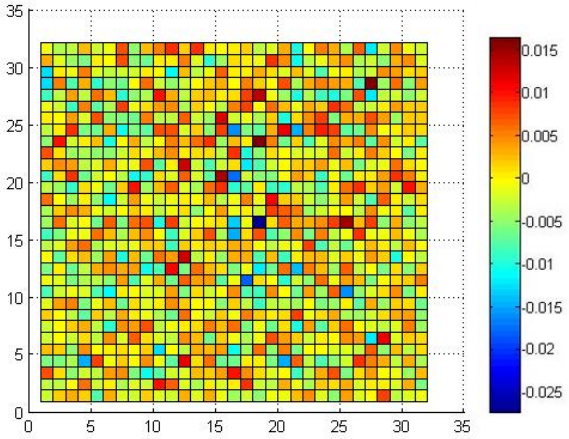


*Figure 5-4. Surface plot of the pressures measured by the sensor at a single time before the pins come into contact with the food; colourbar: pressure (N.mm$^{-2}$).*

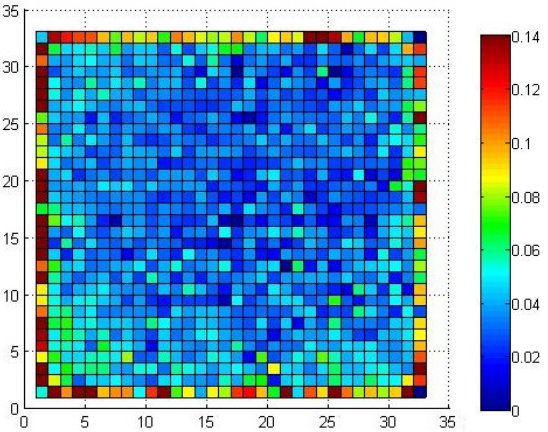


*Figure 5-5. Pressure profile on an elastic material at a depth of 10mm with all pins; colourbar: pressure (N.mm$^{-2}$).*

With the full number of pins in place to compress the elastic rubber, the pins did not puncture into the material, but pushed the rubber outwards, hence the higher pressures measured at the outer edges (Figure 5-5 and Figure 5-6). Similar behaviour may occur if the MPP is applied to elastic foods. This effect will not be observed if the area of the food sample is contained within the MPP array area.

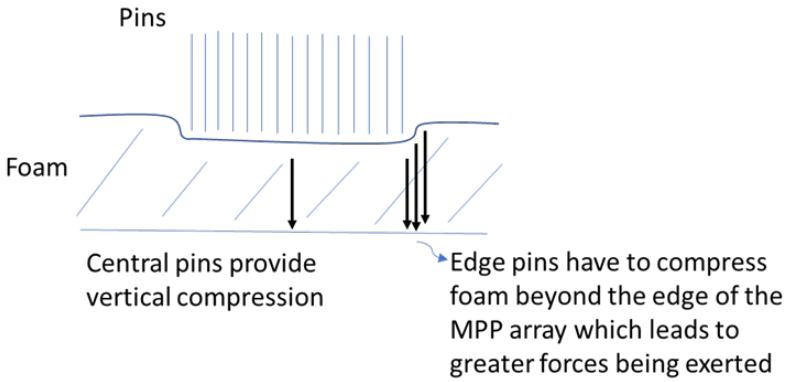


*Figure 5-6: A side diagram illustrating the pins' interaction with the foam resulting in higher pressures measured at the outer edges.*

Figure 5-7 shows the force profiles achieved after pushing the MPP probe 4 mm into the stiff polyurethane foam with pins removed (a, alternate pin; b, alternate rows). For this material, the pins did puncture into the foam material, rather than simply compressing it as observed for the elastic foam rubber.

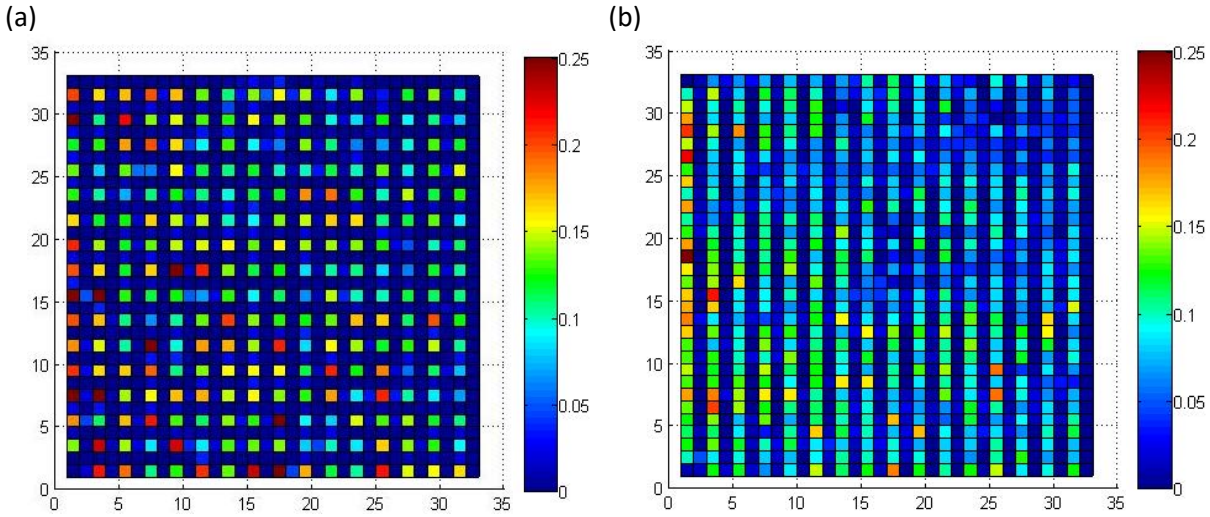


*Figure 5-7. The pressure profiles of the stiff foam at a depth of 4mm with every alternate pin (left) and alternate rows of pins (right) removed; colourbar: pressure (N.mm-$^{2}$).*

In these experiments, ideally, there should be no significant forces measured in the spaces where pins have been removed (Figure 5-7). The sensor did detect small pressures (<0.05 Nmm$^{-2}$) exerted in the empty areas, which suggest that there is some interaction between pins. Due to the structure of the penetrometer, the weight was not completely evenly distributed which caused it to slant towards the heavier side. Thus, higher pressures are measured on that side of the penetrometer as seen in the left and bottom sides of the profiles.

As shown in Figure 5-8, the pressure distributions were bi-modal, suggesting that the distributions at the lower range represent the pressures measured at the points where there are no pins. There were 25% pins present in the penetrometer for the alternate pin orientation, while there were 50% pins for the alternate row orientation. This agrees with the pressure distribution (Figure 5-8), whereby the modes of the lower pressure distributions correspond to the 75$^{th}$ percentile and 48$^{th}$ percentiles. This shows the possibility of using pressure distribution curves to characterise the heterogeneity of a food sample and that while some interactions between pins exists, this is relatively small and can be ignored.

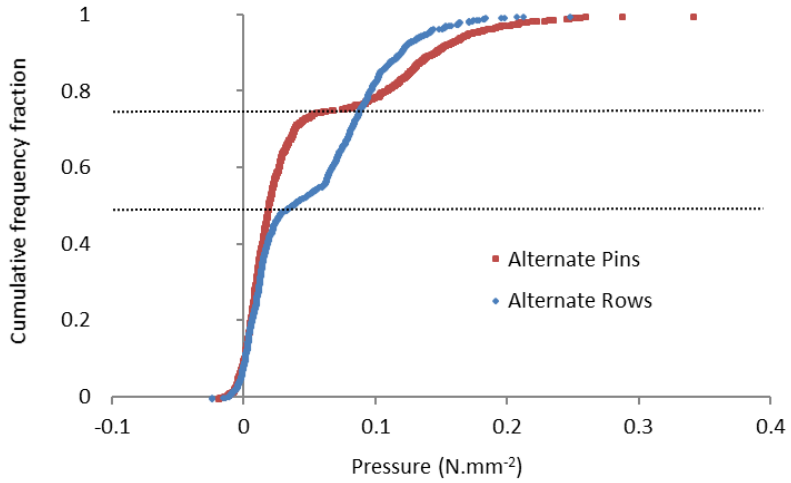


*Figure 5-8. The pressure distributions of the two different pin orientations at a depth of 4mm.*

### 5.1.2. Application to different foods

This part of the chapter explores the textural information that can be obtained from the multiple pin penetrometer using different types of food. There will be a few case studies looking at foods of varying homogeneity and hardness. The selected foods were fresh tomatoes, Tim Tam biscuits (Arnott's Biscuits Holdings, Sydney, Australia), marinated green lipped mussels (Countdown, New Zealand), and four types of chocolate bar (Cadbury, Victoria, Australia).

***Case study 1- fresh tomatoes***

Tomato was selected as its cross section has three distinct sections (Figure 5-9). The test should be able to show the differences between the hard peripheral pericarp, the softer and watery locular gel, and the porous columella. The multiple penetrometer attachment was used to puncture the cross section of a tomato to a depth of 4 mm. The test was run using a pre-test and test speed of 0.65 mm $s^{-1}$ and a trigger force of 0.1 N. Each tomato half is placed on a plastic sheet with a grid and photographed as seen in Figure 5-9, before the test is conducted. The captured image is then used to visually identify and match the various parts of the tomato to the pressure profile measured by the MPP.

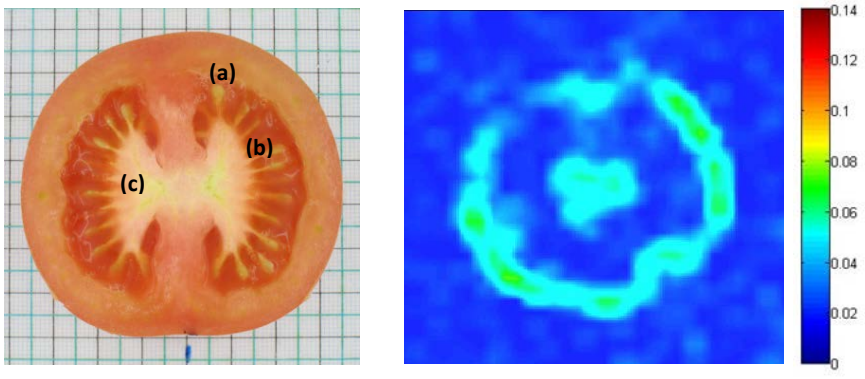


*Figure 5-9. The cross section of the tomato where (a) peripheral pericarp, (b) locular gel and (c) columella (left), and an example of the pressure map of the tomato; colourbar: pressure ($N.mm^{-2}$).*

In general compressional penetrometer texture measurements, the hardness of a food sample is usually indicated by the peak pressure measured during the puncturing. A steady increase of the pressure was observed as the peripheral pericarp was being punctured while the pressure profile of a pin in the columella showed multiple fractures (Figure 5-10). With reference to the various parts of the tomato as seen in Figure 5-9, the cell material of the peripheral pericarp is much harder and less porous as compared to the columella, which explains why there was a smaller peak pressure for the columella. The locular gel is relatively soft and is a semi-fluid, thus the pin was able to puncture through the gel with little resistance.

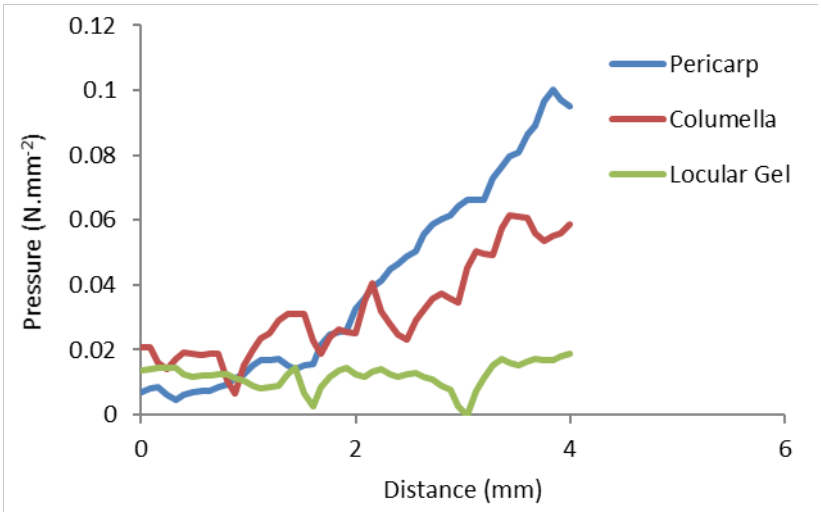


*Figure 5-10. Pressure vs distance profile of single pins in each region of the tomato.*

The results can provide the hardness profile of single pins in each region travelling through the food as well as provide an average hardness profile of all pins in each region. The latter method is more representative of the hardness at each region. The selected pin at the peripheral pericarp in Figure 5-10 was travelling through a harder part of the tomato, thus that single pin gave higher pressure

measurements than that of the average of five pins. Figure 5-11 shows the variation in the hardness profiles of five pins in the same region (std dev=0.024), therefore more pins travelling through a greater surface area would provide a more representative hardness profile.

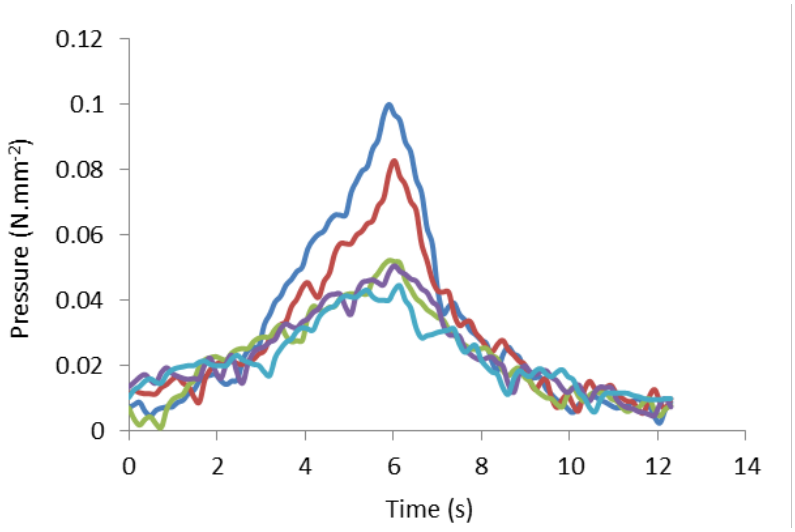


*Figure 5-11. Pressure vs time profile of five pins travelling through different locations within the peripheral pericarp region of the tomato.*

At maximum deformation, the peripheral pericarp is 50 % harder than the columella and 300 % harder than the locular gel. The pressure profile shows that some pressure is still being exerted on the pins as the pins are withdrawn from the tomato (Figure 5-12). However, the pressures are much lower, which indicates that the tomato does not recover after being punctured.

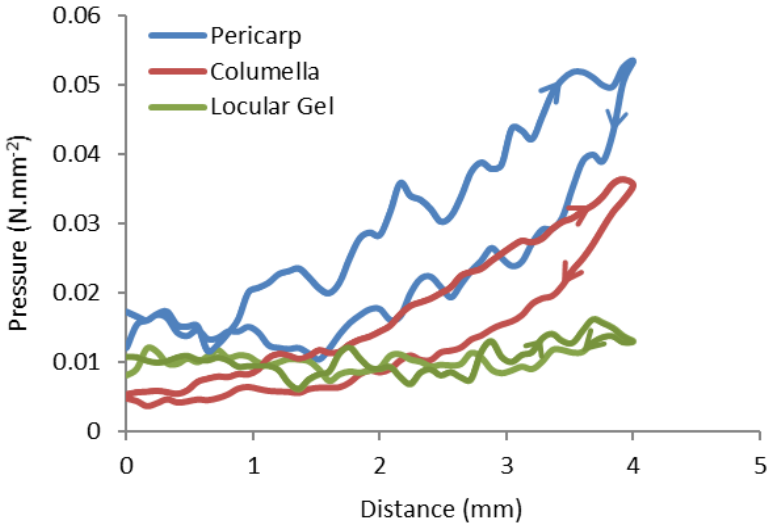


*Figure 5-12. Profile of the average pressure of five pins in each region of the tomato vs distance. The pressure increased and decreased as the penetrometer travelled into and left the food as indicated by the direction of the arrows.*

Figure 5-13 shows the distribution curves with the typical pressure found for each region indicated by the dotted lines. The distribution curve of the pins using the maximum pressure exerted on each

pin (irrespective of time) measured higher pressures compared to that of pressures measured during maximum deformation. This shows that at the point of maximum deformation, the cell walls of the softer parts of the tomato had already fractured. The depths at which the maximum pressures exerted could potentially be determined, and then displayed through a surface plot. This can provide information on the depths of the hardest point within a food.

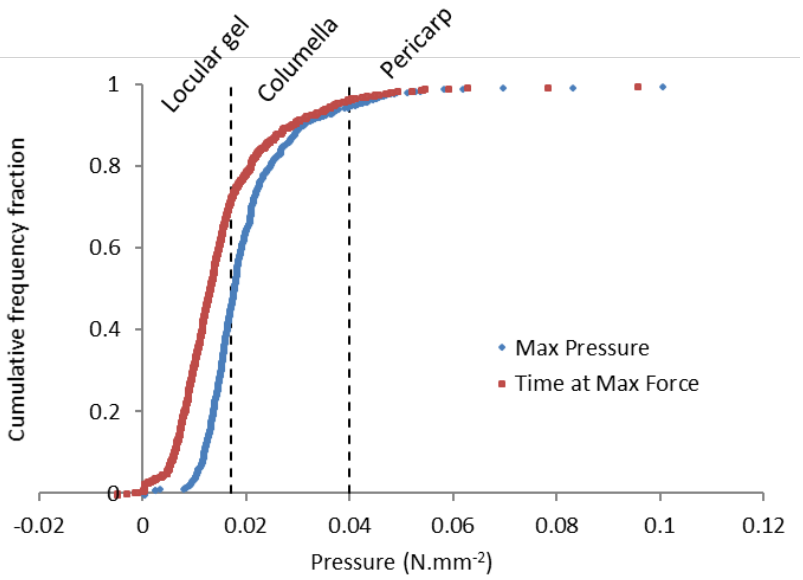


*Figure 5-13. The pressure distribution of pins across the whole tomato using (a) maximum pressure exerted on each pin, (b) pressures of pins at the time at which maximum force/deformation occurred.*

By obtaining a distribution like Figure 5-13, methods of analysis normally applied to particle size distributions could be achieved to characterise the texture. If this could be applied to a bolus, then this may potentially be a method to characterise food breakdown during oral processing.

***Case Study 2- Tim Tam biscuits***

The Tim Tam biscuit is a biscuit sandwich that has a chocolate cream filling in the middle and a chocolate coating around it. The biscuit was selected to test if the test could show differences between the hard chocolate coating, then porous biscuit and then the soft chocolate cream filling. The multiple penetrometer attachment was used to puncture a Tim Tam biscuit to a depth of 8 mm in two orientations as shown in Figure 5-14. The test was run using a pre-test and test speed of 0.65 mm $s^{-1}$ and a trigger force of 0.1 N.

*Figure 5-14. The attachment travelled down to puncture the Tim Tam biscuit (a) from the top and (b) through the cross section (sample was cut in half).*

The biscuit consists of a layer of chocolate cream filling that is sandwiched between two biscuits which are coated in chocolate on the external surface. Figure 5-15 shows the biscuits are much harder than the cream filling in the middle and thus provide clearer details of the hardness of the different layers in the food.

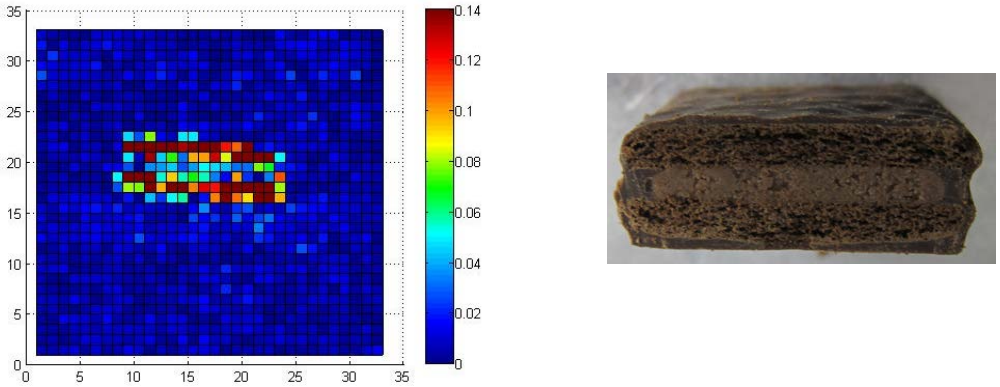


*Figure 5-15. Figure shows the pressure profile at the point where maximum force is exerted as the penetrometer travelled through the cross section of the Tim Tam biscuit; colourbar: pressure (N.mm$^{-2}$).*

Biscuit 1 and 2 shows a steady increase which accounts for the pins puncturing through the biscuit leading to the first peak, and the multiple fractures are due to the biscuit fracturing Figure 5-16. The pressures exerted by the cream remain at around 0.0414 N.mm$^{-2}$ as the cream is soft and the material flows during compression by the pin without much resistance.

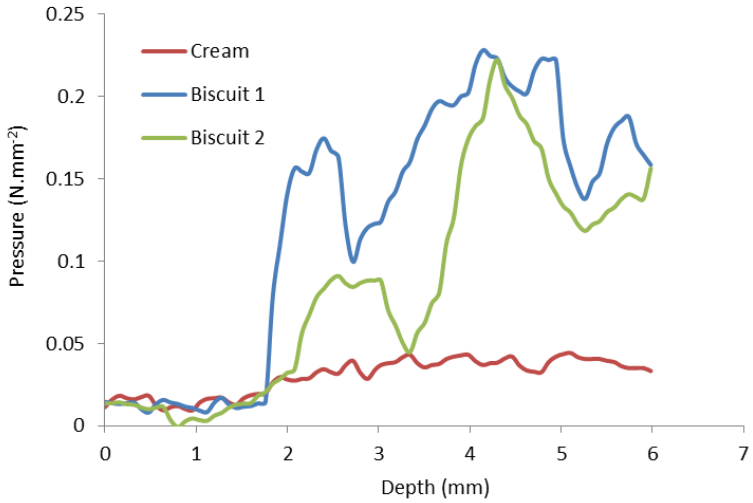


*Figure 5-16. The pressure profile at three locations of the Tim Tam biscuit as the penetrometer travels to a depth of 8mm.*

It has been noted that there is a lag time where there is no measurement of the pressures by the sensor for the first 2 mm due to the gap allowance between the sensor pad and the pins. Although the penetrometer had travelled the specified distance, the pressures measured by the pressure pad would be for a shorter distance. In the first 2 mm of measurement, the pressures experienced by each pin is probably too low to be measured, thus there is no steady increment in the pressure (Figure 5-16). A pressure pad with a lower pressure range would be ideal to correct this problem.

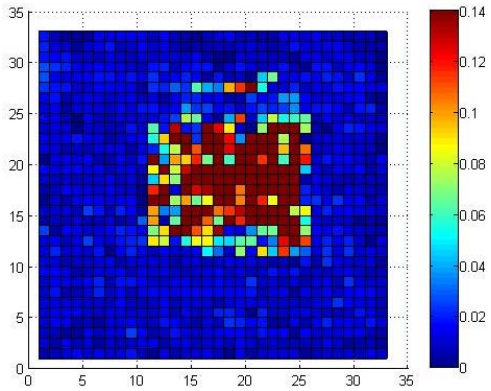


*Figure 5-17. The pressure profile at the point where maximum force is exerted as the penetrometer travelled through the Tim Tam biscuit from the top; colourbar: pressure (N.mm$^{-2}$).*

Figure 5-17 shows the high force detected only in the middle of the biscuit as compared to the edge of the biscuit. It was observed that the pins punctured the chocolate coating but compressed the biscuit instead of puncturing it. This may be due to the fact that the pins are too close to each other, thus acting like a flat surface that is compressing rather than individual pins puncturing through the hard biscuit.

***Case Study 3- precooked marinated green lipped mussels***

The texture measurement of the green lipped mussel is complex as the various parts of the mussel body each possess a different texture based on their inherent tissue structure (Gupta, 2012). The test should be able to provide a textural map of the mussel. The multiple penetrometer attachment was used to puncture the precooked marinated green lipped mussels to a 99% strain (calculated from the point of first contact). The test was run using a pre-test and test speed of 0.65 mm $s^{-1}$ and a trigger force of 0.5 N.

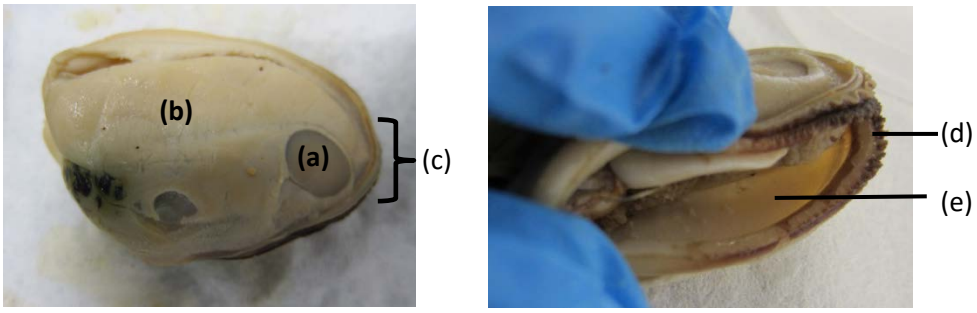


*Figure 5-18. The parts of the mussel as labelled: (a) adductor, (b) body, (c) thickest part of the mussel, (d) mantle edge, (e) mantle.*

The mussel was thickest at the part where the bigger adductor muscle was which also contributed to the higher pressure exerted by that area (Figure 5-19). The thickest part of the body is due to the various organs underneath the mantle, while the part of the mantle closer to the edges is thinner.

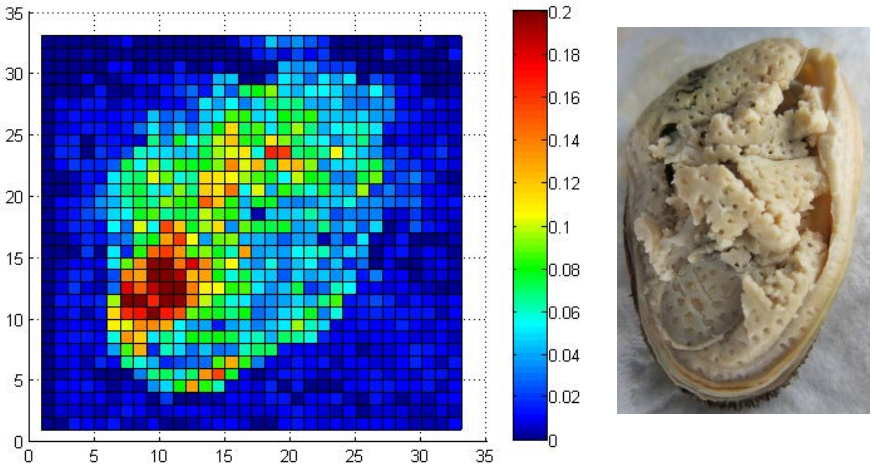


*Figure 5-19.The surface plot of a mussel at 99% strain; colourbar: pressure (N.$mm^{-2}$).*

As the penetrometer travelled deeper, the distribution of the pins shifted upwards. Figure 5-20 shows that at 49% strain, only the thickest part of the mussel is punctured by the pins. At 74% strain, 35% of the pins measured 0.07 N.$mm^{-2}$ or more which included the adductor and the thickest part of the mussel. The pins had not yet punctured the mantle at the thinner part of the mussel at 74%

strain. The whole mussel is punctured at 12.9 mm (99 % strain), and 75 % of the pins measured pressures of 0.0689 N.mm$^{-2}$ or more (Figure 5-21). The mantle of the mussel at coordinates (11,4) to (25,10) are thicker, thus accounting for the higher pressure. The spatial distribution of the mussel allows a better understanding of the texture of the mussel.

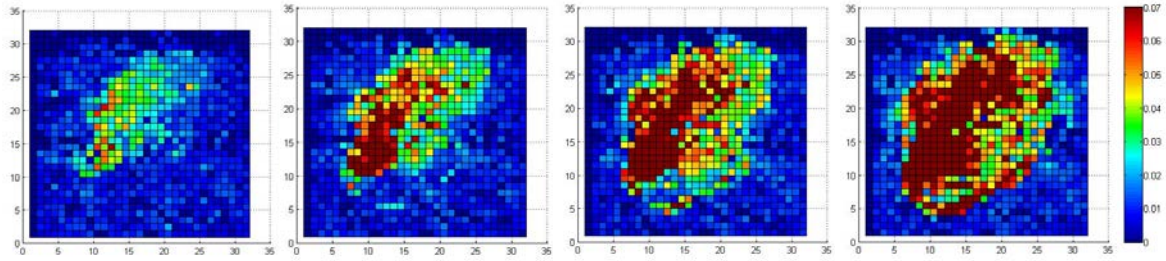

*Figure 5-20.The surface plots of the pressure distribution across the mussel at 49% strain, 74% strain, 86% strain and 99% strain (from left to right); colourbar: pressure (N.mm$^{-2}$).*

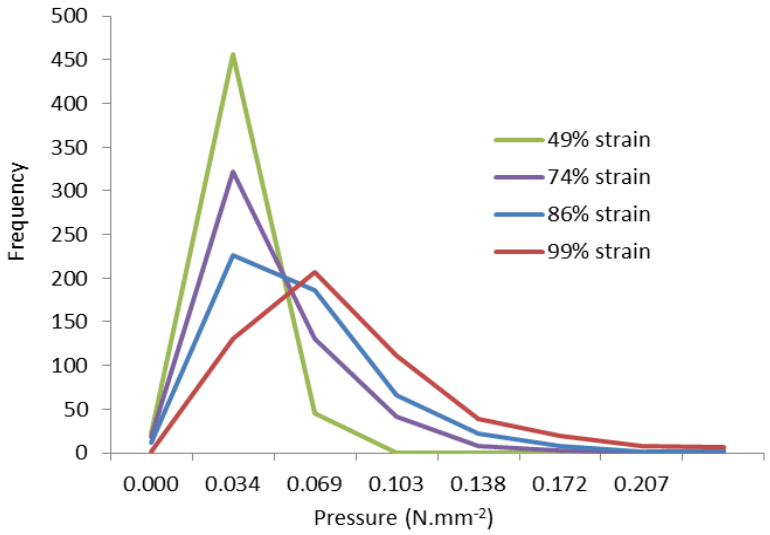


*Figure 5-21. Distribution of the number of pins in each range of pressure measured as the amount of deformation increased.*

The mussel does not have a heterogeneous texture which does not agree with the smooth curve in the pressure distribution (Figure 5-22). This could be due to the fact that there are many different regions of measured pressures thus making it difficult to see the distinct regions. In general, the maximum pressure experienced by each pin is when the mussel is at maximum deformation. This is probably because the mussel is elastic and not porous. Thus, the mussel exerted greater pressure on the pins as the strain increased. Comparing the distributions, the softer regions have a slightly higher pressure when maximum pressure measurements of pins are taken rather than measurements at the point of maximum strain. This is explained by the higher pressures reducing after the initial puncture of the softer regions. It may be because of the lesser resistance in the empty spaces

between the mantles of the mussel which are also less thick as compared to the other parts of the mussel.

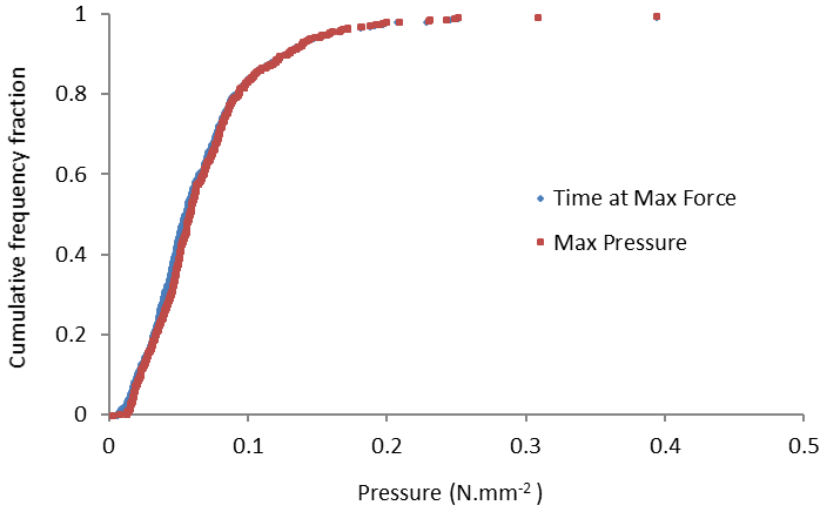


*Figure 5-22. The pressure distribution of the mussel at (a) time at max force: pressures measured at 99% strain and (b) max pressure: maximum pressure measured by each pin.*

The pin measuring the pressure at the body is at the thickest part of the mussel, followed by the adductor, mantle edge and lastly, the mantle at the thinnest part of the mussel. Although the body is the thickest, the adductor is tougher and thus more pressure is being exerted as the pins puncture it. The young's modulus for the adductor and body is 0.319 $N.mm^{-2}$ and 0.242 $N.mm^{-2}$ respectively (Figure 5-23). This agrees with what was observed as the adductor was stiffer compared to the body which was more readily compressed.

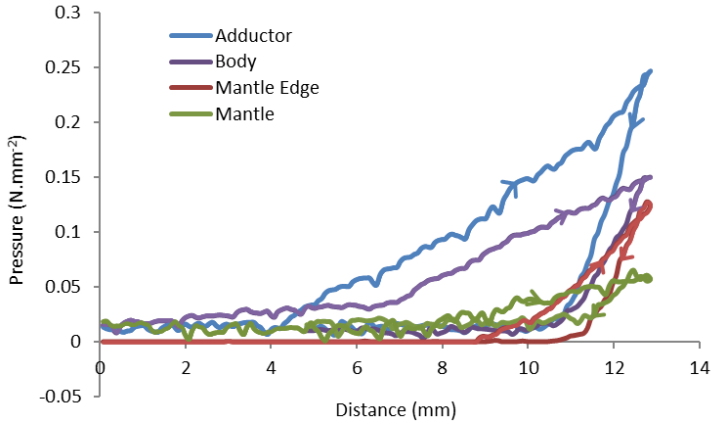


*Figure 5-23.The pressure profiles at different parts of the mussel as the penetrometer punctured into it and returned back to its original position. The pressure increased and decreased as the penetrometer travelled into and left the food as indicated by the direction of the arrows.*

Figure 5-24 shows a contour plot of the pressure map across the mussel at 99% strain. A possible application is to understand how the texture of the different parts of the mussel changes during cooking. Thresholding of the pressures could be done to select parts of the mussel to study the distribution of the various regions in the mussel individually instead of the overall pressure distribution of the whole mussel. For example, the mantle and the body can be separated and the change in pressure distributions with increasing heating time or temperature can be studied (Figure 5-25).

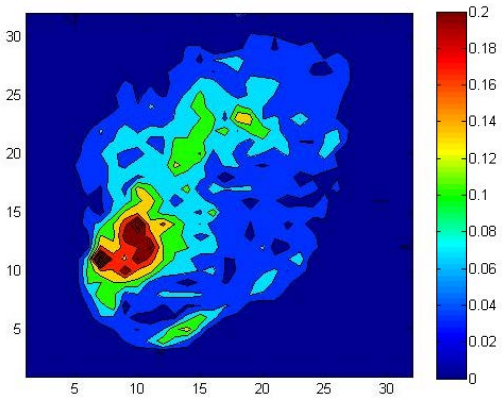


*Figure 5-24. The contour plot of the mussel showing the various regions of pressures across the mussel; colourbar: pressure ($N.mm^{-2}$).*

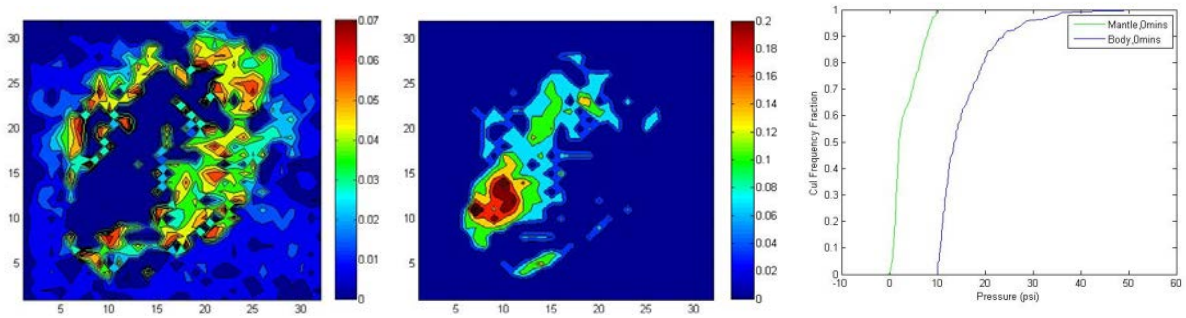


*Figure 5-25. The contour plots of the pressures exerted on the mantle and body of the mussel after thresholding and the pressure distributions of the two parts at zero minutes of heating; colourbar: pressure ($N.mm^{-2}$).*

***Case Study 4- chocolate bars***

The next study aims to demonstrate the ability of the multiple pin penetrometer to be sensitive enough to be able to measure the textures between four types of chocolate with liquid filling, gel-like filling, no filling and with fruit and nuts in it. The multiple penetrometer attachment was used to puncture four different types of chocolate to a depth of 14 mm. The test was run using a pre-test and test speed of 0.65 mm $s^{-1}$ and a trigger force of 0.1 N. Each chocolate sample consisted of four squares of chocolate (Figure 5-26). Each sample was kept in a polyethylene resealable bag and

placed in a 29.5°C water bath for ten minutes before texture analysis was carried out. This was done to soften the chocolate as the chocolates at ambient temperature were too hard and caused the texture analyser to be overloaded.

*Table 5-2. The four types of chocolate bar that was tested and a brief description of them.*

| Name of Chocolate Bar | Description |
|---|---|
| Milk Chocolate | A milk chocolate bar |
| Fruit N Nut Chocolate (FNN) | A milk chocolate bar with raisins and almonds |
| Caramello Chocolate | A milk chocolate bar with caramel filling within each square |
| Turkish Delight Chocolate (TD) | A milk chocolate bar with a Turkish delight jelly within each square |

*Figure 5-26.Top: The whole milk chocolate bar before and after puncture; Bottom: the Caramello chocolate bar before and after puncture (from left to right).*

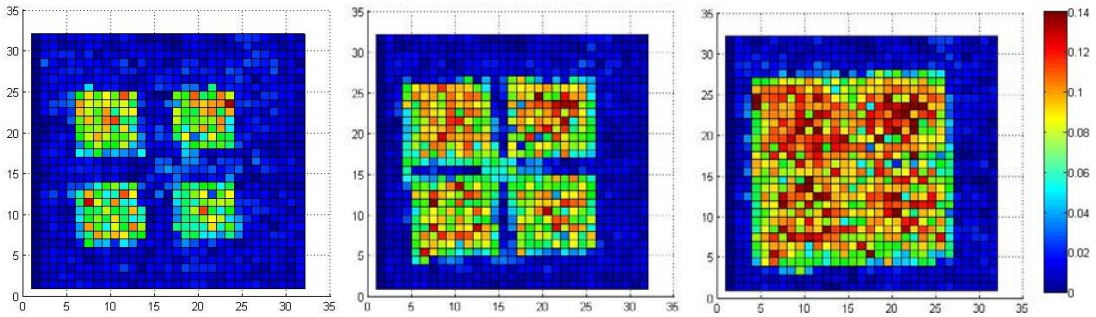

*Figure 5-27.The surface plots of the pressure profile as the penetrometer travelled into the milk chocolate to a depth of 7mm, 11mm, and 14mm (from left to right); colourbar: pressure (N.mm$^{-2}$).*

As the penetrometer travelled down, the thicker parts of the chocolate slab was punctured first. The pins at the thicker parts of the chocolate experienced a greater force exerted back on the pins. The pins at the sloping surface of the chocolate slab probably account for 60% of pins which experienced

a lower total/ maximum pressure. The remaining 40% are the pins puncturing into the four flat surfaces as indicated in Figure 5-27. Since the edges of each chocolate cube have a shorter height, the pins along the edges would experience a lower pressure as compared to other areas. It was observed that as the chocolate deformed, there were parts that have been pushed out of the way by a few bent pins, which accounts for the low pressures measured by the neighbouring pins.

The surface of the milk chocolate slab is not entirely flat; hence there is a bimodal distribution (Figure 5-28). At the 11 mm depth, 50 % of the pins experience less than 0.065 $N.mm^{-2}$. These are probably the pins at the edge that have just started puncturing the chocolate and hence the lower pressure. At the 14 mm depth, all the pins have punctured the chocolate, with the lowest pressure at 0.007 $N.mm^{-2}$. As the penetrometer travelled deeper into the chocolate, the percentage of pins experiencing pressures less than 0.065 $N.mm^{-2}$ reduced to 20%.

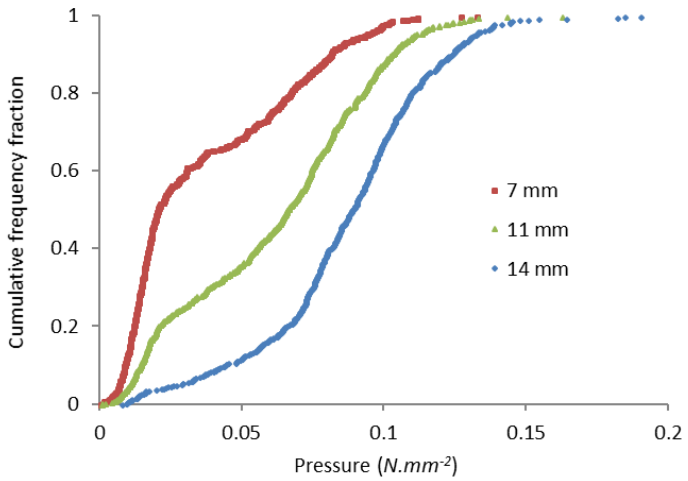


*Figure 5-28: The pressure distribution of pins as the penetrometer attachment travelled to a depth of 7mm to 14mm in the milk chocolate slab.*

The $d_{50}$ is an established parameter in PSD analysis, that was used in previous chapters, to describe a distribution. The $P_{50}$ is equivalent to the $d_{50}$ but refers to the pressure applied where 50% of pins have a pressure measurement lesser than this. In a similar way as done for PSD analysis, the Rosin-rammler function or defining a range ($P_{75}$-$P_{25}$) could be used to characterise the distribution further. Figure 5-29a shows the cumulative distributions compared between the four different chocolate bars at 14mm penetration. Based on the $P_{50}$, the Caramello and Turkish Delight (TD) chocolate are softer than the milk chocolate bar (Figure 5-29b). This agrees with the data as these two chocolate bars are chocolate shells that have a semi solid and jelly filling which is softer and the penetrometer has to puncture a thinner layer of chocolate as compared to the milk chocolate bar. The Fruit n Nut (FNN) chocolate is harder due to the presence of nuts and raisins in the chocolate bar. Figure 5-30

shows the outcome when applying the same methodology to a Fruit n Nut chocolate bar, where an area of high local force (red pixels) corresponds to the presences of a nut particle.

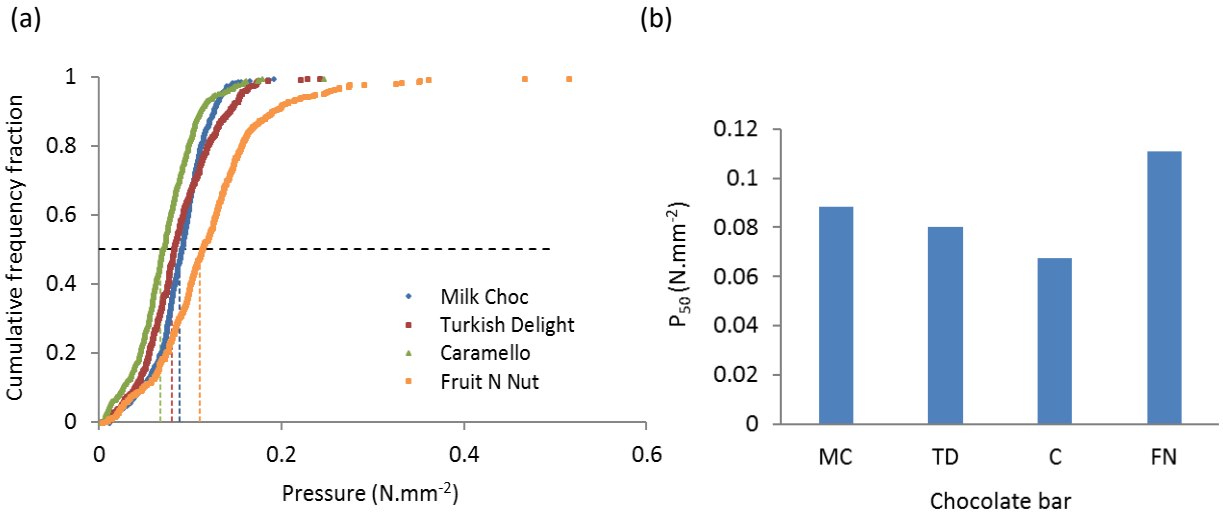


*Figure 5-29: The pressure distributions of the pins puncturing into the four different chocolates at 14mm where (a) shows the cumulative distribution and (b) shows the $P_{50}$ for each type of chocolate bar.*

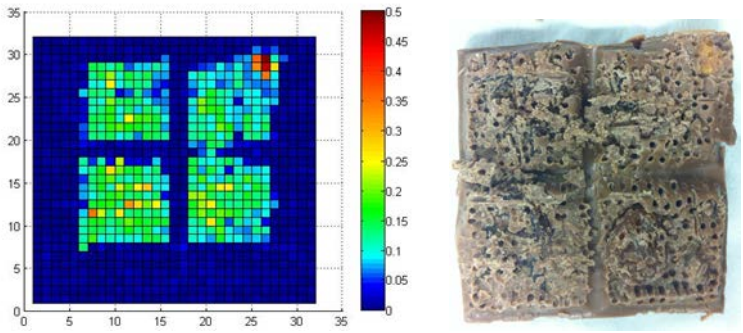

*Figure 5-30: The pressure profile of a Fruit n Nut milk chocolate bar at a depth of 7.4mm; colourbar: pressure (N.mm$^{-2}$). The higher pressures at coordinates (26,30) and at coordinates (11,12) were due to the almond and raisin respectively.*

The chocolate of the milk chocolate, FNN chocolate and TD chocolate bars have similar pressure profiles (Figure 5-31). The pressure of the 'FNN raisin' increased at a shorter depth compared to the 'FNN nut' is due to the fact that the raisin was at the surface while the nut was embedded in the chocolate, thus the pressure measurement of the nut only occurred after a depth of 8 mm. The pressure profile of the 'TD jelly' shows the pressure exerted by the chocolate shell at a depth of 4 mm before it cracked and the pin starts to measure the pressure of the softer jelly which accounts for the decrease and its gradual increase as it meets the chocolate base again.

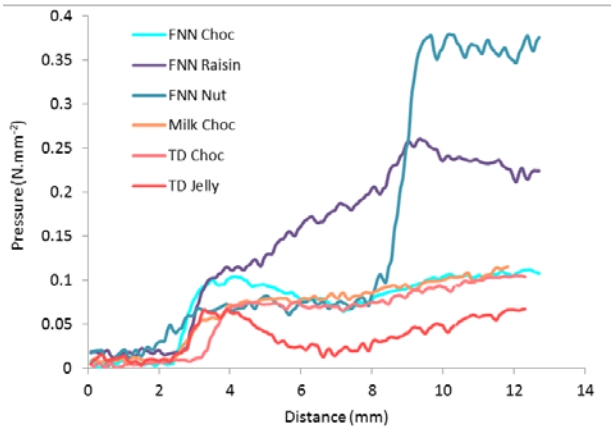


*Figure 5-31.The texture profiles of single pins at various locations across the Fruit n Nut chocolate (FNN), milk chocolate and Turkish Delight (TD) chocolate.*

### 5.1.3. Image analysis: Grey level co-occurrence matrix

Although the cumulative distribution data shown above have similarity to PSD and provide a convenient way of extending bolus evaluation to non -brittle foods, the analysis of the pressure distributions in the previous section do not provide spatial information about the texture. In the image, there is more information such as whether the high force pins are randomly distributed across the image or all clustered in one location. The grey level co-occurrence matrix (GLCM) is a statistical texture method that considers the spatial relationship of the pixels in the grey scale image. GLCM has been widely used to characterise the texture of food images (N.B. image texture refers to 'roughness' of an image and has a different meaning to food texture). Texture features are extracted by statistical approaches from the co-occurrence matrix *p(i, j)* (Haralick et al., 1973).

The GLCM is created by calculating how often a pixel with grey level value *i* occurs in a specific spatial relationship to a pixel with the value *j* for a given grey scale image. The spatial relationship is specified by the distance *d*, and direction θ with angles equal to 0°, 45°, 90° and 135°. The top figure in Figure 5-32 illustrates how the GLCM is created using a spatial relationship of *d*=1 and θ=0°. In the greyscale image I, there is only one instance where two horizontally adjacent pixels have the values 1 and 1, thus the GLCM for element (1,1) contains a value of 1. Element (1,2) contains a value of 2 since there are two instances where two horizontally adjacent pixels have the values 1 and 2. Element (1,3) contains a value of 0 since there are no instances of two horizontally adjacent pixels with the values 1 and 3. The created GLCM is then normalised by a function, R, which is usually the sum of the matrix, thus giving $P_d(i,j) = \frac{P_d(i,j)}{R}$ which is the $(i,j)th$ entry in a normalised grey-tone spatial dependence matrix.

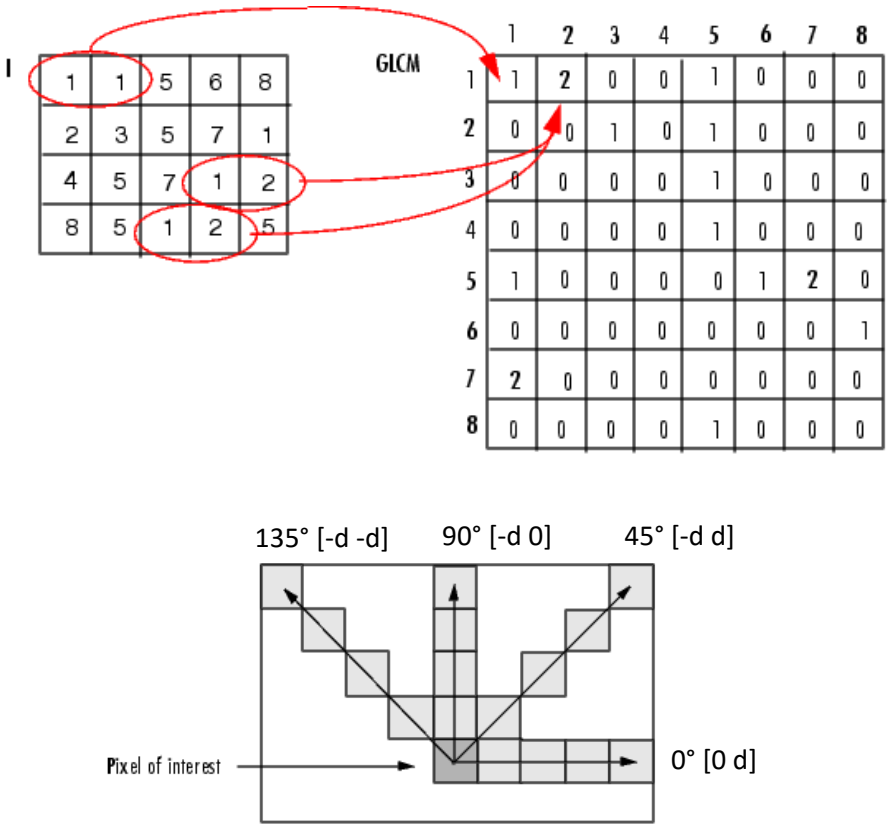


*Figure 5-32: Creating a GLCM from a greyscale image I (top). Illustration of the spatial relationships of pixels that are defined by an array of offsets, where d represents the distance from the pixel of interest (bottom). [Image Processing Toolbox User's Guide]. Retrieved February 25, 2018, from [http://matlab.izmiran.ru/help/toolbox/images/enhanc15.html](http://matlab.izmiran.ru/help/toolbox/images/enhanc15.html)*

There are fourteen image texture features proposed by Haralick et al. (1973), but only 'contrast', 'energy' and 'homogeneity' will be used in this work. $P_d(i,j)$ is the number of elements in the set of pairs of points that have grey level values of *i* and *j*, for a displacement vector *d*. The following notions are used to explain the three textural features:

$\boldsymbol{N_g}$ = Number of distinct grey levels in the image

$$\sum_{\boldsymbol{i}} = \sum_{\boldsymbol{i=1}}^{\boldsymbol{N_g}}$$

$$\sum_{\boldsymbol{j}} = \sum_{\boldsymbol{j=1}}^{\boldsymbol{N_g}}$$

Contrast = $\sum_i \sum_j (i-j)^2 \, P_d(i,j)$

Energy = $\sum_i \sum_j P_d(i,j)^2$

Homogeneity = $\sum_i \sum_j \frac{P_d(i,j)}{1+|i-j|}$

Contrast measures the amount of local variations present in the image through determining the difference between the highest and lowest values between a pixel and its neighbours. In a constant image, the contrast is 0. Unlike contrast, both energy and homogeneity have a normalized range with a maximum value equal to one. Energy measures the textural uniformity of the local grey scale distribution while homogeneity measures the similarity of pixels. High energy values occur when the grey level distribution has a constant or periodic form. A diagonal GLCM gives homogeneity of 1 and the value becomes large if there are minimal changes in the local textures. A homogenous image contains very few dominant grey tone transitions and therefore the matrix for this image will have fewer entries of larger magnitude resulting in a large value for energy. The GLCM of less homogeneous images will have a large number of small entries resulting a in small value for energy.

Multiple GLCMs may be created for each set of spatial relationship, and an average of the textural features of each GLCM is calculated. For example, the bottom figure in
Figure *5-32* shows that the spatial relationship to be explored will be in four different directions (left, right, up, and down). Thus, four GLCMs were created and the calculation of each textural feature was performed for each GLCM before an average is taken.

***Example***

An example with five images (Figure 5-33) is used to demonstrate the application of GLCM analysis using Matlab®. The code written for this analysis is attached in Appendix D. The GLCMs of the five images were created using 9 grey scale levels, and offset settings for four directions (θ=0°, 45°, 90° and 135°) with *d*=1. 'Symmetric' was set to true such that the ordering of the values was not considered during the calculation of the number of occurrences in which a pixel with grey level value *i* was adjacent to a pixel with the value *j.* For example, both 1,2 and 2,1 pairings were counted when calculating the number of times the value 1 was adjacent to the value 2. The *graycoprops* Matlab® function was used to derive the contrast, energy and homogeneity for each of the four matrices and an average was taken.

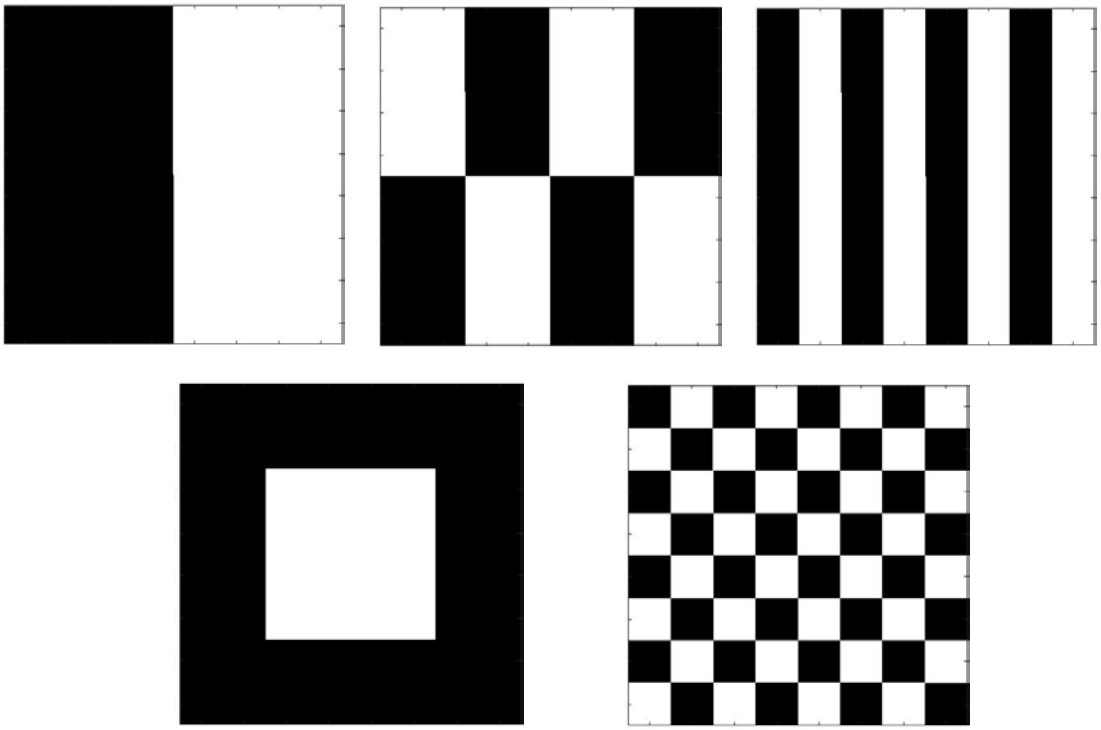

*Figure 5-33: Sample images created using MATLAB® to depict various textures. The labels for the images are as follows: half, quarter, alternate, checkerboard and enclosed (from top left in a clockwise direction).*

Referring to Figure 5-34, for the GLCM defined by offset [0 1], there were 16 occurrences where two horizontally adjacent pixels have the values 1 and 1; 12 occurrences where two horizontally adjacent pixels have the values 1 and 9; and these occurrences were multiplied by two to account for the symmetric setting, thus the number of entries for elements (1,1) and (1,9) were 32 and 24 respectively. For the GLCM defined by offset [-1 1], there were 13 occurrences where a pixel of value 1 was diagonally to the right of another pixel of value 1; 11 occurrences where a pixel of value 1 was diagonally to the right of another pixel of value 9 and these occurrences were multiplied by two to account for the symmetric setting, thus the number of entries for elements (1,1) and (1,9) were 26 and 22 respectively. These GLCMs were normalised and then used to calculate the textural features as shown in Table 5-3. The contrast for the GLCM defined by offset [-1 0] was lowest due to the low occurrences in which two vertically adjacent pixels were of different values. The energy and homogeneity for the GLCM defined by offset [-1 0] were highest due to the large magnitude of the entries in elements (1,1) and (9,9).

*(a)*

*I*

| | | | | | | | |
|---|---|---|---|---|---|---|---|
| 1 | 1 | 9 | 9 | 1 | 1 | 9 | 9 |
| 1 | 1 | 9 | 9 | 1 | 1 | 9 | 9 |
| 1 | 1 | 9 | 9 | 1 | 1 | 9 | 9 |
| 1 | 1 | 9 | 9 | 1 | 1 | 9 | 9 |
| 9 | 9 | 1 | 1 | 9 | 9 | 1 | 1 |
| 9 | 9 | 1 | 1 | 9 | 9 | 1 | 1 |
| 9 | 9 | 1 | 1 | 9 | 9 | 1 | 1 |
| 9 | 9 | 1 | 1 | 9 | 9 | 1 | 1 |

*(b)*

*GLCM*

*(i)*

| | 1 | 2 | 3 | 4 | 5 | 6 | 7 | 8 | 9 |
|---|---|---|---|---|---|---|---|---|---|
| 1 | 32 | 0 | 0 | 0 | 0 | 0 | 0 | 0 | 24 |
| 2 | 0 | 0 | 0 | 0 | 0 | 0 | 0 | 0 | 0 |
| 3 | 0 | 0 | 0 | 0 | 0 | 0 | 0 | 0 | 0 |
| 4 | 0 | 0 | 0 | 0 | 0 | 0 | 0 | 0 | 0 |
| 5 | 0 | 0 | 0 | 0 | 0 | 0 | 0 | 0 | 0 |
| 6 | 0 | 0 | 0 | 0 | 0 | 0 | 0 | 0 | 0 |
| 7 | 0 | 0 | 0 | 0 | 0 | 0 | 0 | 0 | 0 |
| 8 | 0 | 0 | 0 | 0 | 0 | 0 | 0 | 0 | 0 |
| 9 | 24 | 0 | 0 | 0 | 0 | 0 | 0 | 0 | 32 |

*(ii)*

| | 1 | 2 | 3 | 4 | 5 | 6 | 7 | 8 | 9 |
|---|---|---|---|---|---|---|---|---|---|
| 1 | 26 | 0 | 0 | 0 | 0 | 0 | 0 | 0 | 22 |
| 2 | 0 | 0 | 0 | 0 | 0 | 0 | 0 | 0 | 0 |
| 3 | 0 | 0 | 0 | 0 | 0 | 0 | 0 | 0 | 0 |
| 4 | 0 | 0 | 0 | 0 | 0 | 0 | 0 | 0 | 0 |
| 5 | 0 | 0 | 0 | 0 | 0 | 0 | 0 | 0 | 0 |
| 6 | 0 | 0 | 0 | 0 | 0 | 0 | 0 | 0 | 0 |
| 7 | 0 | 0 | 0 | 0 | 0 | 0 | 0 | 0 | 0 |
| 8 | 0 | 0 | 0 | 0 | 0 | 0 | 0 | 0 | 0 |
| 9 | 22 | 0 | 0 | 0 | 0 | 0 | 0 | 0 | 28 |

(iii)

| | 1 | 2 | 3 | 4 | 5 | 6 | 7 | 8 | 9 |
|---|---|---|---|---|---|---|---|---|---|
| 1 | 48 | 0 | 0 | 0 | 0 | 0 | 0 | 0 | 8 |
| 2 | 0 | 0 | 0 | 0 | 0 | 0 | 0 | 0 | 0 |
| 3 | 0 | 0 | 0 | 0 | 0 | 0 | 0 | 0 | 0 |
| 4 | 0 | 0 | 0 | 0 | 0 | 0 | 0 | 0 | 0 |
| 5 | 0 | 0 | 0 | 0 | 0 | 0 | 0 | 0 | 0 |
| 6 | 0 | 0 | 0 | 0 | 0 | 0 | 0 | 0 | 0 |
| 7 | 0 | 0 | 0 | 0 | 0 | 0 | 0 | 0 | 0 |
| 8 | 0 | 0 | 0 | 0 | 0 | 0 | 0 | 0 | 0 |
| 9 | 8 | 0 | 0 | 0 | 0 | 0 | 0 | 0 | 48 |

(iv)

| | 1 | 2 | 3 | 4 | 5 | 6 | 7 | 8 | 9 |
|---|---|---|---|---|---|---|---|---|---|
| 1 | 28 | 0 | 0 | 0 | 0 | 0 | 0 | 0 | 22 |
| 2 | 0 | 0 | 0 | 0 | 0 | 0 | 0 | 0 | 0 |
| 3 | 0 | 0 | 0 | 0 | 0 | 0 | 0 | 0 | 0 |
| 4 | 0 | 0 | 0 | 0 | 0 | 0 | 0 | 0 | 0 |
| 5 | 0 | 0 | 0 | 0 | 0 | 0 | 0 | 0 | 0 |
| 6 | 0 | 0 | 0 | 0 | 0 | 0 | 0 | 0 | 0 |
| 7 | 0 | 0 | 0 | 0 | 0 | 0 | 0 | 0 | 0 |
| 8 | 0 | 0 | 0 | 0 | 0 | 0 | 0 | 0 | 0 |
| 9 | 22 | 0 | 0 | 0 | 0 | 0 | 0 | 0 | 26 |

*Figure 5-34: (a) The grey scale image of the 'quarter' image where 0 represents the white parts and 1 represents the black parts. (b) The GLCMs of the image created using the different offsets: (i) offset vector of [0 1] for ϑ=0° and d=1; (ii) offset vector of [-1 1] for ϑ=45° and d=1; (iii) offset vector of [-1 0] for ϑ=90° and d=1; and (iv) offset vector of [-1 -1] for ϑ=135° and d=1.*

*Table 5-3: The textural features calculated for each GLCM defined by a specific spatial relationship (offset) for the 'quarter' image.*

| **Offset** | **[0 1]** | **[-1 1]** | **[-1 0]** | **[-1 -1]** |
|---|---|---|---|---|
| **Description** | → | ↗ | ↑ | ↖ |
| **Contrast** | 27.43 | 28.73 | 9.14 | 28.73 |
| **Energy** | 0.26 | 0.25 | 0.38 | 0.25 |
| **Homogeneity** | 0.62 | 0.60 | 0.87 | 0.60 |

The values for the textural features in Table 5-4 were the mean of the values calculated for four GLCMs defined by the different offsets for each image. The 'alternate', 'checkerboard' and 'quarter' images have high contrast values due to more variation in the images. The 'alternate' and 'checkerboard' images have the highest energy which can be attributed to the uniform pattern exhibited by these two images. The 'half' and 'enclosed' images have the highest homogeneity since these two images have minimal changes within each image and the magnitudes of the entries along the diagonal are large.

*Table 5-4: A summary of the textural features of the images in Figure 5-33.*

| Image | Contrast | Energy | Homogeneity |
|---|---|---|---|
| **Half** | 6.86 | 0.41 | 0.90 |
| **Quarter** | 23.51 | 0.28 | 0.67 |
| **Alternate** | 48.00 | 0.50 | 0.33 |
| **Enclosed** | 13.71 | 0.41 | 0.81 |
| **Checkerboard** | 32.00 | 0.50 | 0.56 |

GLCM analysis was applied to the pressure profiles for the four different chocolate bars (section 5.1.2, case study 4). The milk chocolate had the lowest contrast, highest energy and homogeneity which reflects that the milk chocolate was the most uniform and homogenous amongst the four bars. Contrast is determined by the difference in the highest and lowest values between a pixel and its neighbours. Since the pressure difference between the chocolate shell and the caramel was larger than that for the chocolate shell and jelly (TD bar), thus, the Caramello bar had a higher contrast than the TD bar. The FNN bar was the least uniform as it had three components within the bar (chocolate, raisins, and nuts) as compared to the other bars which only had two or one.

*Table 5-5: A summary of the textural features used to describe the different types of chocolate bar (case study 4).*

| Chocolate bar | Contrast | Energy | Homogeneity |
|---|---|---|---|
| **Caramello** | 6.98 | 0.07 | 0.53 |
| **Milk Choc** | 1.66 | 0.63 | 0.87 |
| **Fruit N Nut (FNN)** | 5.86 | 0.03 | 0.51 |
| **Turkish Delight (TD)** | 5.95 | 0.19 | 0.63 |

### 5.1.4. Conclusions of the multiple pin penetrometer system

Although the MPP is developed for the application of characterizing the bolus in the current work, it could be used to characterize the texture of foods. The aim was to demonstrate the application of the technique to different foods with varying textures and how the different data analysis treatments could provide different information about the food's texture. This method would be

suitable for foods that do not have a homogenous texture, for example foods with different fillings or ingredients embedded randomly in a matrix such as a fruit cake or a food that has a different texture for each layer such as cream filling sandwiched between two layers of wafer crisp.

In some foods, the texture changes randomly as the penetrometer travels through the food (eg. Fruit N Nut chocolate). For such foods in which the determination of the hardest part of the food is important, only the maximum pressure measured by each pin regardless of time is used. As the penetrometer travels through the food, the pressures exerted by each pin on the pressure sensor is recorded. Since the texture across a plane of the food could be measured, different information could be extracted from the data collected. To understand the textural properties of food with multiple layers, the pressure distribution at different times could be compared. To understand the textural properties across a plane in the food at the point of maximum deformation, the data set at a time at which the maximum force exerted on the food and maximum area in contact with the food was selected for analysis. As demonstrated in the case studies, the pressure profile provided by a full pin orientation could be used to provide a clear image of the food based on the different regions of pressure range. In addition, image analysis using GLCM could be employed to provide statistical textural information about the food. The difference in the sample images could be identified using three textural features: contrast, energy and homogeneity.

This part of the chapter adequately evaluated the multiple pin penetrometer and established the data analysis method to be employed later in the characterisation of bolus properties. The method could be used to characterise fibrous (non-fracturable) foods in a similar way to PSD analysis, offering a method to characterise boluses that do not form discrete particles. The GLCM analysis could also be applied to obtain extra spatial information. This method is not suitable for collections of particles (eg. peanut bolus) as the individual particles will be pushed aside by the pins and thus would not provide a true reflection of the spatial variation.

## 5.2. Slip Extrusion Test

The role of mastication is to prepare a bolus for safe swallowing. There are a few models suggesting different criteria required in a bolus, for swallowing to be triggered. One of these is the Hutchings and Lillford breakdown model (Hutchings, J. B. & Lillford, 1988). It is a conceptual model which suggests that the criterion for swallowing a bolus is its degree of structure and lubrication. The Swallow Safe model (Gray-Stuart, 2016) defined deformability, slippiness and cohesiveness as key

bolus properties required for safe swallowing. Although bolus properties have been defined in literature; a quantitative measurement of bolus swallowability has not previously been developed. Defining these properties numerically is difficult and current instruments used for bolus analysis have limitations. They are usually designed to evaluate certain types of food and do not give meaningful results for all stages of breakdown.

Previous studies which characterise the breakdown of food have employed different types of measurement methods due to the nature of the resulting boluses. For example, particle size determination can be used for brittle foods such as peanut, raw carrot, cake, and cereal bar boluses through sieving analysis (Flynn et al., 2011; Jalabert-Malbos et al., 2007; Mishellany-Dutour et al., 2011; Panouillé, Maud et al., 2016); whereas laser diffraction and viscosity measurements are employed for boluses that are more pasty such as banana and cooked rice (Hwang et al., 2012); texture measurements such as the two-bite compression test (Texture Profile Analysis) are used for cereals, biscuit and rice cake boluses (Peyron, Marie-Agnès et al., 2011; Shiozawa & Kohyama, 2011); the back extrusion test has been used for biscuits (James et al., 2011b); and the cutting test using a double-bladed shearing cell was used for beef boluses (Mioche et al., 2003). Another problem is that some foods require a different type of measurement method at different stages of breakdown. For example, in their characterisation of biscuit breakdown, James et al., (2011) used the 3-point bending test for the initial stages of mastication, however, this was not applicable to studying the whole process of bolus formation due to the texture changing from a crumbly nature to a paste as it is softened and mixed with saliva during the breakdown.

Physical and sensory characterisation methods have been applied to boluses or model boluses that are ready for swallowing (Loret et al., 2011a; Nakauma et al., 2011). Ishihara et al. (2011) studied the rheological properties of model boluses prepared by a mechanical simulator and found that the mechanical cohesiveness and surface lubrication of a bolus determined its swallowability. The rheological methods used are not suitable to follow the changes in the bolus at the initial stages of mastication. Brenner et al. (2014) found that there was better correlation in the extrusion test with the sensory attributes of polysaccharide gels than the texture profile analysis. However, their large deformation extrusion test was concluded to be only useful for characterising solid foods with a yield stress. Thus, this test may not be suitable for evaluating boluses at the end of mastication.

The human mouth is a complicated instrument that can evaluate all foods over the whole period of chewing. Laboratory instruments have been designed to measure specific mechanical or rheological

properties of certain types of food. However, they have not been designed to measure the properties of the bolus that are directly relevant to the formation of a swallow safe bolus. The design of the slip extrusion test (SET) (developed below) mimics swallowing but is not intended to measure swallowing. Based on the conceptual model of Gray-Stuart (2016), it is hypothesized that for a bolus to be safely swallowed it must be able to; deform to respond to peristalsis and flow through the upper oesophageal sphincter, to slip along the walls of the oro-pharynx and oesophagus, and to be cohesive enough to avoid particles separating and being left behind to potentially make their way into the airways when breathing recommences after swallow. In this work, a novel slip extrusion test has been developed to simply approximate the structural changes and manipulation applied to a bolus during swallowing. The SET was adapted from the 'Squeeze Test' (Voisey et al., 1980), which extrudes paste through a tube as it is pulled through a tube extrusion rig. The test measures the force needed to extrude a bolus through a test bag imitating the swallowing action of a bolus. By measurement of the forces applied to the bolus during the test, quantification of bolus deformability, slippiness and retention of bolus integrity is possible for a wide range of foods at different stages of bolus preparation. The test is aimed at quantifying the bolus properties if it were to be swallowed at any point during bolus preparation, whether it has reached swallow point or not.

In this part of the chapter, the SET is introduced and its application is demonstrated using three different food model systems of varying structure and consistency. How it can be used to characterise boluses expectorated from human subjects at different stages of mastication is then demonstrated.

### 5.2.1. Development of Systems

***Development of the Extrusion Rig***

The design of the extrusion rig was adapted from the 'Squeeze Test' by Voisey et al. (1980) and the TA-TR Tube Roller Extrusion Fixture (Texture Technologies Corp, Hamilton, Massachusetts) seen in Figure 5-35.


*Figure 5-35: The TA-TR Tube Roller Extrusion Fixture ("The squeeze test for tubes and packets," 2014).*

The test rig shown in Figure 5-36 shows the new system that was developed as an attachment to a Texture Analyser TA.XT plus (Stable Micro Systems, Surrey, UK). It consists of a pair of cylindrical stainless steel rollers (25mm diameter, 60mm long). A slip extrusion bag containing the sample is pulled through the gap between the rollers. The force needed to extrude the sample as the bag is being pulled through the rollers is recorded. A 50 kg load cell that was mounted on the crosshead with an attached fixture that clamped the test bag measured the pulling force. The gap between the rollers and the height of the frame, which the rollers were mounted on, could be adjusted. The gap between the rollers could be adjusted from 0.75 to 4.0mm. The height of the frame for the rollers was placed at 90 mm, far enough from the base of the rig, so that the test bag would not be folded at an angle.

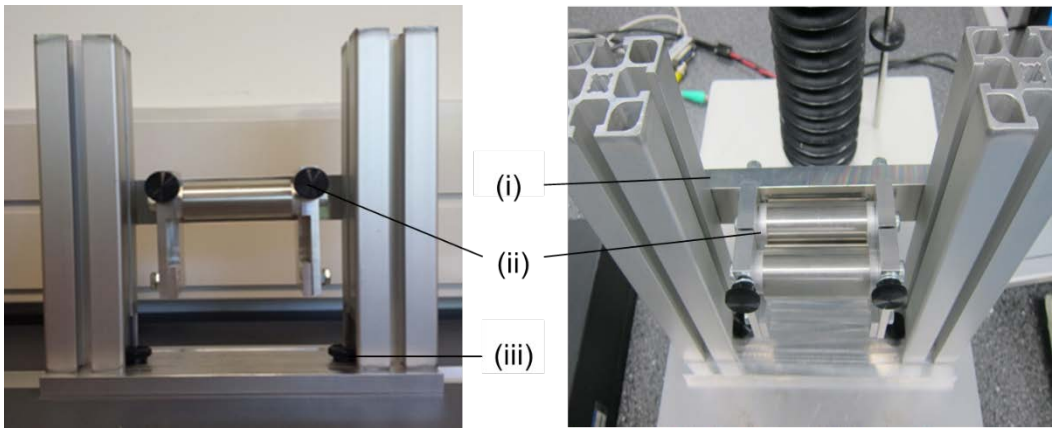


*Figure 5-36: The frontal and top view of the extrusion rig built by the workshop: (i) the frame on which the rollers are mounted on; (ii) a pair of steel rollers (25 mm diameter) with adjustable gap; (iii) the rig is attached to the test platform and held in position by two screws.*

***Development and production of Slip Extrusion Bags***

The slip extrusion bags are flat, funnel shaped, plastic bags and were made out of Nylon Polyethylene material with a thickness of 70 microns. This material was readily available and proved to be strong enough to not lose its shape easily when subjected to forces during the test. These bags were to be used in conjunction with the extrusion rig and texture analyser, therefore the design of the bags was limited by the size of these two devices. A variety of food samples could be placed in these bags so they need to be strong enough to handle soft, dry and hard foods etc. The bag's dimensions were designed such that the bolus is passed from a wider part into a narrow channel as the bag is pulled through the pair of rollers. This mimics the deformation of a bolus being as it is displaced from the larger oral cavity into the pharynx and then the resistance to slip as it travels through the oesophagus. Additional details are shown in Figure 5-37.

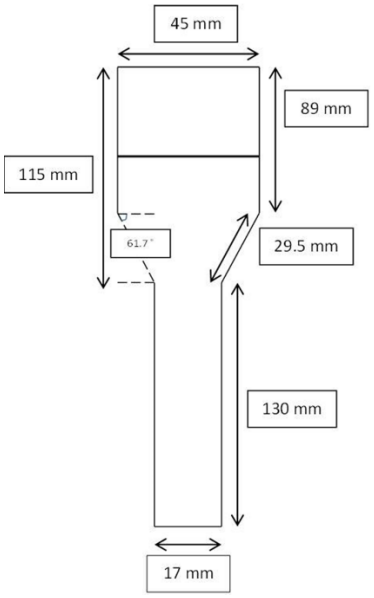


*Figure 5-37: The test bag dimensions.*

To make the bags, a flat plate sandwich maker was modified to create a hot plate press with a mould of the slip extrusion bags. The outline of the shape was mechanically milled into the top side of an aluminium block as seen in Figure 5-38. A PID temperature controller was used to keep the hot plate press at 140°C. The polymer material was placed onto the bottom wooden plate and the top plate is brought down and pressed to create the bags by heat sealing the bags' shapes onto the material. As the top plate was not level, some force needed to be exerted across the plate during the "imprinting" of the bags. To standardise the amount of force exerted onto the press, the hot plate press was placed on a weighing balance and approximately 10kg of force was exerted for 5 seconds

during each press. The bags were then cut when cooled. Before the press was used, a thermocouple was used to measure the temperature at different points on the plate to ensure that the temperature across the press would not have differences of more than 10˚C.

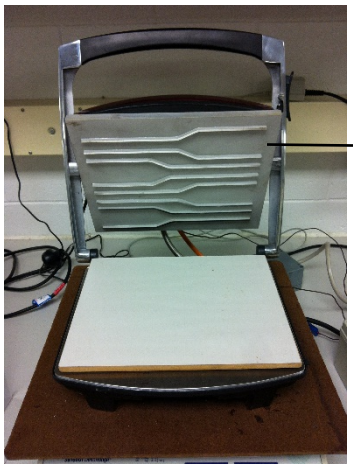


*Figure 5-38: The setup of the hot plate press used for the production of the slip extrusion bags.*

### 5.2.2. Test Protocol

The empty bag is partially slipped through the rollers of the extrusion rig and clamped onto the crosshead of the texture analyser as seen in Figure 5-39. The texture analyser carries out a tension test to pull the bag through the slip extrusion rig with a standard set gap between rollers and at crosshead speed of 20mm $s^{-1}$ to do a baseline measurement. This baseline measurement measures the force needed to pull an empty bag which will then be subtracted from the final measurement so that only the force needed to extrude the food sample is being measured. Sample size is standardised either by volume or by weight. Each bag is clipped tight at the lower end before the sample is placed into the bag. The bag is then partially slipped through the rollers of the extrusion rig and clamped onto the crosshead of the texture analyser and the test is repeated. The clip is released just before the test commences.

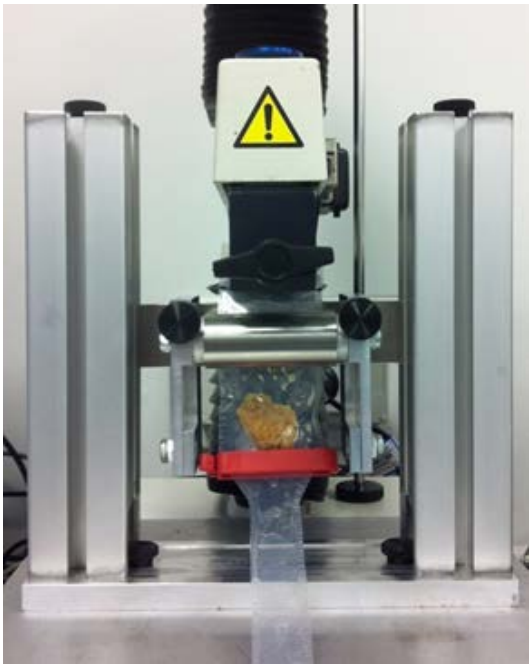

*Figure 5-39: The experimental set up of the test and a loaded test bag which is clipped shut to keep the sample in the wider part of the test bag.*

To better simulate the moist and lubricated environment of the mouth due to the presence of saliva, the slip extrusion bag was internally wetted by 0.25ml of 0.1% xanthan gum solution before the baseline measurement. Although the bag and xanthan gum solution are quite different from the mucosal surface and saliva in terms of material properties such as viscosity and wettability etc, it was decided that the set up be kept simple at this stage. In consideration of practical limitations associated with replicating saliva and mucosa, the set up provides adequate simulation of the swallowing process, and a level of background consistency against which experimental variation can be reliably measured. During the baseline measurement, the xanthan gum solution would be spread in the wider part of the test bag. As only a small amount is added, it was observed that the addition had no significant effect on the baseline measurement. In any case, any force due to the addition of the xanthan gum solution would be accounted for during the subtraction of the baseline force measured.

***Data Analysis***

During extrusion, the force and distance travelled are recorded using the Texture Exponent Software (Stable Micro Systems, Surrey, UK). The work done during extrusion was calculated as the area under the curve of the force-distance graph over a distance of 30mm corresponding to the region where the bag changes width (Figure 5-40). This work done was taken as a measure of deformation resistance, a measure of how difficult it is to deform the shape of the bolus into a narrower

aperture. The resistance to slip was taken as the average force measured as the food travels in the narrow tube, before the bolus started exiting from the bag (30-50mm on the force-distance graph). The range varies depending on the volume/nature of the sample as viscous fluids had a larger volume and started exiting the bag earlier as compared to the other samples. The resistance to slip is a measure of lubrication of the bolus on the walls of the extrusion bag and no change in shape of the bolus occurs in this section of the test.

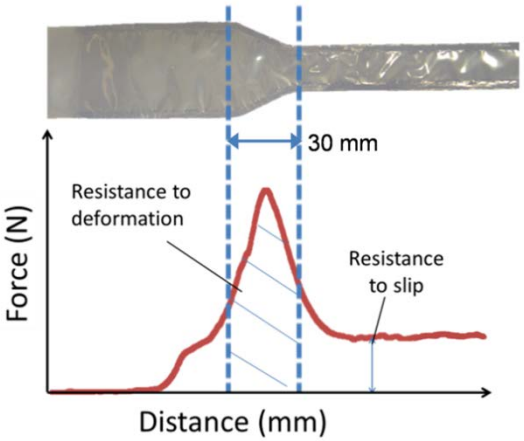


*Figure 5-40: The slip extrusion bag and how the measurements are taken on a typical force profile.*

***Refining the test***

Preliminary tests with the slip extrusion bags were carried out using rehydrated instant mashed potato (Cinderella, James Crisp Ltd, New Zealand) of different softness by varying the amount of water added. The compositions of the mashed potatoes were varied at 75%, 85% and 95% of water added. The gap between the rollers was 0.6mm since it was the minimum gap required to pull an empty bag through. 8g of mashed potato was extruded for each of the three compositions of mashed potato.

Examples of the force profiles measured during the extrusion of the mashed potato are shown in Figure 5-41. The forces measured between 30 to 60 mm are the forces needed to extrude the mashed potato from the larger cavity to the narrow tubing of the bag. The higher the composition of water added resulted in mashed potatoes of increasing softness and was more flowable and deformable. The mashed potato that only had 75% water added required the most force as it was least deformable as compared to the other mashed potato samples. The force measured between 80 to 160mm was a good indicator of the forces needed to overcome the frictional forces encountered with the surface of the bag. The force measured for the 75% water mashed potato

sample was significantly higher than the other samples as there was insufficient liquid to provide lubrication during its extrusion through the narrow channel. The increase in forces after 120 mm was probably due to the forces pushing against the narrow channel of the bag as the mashed potato exited the narrow channel. This is because the narrow channel became turgid as all the mashed potato was in the narrow channel and the end of the channel was being dragged along the base of the extrusion rig.

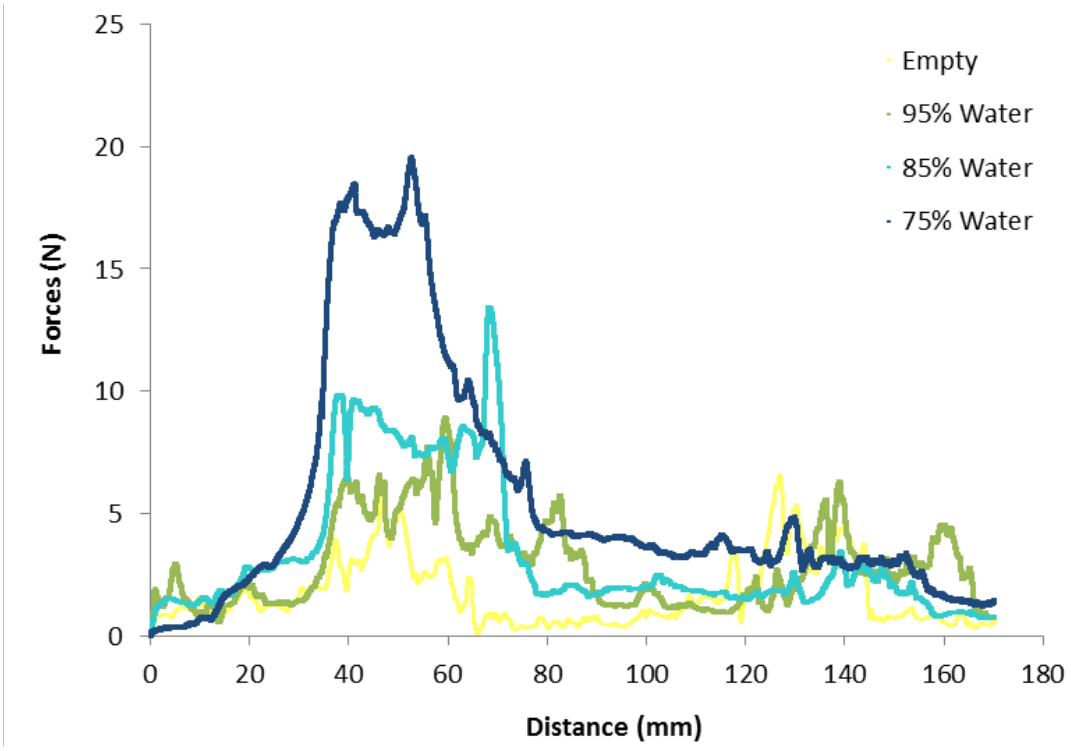


*Figure 5-41. Example of the force profiles for reconstituted mashed potatoes made by adding 75%, 85% and 95% of water (by weight) to dried potato flakes.*

Figure 5-42 shows that the force profiles of both the baseline measurement and the extrusion of the 95% mashed potatoes were quite similar and were not significantly different. Much of the force measured in the baseline measurement was due to the frictional forces acting on the bag as it was being pulled through the rollers. As the gap was too small, the frictional force between the bag and the rollers was more than 5N, which made it impossible to measure fluid samples due to the noise. To reduce the noise, a series of tests was carried out to find an optimum gap setting that was wider to reduce the frictional forces but narrow enough to measure the force needed to extrude extremely soft or flowable materials. The gap between rollers was determined by measuring the force needed to pull an empty extrusion bag through the rollers starting from a gap of 0.3mm and increasing in 0.05mm increment until the force measured was below 0.5N.

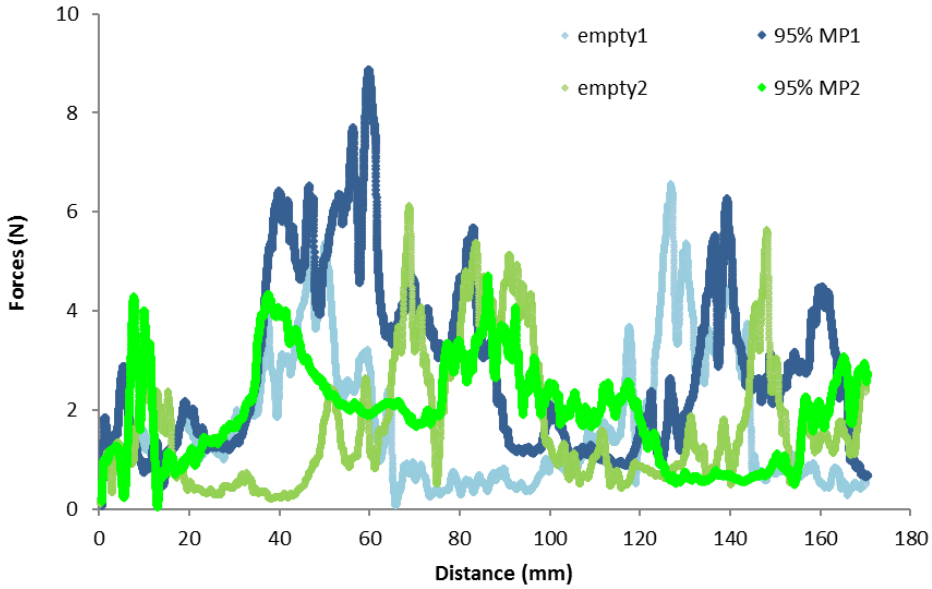


*Figure 5-42: Force profile of baseline measurement of empty bags and the extrusion of 95% water mashed potato at gap setting of 0.6mm.*

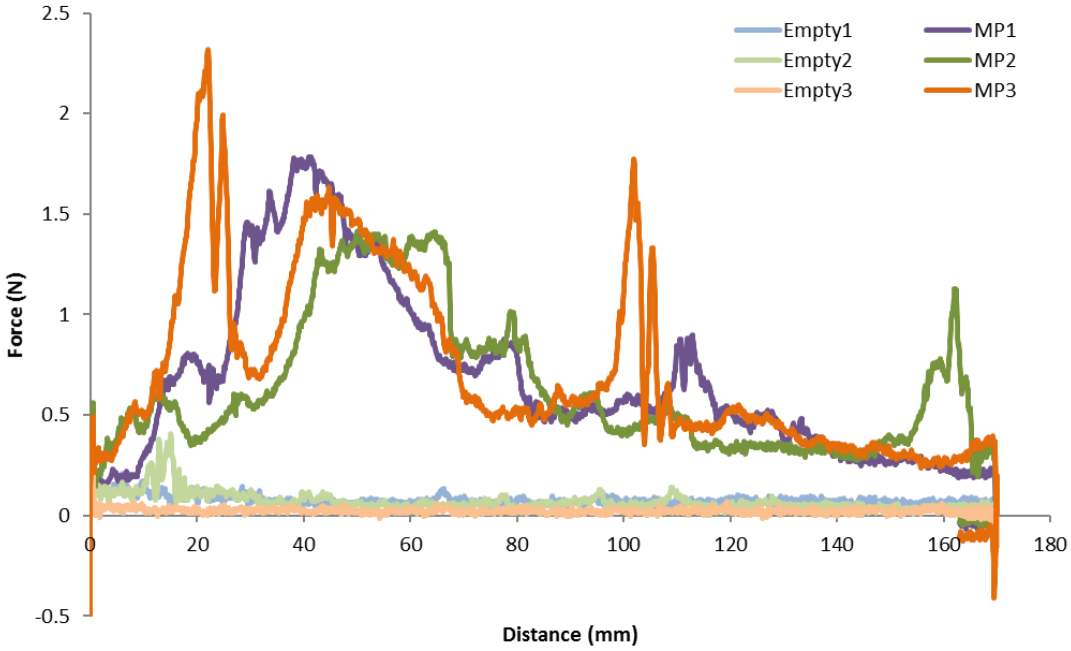


*Figure 5-43: Force profile of baseline measurement of empty bags and the extrusion of 95% water mashed potato at gap setting of 0.75mm.*

The final gap setting was determined at 0.75mm as it allowed the test to be sensitive enough to measure the forces needed to extrude the 95% water mashed potatoes with the noise greatly reduced (Figure 5-43). The peak force measured for the extrusion of the empty bags was less than 0.5N. The initial spike at the start of the test is due to the sudden change of speed as the crosshead started to move.

### 5.2.3. Evaluation Using Three Model Food Systems

The SET was developed to investigate bolus properties. However, this test should be able to measure both unswallowable (boluses from initial stages of mastication) and swallowable boluses. Therefore, three model food systems with different rheological properties and hardness were selected to evaluate the SET so as to understand the limits of this test system, its sensitivity and the bag's seam strength. The SET was tested with a viscous fluid with varying viscosity, gelatine gels with varying hardness and a liquid-particulate mixture of varying cohesion to simulate a range of conditions relevant to human swallowing. Triplicates were conducted across all samples.

***Preparation of model food systems***

The viscous fluids were made using Xanthan gum solutions ranging from 1% to 2% (w/w), increasing at 0.25% intervals. Xanthan gum solutions have been previously used as model fluid food systems (Cutler et al., 1983; Garcia et al., 2005) since most fluid foodstuffs are shear thinning. In each test, five grams of xanthan gum solution was extruded through the slip extrusion bag.

Gelatine gels differing in hardness but identical in size and shape were made from five grades of gelatine (Gelita 125, 150, 175, 200 and 250 blooms; Gelita NZ. Ltd., Christchurch, New Zealand) according to the formulations in

Table 5-6. The compositions and procedure of making the gels were similar to those described by Lassauzay, Claire et al. (2000) and Gray-Stuart (2016) respectively. Half the water was used to dissolve the gelatine in a water bath at 75°C while the remaining water was added to the glucose and sucrose and heated until the solution reached 100°C. The sugar solution, citric acid and colour (to differentiate between gel samples) were added to the gelatine and the mixture was stirred to ensure it was well mixed. The mixture was placed back in the water bath at 75°C for 60 minutes to de-gas. After heating, the molten gel was poured into aluminium moulds (200 x 15 x 10 mm), and left to cool at room temperature for 24 hours. A sharp kitchen knife was used to cut the gels into cuboids (20 x 15 x 10 mm) of 4.5 ± 0.2g each.

*Table 5-6: The mass composition (%) of the gelatine gel samples.*

| Bloom | Gelatin | Water | Glucose | Sucrose | Citric acid |
|---|---|---|---|---|---|
| **125** | 6.21 | 23.17 | 36.41 | 30.62 | 3.59 |
| **150** | 6.85 | 23.01 | 36.16 | 30.41 | 3.56 |
| **175** | 7.86 | 22.76 | 35.77 | 30.08 | 3.52 |
| **200** | 8.85 | 22.52 | 35.39 | 29.76 | 3.49 |
| **250** | 10.88 | 22.02 | 34.60 | 29.10 | 3.41 |

A series of particulate samples was created by mixing glass ballotini (between 510 to 750 microns) with different amounts of xanthan gum solution. Glass particles were used as an extreme example of a non-deforming particle-liquid binder system. Work done by Flynn (2012) showed that the amount of moisture in a peanut bolus collected at the point of swallow is around 50% of the initial dry weight. Based on this finding, a range of xanthan gum solution masses were added to 5 g of glass ballotini as shown in Table 5-7 producing five sets of particulate samples.

*Table 5-7: The amount of 0.1% (w/w) xanthan gum solution to be added to 5 g of glass ballotini to produce five sets of samples in the particulate system. Note: (*): SP corresponds to the amount of liquid reported by Flynn (2012) for a peanut bolus at swallow point.*

| Sample | Amount of Xanthan Gum Solution (g) | XG Solution in mixture (%) |
|---|---|---|
| **Dry** | 0.00 | 0 |
| **¼ SP*** | 0.625 | 11.11 |
| **½ SP *** | 1.25 | 20 |
| **SP*** | 2.50 | 33.33 |
| **2 SP*** | 5.00 | 50 |

***Instrumental characterisation***

The SET was carried out using the following test conditions. The crosshead speed was 20mm/s and it travelled to a distance of 170mm operating in tension mode. The gap between rollers was 0.75mm for all samples except for the particulate system, which needed a gap of 1.45mm.
Viscosity measurements of the viscous fluids were carried out using the a MCR 301 (Anton Paar 19 GmbH, Graz, Austria) rheometer, using a bob and cup geometry at 25°C (bob diameter: 26.637mm, cup diameter: 28.93mm). The viscosity measurement was taken at the shear rate of $3.5s^{-1}$ which was the estimated shear rate experienced at the start of the extrusion test. The shear rate was estimated using Equation (5-1) (Darby, 2001) by assuming that the bag deforms to a cylinder with a diameter of 45mm and that Newtonian viscosity holds.

$$\dot{\gamma} = \frac{8v}{d} \qquad \text{Eq. (5-1)}$$

Where $\dot{\gamma}$ is the shear rate; $v$ is the linear fluid velocity and $d$ is the inside diameter of the pipe.

The hardness of the gelatine gels were measured using the TA.XT plus texture analyser using a uniaxial compression method described by Foster et al. (2006). The gel cuboids were placed on their largest face (20 x 15 x 10 mm) and compressed by a piston head of 50mm diameter. The hardness of the gels corresponds to the force at 70% compression. Oil was applied to provide lubrication, avoiding adhesion between the gel, the piston head and surface of the platform. Compressions were performed at a constant displacement rate of 1mm/sec, up to 70% compression of the initial gel height. All the tests were carried out at room temperature at 20°C.

***Statistical Analysis***

The t-test assuming equal variance (Analysis ToolPak, Microsoft Excel 2010, United States) was used to determine if the effect of increased liquid on the deformation and slip resistance in the particulate system was significant. The Pearson's correlation coefficient was used to quantify correlations between the SET and traditional techniques and the coefficient of variation was used to quantify the reproducibility between replicates.

***Results and discussion***

Figure 5-44 shows example SET data for the three model food systems. As a bag containing a sample was pulled up through the rollers, the forces started to increase at about 20 mm as the rollers start to extrude the sample through the larger portion of the test bag. The forces further increase to the maximum force needed to extrude the sample through the narrowing orifice. The forces decreased as most of the sample had entered the narrow channel. At 100mm, the sample had completely entered the narrow channel and thus the force measured is relatively constant. Similarly shaped force curves were produced for all three model food systems, although the magnitude of the forces were significantly different. This result demonstrates that the test is applicable across a wide variety of food systems.

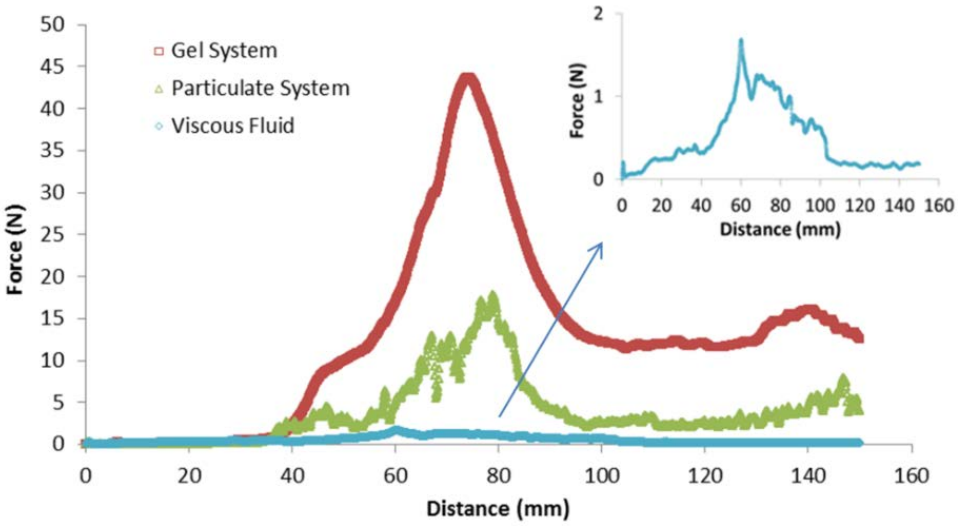


*Figure 5-44: Example force profiles for the extrusion of the different food model systems.*

Figure 5-45a shows the deformation and slip resistance plotted against the viscosities of the xanthan gum solution samples. The forces needed to extrude the xanthan gum solutions are much lower than for the gel and particulate systems as they are easily deformable and flowable. The results show that the test is sensitive enough to detect the differences in the viscosities of the liquid samples.

Figure 5-45b shows how deformation and slip resistances changed during SET testing of gelatine gels of varying hardness. The deformation and slip resistances increased with increasing hardness. The increasing deformation resistance agrees with the idea that as the gelatine gel gets harder, more force is needed to deform it on entrance into the narrow channel. It was noticed that the 250 bloom gels were more rigid and the structure of the gel was least damaged as compared to the other gels. Due to their rigid structure, the 250 bloom gels were packed more tightly against the walls of the narrow channel as it was being extruded, a result that accounts for the great increase in the slip resistance. In this example, the extrusion of the gels without prior processing corresponds to their fracture prior to swallowing; however, the SET is intended to be applied to preprepared boluses for the measurement of bolus properties. The purpose of the gels was to simulate unswallowable foods that required further oral processing prior to swallow.

Figure 5-45c shows the SET applied to liquid-particle mixture model systems as a function of the mass fraction of liquid present. The dry particulate system required the highest force to move it through the bag. This force decreased as more moisture was present to lubricate the cluster of glass ballotini.

Table 5-8 shows that there is significant difference in the forces needed to extrude the XG-ballotini mixtures. However, only the 0% XG mixture was significantly different (P>0.05; t-test assuming equal variance) from the other samples (11% to 50% XG solution added). The addition of the liquid made a difference but adding more liquid did not significantly change the deformation and slip properties of the samples.

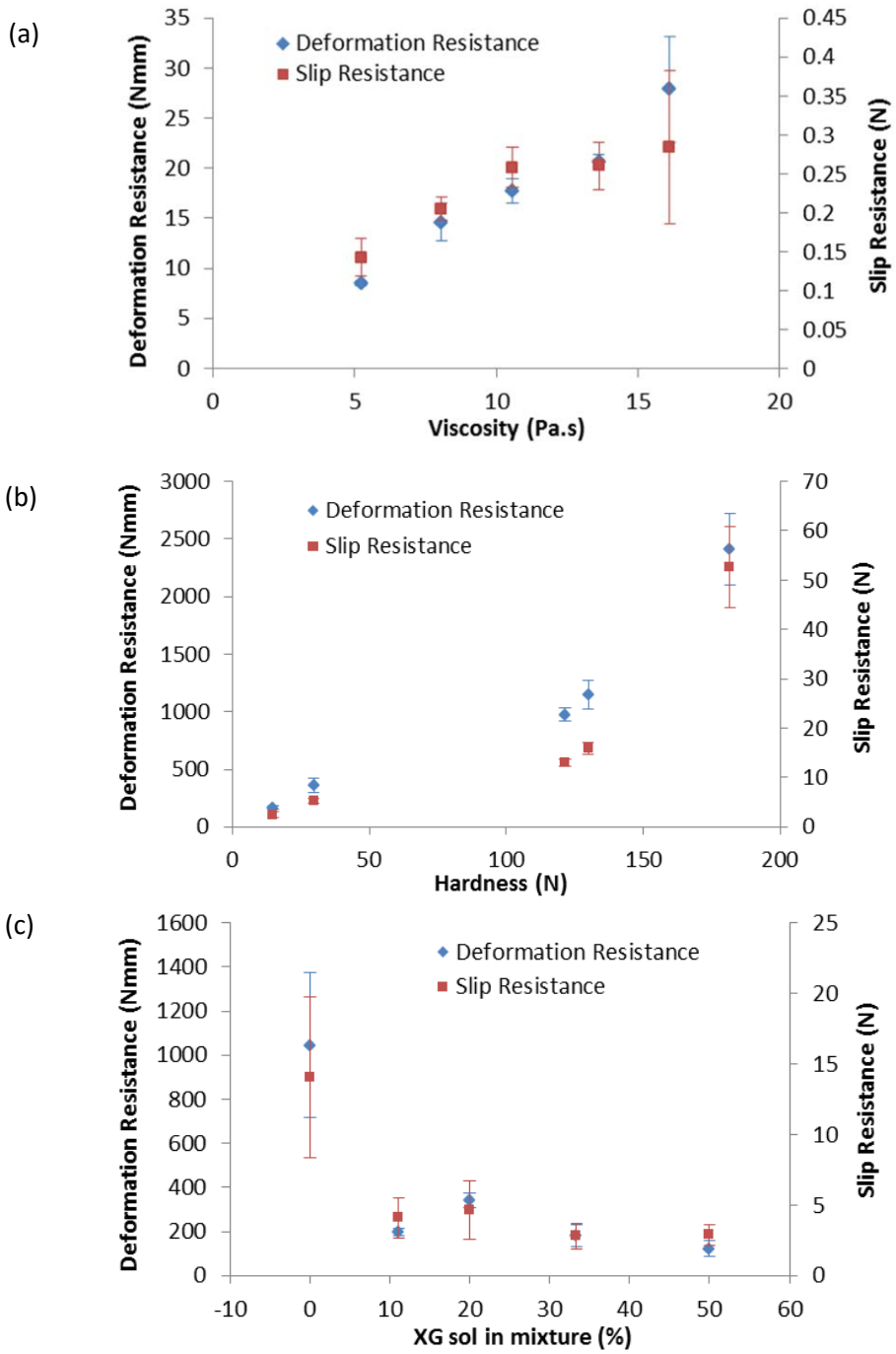


*Figure 5-45: SET results for the three model food systems: (a) Deformation resistance and slip resistance for xanthan gum solutions with different viscosities. (b) Deformation resistance and slip resistance for gelatine gels with different hardness. (c) Deformation resistance and slip resistance of the particulate system versus concentration of xanthan gum (XG) solution in the XG-ballotini mixtures. The mean deformation resistance (◆) and slip resistance (■) are from triplicate measurements and the error bars are the standard error of the mean.*

*Table 5-8:* Analysis of variance (ANOVA) results for the XG-ballotini mixtures varying from 0% to 50% XG solution.

| *Source of Variation* | *SS* | *df* | *MS* | *F* | *P-value* |
|---|---|---|---|---|---|
| Within Groups | 1051.731 | 2 | 525.8655 | 0.106536 | 0.900605 |
| Between Groups | 78206.52 | 3 | 26068.84 | 5.281334 | 0.040372 |
| Error | 29616.2 | 6 | 4936.033 | | |
| Total | 108874.4 | 11 | | | |

In the sample foods studied in this work, there was a strong correlation between the deformation and slip resistance (Pearson's correlation coefficient r=0.99 for gel system, r=0.99 for particulate system, and r=0.93 for the fluid system), thus it appears that the test is effectively measuring a single property. Considering the different stresses applied to the food during the deformation and slip stages of the test, this correlation may not always be observed across all foods. For example, a food like banana may present differently as it should slip on the walls of the bag quite easily after the initial deformation into the narrow channel of the bag. The measurements for the three systems are of different orders of magnitude, but there is good reproducibility across all the model food systems. The average coefficient of variation (CV) between replicate deformation resistances was 15.6%, 19.2% and 32.7% for xanthan gum, gel and particulate samples respectively. For slip resistance, the average CVs were 28%, 19.9% and 60% for these same samples. The results showed that the test was sensitive enough to measure a system that was easily deformable as demonstrated with the viscous food system. Thus, the SET can evaluate boluses that are ready for swallow.

The deformation and slip resistance measurements of the SET followed expected trends with respect to the hardness and viscosity measurements of the gelatine gels and XG solutions respectively (Pearson's correlation coefficient r= 0.94 for correlation between deformation resistance and hardness; r=0.85 for slip resistance and hardness in gels; r=0.98 for deformation resistance and viscosity; r=0.93 for slip resistance and viscosity in XG solutions). While the SET results correlate with viscosity and hardness, two different traditional measures were needed to characterize the different model food systems, while the SET could be applied across all the systems. Another advantage of the test is that the SET could be applied to a wider range of textures than uniaxial compression which is not suitable for liquids and solids that are not self-supporting (Brenner et al., 2014). Although this study has been applied to different model food systems, the SET should be investigated with a larger range of real foods with varying rheological properties and with food boluses chewed by human subjects.

### 5.2.4. Boluses obtained in vivo

The SET proved to be useful in characterizing the deformation and slip properties of different model food systems, thus the next step was to demonstrate the application of the test in characterising properties of bolus expectorated at different stages of the mastication process.

***Methodology***

Peanuts (ETA Dry Roasted Peanuts, Griffins Foods Limited, Auckland, New Zealand) were presented as split kernels and the portion size was standardised by weight (3 ± 0.02 g). A single subject was instructed to chew a serving of peanuts and swallow naturally while being video recorded. The number of chews taken to reach swallow point was determined from the recording when the subject indicated by raising her hand. The average number of chewing cycles taken to reach the swallow point ($CC_{SP}$= 34 ± 2) was determined from triplicate measurements. Subsequently, the subject was instructed to expectorate the bolus after a certain number of chewing cycles as seen in *Table 5-9*. The order in which samples were prepared was randomised. The boluses were expectorated into small cylindrical containers and capped immediately. Upon completion of the collection of boluses, the boluses were transferred to the SET bag, weighed and characterised using the SET. Each bolus is only transferred into the SET bag just before the test is carried out to minimize drying of the bolus surface. Triplicates were collected for each stage of the mastication.

*Table 5-9: The number of chewing cycles corresponding to the stage of mastication where $CC_{sp}$ is the number of chewing cycles taken to reach the swallow point.*

| Stage of Mastication | No. of Chews |
|---|---|
| - | 0 |
| **1/4 of $CC_{sp}$** | 8 |
| **1/2 of $CC_{sp}$** | 17 |
| **3/4 of $CC_{sp}$** | 25 |
| **$CC_{sp}$** | 34 |
| **1.5 of $CC_{sp}$** | 51 |

***Results and discussion***

Figure 5-46 shows the preliminary results of the test applied to actual bolus at different stages of mastication. The expectorated bolus weight varied due to potential losses in peanuts during chewing and due to the addition of saliva. The work done on any given sample, to deform it from its original shape (in the wider region) into the narrower region of the bag, will be dependent on the volume of

material that must be reshaped. As such, it is appropriate to normalise the deformation resistance against the sample volume. Similarly, the slip resistance force is dependent on the surface area of the bolus in contact with the slip extrusion bag, which will also vary linearly with the sample volume. In this experiment, the density of the peanut bolus is expected to be relatively constant and so for convenience the deformation and slip resistances were normalised against sample weight. In the early stages of chewing (i.e. after 8 chews), the variance between the replicates is greater than the other samples. This is because in the initial stage, the peanuts are still in the process of being broken down to smaller particles and it was noted that there were some large particles present in one of the replicates. Thus, a larger amount of force was needed to extrude the bolus. The heterogeneity of the boluses is reduced after the initial stages of chewing as the peanuts are completely broken down to smaller particles and the subsequent chews facilitate mixing and clustering of the particles with saliva to form "safe-to-swallow" boluses. This result is in agreement with the studies by Flynn (2012) stating that there was a slower rate of change in the particle size distributions of peanut boluses after 15 chewing cycles and by Peyron, Marie-Agnès et al. (2011) stating that the particle size and hardness values of the cereal boluses changed little after the first half of the masticatory sequence.

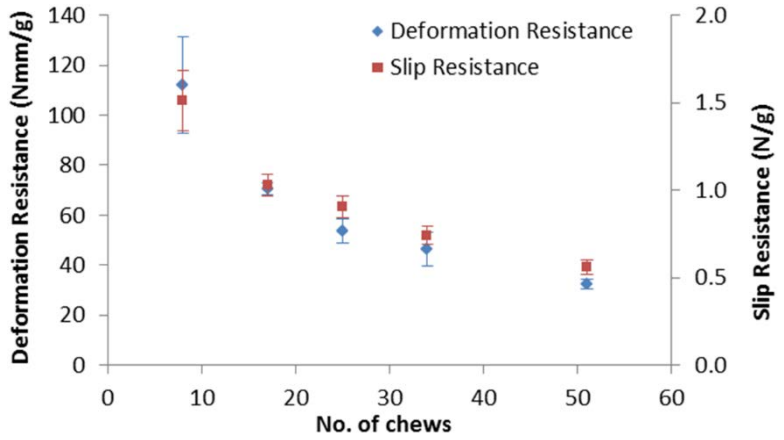


*Figure 5-46: SET results for the boluses obtained in vivo: The normalised resistance to deformation and slip of the peanut boluses with increasing number of chewing cycles. The mean deformation resistance (◆) and slip resistance (■) are from triplicate measurements and the error bars are the standard error of the mean.*

The characterisation of the peanut boluses at different stages of the breakdown process could be further explored by correlating the resistance to deformation and slip to other bolus properties such as the moisture content since it plays a crucial role in forming a bolus. The resistance to deformation and slip continued to decrease further for the bolus that was processed past the swallow threshold. Thus, it was decided that for subsequent studies (chapters 6 and 7), boluses should be processed 25% and 50% past the swallow threshold and collected for characterization

### 5.2.5. Tensile Property of Slip Extrusion Bag

The tensile property of the slip extrusion bag was evaluated as the bags were subjected to plastic deformation and tearing during the extrusion of the harder and more rigid food models. The tensile strength of the bags was measured to determine the range of force that could be exerted on the bag before it became deformed. The bags were cut to 80mm pieces as seen in Figure 5-47 and each end was clamped to a set of grips on the TAXT plus Texture Analyser. A tensile test was conducted to stretch the cut sections at a crosshead speed of 20mm/sec.

(a) (b)

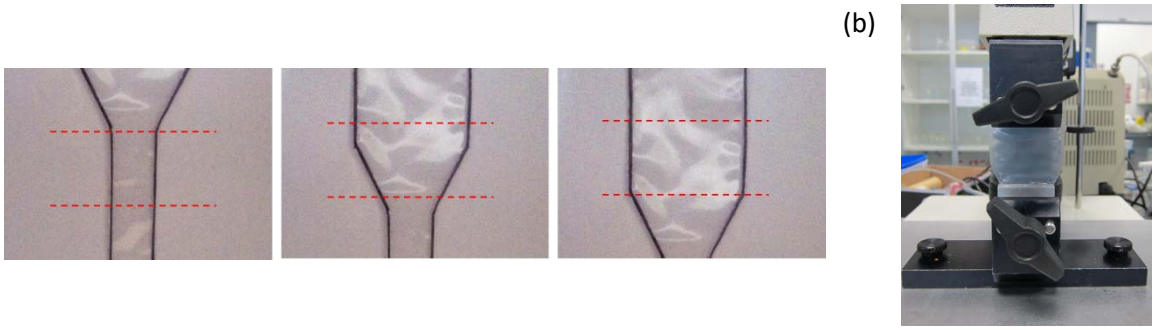

*Figure 5-47: (a) The cut bags were clamped as indicated by the red dotted lines so that the different parts (narrow, middle and wide sections) of the bag was tested. (b) The cut sections of the bags were clamped to a set of grips to determine the maximum force that the section could withstand before failing.*

The bags tore apart at the narrow channel, which required the least force as compared to the bags that tore apart at the middle and wide sections as seen below in Figure 5-48. With the wide sections, the bags can withstand a larger force and yielding of the plastic before the bags tore. Rather than the maximum force measured before the bags tore, the maximum force measured before the plastic started to stretch was taken as the upper limit. Thus, the maximum force before yielding for the wide, middle and narrow section of the bag was 141.26N ± 3.82N, 115.93N ± 0.96N and 74.52N ± 0.69N respectively. Samples that require larger extrusion forces than these values would not be suitable for the SET.

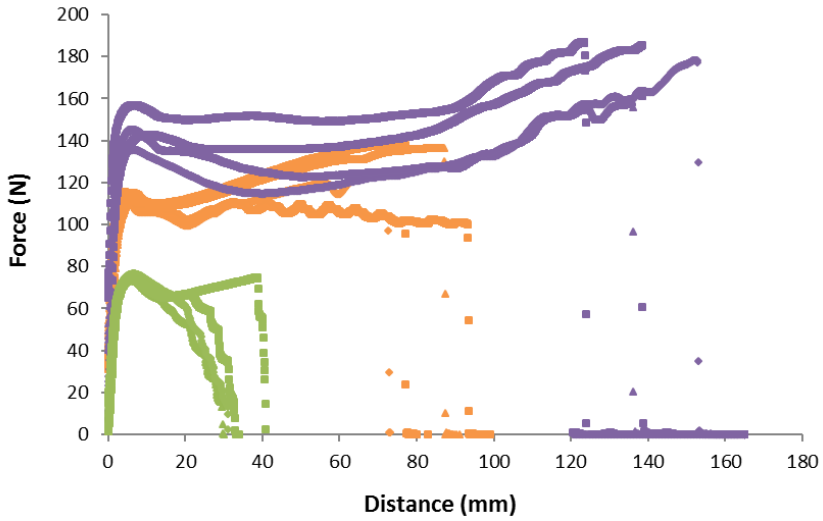


*Figure 5-48: The distanced travelled by the upper grip indicates the length the section of plastic (narrow: green; middle: orange; wide: purple) was stretched for before failing and the corresponding forces measured during the tensile test.*

### 5.2.6. Conclusions on SET

The SET was developed to objectively measure the swallowability of the bolus through determination of its resistance to deformation and slip. The design, manufacture and test parameters were established after troubleshooting the issue with the noise measurement due to the frictional force between the bag and rollers. Finally, the test was evaluated using three model food systems and the results correlated well with the properties of the model foods. As the test was successfully applied across liquids to solids as well as the preliminary bolus study, the SET could be used to quantify the resistance to deformation and slip for all types of foods including solid foods and boluses produced throughout the various stages of oral processing. It was noted that the SET bag started stretching if the extrusion forces exceeded the tensile strength of the material and thus, this was a limitation especially for the measurement of unchewed solid foods. However, it could still potentially be used to investigate the properties of boluses expectorated up to and including the swallow point.

## 5.3. Overall conclusions on novel bolus characterisation methodologies

In this chapter, two novel techniques, the multiple pin penetrometer test and the slip extrusion test were developed and evaluated for their potential usage in characterizing boluses. The MPP test provides a distribution of pressure data that could be analysed with the Rosin-Rammler function as used in previous chapters to describe the particle size distribution of boluses. This method is suitable

for foods that do not break down into discrete particles, and thus fills in the gap for the characterisation of foods/ boluses that are non-fracturable. The SET was developed to characterise the deformation and slip properties of boluses and it was successfully applied in a preliminary experiment to peanut boluses collected at various stages of mastication. Thus, the next step would be to demonstrate how these developed methods can be used together with the mastication robot to track the dynamic changes in the bolus properties during mastication.

# Chapter Six Human study and determination of chewing parameters for robot mastication

The previous chapters described the development and validation of the three potential techniques, the slip extrusion test, the multiple pin penetrometer and the mastication robot, which could be used to characterize boluses during food breakdown. However, the application of these has not yet been demonstrated. In this chapter, a human study was conducted to characterise chewing during the breakdown of five different foods so that the chewing process could be simulated using the MR to produce boluses for characterization. The parameters needed were: (a) the amount of simulated saliva to be added during the chewing cycles in the MR; (b) the chewing trajectory by the MR; and (c) the baseline force needed for mastication in the MR in order to break these foods down into an equivalent bolus in the same number of chews as done by people. Once these parameters are known, boluses can be prepared in a reproducible way using the MR at different degrees of mastication, and the rate of bolus breakdown can be studied (see Chapter 7).

## 6.1. Sample preparation

Five foods were selected from the food categories that Aguilera and Lillford (2007) had created for natural foods based on their structure: (a) embryos containing starch, protein and fat such as grains, legumes and eggs; (b) fleshy cellular parts of plants that retain water such as tubers, fruits and vegetables; and (c) tissue structures such as muscle fibers in meat. Peanuts were selected to represent a brittle food that would break down into individual particles. Much of the published work done to track the breakdown of brittle food has been through particle size studies (Hiiemae, M. K. & Palmer, 1999; Peyron, M. A. et al., 2004). Peyron, Marie-Agnès et al. (2011) found that other than the particle size, factors such as the cohesiveness and lubrication contribute to the triggering of a swallow. Thus, there is value to apply these novel techniques to characterize the breakdown of peanuts in terms of the slip and deformability properties. Apples were selected for their initial crunchy texture due to the cellular structure that gets broken down to a pulp upon mastication. Ham was selected to represent the food that has a fibrous structure that would undergo softening and breaking down of connective tissue and myofibrillar protein fibre during mastication. For such fibrous food, the properties of the bolus at swallow is not well documented. In previous studies, the boluses were analysed using shear (cutting) tests, which is very sensitive to the orientation of the myofibers, may not be the best characterization test since the structure of the meat bolus is disorganized without visible fiber orientation, thus measurement had to be done in several points of the bolus (Yven, C et al., 2005). Thus, the novel techniques developed may potentially be better in

characterizing the boluses. Weet-Bix bites have a crisp and extremely dry texture which softens and turns pasty upon contact with moisture. It was selected due to interest in understanding how moisture uptake into the dry particles during breakdown affect the bolus properties. Muesli bars have many different food components bound together by a syrup. These were selected to represent a heterogenous food with various structures.

The five foods selected were ETA Dry Roasted Peanuts (The Griffin's Food Company, Auckland, New Zealand), Weet-Bix wild berry bites (Sanitarium Health and Wellbeing Company, Auckland, New Zealand), Braeburn apples (Countdown packed bags), Continental carve leg ham (Heller Tasty Limited, Christchurch, New Zealand), Superfruits raspberry & pomegranate muesli bar (Nice & Natural, The Griffin's Food Company, Auckland, New Zealand). The samples were prepared as described in Table 6-1.

*Table 6-1: Description of the portion sizes of the food samples.*

| Food | Weight (g) | Volume ($cm^3$) | Dimensions (cm) | Sample Description |
|---|---|---|---|---|
| **Peanuts** | 3.00 ± 0.05 | 5.04 | 1.4 x 0.9 x 0.5 | Eight peanut halves |
| **Weetbix** | 2.75 ± 0.25 | 5.94 | 2.7 x 2.0 x 1.1 | A single piece |
| **Apple** | 6.00 ± 0.25 | 7.50 | 2.5 x 2.0 x 1.5 | A cuboid cut from an apple (without skin) |
| **Ham** | 6.75 ± 0.50 | 7.07 | 3.0 ϕ x 1.0 | A circular slice cut from a block of ham |
| **Muesli bar** | 6.75 ± 0.25 | 8.10 | 1.8 x 3.0 x 1.5 | A cuboid cut from a bar |

## 6.2. Methodology for human mastication study

The same subjects recruited for the validation study (Chapter 4) were instructed to chew a given portion of the food samples in Table 6-1 on their preferred side (i.e. one-sided chewing) and expectorate the bolus into prepared containers when instructed to stop. Samples were collected after three chewing cycles and at the swallow point. For the swallow point samples, subjects were also asked to chew until they felt the bolus was ready to swallow and indicate by raising their hand. The number of chews taken to reach swallow point was recorded. Subjects were asked to rinse their mouth between each sample to remove any remaining particles. The sample collection was repeated five times at each collection point, for each subject, and all trials were randomised. Video recording was done to track the jaw movement during the chewing sequence. The chewing behaviour of

subjects were profiled using the JBMB™ (Jeltema/Beckley Mouth Behavior) Classification Tool (Jeltema et al., 2015).

## 6.3. Analysis of Boluses

The collected samples were immediately weighed before being transferred into the SET bags for the SET. After the SET, the samples were placed in a moisture dish for moisture content analysis. This was done for all samples expectorated by subject A, but SET was not conducted on the boluses collected after three chewing cycles for the remaining subjects. Subject A was selected as he was the median person based on the number of chewing cycles needed to approach the swallow point. To determine the moisture content, the food samples and boluses were placed into dishes, weighed and allowed to dry for 16h at 108°C in an air oven. After drying in the oven, the samples were cooled in a desiccator before they were weighed again.

The statistical analysis evaluating the variables affecting the slip resistance was analysed by ANOVA using Minitab 17, Minitab Software Inc., USA. The factors were DR, subject, moisture content. To explain the variation in DR, ANOVA was applied to the factors SR, subject, moisture content. The moisture content ($MC_{db}$) of the boluses collected after three chews and at swallow point were plotted against the number of chews. A line was fitted using the least squares method (LINEST function in Microsoft Excel). This was used to estimate the initial amount of saliva added to the food at the start of mastication (y-intercept) and the rate of saliva addition over time (slope). It was assumed that the increased moisture content in the bolus is due to the absorption of saliva during mastication. Please refer to in section 4.2.2. for more details of the analysis.

## 6.4. Results

### 6.4.1. Comparison of boluses at swallow point using SET

Table 6-2 shows the results of the boluses characterised by the SET. The food that required the least number of chews on average to approach swallow point was apple, followed by weetbix, then peanuts and ham, with muesli bar requiring the most chews. The differences in the number of chews required between the subjects was largest for apple (SD = 11.54) and the smallest differences were seen in ham (SD = 6.94) and peanuts (SD = 6.88).

*Table 6-2: Summary of the deformation resistance, slip resistance and moisture content of the boluses collected at swallow point for the five foods. The results are the mean of five replicates and presented as means ± SD.*

| Food | Subject | Number of chews | DR (N mm/g) | SR (N/g) | Bolus MC (g/g dry wt) |
|---|---|---|---|---|---|
| Apple | Subject A | 18 | 194.09 ± 38.35 | 4.14 ± 0.65 | 8.14 ± 0.64 |
| | Subject B | 18 | 198.54 ± 49.64 | 5.00 ± 1.05 | 8.08 ± 0.73 |
| | Subject C | 38 | 67.15 ± 17.45 | 1.81 ± 0.31 | 8.54 ± 0.45 |
| | Subject D | 8 | 217.70 ± 51.84 | 5.88 ± 3.31 | 7.42 ± 0.84 |
| | Subject E | 12 | 155.64 ± 29.58 | 4.10 ± 0.90 | 7.34 ± 0.12 |
| Ham | Subject A | 25 | 95.07 ± 28.45 | 1.19 ± 0.45 | 4.02 ± 0.57 |
| | Subject B | 35 | 109.80 ± 18.43 | 1.36 ± 0.27 | 3.63 ± 0.46 |
| | Subject C | 27 | 100.20 ± 39.53 | 1.06 ± 0.37 | 3.75 ± 0.56 |
| | Subject D | 20 | 108.76 ± 19.22 | 1.36 ± 0.31 | 3.45 ± 0.20 |
| | Subject E | 17 | 91.82 ± 22.77 | 0.98 ± 0.30 | 3.70 ± 0.30 |
| Peanuts | Subject A | 27 | 59.40 ± 18.75 | 1.14 ± 0.34 | 0.58 ± 0.17 |
| | Subject B | 30 | 56.73 ± 10.30 | 1.19 ± 0.16 | 0.56 ± 0.06 |
| | Subject C | 31 | 48.81 ± 11.33 | 0.87 ± 0.17 | 0.69 ± 0.06 |
| | Subject D | 15 | 117.28 ± 23.29 | 1.88 ± 0.39 | 0.35 ± 0.05 |
| | Subject E | 20 | 80.04 ± 18.98 | 1.23 ± 0.19 | 0.47 ± 0.07 |
| Muesli Bar | Subject A | 30 | 51.03 ± 22.66 | 0.79 ± 0.19 | 0.56 ± 0.06 |
| | Subject B | 43 | 78.08 ± 20.34 | 1.48 ± 0.40 | 0.49 ± 0.06 |
| | Subject C | 47 | 49.49 ± 11.65 | 0.63 ± 0.22 | 0.75 ± 0.08 |
| | Subject D | 23 | 90.20 ± 14.23 | 1.26 ± 0.14 | 0.37 ± 0.03 |
| | Subject E | 28 | 113.50 ± 14.81 | 1.50 ± 0.32 | 0.34 ± 0.019 |
| Weetbix | Subject A | 17 | 111.56 ± 36.10 | 1.62 ± 0.52 | 0.78 ± 0.06 |
| | Subject B | 37 | 192.45 ± 74.48 | 3.97 ± 1.48 | 0.68 ± 0.08 |
| | Subject C | 30 | 80.21 ± 39.41 | 1.28 ± 0.58 | 0.93 ± 0.04 |
| | Subject D | 15 | 707.27 ± 139.41 | 11.49 ± 2.38 | 0.48 ± 0.05 |
| | Subject E | 17 | 351.89 ± 90.28 | 6.07 ± 1.69 | 0.61 ± 0.04 |

In general, for the same food, the five subjects required different number of chews before they felt that the bolus was ready for swallowing. This inter-individual variability was observed in other studies (Jemt et al., 1979; Lassauzay, C. et al., 2000; Pröschel & Hofmann, 1988). Apart from subject B, the amount of saliva added increased with increasing number of chews across all foods except for ham (Figure 6-1). Although subject B required more chewing cycles, his boluses did not have an increase in the saliva added which suggests that subject B had a lower rate of saliva secretion compared to the other subjects. Salivary rates in terms of chewing cycles were different across the five subjects, this was observed in subjects that had same number of chewing cycles but produced boluses with different moisture content. For example, in the Weetbix boluses collected from the human subjects, the moisture content of the boluses from subject A was 20% more than subject E although they took the same number of chewing cycles.

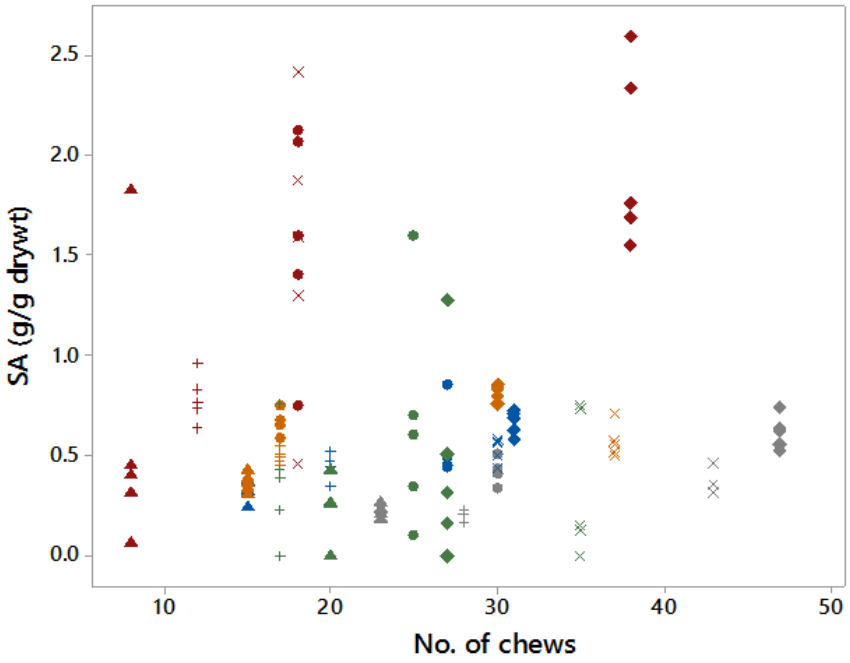


*Figure 6-1: The amount of saliva added assuming all plotted against the number of chewing cycles at swallow point for the five subjects. Colour of symbols represent the food type while symbol shape represents the subject: red = apple, green = ham, grey = muesli bar, blue = peanuts, orange = Weetbix; ● = subject A, × = subject B, ◆= subject C, ▲= subject D, + = subject E.*

In general, the deformation resistance decreased for boluses with higher moisture content within each type of food (Figure 6-2). The effect of moisture on the deformation resistance of the weetbix boluses was greatest as observed in subjects D, E and B. Since the swallow points were different amongst the subjects, the particle sizes and moisture content of the resulting boluses were different. Although particle size analysis was not conducted on the boluses, in some of the foods, the differences in bolus properties and particle size were visually apparent. For example, in Figure 6-3, the apple boluses obtained at swallow point from subject E consisted mostly of small pieces of apple while those obtained from subject B had been well chewed such that the bolus were pulpy with most of the structure destroyed.

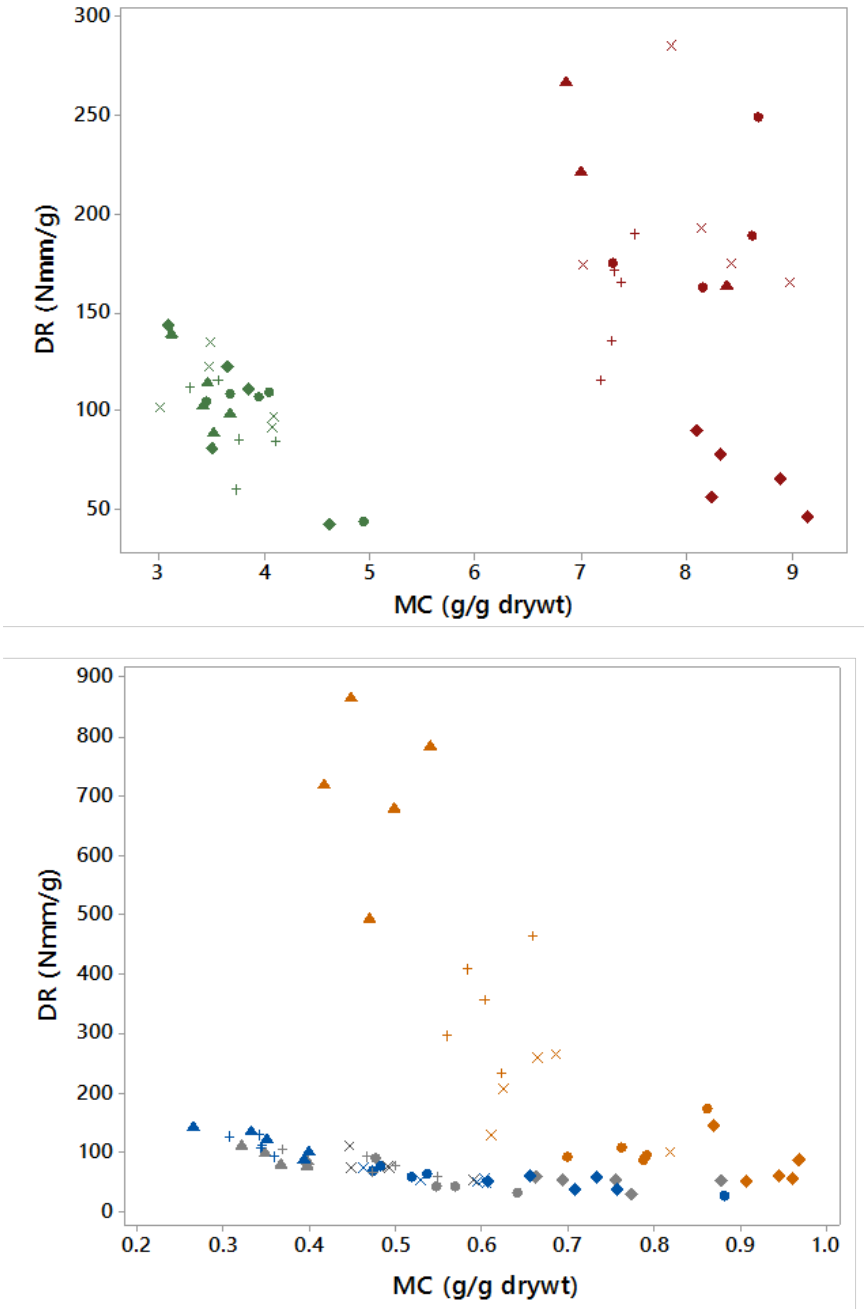


*Figure 6-2: The deformation resistance measured during the extrusion test is plotted against the moisture content of the boluses collected at swallow point for the five subjects. Colour of symbols represent the food type while symbol shape represents the subject: red = apple, green = ham, grey = muesli bar, blue = peanuts, orange = Weetbix; ● = subject A, × = subject B, ◆= subject C, ▲= subject D, + = subject E.*

*Figure 6-3: Apple boluses collected at swallow points of 12 cycles for subject E (left) and 18 cycles for subject B (right).*

Figure 6-4 compares the deformation and slip resistance between subjects (at swallow point) for each food. It may seem that the DR and SR are highly correlated for all the foods except for ham. However, when intersubject variation is considered as in Figure 6-5, the correlation between SR and DR were not always highly correlated for most of the foods. Only the DR and SR of the weetbix boluses were highly correlated for all the subjects. The weetbix boluses at swallow point had been fully broken up into small bits that had smaller dimensions than the narrow channel of the test bag and were a pasty mass which was softening thorugh the addition of saliva with each chew. By this point, the changes in the bolus properties were solely dependent on the increasing moisture and thus, both the DR and SR seem to be measuring the same property.

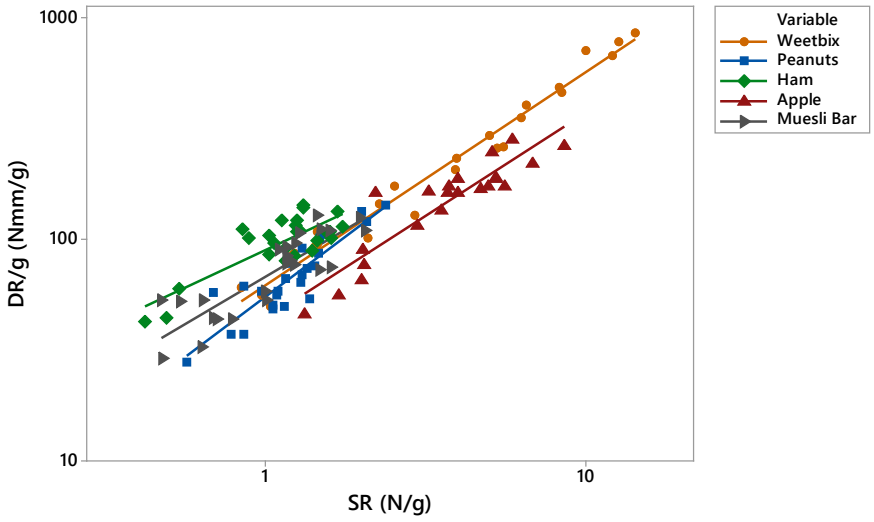


*Figure 6-4: Scatterplot showing the correlation between DR and SR for each food.*

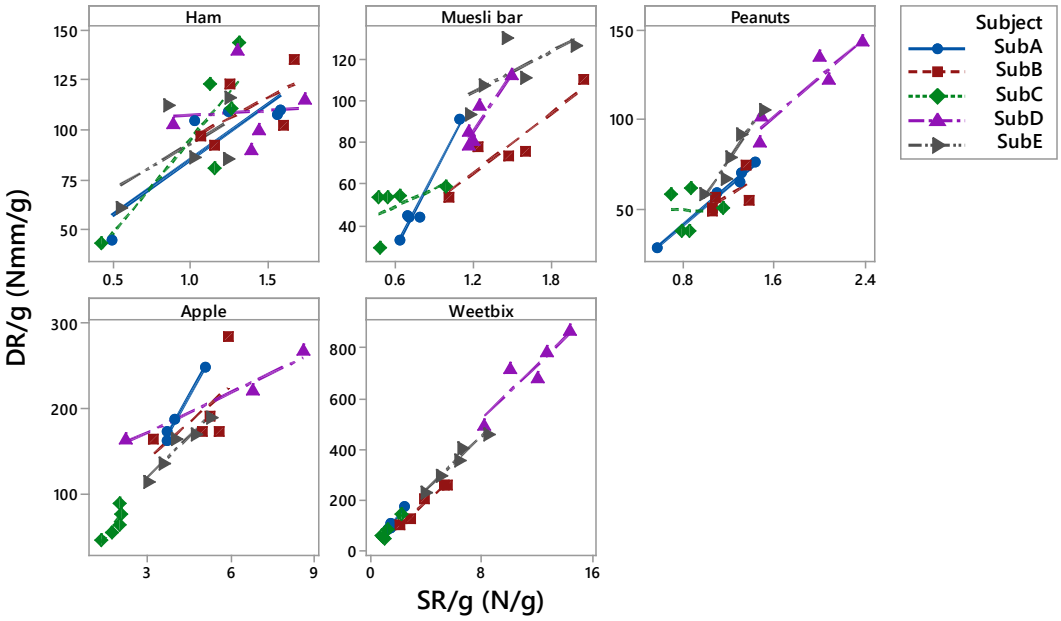


*Figure 6-5: Scatterplots to show the correlation between DR and SR for replicates within each subject for ham, muesli bar, peanuts, apple, and weetbix (from top left in a clockwise direction).*

For some of the foods such as the muesli bar and peanuts, the SR decreased when the boluses had higher amount of moisture comparing within the replicates of each subject (Figure 6-6). This suggests that the effect of moisture content on the SR is high for such boluses. For the peanut boluses, the moisture content was significant in explaining the variance in SR ($p = 0.013$) but not for DR ($p = 0.337$). Although not significant but approaching significance, the F value for moisture content ($F = 3.82$, $p = 0.066$) was higher in explaining the variance in the SR than that for moisture content ($F = 0.62$, $p = 0.442$) in explaining the variance in the DR.

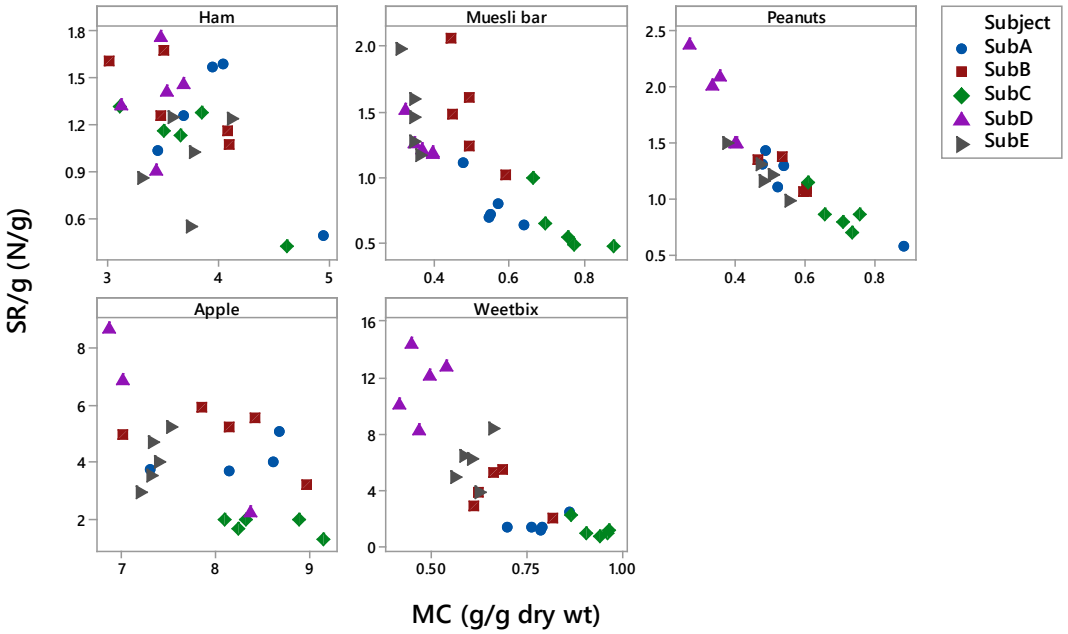


*Figure 6-6: Scatterplots to show the relationship between SR and the moisture content of boluses for replicates within each subject for ham, muesli bar, peanuts, apple, and weetbix (from top left in a clockwise direction).*

It was observed that subjects were consistent in their chewing behaviour such that they used small or large number of chews across all types of food. This agrees with the idea that there are slow and fast swallowers as proposed by Engelen et al. (2005). Similarities in the chewing behaviour and resulting boluses were observed in subjects that belonged to the same category of the JBMB™ Classification Tool. Subjects D and E needed less mastication cycles for their boluses to approach the swallow point, which agrees with their preferred mouth behaviour, as 'crunchers' tend to deem a food ready for swallowing when it is no longer crunchy. Subjects A and B were typed as 'chewers' and the number of chewing cycles needed to approach swallow point was the median or higher. Although subject B had more chewing cycles than subject A, subject B's boluses had a lower moisture content across all foods. This may suggest that foods may be masticated more to compensate for slower salivary uptake into the food so that boluses will be moist enough for swallowing. Subject C has a clear preference for soft foods and was typed as a 'smoosher'. Most of subject C's boluses had the highest moisture content and the number of chewing cycles needed to

approach swallow point was in the 75th percentile or higher across all foods. The variation in the moisture content of boluses at swallow point is proof that subjects' thresholds for bolus properties vary.

In conclusion, subject D and E required less chewing cycles before they felt ready to swallow, while subject B and C required more. Selecting a single subject would eliminate the inter-subject variation and allow focus on the food effects. Based on the number of chewing cycles needed to reach swallow point, subject A was the median. Thus, subject A's data on the number of chewing cycles and amount of moisture addition for each food were used to establish the parameters for the chewing robot's set up in the next phase of work.

### 6.4.2. Chewing trajectories and estimation of saliva added to boluses

Videos of the subjects masticating the five foods were analysed by Arran Wilson from Plant and Food Research, New Zealand, using the method detailed in section 4.1.2. The width, height and inclination of closing slope of each chewing cycle were determined for one video recording of each food per subject. The plots in Figure 6-7 show that peanuts tended to have a small width and height as compared to the other foods indicating that the peanuts were mostly chewed in the vertical trajectory while trajectories used for the muesli bar tended to have a larger width for most of the subjects. The chewing patterns for the other foods differed across the subjects. For example, the chewing trajectory for ham appeared to be more vertical for subject A, C and E but was more lateral for subject B and D.

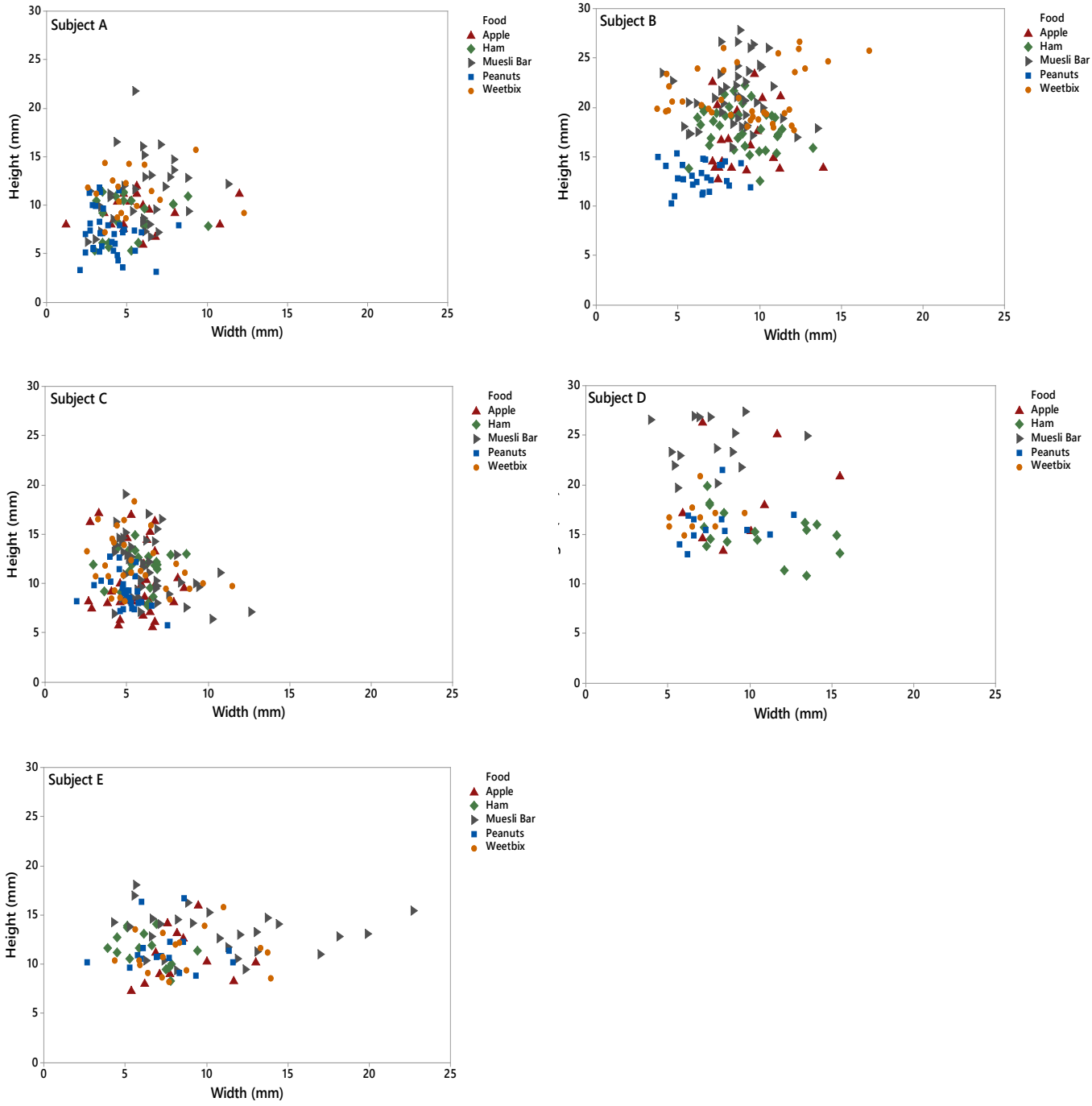


*Figure 6-7: Width and height of each chewing cycle for one mastication recording of each food per subject.*

A greater incline in the closing slope indicates a more vertical chewing trajectory. The tracking of the position on the chin is quite different from that of the measurement on the robot. The dot on the chin may move around more during the tracking as the skin is more flexible and the chin is not completely fixed to the jaw. Figure 6-8 shows that only the closing slopes for the muesli bar had smaller incline across all the subjects.

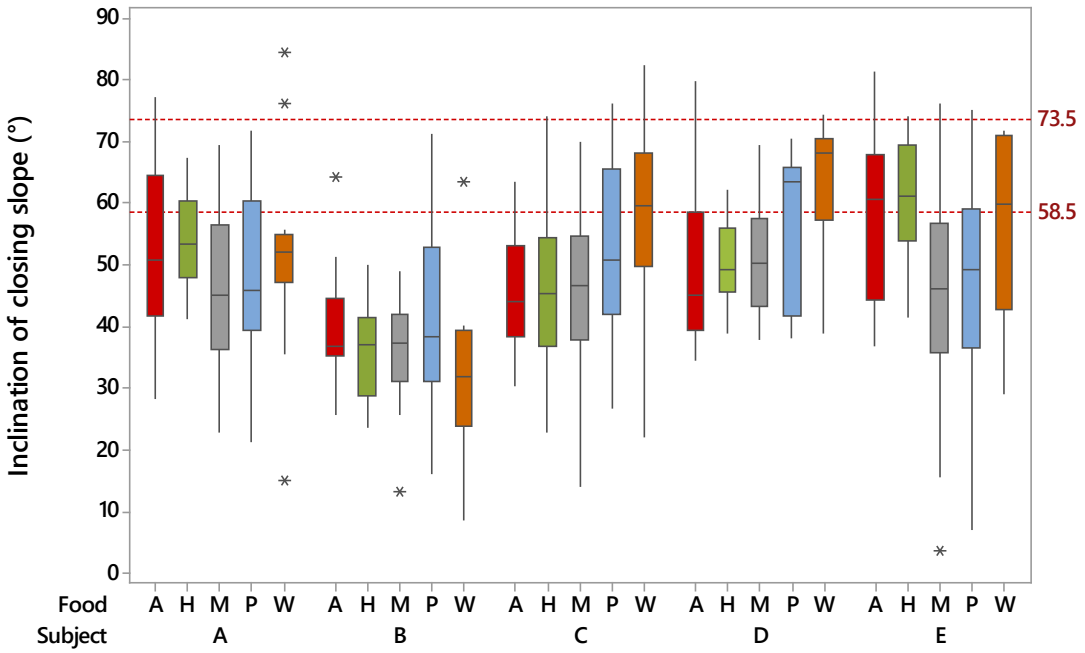


*Figure 6-8: Boxplot of the closing slopes in degrees for chewing cycles in one mastication recording for each food per subject. The reference lines at 58.5° and 73.5° represent the average inclination of the closing slope for the chewing cycles in the lateral and vertical trajectory respectively. The foods are: A- apple, H- ham, M- muesli bar, P- peanuts, W- weetbix.*

To determine if there was an effect of the stage of mastication process on the properties of the chewing trajectories, the average width, height and angle of closing slope for every three chewing cycles was plotted against the number of chews. The average width of the chewing cycles (Figure 6-9) was plotted against the mastication stage for each food. The maximum average width of the chewing cycles for apple and peanuts were the smallest as compared to the other foods. Since a wider chewing cycle indicated a more lateral trajectory, it appears that ham, muesli bar and weetbix were broken down by more lateral chewing cycles while apple and peanuts were broken down by more vertical chewing cycles. For most of the mastication sequences, the width of the chewing cycles at the final stages were either same or larger than at the initial stages. This agrees with previous findings that lateral movements do increase (Hiiemae, K. et al., 1996) or fluctuate about a reasonably constant value (Lucas et al., 1986) throughout a mastication sequence.

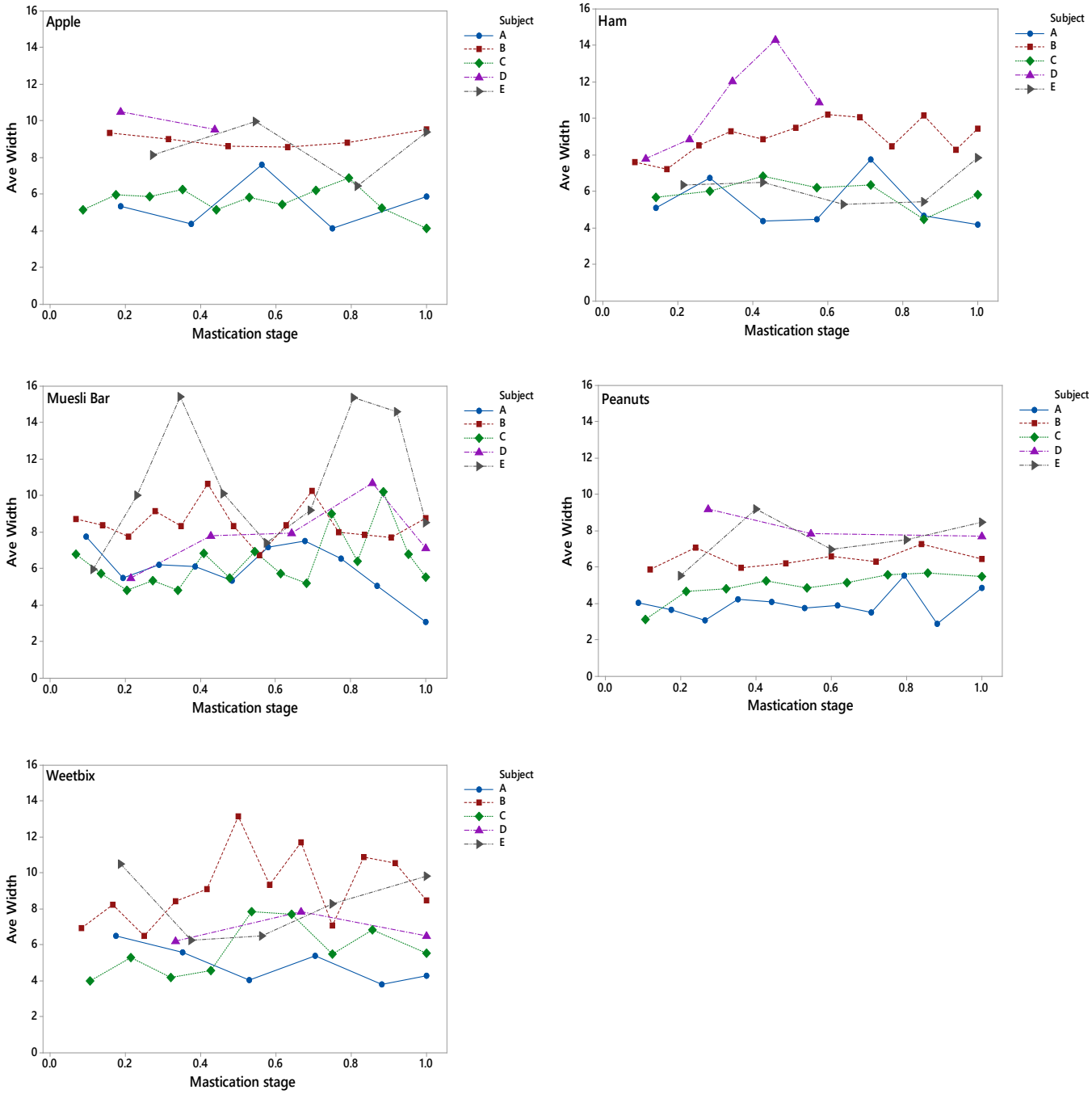


*Figure 6-9: The average width of three chewing cycles plotted against the chewing cycle for the mastication process of each food for each of the subjects. For example, the average width at three chews (first data point) is the average for the first three chews, and the average width at six chews (second data point) is the average width of the fourth to sixth chews, the average of every three chews were determined until the end of each mastication process. For some of them, the final data point was the average of two or four chews, depending on the number of chews in the mastication process.*

The average height of the chewing cycles (Figure 6-10) was either similar or decreased as the mastication stage progressed. As the food got broken down into smaller particles during chewing, resulting in a reduction in the volume of food broken by the teeth in the next closing stroke, the maximum opening of the jaw decreased. This agrees with the suggestion that the jaw is opened no more than necessary for the food to be placed between the molars for mastication (Lucas et al.,

1986; Van der Bilt, A. et al., 1991; Watt, 1976). The muesli bar samples, especially in the initial stage of mastication, required the largest jaw opening across all subjects. The initial higher hardness and adhesiveness properties of the muesli bar required larger jaw opening as compared to the other foods. This agrees with previous work by (ÇAkir et al., 2012); Filipić and Keros (2002); Koç et al. (2014), who reported that greater hardness and adhesiveness resulted in larger vertical and lateral movements. In addition, Allen et al. (2015) found that the extent of reduction in the physiological parameters during a chewing sequence appeared to be greater for larger and/or harder foods as more work was required to begin the initial breakdown of the food.

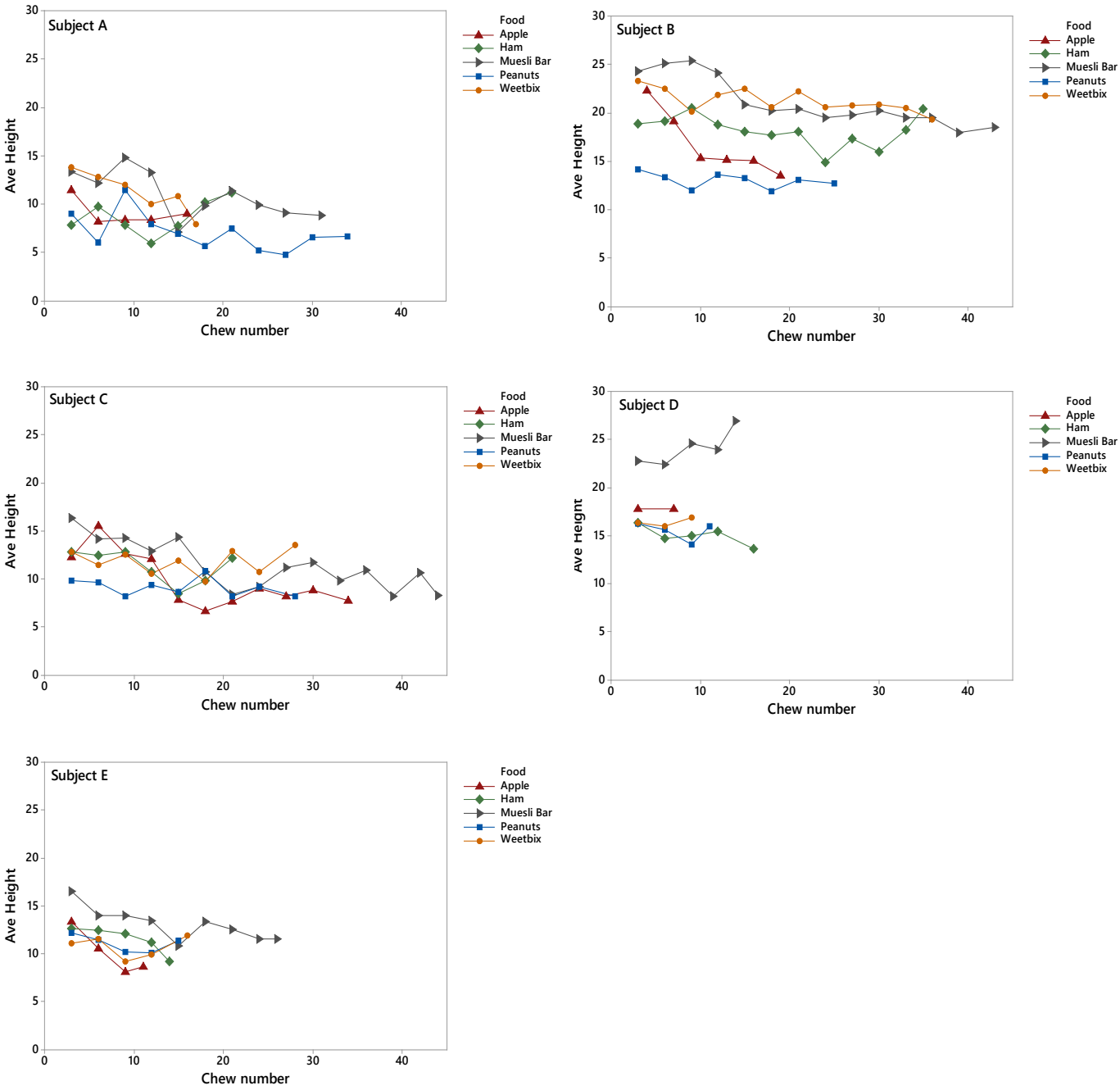


*Figure 6-10: The average height of three chewing cycles plotted against the chewing cycle for the mastication process of each food for each of the subjects.*

The inclination of the closing slope (Figure 6-11) was plotted against the mastication stage for each food. The mastication stage was determined by dividing the chew cycle by the total chewing cycles taken for each subject before reaching swallow point. The chewing cycles in the mastication of apple had high degree of inclination in the initial stages of mastication which decreased, indicating that vertical chewing trajectories were employed in the initial stage of mastication which subsequently proceeded to lateral chewing. In the mastication of ham, there was no clear trend of either an increased or decreased inclination between the initial and final stages of mastication. Except for the increase in the inclination for subject D, the inclination at the initial and final stages of mastication did not change much. The chewing cycles at the initial stages of mastication of the muesli bar followed a lateral trajectory which became more vertical at the later stages of mastication. In the mastication of peanuts, the inclination of the closing slopes was high at the initial stages and gradually decreased with increasing number of chews. The inclination at the final stages of mastication for subjects A, C and D were lower than at the initial stages, which suggests that the initial chews followed vertical trajectories which subsequently became lateral in the final stages of mastication. In the mastication of weetbix, the subjects started with a more vertical trajectory, then changed to a lateral trajectory before switching back to a vertical trajectory at the later stages of the mastication process of weetbix. Only subject B had higher inclination of the closing slopes at the final stages of mastication than at the start. Subject B had the lowest inclination for most of the closing slopes across all the foods although the inclination in the initial stages of mastication was similar to the other subjects (except for weetbix). This suggests that subject B used more shearing action to grind the particles as the mastication stage progressed. To compensate for the slower salivary uptake into the food in subject B, this could be a response to create smaller particles with greater surface area for moisture adsorption and facilitate bolus formation.

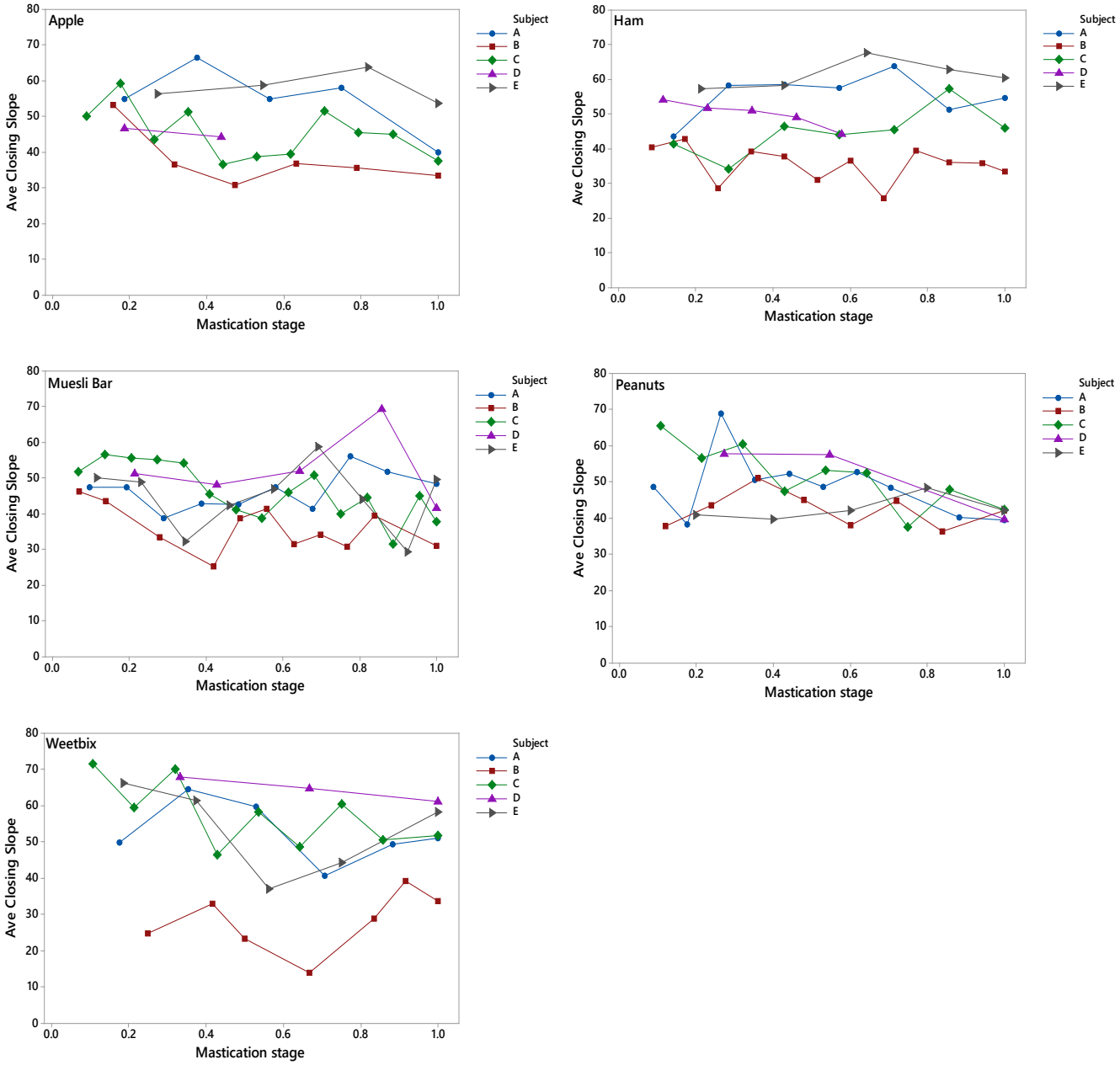


*Figure 6-11:The average inclination of the closing slope in degrees of three chewing cycles plotted against the chewing cycle for the mastication process of each subject for each of the foods. From left to right: apple, ham (first row), muesli bar, peanuts (second row), weetbix (third row).*

It has been shown that saliva plays a significant role in preparing a bolus for swallowing (Chen, Jianshe, 2012; Gavião et al., 2004; Mosca & Chen, 2017). At this stage of the work, the focus was on how the moisture imparted by saliva affects the breakdown and structure of the food as a bolus is formed. To simulate the action of moisture imparted by saliva during mastication, 0.1% xanthan gum (XG) solution will be added during the mastication process in the robot. The moisture content of the collected boluses served as an estimate as to how much saliva was absorbed by the bolus, assuming that all additional moisture other than the food's initial moisture content is due to the addition of

saliva. A summary of the results from the moisture analysis is detailed in Table 6-4. The rate of moisture addition per chew is the slope of the line fitted to the moisture content of boluses plotted against the number of chews. The initial moisture content is the y-intercept of the fitted line. The saliva added is the difference between the moisture content of food and that of the initial moisture content of the bolus, and is taken as the initial uptake of saliva by the food sample when placed in the mouth. The linear regression model fitted the data for weetbix, peanuts and muesli bar well as demonstrated by the high $r^2$ values. The model for the peanut boluses by subject A had a lower $r^2$ value as the first bolus collected at swallow point had 52% more moisture than the average moisture content of the 5 replicates and was probably an outlier. There was poor fit for apple and ham boluses as the individual variation in the moisture of the ham and apple samples were huge as compared to the dry foods. The 'rate per chew' and 'initial saliva added' for subject A were used as parameters for the addition of the XG solution during the mastication in the robot (*Table 6-3*). Calculations are detailed in section 4.2.2.

*Table 6-3: The saliva parameters for subject A in dry weight is converted to a wet weight basis using a moisture factor for each food. The values for 'initial addition' and 'rate per chew' are the mean of five replicates presented as mean ± SD.*

| | Saliva (subject A) | | | XG solution | |
|---|---|---|---|---|---|
| Food | Initial addition (g/g dry wt) | Rate per chew (g/g dry wt) | Moisture factor | Initial Addition (g) | Rate per chew (g) |
| Apple | 1.191 ± 0.336 | -0.011 ± 0.026 | 0.108 | - | - |
| Ham | 0.395 ± 0.308 | 0.011 ± 0.017 | 0.212 | 0.566 | 0.016 |
| Muesli bar | 0.092 ± 0.024 | 0.011 ± 0.001 | 0.794 | 0.512 | 0.061 |
| Peanuts | 0.189 ± 0.067 | 0.013 ± 0.003 | 0.799 | 0.452 | 0.031 |
| Weetbix | 0.235 ± 0.047 | 0.026 ± 0.004 | 0.706 | 0.498 | 0.055 |

*Table 6-4: Results of moisture content analysis for each food based on moisture content of boluses collected from subjects in human study. Note: the rate of saliva addition is determined as the slope of the line fitted to the moisture content of boluses collected after three chewing cycles and at swallow point. The initial moisture content is the y-intercept of the fitted line.*

| Food | Subject | Rate per chew (g/g dry wt) | SD (g/g dry wt) | Initial MC (g/g dry wt) | SD (g/g dry wt) | $r^2$ | Initial saliva added (g/g dry wt) | $MC_{dbbolus}$ (g/g dry wt) |
|---|---|---|---|---|---|---|---|---|
| Apple | A | -0.011 | 0.026 | 8.340 | 0.336 | 0.022 | 1.191 | 8.144 |
| | B | 0.064 | 0.025 | 6.934 | 0.317 | 0.458 | -0.215 | 8.083 |
| | C | 0.057 | 0.006 | 6.383 | 0.175 | 0.906 | -0.767 | 8.540 |
| | D | 0.090 | 0.065 | 6.446 | 0.392 | 0.193 | -0.703 | 7.164 |
| | E | 0.017 | 0.019 | 7.141 | 0.165 | 0.088 | -0.008 | 7.340 |
| Ham | A | 0.011 | 0.017 | 3.739 | 0.308 | 0.049 | 0.395 | 4.016 |
| | B | -0.003 | 0.010 | 3.730 | 0.259 | 0.009 | 0.386 | 3.632 |
| | C | 0.003 | 0.014 | 3.671 | 0.274 | 0.005 | 0.327 | 3.749 |
| | D | -0.018 | 0.013 | 3.810 | 0.191 | 0.188 | 0.466 | 3.570 |
| | E | -0.007 | 0.019 | 3.822 | 0.236 | 0.018 | 0.478 | 3.696 |
| Muesli bar | A | 0.011 | 0.001 | 0.227 | 0.024 | 0.925 | 0.092 | 0.556 |
| | B | 0.007 | 0.001 | 0.192 | 0.021 | 0.930 | 0.057 | 0.494 |
| | C | 0.012 | 0.001 | 0.188 | 0.029 | 0.959 | 0.053 | 0.753 |
| | D | 0.008 | 0.001 | 0.184 | 0.014 | 0.917 | 0.049 | 0.366 |
| | E | 0.007 | 0.000 | 0.153 | 0.009 | 0.966 | 0.018 | 0.339 |
| Peanuts | A | 0.013 | 0.003 | 0.214 | 0.067 | 0.652 | 0.189 | 0.515 |
| | B | 0.013 | 0.001 | 0.162 | 0.026 | 0.936 | 0.137 | 0.637 |
| | C | 0.019 | 0.001 | 0.103 | 0.024 | 0.975 | 0.077 | 0.549 |
| | D | 0.018 | 0.002 | 0.081 | 0.024 | 0.891 | 0.056 | 0.667 |
| | E | 0.014 | 0.002 | 0.195 | 0.030 | 0.843 | 0.170 | 0.497 |
| Weetbix | A | 0.026 | 0.004 | 0.345 | 0.047 | 0.848 | 0.235 | 0.781 |
| | B | 0.013 | 0.001 | 0.215 | 0.031 | 0.934 | 0.105 | 0.681 |
| | C | 0.022 | 0.001 | 0.260 | 0.023 | 0.981 | 0.150 | 0.930 |
| | D | 0.017 | 0.002 | 0.216 | 0.024 | 0.881 | 0.106 | 0.475 |
| | E | 0.015 | 0.002 | 0.343 | 0.023 | 0.898 | 0.233 | 0.606 |

## 6.5. Methodology for mastication robot

In chapter three, it was found that chewing trajectory and the baseline force influenced the breakdown rate of peanuts. In addition, it was established that the amount of moisture imparted by saliva had an effect on the bolus properties. The objective of this next phase was to identify the trajectory, amount of saliva and amount of baseline force needed for the mastication robot to produce a bolus with similar deformation and slip resistance properties as the ones produced by subject A for each food system. This would form a basis for full characterization of bolus formation using the novel methodologies developed in this work.

### 6.5.1. Experimental design for robot mastication study

A full factorial design of 3 factors with 2 levels was used to identify the parameters to be used for the mastication process that could provide bolus properties closest to those obtained from the median subject, subject A, based on the slip extrusion test (SET) results. The factors were: chewing trajectory, the rate of 0.1% XG solution (artificial saliva) addition, and the baseline force as shown in Table 6-5. Trajectories produced by the ground link length of 50mm and 3mm are referred to as the lateral and vertical trajectories respectively. To simulate the saliva addition, the amount of XG solution added for the corresponding level for each food is shown in Table 6-6. The baseline force was controlled by adjustment of the table height, which is the distance between the lower molar repositioning table and the base plate (*Figure 6-12*), and is detailed in Table 6-7. The response monitoring was based on the deformation and slip resistance from the SET after the specified number of chews for each food.

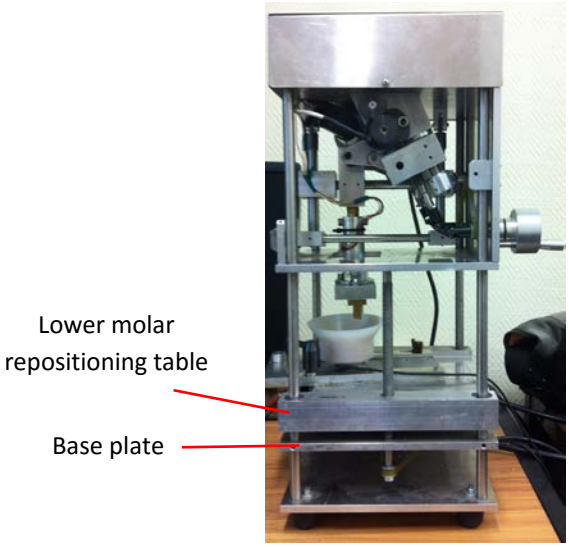


*Figure 6-12: The table height is adjustable to achieve desired baseline force by changing the distance between the lower molar repositioning table and the base plate.*

*Table 6-5: $2^3$ full factorial design conducted for each food to determine the settings to be used for phase 2 of mastication study.*

| **Independent factors** | **Levels** | |
|---|---|---|
| | -1 | +1 |
| **Trajectory** | Lateral | Vertical |
| **XG addition (ml/chew)** | 1* rate of saliva addition | 1.5*rate of saliva addition |
| **Baseline force (N)** | 200 | 270 |

*Table 6-6: The amount of 0.1% XG solution to be added to each food at the start (initial addition), and before each chewing cycle (rate per chew or 1.5*rate per chew depending on the level).*

| **Food** | **Initial Addition (g)** | **Rate per chew (g)** | **1.5*rate per chew (g)** |
|---|---|---|---|
| Apple | - | - | - |
| Ham | 0.566 | 0.016 | 0.024 |
| Muesli bar | 0.512 | 0.061 | 0.092 |
| Peanuts | 0.452 | 0.040 | 0.060 |
| Weetbix | 0.498 | 0.069 | 0.104 |

*Table 6-7: The stage height was adjusted to the following values to achieve the required baseline force in the lateral and vertical chewing trajectories.*

| Baseline Force (N) | Trajectory | Table Height (mm) |
|---|---|---|
| 200 | Lateral | 5.05 |
| 270 | Lateral | 5.80 |
| 200 | Vertical | 6.45 |
| 270 | Vertical | 8.75 |

Each food was chewed by the MR until swallow point, which was defined as the number of chews required by subject A to achieve a bolus that was ready for swallow. The bolus at swallow point was collected and the SET was done before being dried in the oven for moisture analysis. There were eight trials per food ($2^3$ full factorial design), and four replicates for each trial. It was observed that the juice expelled from the apple during mastication was flooding the occlusal surface, thus it was decided that no additional XG solution would be added to the bolus. Thus, for apple a $2^2$ full factorial design was used resulting in only four runs. The factorial design and analysis were performed using Minitab 17, Minitab Software Inc., USA. Solver function in Excel was used to optimize the factors through the regression model from the factorial analysis. This was done by making the DR of the bolus at swallow point for each food from subject A the objective and using suitable constraints.

## 6.6. Results and discussion

The experimental design and results for each run is summarized in Table 6-8.

*Table 6-8: Factorial design and results of deformation resistance, slip resistance and moisture content of boluses for the five foods. The results shown were the mean of four replicates presented as mean ± SD.*

| Run | Coded Factors | | | DR | SR | MC |
|---|---|---|---|---|---|---|
| Code | T | XG | BF | (N mm/g) | (N/g) | (g/g dry wt) |
| A1-1 | -1 | - | -1 | 120.97 ± 8.86 | 4.03 ± 0.38 | 7.41 ± 0.18 |
| A1-2 | -1 | - | +1 | 139.42 ± 6.53 | 3.62 ± 0.24 | 6.66 ± 0.07 |
| A2-1 | +1 | - | -1 | 208.64 ± 32.48 | 5.06 ± 0.66 | 6.52 ± 1.04 |
| A2-2 | +1 | - | +1 | 153.16 ± 35.11 | 4.04 ± 0.56 | 7.57 ± 0.60 |
| H111 | -1 | -1 | -1 | 94.21 ± 12.23 | 0.91 ± 0.10 | 4.00 ± 0.21 |
| H112 | -1 | -1 | +1 | 97.60 ± 11.73 | 1.11 ± 0.23 | 4.09 ± 0.19 |
| H121 | -1 | +1 | -1 | 85.70 ± 27.89 | 1.02 ± 0.49 | 4.11 ± 0.16 |
| H122 | -1 | +1 | +1 | 77.61 ± 14.91 | 0.89 ± 0.21 | 4.16 ± 0.07 |
| H211 | +1 | -1 | -1 | 77.56 ± 13.14 | 0.82 ± 0.11 | 4.34 ± 0.17 |
| H212 | +1 | -1 | +1 | 88.52 ± 17.51 | 0.98 ± 0.27 | 4.07 ± 0.21 |
| H221 | +1 | +1 | -1 | 76.98 ± 4.78 | 0.73 ± 0.04 | 4.12 ± 0.07 |
| H222 | +1 | +1 | +1 | 81.37 ± 17.70 | 0.81 ± 0.17 | 3.99 ± 0.30 |
| M111 | -1 | -1 | -1 | 61.83 ± 10.38 | 0.94 ± 0.20 | 0.55 ± 0.01 |
| M112 | -1 | -1 | +1 | 63.29 ± 7.80 | 0.94 ± 0.17 | 0.55 ± 0.01 |
| M121 | -1 | +1 | -1 | 50.24 ± 10.07 | 0.77 ± 0.05 | 0.68 ± 0.01 |
| M122 | -1 | +1 | +1 | 36.02 ± 5.33 | 0.53 ± 0.04 | 0.68 ± 0.01 |
| M211 | +1 | -1 | -1 | 85.21 ± 8.02 | 1.03 ± 0.20 | 0.47 ± 0.01 |
| M212 | +1 | -1 | +1 | 68.28 ± 12.06 | 1.02 ± 0.22 | 0.53 ± 0.05 |
| M221 | +1 | +1 | -1 | 48.31 ± 6.11 | 0.71 ± 0.05 | 0.61 ± 0.01 |
| M222 | +1 | +1 | +1 | 55.88 ± 10.58 | 0.74 ± 0.13 | 0.62 ± 0.00 |
| P111 | -1 | -1 | -1 | 118.32 ± 10.29 | 1.65 ± 0.17 | 0.55 ± 0.02 |
| P112 | -1 | -1 | +1 | 113.04 ± 16.11 | 1.66 ± 0.26 | 0.52 ± 0.05 |
| P121 | -1 | +1 | -1 | 84.61 ± 15.78 | 1.12 ± 0.21 | 0.66 ± 0.04 |
| P122 | -1 | +1 | +1 | 85.06 ± 7.77 | 1.19 ± 0.14 | 0.70 ± 0.04 |
| P211 | +1 | -1 | -1 | 117.94 ± 13.01 | 1.65 ± 0.19 | 0.54 ± 0.02 |
| P212 | +1 | -1 | +1 | 110.19 ± 14.42 | 1.62 ± 0.07 | 0.55 ± 0.01 |
| P221 | +1 | +1 | -1 | 69.67 ± 6.63 | 0.90 ± 0.02 | 0.73 ± 0.01 |
| P222 | +1 | +1 | +1 | 76.35 ± 8.09 | 1.06 ± 0.14 | 0.73 ± 0.01 |

| | | | | | | |
|---|---|---|---|---|---|---|
| W111 | -1 | -1 | -1 | 332.03 ± 67.41 | 5.23 ± 1.34 | 0.79 ± 0.04 |
| W112 | -1 | -1 | +1 | 270.21 ± 26.39 | 4.29 ± 1.24 | 0.80 ± 0.04 |
| W121 | -1 | +1 | -1 | 165.84 ± 11.94 | 2.30 ± 0.39 | 0.98 ± 0.04 |
| W122 | -1 | +1 | +1 | 95.57 ± 24.14 | 1.52 ± 0.22 | 1.02 ± 0.02 |
| W211 | +1 | -1 | -1 | 311.90 ± 51.46 | 4.52 ± 1.11 | 0.80 ± 0.03 |
| W212 | +1 | -1 | +1 | 337.51 ± 23.44 | 5.36 ± 0.89 | 0.80 ± 0.05 |
| W221 | +1 | +1 | -1 | 151.30 ± 36.62 | 2.03 ± 0.59 | 1.06 ± 0.03 |
| W222 | +1 | +1 | +1 | 158.35 ± 2.88 | 2.27 ± 0.26 | 1.05 ± 0.04 |

The first alphabet of the run code indicates the food, where A: apple; H: ham; M: muesli bar; P: peanuts; W: weetbix and the numbers represent the level of the factors to be applied for the run, where 1 represents level -1 and 2 represents +1. T: trajectory; XG: 0.1% XG solution addition; BF: baseline force; DR: deformation resistance; SR: slip resistance; MC: moisture content.

In general, the DR and SR of the boluses across all foods were highly correlated (correlation coefficient r = 0.898) and displayed similar trends in the scatterplots (Figure 6-13). The lateral chewing trajectory resulted in boluses with lower DR and SR, but the baseline force had no effect on the deformation and slip properties of the apple boluses. The effect of higher XG solution addition resulted in ham boluses with lower DR and SR while the effect of trajectory was only observed in boluses that had less XG solution added. The baseline force had no effect on the deformation and slip properties of the ham boluses. There were two distinct clusters of observations along the reference lines for the desired moisture added for the peanut and weetbix boluses. The effect of higher XG solution addition in reducing the DR and SR was clearly observed in the muesli bar, peanut and weetbix boluses. This reflected that the amount of XG solution added was well absorbed by the boluses and that the initial moisture content of the food samples had little variation as compared to the apple and ham samples. The moisture added for the muesli bar boluses were lower than the desired values, this could be attributed to the fact that the particles in muesli bar had poorer ability to bind with the XG solution as compared to saliva. Although the muesli bar boluses that were chewed in the lateral chewing trajectory had lower DR and SR, these boluses had higher moisture content compared to those chewed in the vertical trajectory. It is unsure if the trajectory had an effect on the moisture absorbed by the particles, or this was just part of random error. The different chewing trajectories and baseline force had no effect on the deformation and slip properties of the peanut and weetbix boluses.

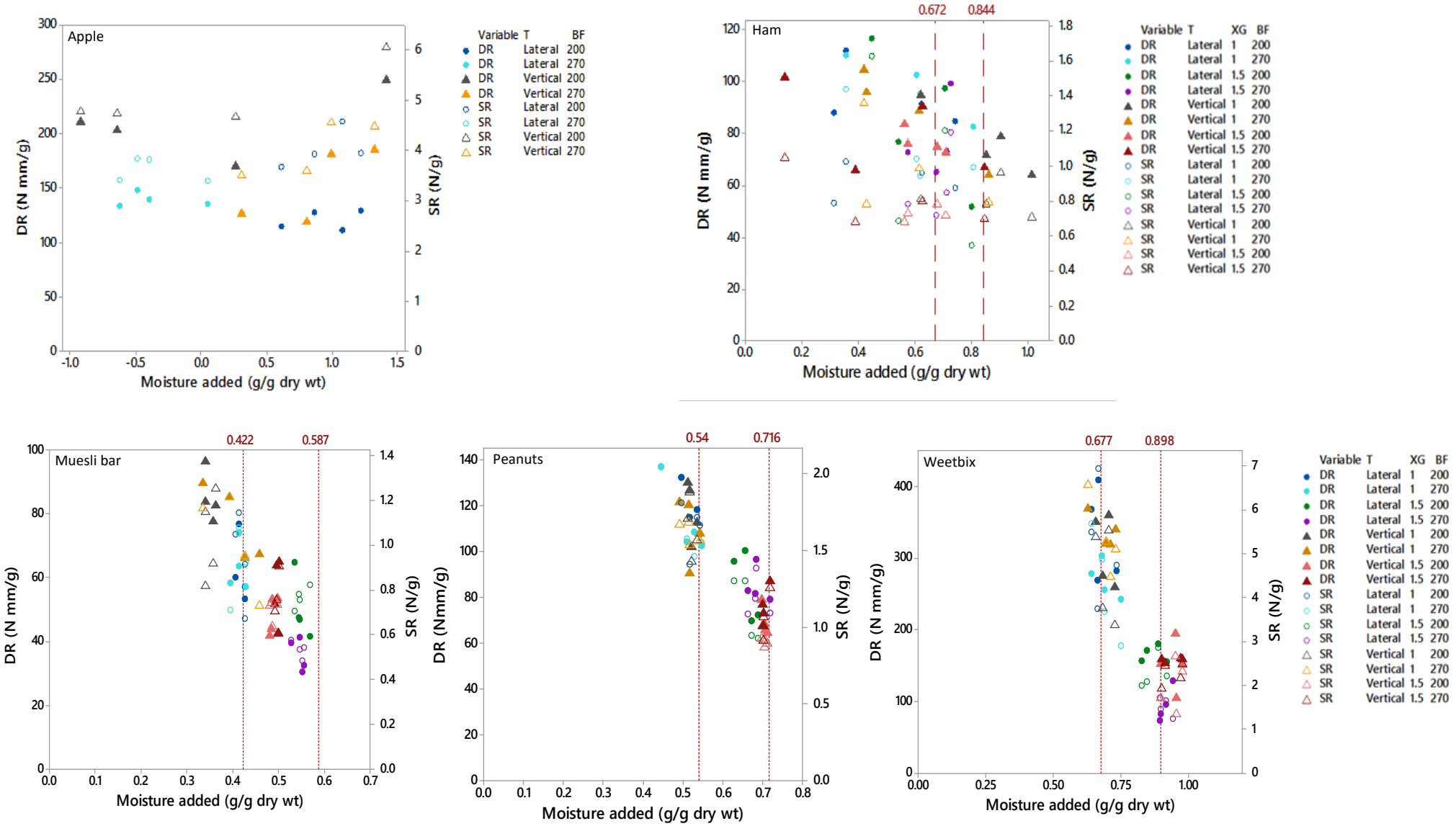


*Figure 6-13: Scatterplot of DR and SR of the boluses plotted against the saliva addition for the different runs (filled symbol- DR; hollow symbol- SR). Red dashed lines indicate the desired moisture added (g/g dry wt) for the low and high levels respectively.*

Figure 6-14 shows the DR and SR of the boluses collected from the MR and subject A. The apples boluses from lateral chewing trajectories had lower resistance to deformation but had similar resistance to slip compared to those from subject A. The DR and SR for the boluses chewed with a smaller baseline force was smaller than those chewed with a larger baseline force which suggests that the lateral trajectory was so efficient in breaking down the apple samples such that the effect of the baseline force was not observed. The apple boluses from vertical chewing trajectories had higher resistance to slip but had similar resistance to deformation compared to those from subject A. The peanut boluses that had higher level of XG solution added had similar resistance to deformation but had lower resistance to slip as compared to the peanut boluses from subject A. The weetbix boluses chewed in the lateral trajectory with higher level of XG solution added and higher baseline force had the most similar DR and SR properties to the weetbix boluses from subject A.

Although Figure 6-14 provided some insight on the relationship between the DR, SR and the factors, the conclusion was not clear due to variation in the observations, thus ANOVA was used to examine the variability and determine if the factors had a significant effect. The response data, 'DR', in *Table 6-8* were analyzed using ANOVA and each individual factor was evaluated using F-test. The results of the ANOVA is shown in Table 6-9. An equation for each food was generated using regression analysis. The final equations for apple, muesli bar, peanuts, and weetbix are shown in Table 6-10. There were no significant model terms for ham, which could be due to the large variation within the ham samples. It was found that the variability of moisture content within the initial samples before mastication was greater than the amount of XG solution added. Thus, no clear effect could be observed. The deformation and slip resistance of the boluses obtained from the robot was like those of subject A but some of the runs produced boluses that had lower resistance to deformation and slip (Figure 6-14). It has been found that more lateral chewing movements were used in the mastication of fibrous foods (Ahlgren (1976); Langley, and Marshall (1993)), thus the lowest levels for XG addition and baseline force in the lateral trajectory was selected as the parameters for mastication in the final study.

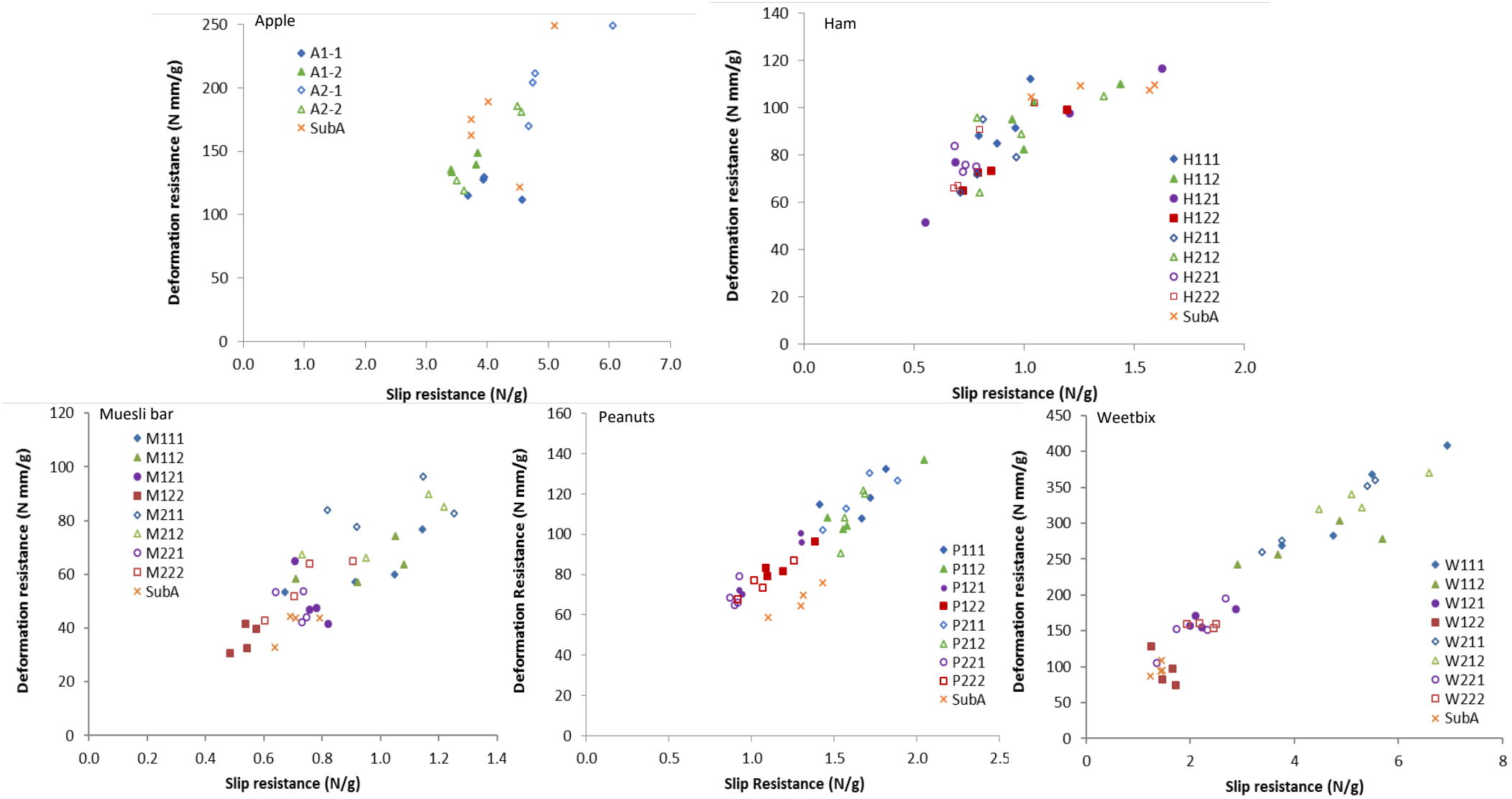


*Figure 6-14: Comparison of DR and SR of boluses from the different runs and subject A through use of the scatterplot of the DR plotted against the SR (filled symbol- lateral trajectory; hollowed symbol- vertical trajectory; ). A single outlier observation from subject A was removed for ham, muesli bar, peanut and weetbix boluses.*

Hierarchical model reduction was used to remove terms that were insignificant but all lower order terms were retained in the model if a higher order term was significant. The pareto charts in Figure 6-15 and ANOVA results in Table 6-9 summarised the terms that had significant effect on the deformation resistance. For apple, the trajectory was significant, but the baseline force was not ($p > 0.05$). Although the baseline force was not significant as a factor on its own, the interaction between the trajectory and the baseline force was significant. Thus, the baseline force was retained in the final model. None of the terms had a significant effect on the DR response for ham boluses. For muesli bar, the amount of XG solution added was the most significant, followed by the chewing trajectory. Although the baseline force was not a significant factor, the interaction between the three factors was significant. For peanuts, the amount of XG solution added was the only significant factor. For weetbix, the amount of XG solution added was the most significant, followed by the interaction between the chewing trajectory and baseline force and the baseline force as a factor on its own was significant too.

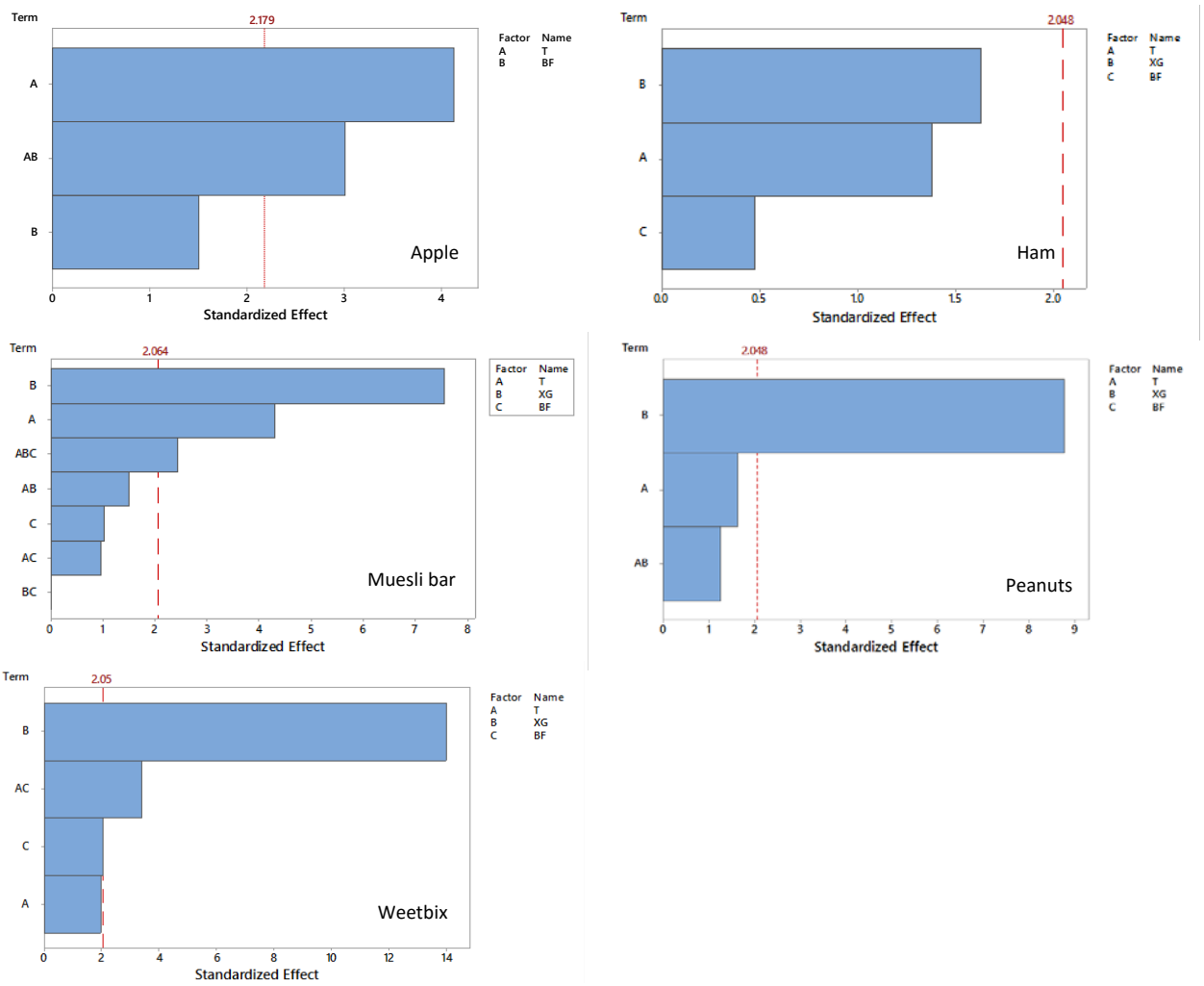


*Figure 6-15: Pareto chart showing the standardized effects of each term on the response (DR) with the red dashed reference line to indicate which effects were statistically significant (α = 0.05). Terms with a larger value than the reference value were statistically significant at the 0.05 level with the current model terms. T=trajectory, XG=XG addition, BF=baseline force.*

*Table 6-9: Analysis of variance (ANOVA) results for apple, muesli bar, peanuts and weetbix.*

| Food | Source of variation | SS | DF | MS | F-value | P-value |
|---|---|---|---|---|---|---|
| Apple | T | 10282 | 1 | 10281.50 | 17.07 | 0.001 |
| | BF | 1371 | 1 | 1371.40 | 2.28 | 0.157 |
| | T*BF | 5466 | 1 | 5465.70 | 9.08 | 0.011 |
| | Residual | 7227 | 12 | 602.20 | - | - |
| | Total | 24346 | 15 | - | - | - |
| Muesli bar | T | 1522.87 | 1 | 1522.87 | 18.53 | 0.000 |
| | XG | 4707.03 | 1 | 4707.03 | 57.29 | 0.000 |
| | BF | 87.75 | 1 | 87.75 | 1.07 | 0.312 |
| | T*XG | 186.64 | 1 | 186.64 | 1.06 | 0.145 |
| | T*BF | 75.27 | 1 | 75.27 | 2.27 | 0.348 |
| | XG*BF | 0.00 | 1 | 0.00 | 0.00 | 0.998 |
| | T*XG*BF | 489.73 | 1 | 489.73 | 5.96 | 0.022 |
| | Residual | 1972.03 | 24 | 82.17 | - | - |
| | Total | 9041.32 | 31 | - | - | - |
| Peanuts | T | 361.30 | 1 | 361.30 | 2.70 | 0.112 |
| | XG | 10339.40 | 1 | 10339.40 | 77.19 | 0.000 |
| | T*XG | 208.70 | 1 | 208.70 | 1.56 | 0.222 |
| | Residual | 3750.30 | 28 | 133.90 | - | - |
| | Total | 14659.70 | 31 | - | - | - |
| Weetbix | T | 4553 | 1 | 4553.00 | 3.85 | 0.060 |
| | XG | 231600 | 1 | 231600.00 | 195.70 | 0.000 |
| | BF | 4942 | 1 | 4942.00 | 4.18 | 0.051 |
| | T*BF | 13571 | 1 | 13571.00 | 11.47 | 0.002 |
| | Residual | 31953 | 27 | 1183.00 | - | - |
| | Total | 286619 | 31 | - | - | - |

Ordinary least squares regression assumptions need to be satisfied to ensure that the coefficient estimates in the regression models were unbiased. The residual plots in Figure 6-16 were used to determine if the residuals were stochastic. The normal probability plots and histograms indicated normal distributions for all although the residuals for muesli bar was slightly skewed to the left in the histogram plot. The residuals in the residual versus fits plots had a symmetrical pattern and had a constant spread centered around zero throughout the range of fitted values. Apple shows nonconstant variance as the variance of the residuals increases with the fitted values. The residuals in the residuals versus order plots were in a random pattern across all foods. Thus, the assumptions were satisfied and the regression models for each food in could be accepted (Table 6-10).

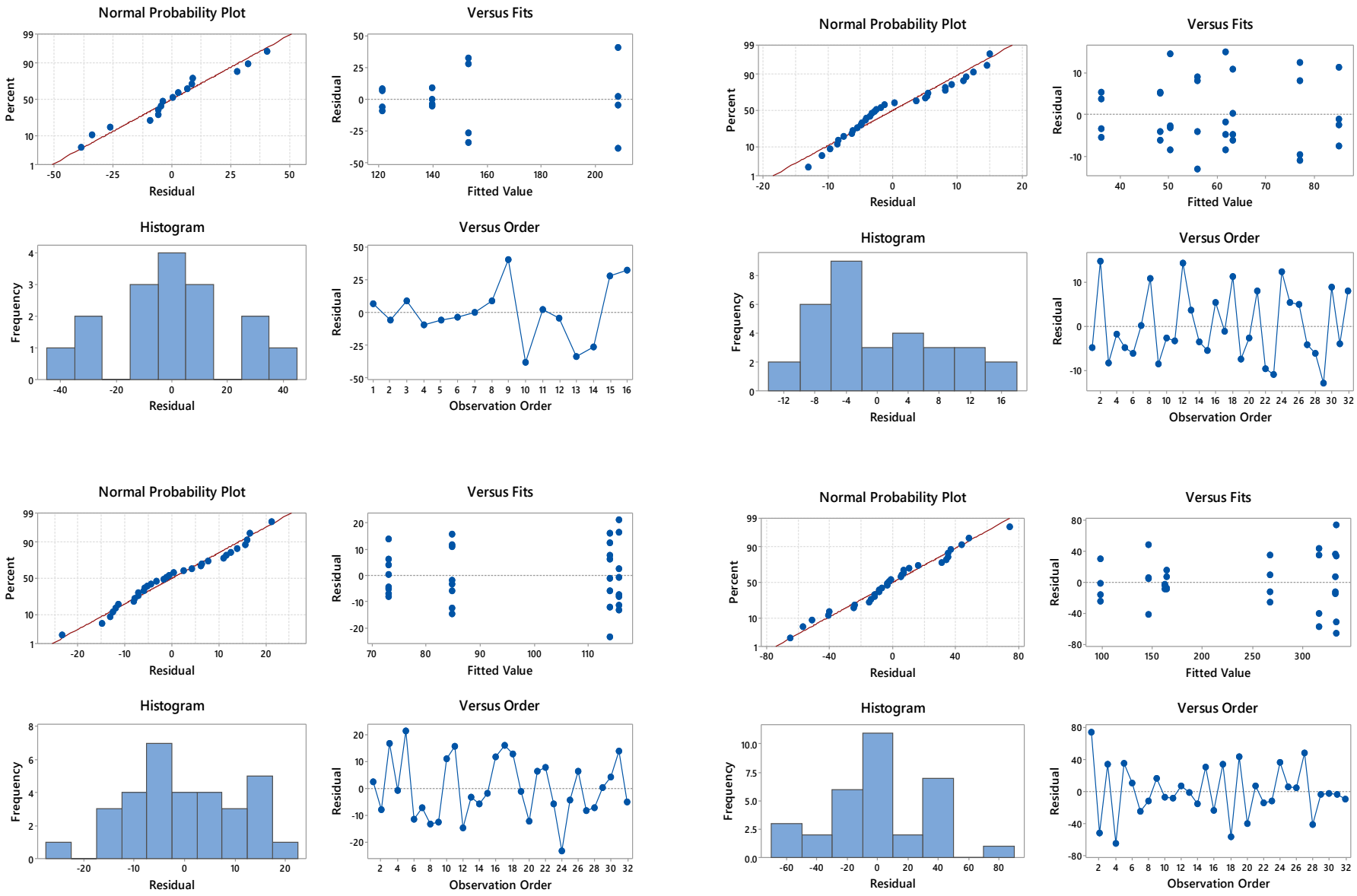


*Figure 6-16: Residual plots for apple, muesli bar (top), peanuts and weetbix (bottom).*

*Table 6-10: Regression equations in terms of coded factors for apple, muesli bar, peanuts and weetbix.*

| Food | Equation | $r^2$ (%) |
|---|---|---|
| Apple | DR = 155.55 + 25.35 T- 9.26 BF - 18.48 T*BF | 70.32 |
| Muesli bar | DR = 59.74 + 6.90 T - 12.13 XG - 1.66 BF - 2.42 T*XG + 1.53 T*BF - 0.01XG*BF + 3.91 T*XG*BF | 78.19 |
| Peanuts | DR = 96.90 - 3.36 T - 17.98 XG - 2.55 T*XG | 74.42 |
| Weetbix | DR = 227.84 + 11.93 T - 85.07 XG - 12.43 BF + 20.59 T*BF | 88.85 |

The models were developed to optimize the factors for the mastication robot to produce boluses with similar deformation and slip properties as those of the median subject. The average DR measurement from subject A was substituted into the corresponding equation for each food and the solved solutions are in Table 6-11. As none of the factors were significant for ham in describing the variance, the conditions from the run that had the closest DR measurement to subject A were selected. The next phase of mastication study using the robot in chapter 7 was carried out using these optimized conditions.

*Table 6-11: The optimised coded levels for the factors solved from the equations in Table 6-10 for apple, muesli bar, peanuts and weetbix. The factor levels for ham were selected based on the run that produced boluses with DR most similar to subject A.*

| Food | Factors | | |
|---|---|---|---|
| | T | XG | BF |
| Apple | +1 | - | +0.045 |
| Ham | -1 | -1 | +1 |
| Muesli Bar | -1 | +0.625 | +1 |
| Peanuts | +1 | +1.279 | -1 |
| Weetbix | -1 | +1.023 | +1 |
| T: trajectory; XG: 0.1% XG solution addition; BF: baseline force | | | |

## 6.7. Comparison of optimized MR to human chewing parameters

The previous section discussed the bolus deformation and slip properties resulting from the range of chewing parameters employed in the MR. Based on the regression analysis in the previous section, a vertical chewing trajectory was recommended for apple and peanuts while a lateral chewing trajectory was recommended for muesli bar and weetbix to achieve boluses similar to subject A. Subject A had employed a vertical chewing trajectory when chewing apple and peanuts, since the average widths of the chews were smaller for most of the mastication stages (Figure 6-9). The average width of the chews was larger for muesli bar and in the initial stages of mastication for weetbix, indicating that subject A used a lateral chewing trajectory for those foods. As the weetbix rapidly soften within the first few chews, a lateral trajectory may be no longer needed in the later

stages of mastication. Thus, the trajectories recommended for each food based on the regression models were coincides with how subject A chewed each food.

## 6.8. Conclusion

In this chapter, subjects were asked to masticate five different foods to determine their chewing behaviour and the bolus properties at swallow point. Although boluses were tested within an hour after bolus collection, there is considerable impact on the boluses due to the enzymatic action from the saliva. For future studies, It is recommended to have the subject seated beside the texture analyser so that the test can be done immediately after each bolus is expectorated. In addition, the time delays in measurement during the human study should be similar to that of the MR study. The boluses were characterized using the slip extrusion test. The DR and SR was only highly correlated for weetbix but not the other foods when intersubject variation was taken into consideration. For foods such as the muesli bar and peanuts, the SR decreased when the boluses had higher amount of moisture when comparing within the replicates of each subject. This suggests that DR and SR measure different bolus properties and the effect of moisture content on the SR is high for certain foods.

There was inter-individual variation in the mouth behaviour and the salivary rates during mastication amongst the subjects. Thus, a single subject was selected as an “instrumental” measure that could be compared with the mastication robot. Subject A was the median subject and his data on the number of chewing cycles and amount of moisture addition for each food were used to establish the parameters for the mastication robot’s set up for the factorial design of experiments. The factors investigated were: (a) chewing trajectory, (b) 0.1% XG solution addition, and (c) baseline force. The developed models from the factorial study was used to optimize the conditions needed for the MR to achieve boluses with similar DR and SR properties as subject A.

# Chapter Seven Application of the characterisation techniques on five different foods

In the previous chapter, different settings were employed in the mastication robot and the bolus properties measured by the SET was compared with that of subject A. Through factorial regression analysis, the settings that would produce boluses with deformation and slip properties similar to the boluses from subject A was predicted for each food. The purpose of the work in this chapter was to demonstrate the application of the characterisation techniques developed in this work (SET, MPP, MR), to track the dynamic changes in the bolus properties of five foods across the different stages of mastication using the mastication robot. Thus, in this section, the five foods were broken down using the identified parameters, and bolus properties were evaluated at various stages of the mastication process through the application of the slip extrusion test, textural mapping using the multiple pin penetrometer, and the back extrusion test.

## 7.1. Methodology

Five foods: peanuts, weetbix bites, apple, ham and muesli bar, were prepared as listed in Table 6-1. The foods were chewed to various stages of mastication by the mastication robot and the number of chewing cycles were approximately spaced with respect to the complete mastication sequence as detailed in Table 7-1. This enabled the boluses to be compared at the same stages of mastication rather than after an arbitrary number of chews. For each food, the number of chews required by subject A to reach swallow point was used to define the corresponding number of chews for each stage of mastication. The chewing parameters for the robot, based on the results from chapter 6,are detailed in Table 7-2. The boluses were collected, and bolus properties were characterised by the slip extrusion test (SET) followed by moisture analysis, or the back extrusion test (BET), or the multiple pin penetrometer test (MPPT). Replicates of two boluses were measured for each test at each mastication stage. The MPPT was not suitable for peanut boluses as the pins pushed the peanut particles into the surrounding spaces between pins rather than penetrating the particles. Except for peanuts, 54 bolus samples per food were collected for analysis. 3-D force data measured by the mastication robot were also analysed. Visual observation of the boluses was captured using a camera (Canon PowerShot S95).

*Table 7-1: Stages of mastication and the corresponding number of chewing cycles for each food.*

| Mastication Stage (%) | 10 | 20 | 30 | 50 | 75 | 100 | 125 | 150 |
|---|---|---|---|---|---|---|---|---|
| **Peanuts** | 2 | 5 | 8 | 13 | 20 | 27 | 34 | 41 |
| **Ham** | 2 | 5 | 8 | 13 | 18 | 25 | 31 | 38 |
| **Weetbix** | 1 | 3 | 5 | 9 | 13 | 17 | 21 | 26 |
| **Apple** | 1 | 3 | 5 | 9 | 13 | 18 | 22 | 27 |
| **Muesli Bar** | 3 | 6 | 9 | 15 | 22 | 30 | 37 | 45 |

*Table 7-2: Chewing parameters set for mastication by the robot for each food. 'XG Initial' is the amount of 0.1% XG solution added to the sample upon loading onto the occlusal surface while 'XG Rate' is the amount of 0.1% XG solution added to the sample after every chew.*

| Food | Trajectory | XG Initial (ml) | XG Rate (ml) | Baseline Force (N) | Stage Height (mm) |
|---|---|---|---|---|---|
| **Apple** | Vertical (3mm) | - | - | 236N | 7.45 |
| **Peanuts** | Vertical (3mm) | 0.452 | 0.063 | 200N | 6.45 |
| **Ham** | Lateral | 0.566 | 0.016 | 270N | 5.80 |
| **Weetbix** | Lateral | 0.480 | 0.104 | 270N | 5.80 |
| **Muesli Bar** | Lateral | 0.512 | 0.086 | 270N | 5.80 |

### 7.1.1. Slip extrusion test

After a baseline measurement, the bolus was placed into the slip extrusion test bag, weighed and the test was carried out. The bolus was extruded into a pre-weighed moisture dish, which was weighed again before drying in the oven for moisture analysis. More detailed explanation of the methodology for the slip extrusion test and moisture analysis is found in section 5.2.2. and 4.2.2.

### 7.1.2. Multiple pin penetrometer test

The bolus was placed in a mould that was shaped according to its original sample shape before mastication (Figure 7-1). For each food, the configuration of the pins was rearranged such that only those pins that would come into contact with the bolus were retained and the rest of the pins were removed. An example is shown in Figure 7-2. The crosshead speed used was 1mm $s^{-1}$ and the distance travelled was 15mm. The depth travelled by the pins were 1mm above the maximum possible distance before the pins would meet the base plate.

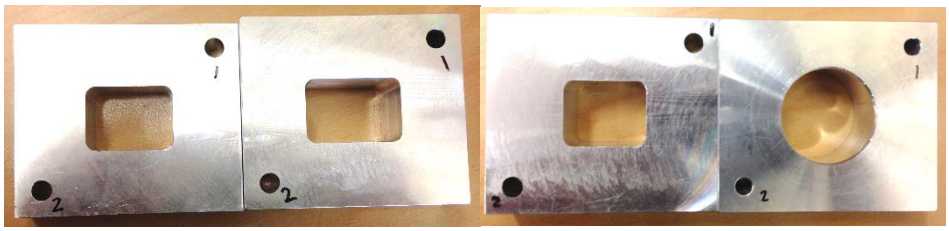

*Figure 7-1: The moulds for apple, muesli bar, weetbix, and ham.*

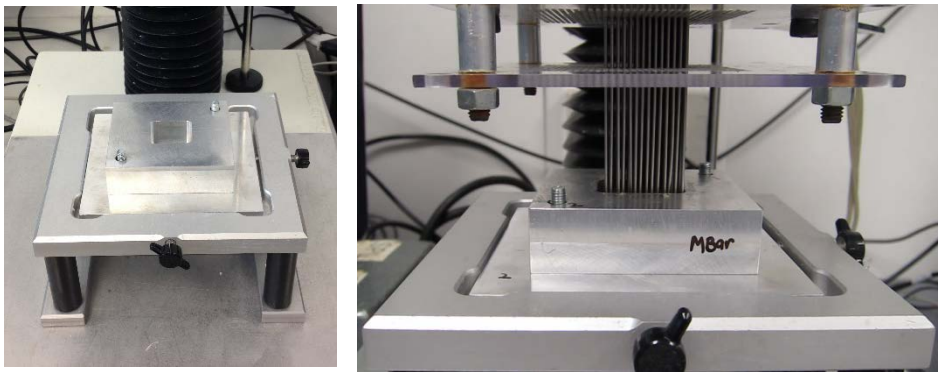


*Figure 7-2: An example of the set up for bolus measurement: the mould for the respective food is fixed to the platform of the texture analyser (left) and the pin configuration for measuring the bolus (right).*

### 7.1.3. Back extrusion test

The back extrusion test is a modified Texture Profile Analysis (TPA) test used by James et al. (2011b) and Peyron, Marie-Agnès et al. (2011) to evaluate the bolus properties. Two consecutive compressions of the piston, at a speed of 100mm $min^{-1}$, to 80% of the height of the bolus was used. The bolus was placed into a cylindrical cup of internal diameter 22mm and gently levelled. A flat stainless steel piston (Ø=18mm) was mounted on TA-XT plus texture analyser (Stable Micro Systems Ltd, UK) and a 50kg or 700kg load cell was used depending on the hardness of the sample being tested. Muesli bar, peanuts and weetbix samples at zero, ten and twenty percent of the mastication stages required the use of the 700kg load cell.

### 7.1.4. Data analysis

The deformation and slip resistance (DR and SR) as well as the DR/SR ratio was determined from the force deformation measurements collected from the SET. Hardness, impulse, adhesiveness, cohesiveness was extracted from the force deformation curves of the BET. Force distributions were obtained from the MPPT after the data was extracted and treated as detailed in section 5.1.. Image texture analysis was conducted using the GLCM as detailed in section 5.1.3. and three textural features (contrast, energy and homogeneity) were calculated. Impulse, which is a measure of work

done was determined by subtracting the baseline force from the forces measured in the x, y and z axis during chewing. Negative and positive values indicate the direction in which the force was applied in the lateral, sagittal and vertical planes (x, y, and z-axis). To examine the amount of work done during mastication, the absolute value of the force measurement was used.

Pearson correlation analysis was done to determine the most suitable variables to be used for the factor analysis. A factor analysis using the principal components factor extraction method and Varimax rotation was applied so that the factors remain uncorrelated throughout the rotation process. The scree plot and eigenvalues (>1) were used to select the factors. The correlation coefficients for each variable were used to calculate the factor scores for each observation (4 foods x 8 mastication stages x 2 replicates) and plotted on factorial maps to track the changes across the mastication stages.

## 7.2. Results and discussion

### 7.2.1. Visual Observation

After 20% mastication (5 chews), the ham sample was still generally connected as a whole piece by strands of fibres that have not been cut through thoroughly. After 50% mastication, the ham sample was broken down into small pieces of fibres and the fibres were torn and shortened with increasing chews. At 75% mastication, the bolus was fairly dry and at 100% mastication, the bolus was wetter. It should be noted that the bolus appeared to be most cohesive at 125% mastication. This may be due to the difference in the rheological properties between saliva and the XG solution.

At 20% mastication, the apple sample was broken down into large chunks measuring between 5-10mm in length. At 50 % mastication, these chunks were mostly reduced to smaller pieces between 3-5mm. At 75% mastication, a pulpy mass had started to take form although there were still a few large pieces. At 100 and 125% mastication, the bolus was a pulpy mass with a few small pieces which gradually reduced to just a pulpy mass with few distinct pieces.

At 20% mastication, the muesli bar was broken down into multiple chunks which were still sticky on the surface as the XG solution had not been absorbed much yet. At 30% mastication, the bar was no longer sticky, and the chunks were broken up into the individual oat pieces. At 50% mastication, the bolus started to be more cohesive, although a few pieces would drop from the main cluster of bolus.

Individual oat pieces were broken up further to 1-2mm pieces. At 100% mastication, the bolus was a sticky and cohesive mass. At 150% mastication, the bolus was slurry like and very flowable, which was less cohesive due to the excess XG solution.

At 20% mastication, all the peanuts had been halved and the particles were dry. At 30% mastication, there were a mixture of small (6mm) and large particles (10mm). At 50% mastication, the larger particles were about 6mm and the bolus was not cohesive. At 75% mastication, the bolus started to be more cohesive and the larger particles present was about 2-3mm. At 100% mastication, the bolus was cohesive but did not have a wet appearance on the surface of the particles. At 150% mastication, some of the particles had been chewed to a pasty fraction and when mixed with the XG solution, the bolus was more cohesive than at 100% mastication.

At 20% mastication, the weetbix was broken up into large chunks, and some pieces were still dry and crispy as the XG solution had not come into contact with those pieces. At 30% mastication, the pieces had broken up into small dry flakes that were barely clumping together as the XG solution was rapidly absorbed and there was insufficient surface moisture. At 50% mastication, a partial bolus could be formed although there was still insufficient XG solution to bind all the dry flakes together. At 75% mastication, the majority of the bolus was a pasty cohesive mass, although there were still some dry flakes. At 100% mastication, a cohesive bolus was formed, and there were no more dry flakes present. The bolus continued to remain as a sticky and cohesive mass which became softer as the mastication stage progressed to 150%.

(a)

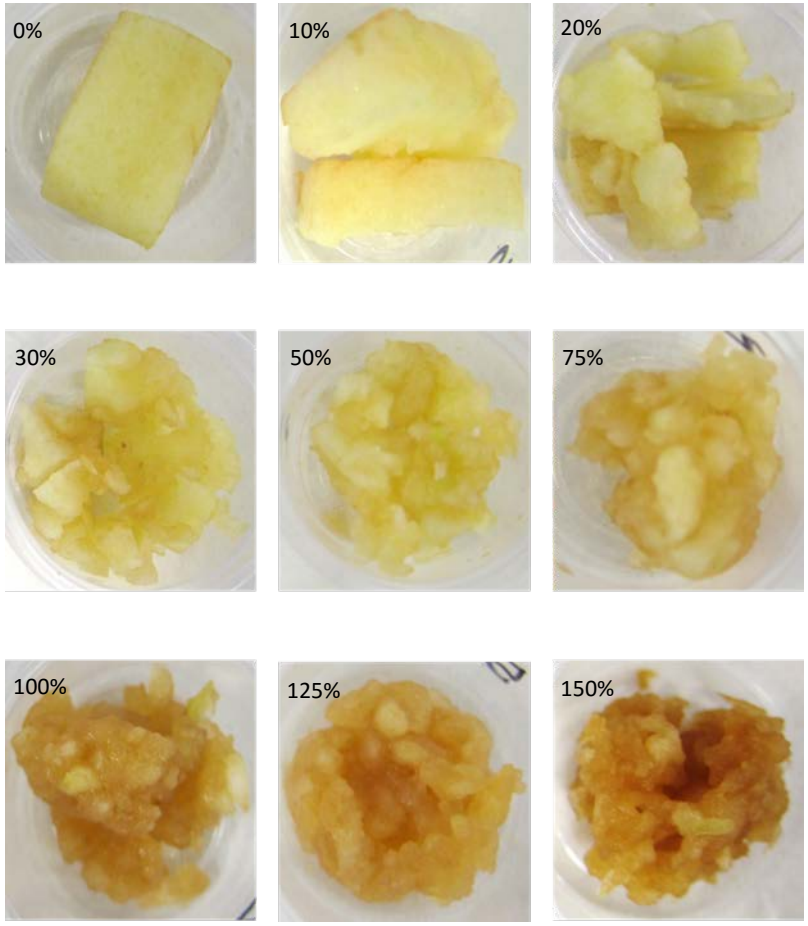


(b)

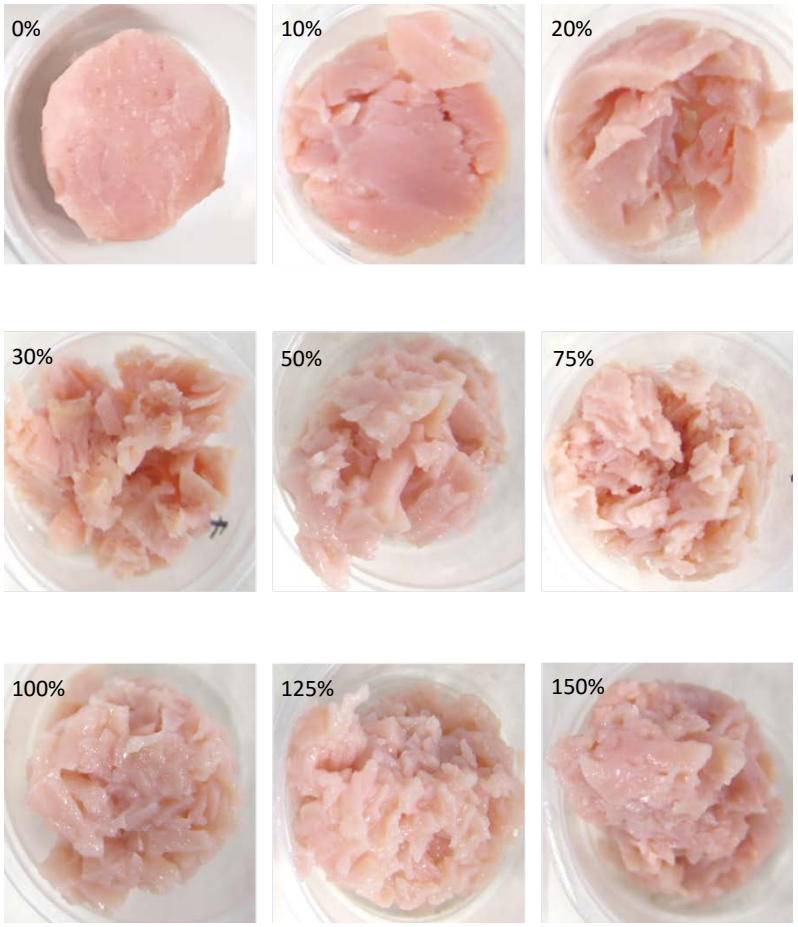

(c)

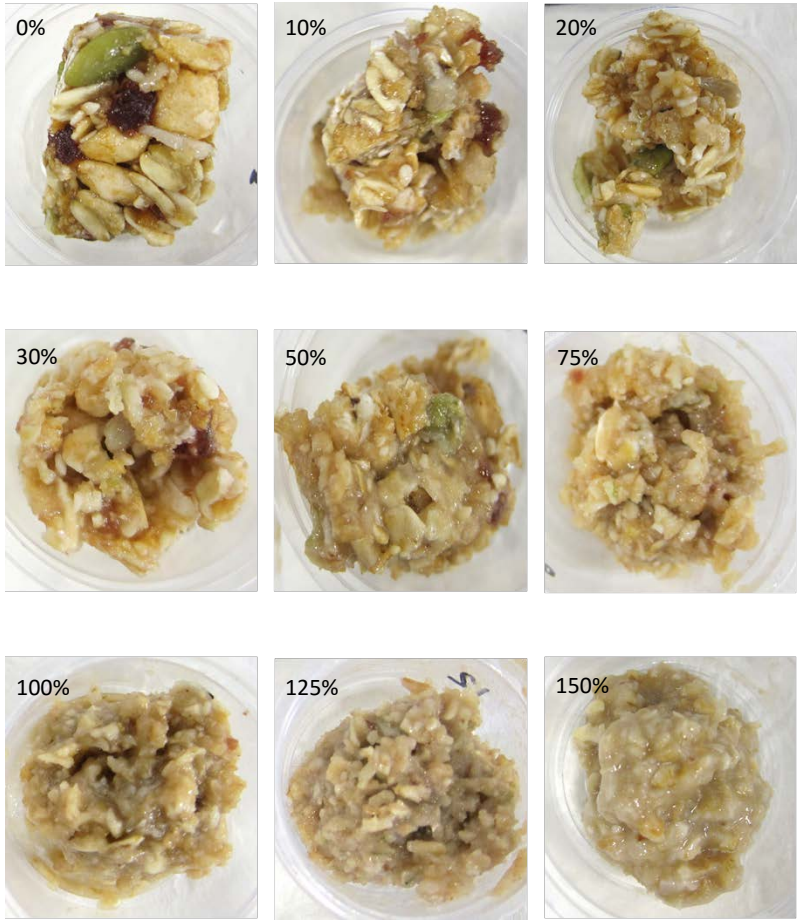


(d)

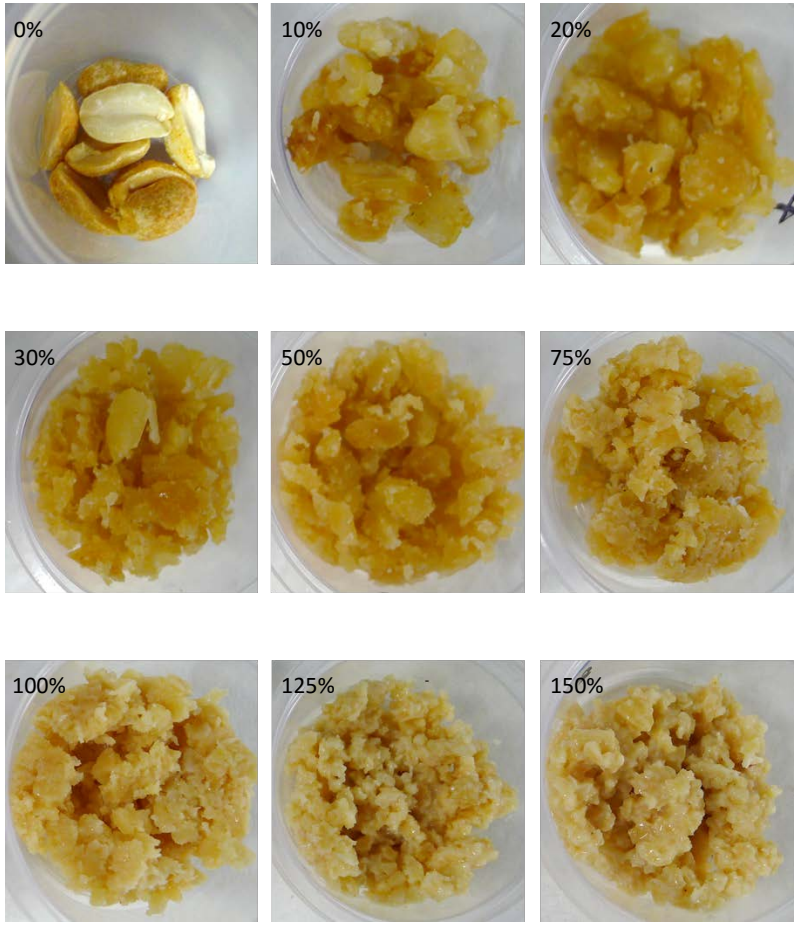

(e)

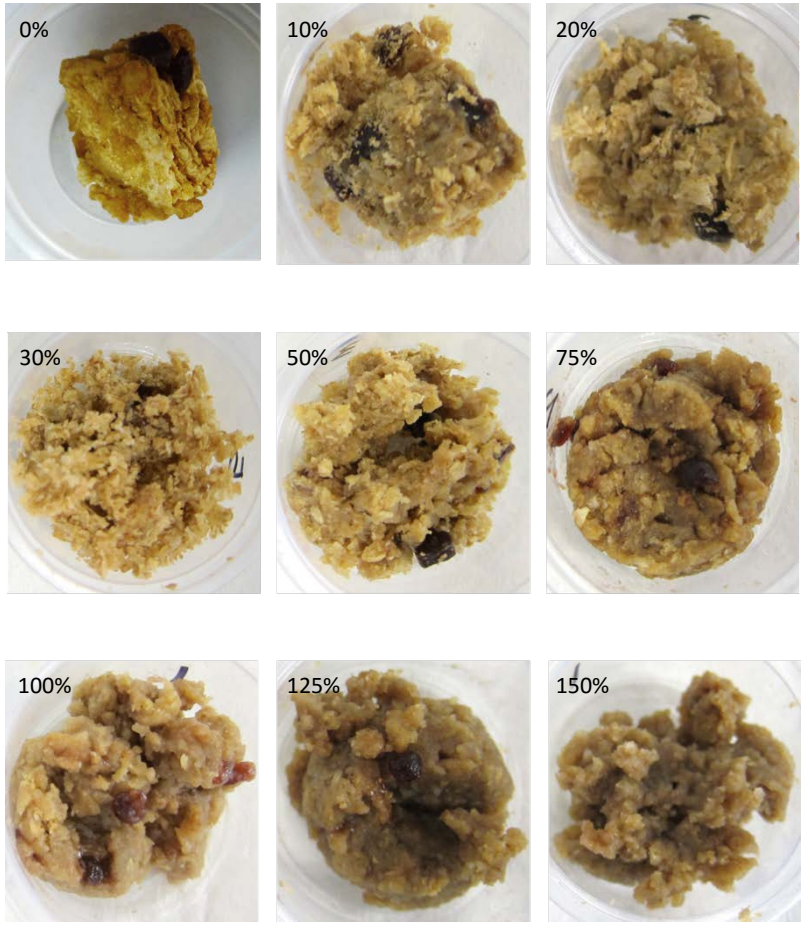


*Figure 7-3: Photos of the (a) apple, (b) ham, (c) muesli bar, (d) peanuts, (e) weetbix boluses collected at the various mastication stages to show the breakdown from the initial sample to past the swallow point (the stages are indicated in each photo).*

### 7.2.2. Slip Extrusion Test

The DR for all the foods except for weetbix, were similarly low as they approached their swallow point. This could be due to the sticky surface of the pasty weetbix bolus as it adhered to the walls of the SET bag during the extrusion. Ham was softest and most deformable as compared to the other foods. It could fold and deform into the narrow channel of the SET bag and was wet enough to slip through the bag. Weetbix, apple, muesli bar and peanuts were not deformable at zero and 10% of the mastication stage (with the exception of peanuts). These unchewed samples and 10% chewed boluses could not deform into the narrow channel of the SET bag and the bags were stretched till they failed during the test. As a result, these points are missing from Figure 7-4. The SR had similar trends to the DR for all foods except for the muesli bar. The muesli bar had much lower SR at the initial stages of mastication. The muesli bar boluses had a higher number of chews at each mastication stage as compared to apple and weetbix, and thus the chews had already broken down the muesli bar into small chunks that faced lesser resistance when being extruded through the narrow channel of the SET bag.

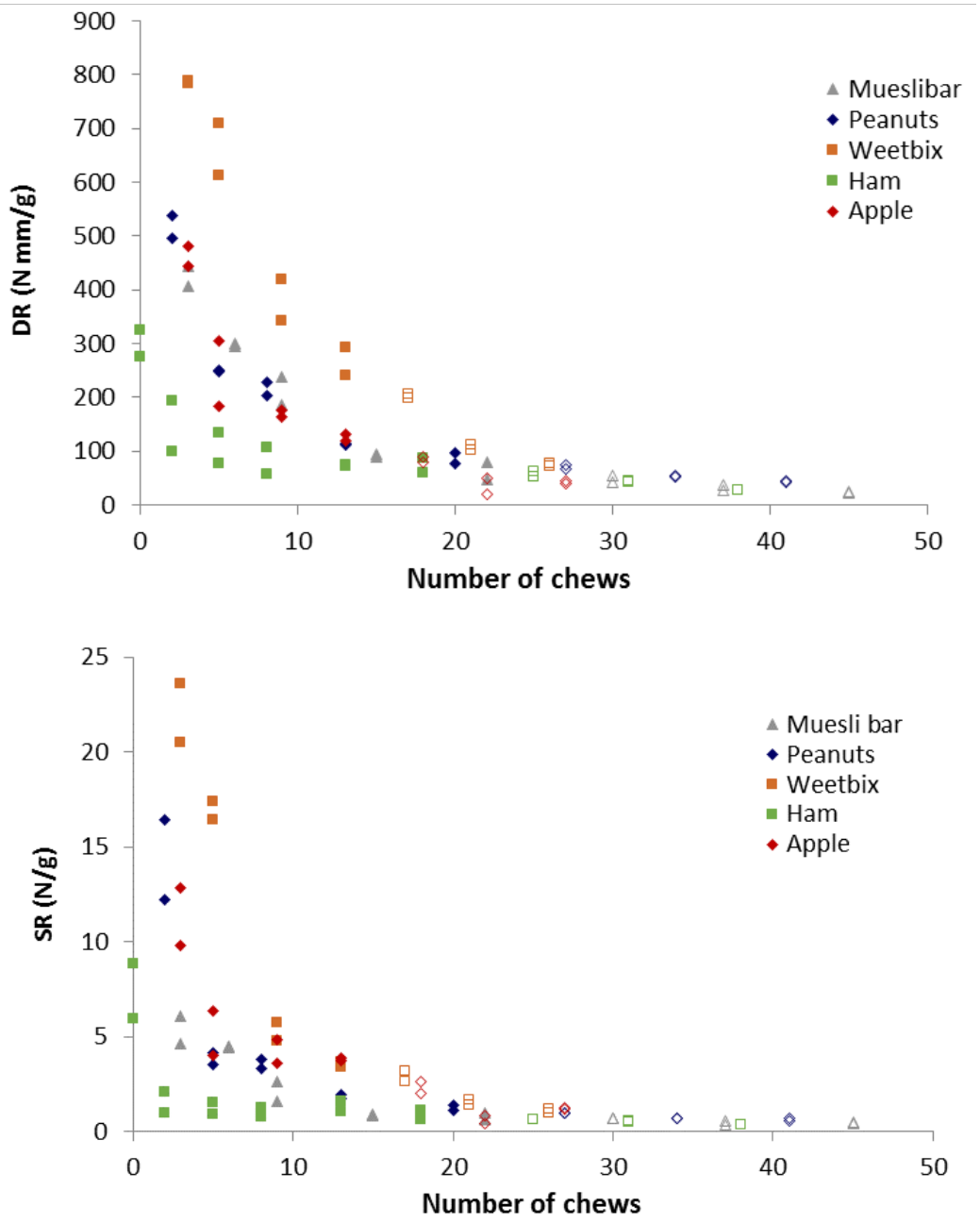


*Figure 7-4: The DR and SR of the boluses collected from the robot after certain number of chewing cycles plotted against the number of chewing cycles. Hollowed symbols represent the boluses collected at and past swallow point.*

Peanuts which has been commonly used as a model food had the most similar boluses in terms of deformation and slip resistance properties between the subjects and robot (Figure 7-5). Although these were boluses collected at the swallow points from five different subjects, the deformation and slip properties were similar to the boluses collected from the robot at the same mastication stage. However, for certain foods such as the weetbix, the spread of the DR of the boluses collected from two of the subjects was large. Comparison of the spread of the DR of boluses between the robot and within a subject showed that the robot was able to produce boluses that were more consistent as compared to the subjects.

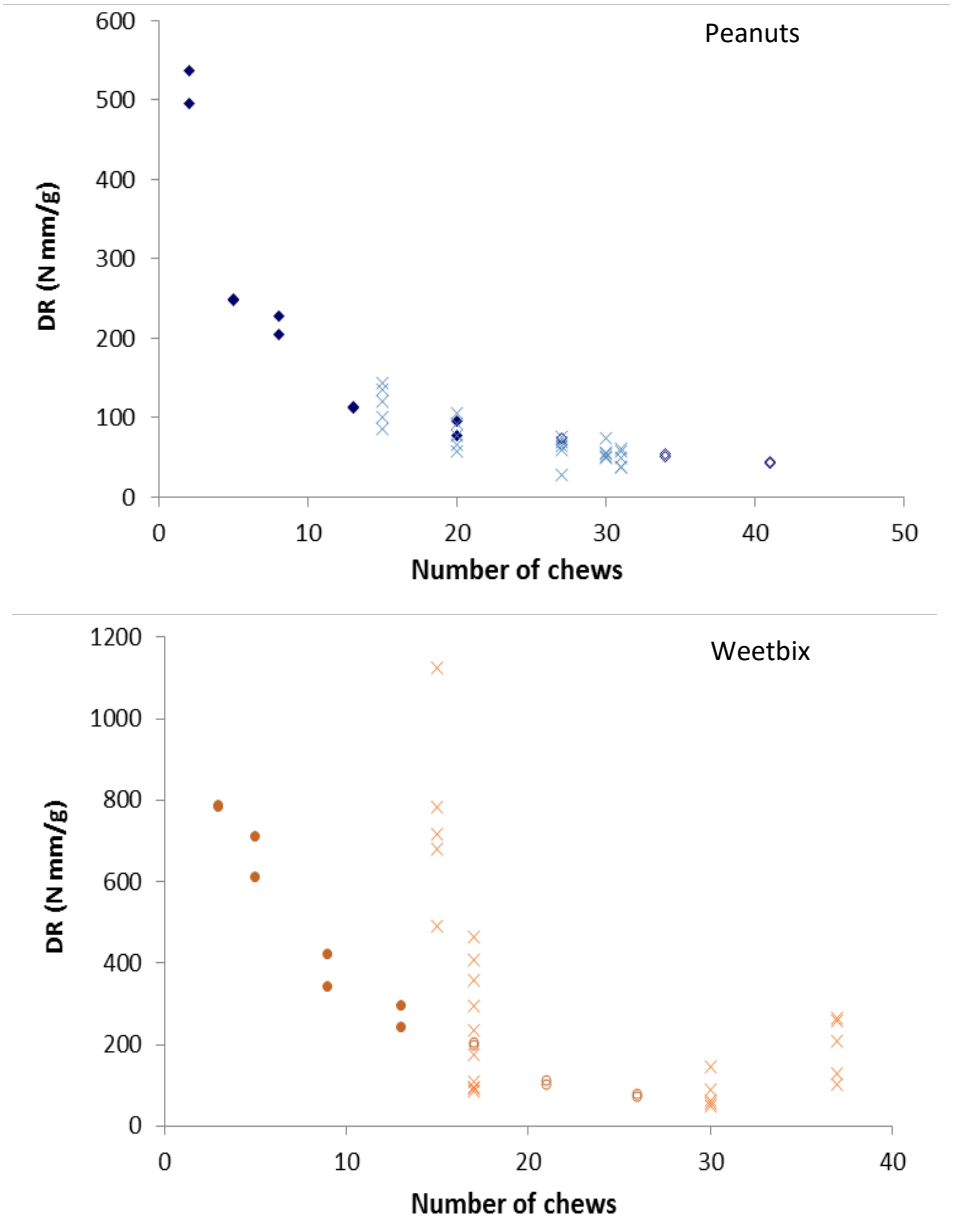


*Figure 7-5: The DR of peanut (top) and weetbix (bottom) boluses collected from the robot and subjects after certain number of chewing cycles plotted against the number of chewing cycles. Circular symbols (●) represent boluses collected from the robot with the unfilled symbols representing boluses collected at and past swallow point, cross symbols (×) represent boluses collected at swallow points from the five subjects. For the boluses collected from subjects, these were at the respective swallow point for each of the five subjects.*

Figure 7-6 shows the DR/SR ratio of the boluses plotted against the number of chewing cycles. Across all foods except for weetbix, the DR/SR ratio of boluses collected from the mastication robot at 10% mastication stage were in the same range as that of boluses collected from subject A after three chews. There were no results collected for the weetbix boluses after three chews as they were too large and were not able to deform to pass into the narrow channel of the SET bag. The bags were stretched and tore thus the measurements collected could not be used.

The DR and SR reduced as the apple got broken down into smaller pieces, and finally were reduced to a pulpy mass and juice. There was no trend in the DR/SR ratio throughout the mastication cycle. A possible explanation is that the DR and SR were measuring similar properties as there was no addition of moisture to the apple bolus during the mastication by the robot. The ham sample without any chews experienced a high SR as the diameter of the sample is almost twice the diameter of the narrow channel of the SET bag. This resulted in a low DR/SR ratio as the ham was soft enough to be deformed into the narrow channel. As the sample is being extruded, the ham is tightly packed against the wall of the SET bag, thus there is much higher resistance to slip. As the ham gets chewed, the fibres get cut and moisture is released in the process. This moisture also contributes to the lubrication which contributes to the decrease in SR. After two chews, the decrease in the diameter of the ham sample greatly reduced the resistance during extrusion in the SET bag, resulting in the increase of the DR/SR ratio which then decreased again as the ham was broken down into small chunks before the fibres were cut after 30% of the mastication stage.

After twenty chewing cycles, as the number of chewing cycles increase, the peanuts were broken down more by subjects than the robot, thus the DR of the boluses collected from the subjects were smaller. As the particles got smaller, the selection of particles for breakage by the robot was poorer than the subjects. Subjects have a more efficient system of ensuring the peanut particles are selected using the cheeks and tongue that keep the particles on the occlusal surfaces. The tongue is more sensitive to pick out the larger particles that need breakdown down as compared to the robot. This was proved by the validation study in chapter 4 which showed that the robot was unable to produce boluses similar to the PSD of boluses collected from the subjects. The robot produced boluses that had larger particle size distributions. The DR (average: 59.4 Nmm/g) of boluses collected from the subjects after 27 chews were smaller than the DR (average: 70.5 Nmm/g) of boluses collected from the robot, while the SR (1.14 N/g) of boluses collected from the subjects were higher than that from the robot (0.969 N /g) due to the higher moisture content in the boluses from the robot. Thus, there was a divergence in the DR/SR ratio in the comparison between the boluses from the robot and subjects after 27 chewing cycles.

In the initial stages of the mastication process of the muesli bar up to 15 chewing cycles, the DR/SR ratio increased as the rate of reduction in the SR was higher than that of the DR. This was due to the rapid loss of the sticky surface of the muesli bar as the XG solution was added the bolus, allowing the bolus to slip along the walls of the extrusion bag with lesser resistance. The first six chews broke down the muesli bar into chunks of 5-10mm, and as the chews progressed to 15 chews, the chunks

were no longer present, which also significantly reduced the SR. After 15 chews, individual particles got broken down, thus reducing the DR more than the SR, which resulted in a decrease in the DR/SR ratio.

Although the DR/SR ratio of the weetbix boluses was similar between the robot and subjects at 17 chews, the DR and SR of the robot was twice that of the subject's. Boluses collected at this point were pasty in nature and moisture addition resulted in softening of the bolus. The moisture content of the boluses produced by the robot at 17 chews were 20% higher than that of boluses collected from subject A, but the boluses from the robot were less deformable and not as well lubricated. Boehm et al. (2014) had found that amylase affected the rheology of comminuted potato chips, thus this could be a possible explanation for the lower deformation and slip resistances measured for the boluses from the subject. The mucins in the saliva may also provide better lubrication to the bolus as compared to the XG solution. In addition, the absorption of the moisture into the bolus was not as efficient as not all the surfaces of the bolus were in contact with moisture all the time, unlike in the mouth. Through the motion of the tongue, moisture is also more evenly distributed throughout the bolus, which may explain why the boluses obtained from subject A at 17 chews were more deformable and had lesser resistance to slip.

It is interesting to note that the DR/SR ratio for the boluses collected at the swallow point (subject A) were smaller than 55 for apple and peanuts, between the range of 50-80 for weetbix and muesli bar, and between the range of 70-100 for ham. The ratio was smallest for foods that required the food to be broken down more to achieve a smaller particle size for better bolus deformability. It appears deformability was more critical for the apple and peanuts. For dry foods, the ratio increased indicating that the SR was much smaller relative to the DR. This suggests that the degree of lubrication was more critical for the bolus to be swallowed. As ham was very well lubricated, the SR was very small, resulting in the largest DR/SR ratio amongst all the foods.

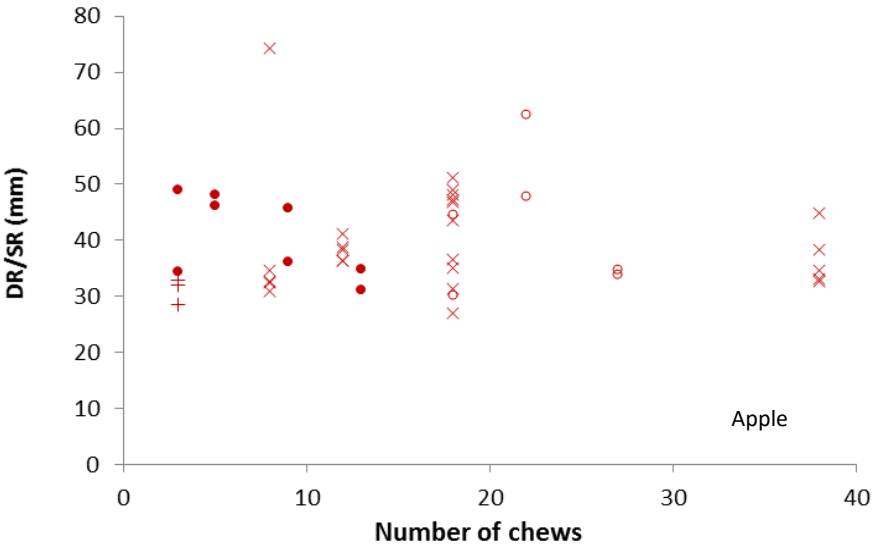
DR/SR (mm)
Number of chews
Apple

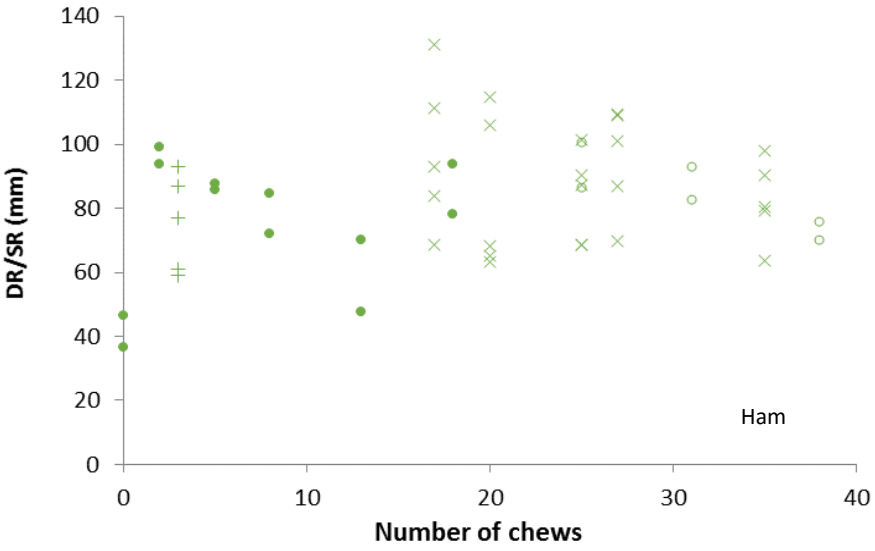
DR/SR (mm)
Number of chews
Ham

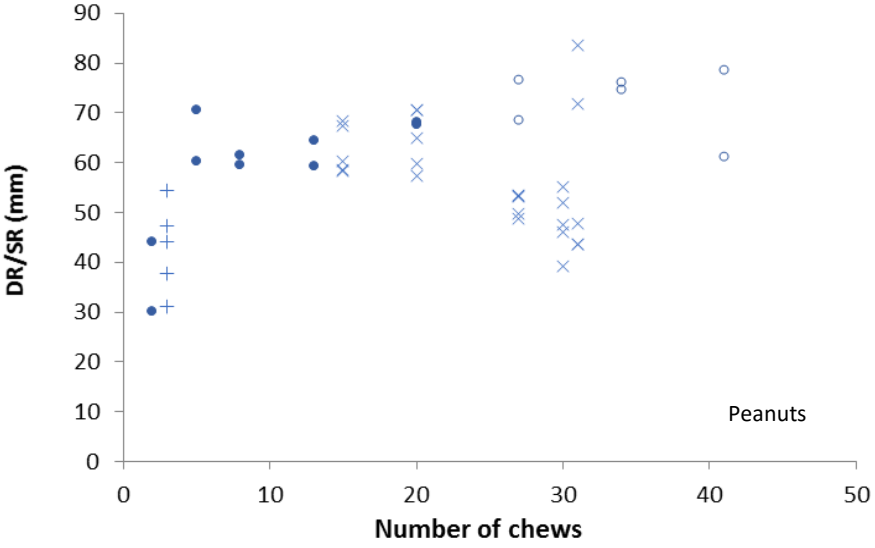
DR/SR (mm)
Number of chews
Peanuts

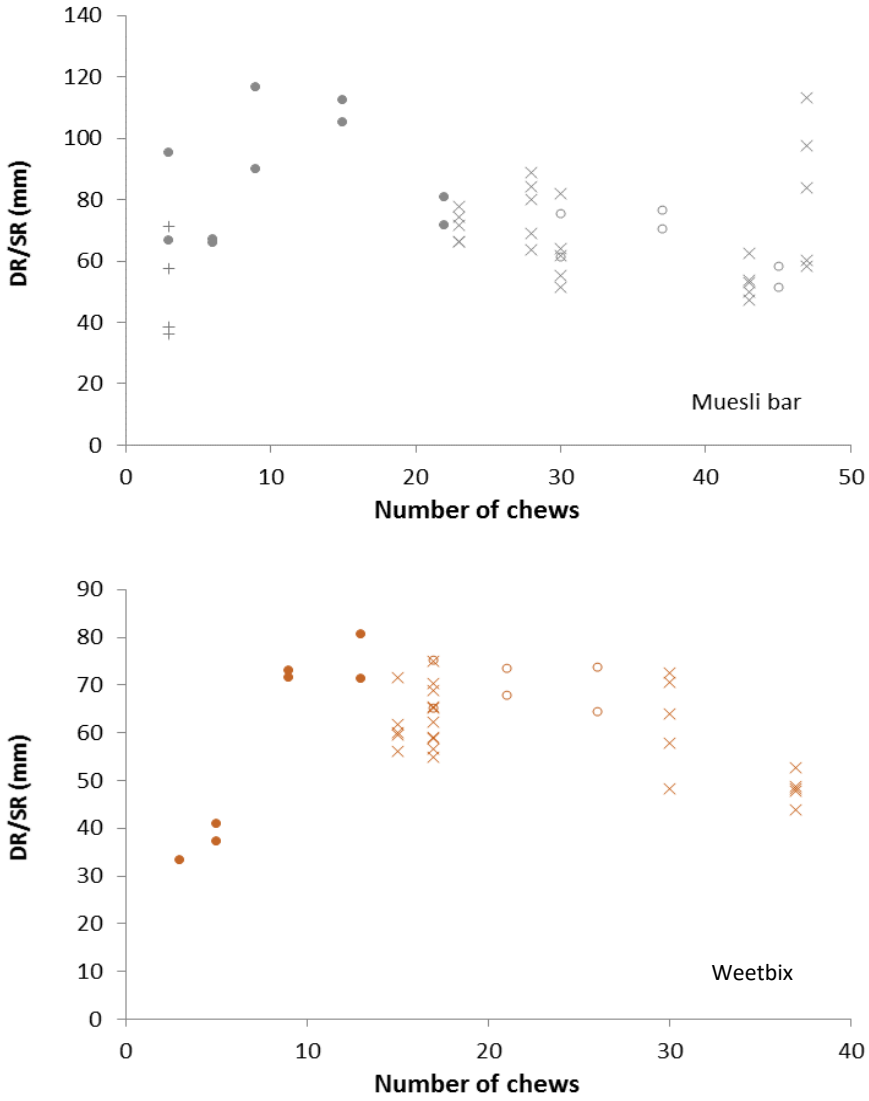


*Figure 7-6: Ratio of the deformation and slip resistance of apple, ham, peanuts, muesli bar, and weetbix boluses (from top to bottom) plotted against the number of chewing cycles. Circular symbols (●) represent boluses collected from the robot with the unfilled symbols representing boluses collected at and past swallow point, cross symbols (×) represent boluses collected at swallow points from the five subjects, and plus symbols (+) represent boluses after three chews from subject A.*

### 7.2.3. Back Extrusion Test

Hardness is the peak force of the force deformation curve obtained during the BET. The hardness of the boluses collected was plotted against the various mastication stages and the corresponding number of chews for each stage (Figure 7-7). Although the samples had different hardness during the initial stage of mastication, by the 75% mastication stage, the hardness tended to be approaching similar values as it approached the swallow point. It is interesting to note that weetbix, apple and ham had earlier swallow points at 17, 18 and 25 chewing cycles while peanuts and muesli bar were chewed for 27 and 30 cycles to reach swallow point. This could explain why the peanuts and muesli bar boluses were less hard as compared to the other foods at and past the swallow point.

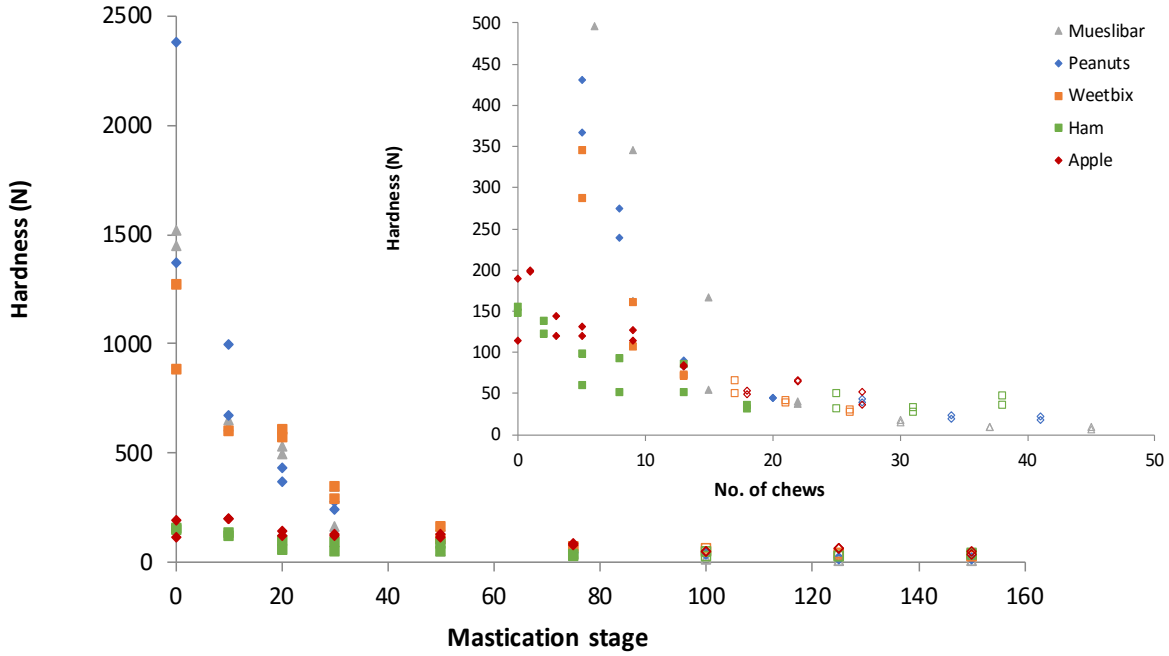


*Figure 7-7: Hardness of boluses collected from the chewing robot plotted against the mastication stage and no of chews (inset).*

Adhesiveness is defined as the work done to pull the probe away from the bolus after the first compression and is quantified by the negative area in the force deformation curve from the BET. Figure 7-8 shows the adhesiveness of the boluses plotted against the number of chewing cycles. The adhesiveness of the weetbix boluses increased as the number of chewing cycles increased, reflecting the action of the XG solution, which changed the dry surface of the weetbix to one which was sticky as the bolus became pasty at the swallow point. The average adhesiveness of the peanut boluses increased as the chews increased and was highest at the swallow point. After which, the adhesiveness deceased as the number of chews past the swallow point increased. The adhesiveness

of the muesli bar was highest at zero chews due to the glucose syrup used as a binder to form the bars. As XG solution was added to the bolus during the chews, the surface lost its stickiness, which explains the reduction as the number of chews increased. However, after 22 chews, the adhesiveness started to plateau. The adhesiveness of the apple boluses increased with increasing number of chews, was highest at five chews and plateaued at five to eighteen chews before decreasing after it was past the swallow point. The adhesiveness of the ham boluses is not a good measure as there seemed to be no observable difference throughout the chewing stages. The adhesiveness in the initial stages maybe be high due to the XG solution that was added to the surface of the ham sample, resulting in some adhesive forces between the ham sample and the probe. As the ham gets more broken down, the XG solution is no longer on the surface of the ham sample but distributed within the broken up chunks and fibres of the ham bolus, thus the adhesiveness decreased. As the bolus gets more well mixed and with more XG solution added, the adhesiveness increased again.

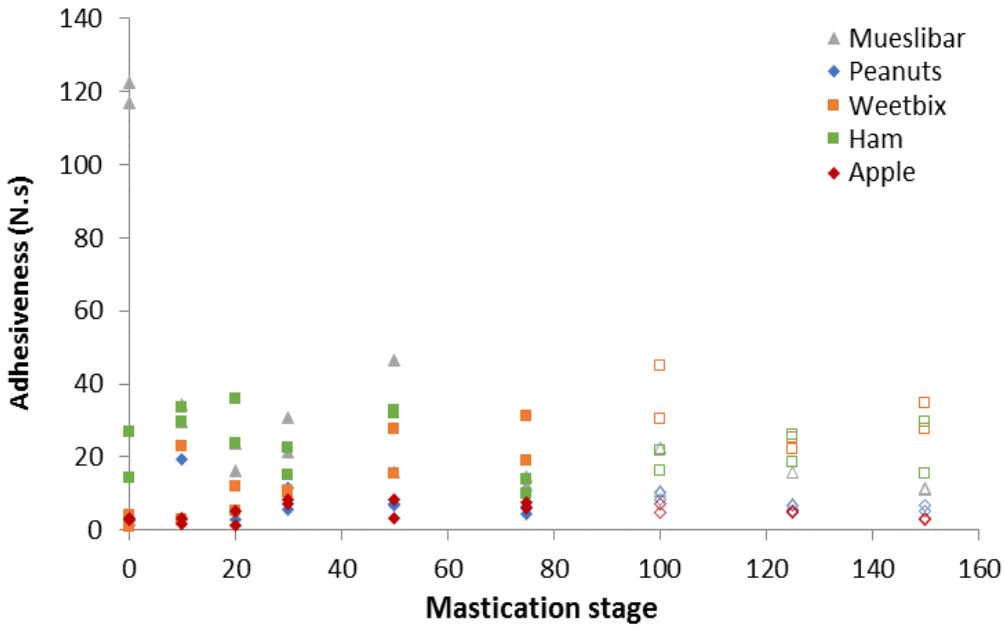


*Figure 7-8: The adhesiveness of the boluses collected from the robot after a certain number of chews plotted against the number of chews. The hollowed symbols represent the boluses collected at 100% (swallow point), 125% and 150% of the mastication stage based on the median subject in chapter. Inset graph is the same data set with the removal of the zero chew data points for the muesli bar and trendlines of the average data so that there is better resolution.*

Cohesiveness measures how well the bolus withstands a second deformation relative to its resistance under the first deformation and is quantified by dividing the area of the second compression over the area of the first compression (Bourne, M., 2002; James et al., 2011b). Figure 7-9 shows the cohesiveness of the boluses plotted against the number of chewing cycles. In general, the cohesiveness of the boluses increased with increasing number of chews, with weetbix boluses

exhibiting the highest cohesiveness amongst the other foods. Although the trend is similar across foods, the reason behind the increase in cohesiveness is different. In the initial stages of mastication, the Weetbix boluses are dry and brittle, thus the amount of work needed in the second compression are small in comparison to the first. With increasing number of chews and more XG solution being mixed into the weetbix, the boluses became pasty and this property allowed the bolus to recover after the first compression. Hence, the ratio of the amount of work needed between the first and second compressions increased. The peanuts and muesli bar boluses also become more cohesive as the individual oat grains, rice puffs, seeds and nuts start to get pasted. However, in the case of apple, as the number of chews increased, the apple boluses became pulpy and there were less undestroyed cellular structures available to be broken down during the first compression of the test. Thus, with less work needed in the first compression, it seemed that the cohesiveness was increasing.

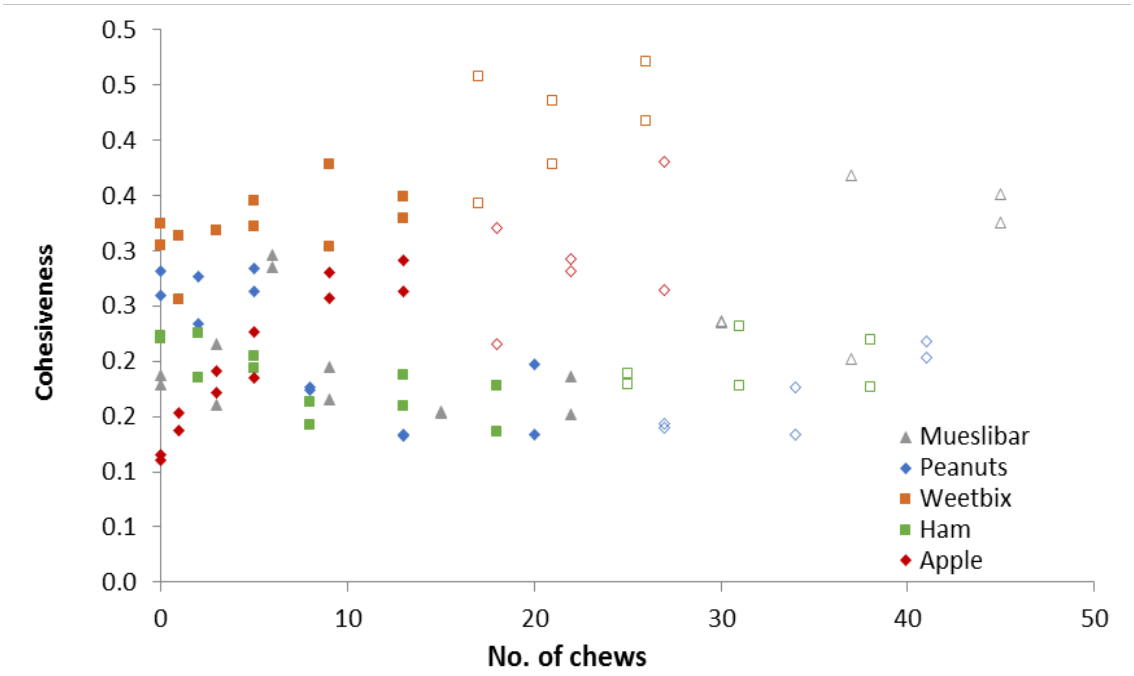


Figure 7-9: The cohesiveness of the boluses plotted against the number of chews. The hollowed symbols represent the boluses collected at 100% (swallow point), 125% and 150% of the mastication stage based on the median subject in chapter six.

The results from the back extrusion may not be relevant for the samples at zero chews and 10% mastication whereby the sample's dimensions result in the samples being placed in different orientations as that of the bolus. Thus, the sites at which the forces were exerted for breakage was different between the BET and the mastication in the MR.

### 7.2.4. Multiple Pin Penetrometer

Boluses produced by the mastication robot (MR) at different degrees of oral processing were characterised using the MPP as discussed above. Figure 7-10 shows the contour plots of the force profiles for each food bolus collected at various stages of mastication. Figure 7-11 shows the force distribution of the boluses from the MPP test plotted as box plots to reflect the $25^{th}$, $50^{th}$ and $75^{th}$ percentile of force measured for the pooled distribution of the duplicates for each mastication stage. The force distributions for apple and ham were much lower than that as compared to muesli bar and weetbix in the initial stages of mastication, reflecting the difference in initial texture properties of the foods. In the case of weetbix, the inter quartile range (IQR) increased after the first chew reflecting the decrease in forces measured at the part of the bolus that was chewed as compared to the bolus at zero chews. The IQR decreased rapidly after three chews due to the brittle nature of the weetbix in addition to the effect of XG solution softening the bolus as it is absorbed by the weetbix. Although the force distributions of the boluses continued to decrease, the differences were not significant after nine chews. This is seen in Figure 7-10d where the first plot had a range of forces measured across the matrix at zero chews; the second plot showed that the first chew was made on the left half of the weetbix; the third plot showed that most of the weetbix bolus had been chewed and that after nine chews, the force maps were less than 1 N throughout the bolus.

As the muesli bar is comprised of different components bound together by sticky syrup, the decrease in forces over chewing progression is more gradual. In the first nine chews, the muesli bar was broken into smaller chunks, and then eventually into the individual components that make up the bar. The individual components of the bar such as the nuts and pumpkin seeds are much harder and required more chews to break down as shown by no significant changes in the force distributions at 15 and 22 chews. Although the rice puffs could be softened by absorbing moisture through the XG solution added, the layer of syrup coating slowed the adsorption of XG solution. No significant differences were observed in the force distributions after the swallow point at 30 chews. Although the initial force distributions for the apple and ham boluses were much smaller than that of the weetbix and muesli bar boluses, the force distributions were similar at the swallow point with ham having the largest force distribution amongst the four foods.

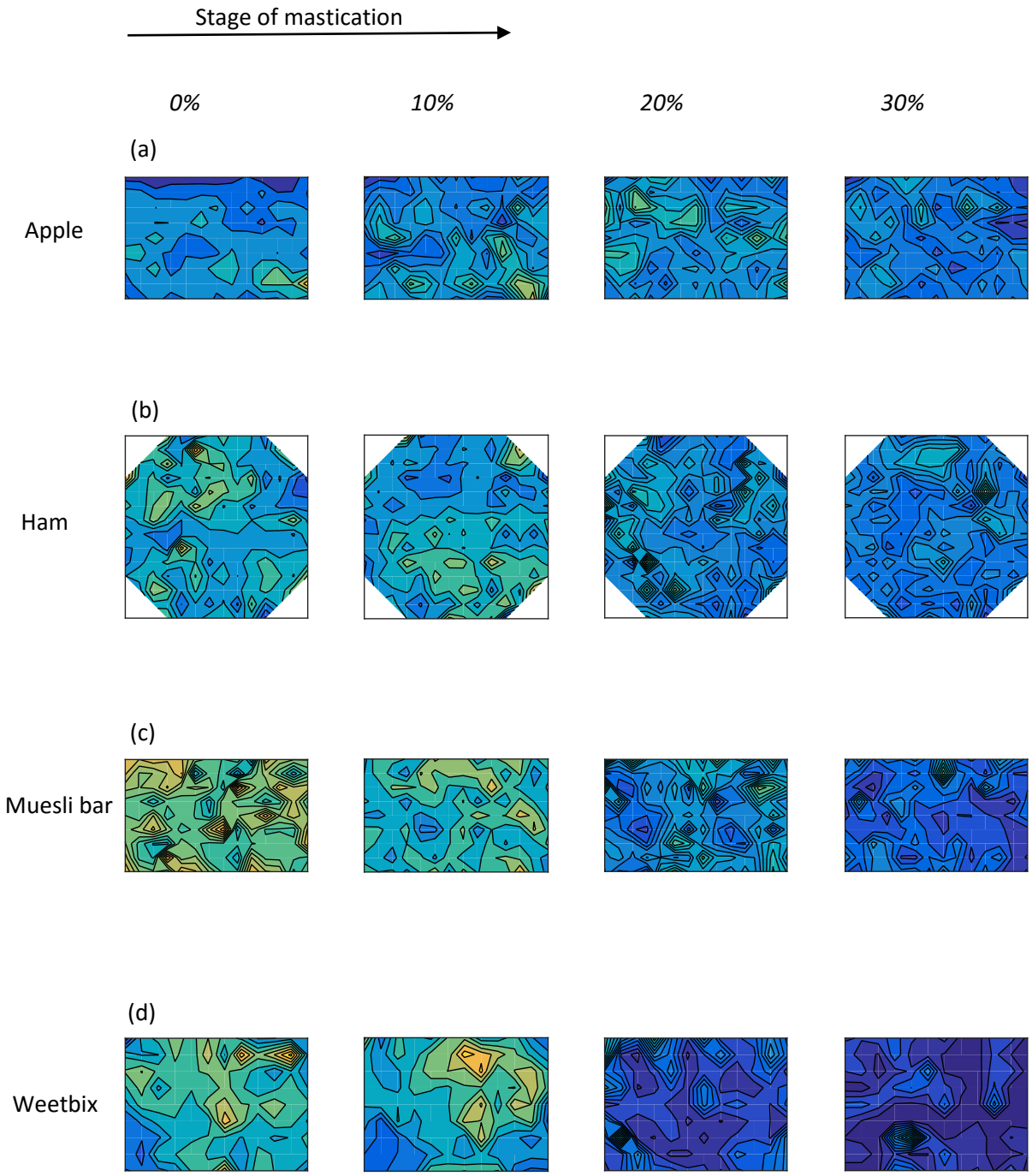


*Figure 7-10: Contour plots of (a) apple boluses after 0,1,3,5,9,13,18,22, and 27 chews based on a 13 x 9 matrix; (b) ham boluses after 0,2,5,8,13,18,25,31, and 38 chews based on a 14 x 14 matrix with six pins removed at each corner; (c) muesli bar boluses after 0,3,6,9,15,22,30,37, and 45 chews based on a 14 x 9 matrix; (d) weetbix boluses after 0,1,3,5,9,13,17,21, and 26 chews based on a 12 x 9 matrix.*

*50%* *75%* *100%* *125%* *150%*


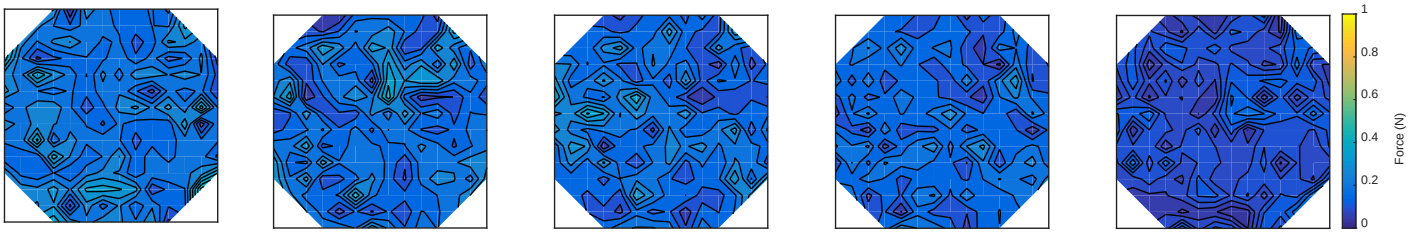



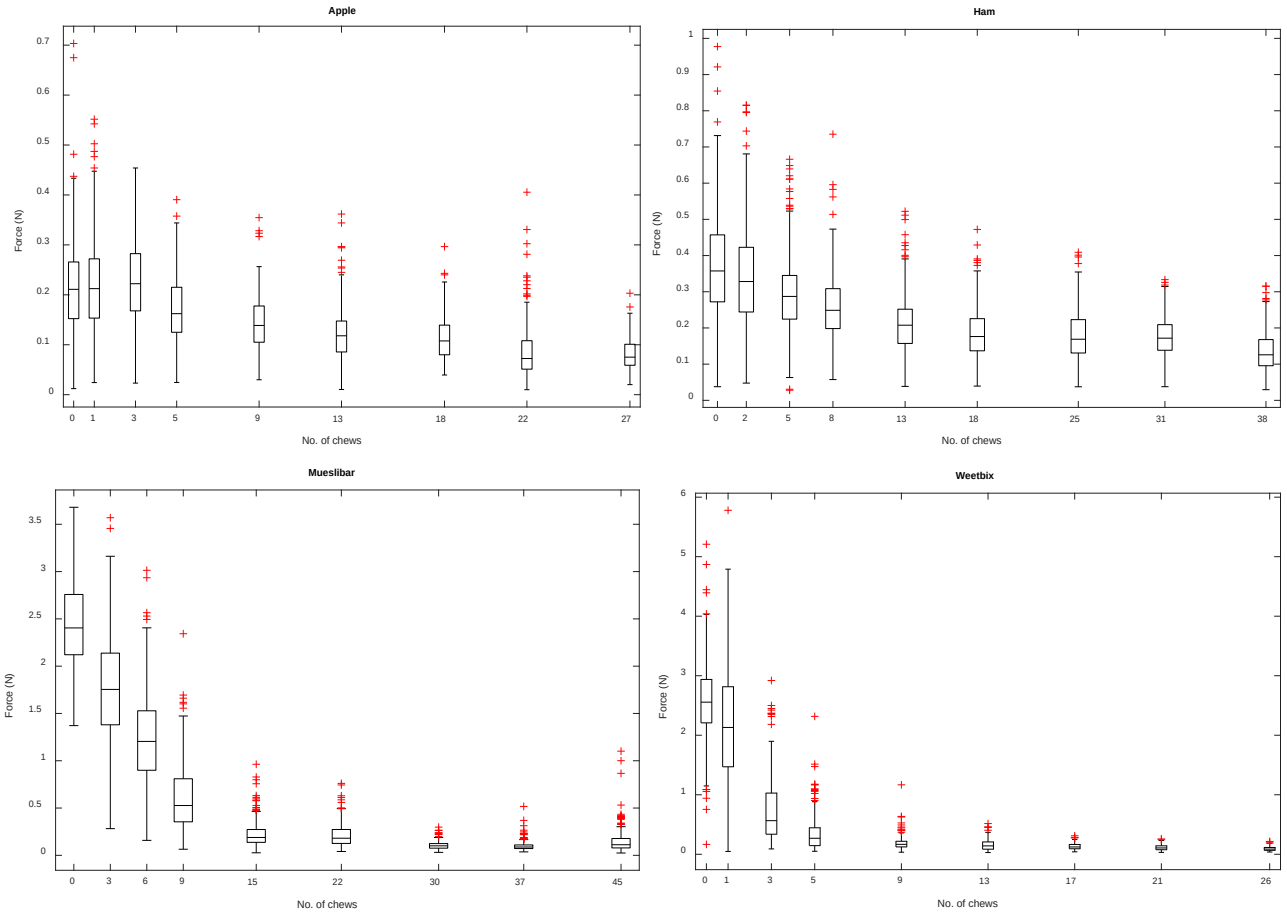


*Figure 7-11: Box plot of the force distributions of the duplicate boluses collected after the required number of the duplicates were pooled together to form the distribution for each chewing cycle. The box represents the 25$^{th}$ percentile, median and 75$^{th}$ percentile, while the whisker length is 1.5*IQR (inter quartile range) and the red crosses represent the outliers.*

In general, the GLCM for the boluses were concentrated around the principal diagonal and shifted down the principal diagonal as the stage of mastication progressed (Figure 7-12). This meant that the areas of particular force levels were surrounded by force levels at the same or similar levels. At zero chews and at 10% of the mastication process, the muesli bar was the only food that had neighbouring pixels with gray level of eight, reflecting that the hard parts were of larger areas as compared to the other foods. At 10% of the mastication process, the spread of the GLCM for the muesli bar increased, reflecting the increase in occurrences in which a pixel of lower gray level was beside another pixel of higher gray level. This is probably due to the broken chunks containing different components of the muesli bar.

The GLCM of the weetbix bolus after three chews (20% mastication stage), showed that the bolus had softened significantly with only a few fragments of crisp weetbix that were above 1.5N. The GLCM of the apple and ham boluses were still changing after the swallow point, which may be due to the smaller differences in the scale for the gray levels as compared to the weetbix and muesli bar boluses since they were initially much harder.

In all the boluses at 10% mastication stage, almost half of the bolus was distinctly softer than the other part reflecting the area in which the food had been broken down during the initial chews (Figure 7-10). The muesli bar sample without chews showed that 85% of the area in contact was above 2N and the remaining 15% was between 1.3N to 2N. The areas with a lower force measured were probably the spots where it consisted of rice puffs which is porous and easier to penetrate. After three chews, the bar was broken down into chunks and the lower forces on the plot reflect the fractured parts since the bar was no longer tightly packed. At six to fifteen chews, most of the bar was broken up into individual components, and the green and yellow areas on the plot were probably seeds or nuts that had not been broken up yet. After 20 chews, most of the boluses were broken down and soft although there was still some variation as the rice puffs and some of the nuts had formed a pasty mass with some bits of nuts and seeds.

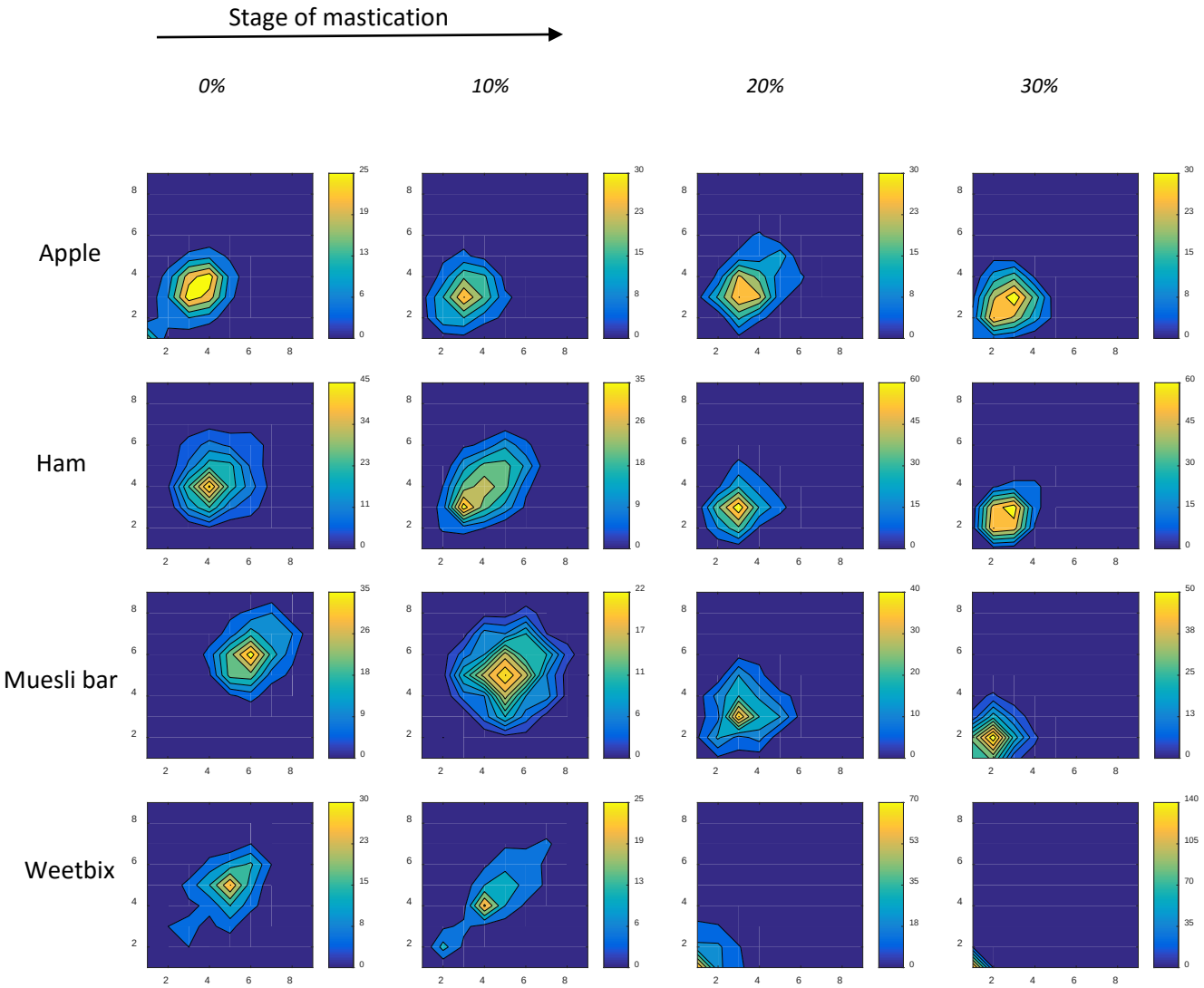


*Figure 7-12: Contour plots of the GLCM for (a) apple, (b) ham, (c) muesli bar, (d) weetbix boluses at various stages of the mastication process plotted on a 9 x 9 matrix (9 gray levels). Ham was the only food that had changing GLCM up till 150% stage of mastication. The nine gray levels for were scaled differently for each food as detailed in appendix D.*

*50%* *75%* *100%* *125%* *150%*

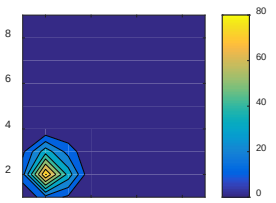


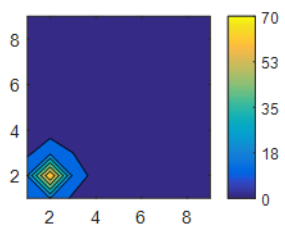


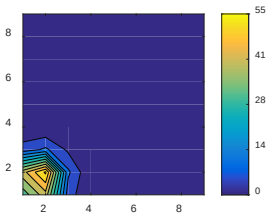


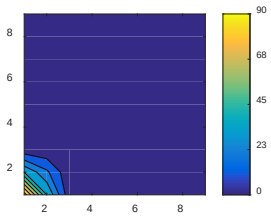


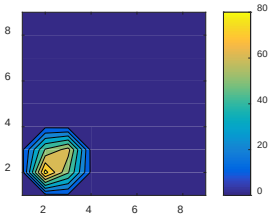


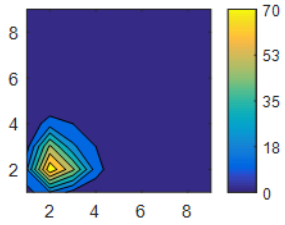


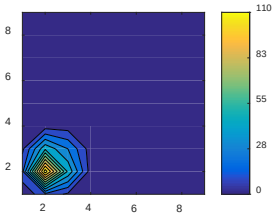


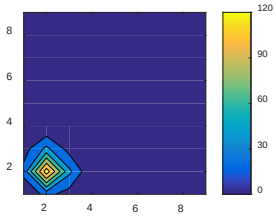


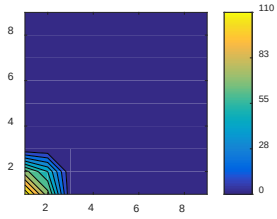


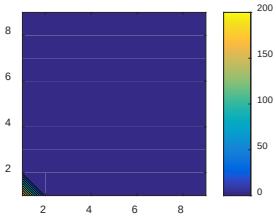


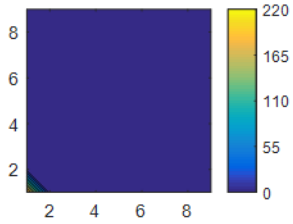


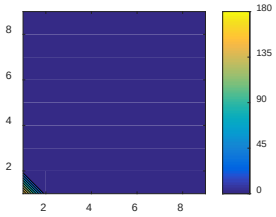

A bolus becomes more homogeneous as the mastication stage progresses, thus the standard deviation of the maximum forces (irrespective of spatial location) measured across the bolus decreased as the number of chews increased. However, for foods like the apple and ham, the decrease in standard deviation became very small such that it was difficult to observe the changes after a certain number of chews (Figure 7-13).

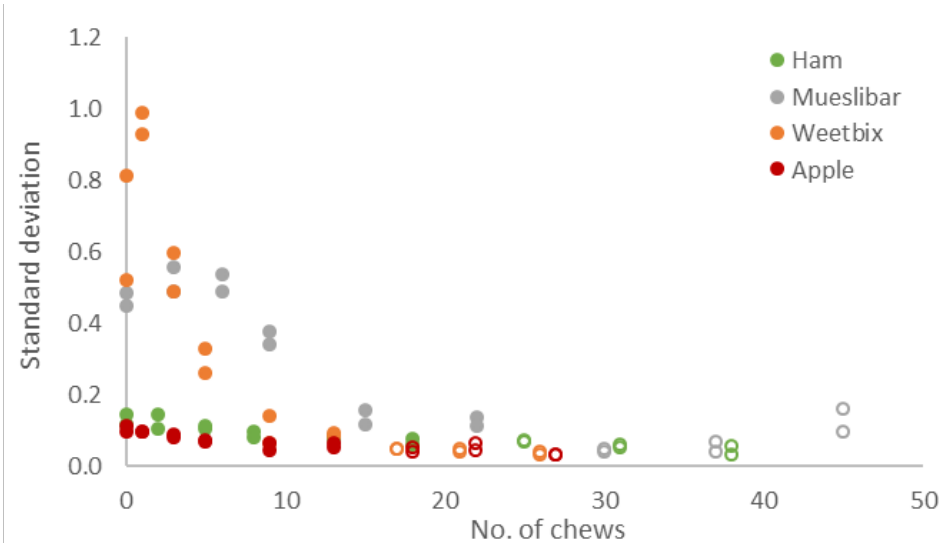


*Figure 7-13: The standard deviation of the force measurements for each bolus is plotted against the number of chews; inset plot has the y-axis set to a lower limit for better resolution.*

The contrast (derived from the GLCM) amplified the differences during the masticatory process, as it is the difference between the highest and lowest values of a pair of neighbouring pixels. As the boluses were chewed, the contrast decreased (Figure 7-14a), reflected by an increase in the number of occurrences around the principal diagonal in the GLCM (Figure 7-12). The energy and homogeneity factors increased with the number of chews towards a maximum value of one which represents a uniform and homogenous bolus (Figure 7-14b&c). The forces measured for the weetbix and muesli bar boluses were within the same gray level after 50% mastication and after swallow point for weetbix and muesli bar respectively. The ham and apple boluses at and after swallow point had a degree of heterogeneity as can be seen in Figure 7-10a&b, where the apple bolus consisted of pieces of pulp and the ham bolus had varying sized bundles of meat fibres. To test the assumption that a bolus should have a more homogenous texture with increasing number of chews, the energy and homogeneity features may be used to differentiate boluses that display similar contrast but were from different stages of the mastication process. For example, the apple boluses at 9 and 22 chews, had similar contrast (0.6% difference) while the energy and homogeneity of the bolus at 22 chews was higher (24% and 3% respectively).

(a)

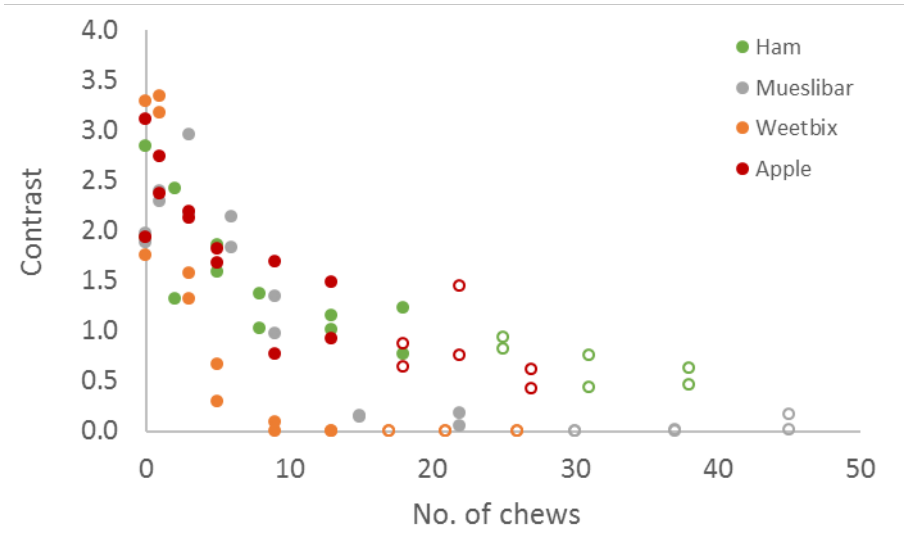


(b)

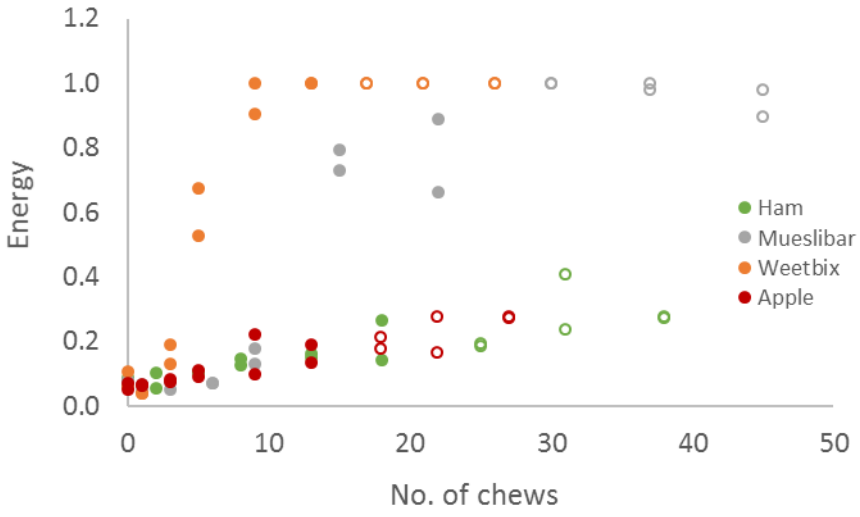


(c)

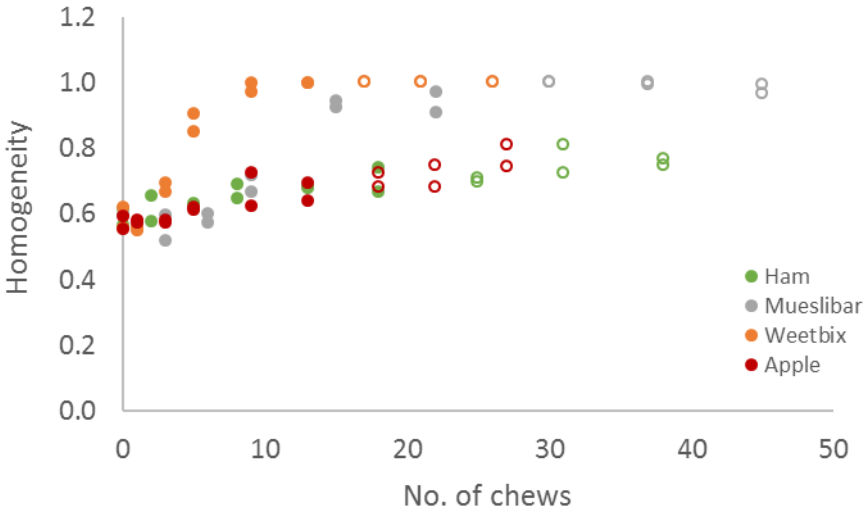


*Figure 7-14: The three textural features from the analysis of the GLCM, (a) contrast, (b) energy, (c) homogeneity, plotted against the number of chews.*

### 7.2.5. 3-Dimensional forces from the Mastication Robot

Figure 7-15 shows an example of the forces measured during chewing. On the left, the x, y and z direction forces are shown during the baseline chew and the first chew of each food. In the plots on the right, the resulting force measured in the z direction after the removal of the baseline force is shown. The shapes of the base peaks were similar for apple and peanuts, which showed a rapid increase and decrease in force on the x and z axes as the teeth occluded and separated. There was no force exerted on the y axis (lateral direction) as these foods were chewed using the vertical trajectory. The shapes of the base peaks on all axes for ham, muesli bar and weetbix were similar with a gradual increase as the teeth occlude and an initial rapid decrease as the upper teeth lift off, but due to the lateral path, there is still some contact with the lower teeth, reflected by the gentle slope before rapidly decreasing again when the upper and lower teeth are no longer in contact. The widths of the base peaks in the vertical trajectory were smaller than that for the lateral trajectory as the upper teeth come in at an angle and meet with the tips of the lower teeth before coming into occlusion at the lowest point. Thus, the upper and lower teeth come into contact for a longer period in the lateral trajectory as compared to the vertical trajectory. The shapes of the base peaks reflect the difference in the force exerted by the upper teeth between a vertical and lateral chewing trajectory.

The decrease after the first peak in the first chew of the apple showed that the forces needed to chew the apple were small and the apple fractured before the teeth were in complete occlusion. The multiple fractures on the peaks during the first chew for weetbix and peanuts reflect the crispy and brittle nature of the respective foods. The increase in force exerted by ham and apple during the first chew was much smaller than peanuts, muesli bar and weetbix which were larger than 100 N. As apple and ham were much softer, they were broken down by the occluding forces. In comparison, the peanuts, muesli bar and weetbix had a higher hardness, accounting for the increase in force before they were broken down. The increase in the width of the peak for the first chews were directly proportional to the thickness of the food sample. This is because the upper teeth would meet the food earlier in the chewing trajectory, resulting in a force exerted for a longer time.

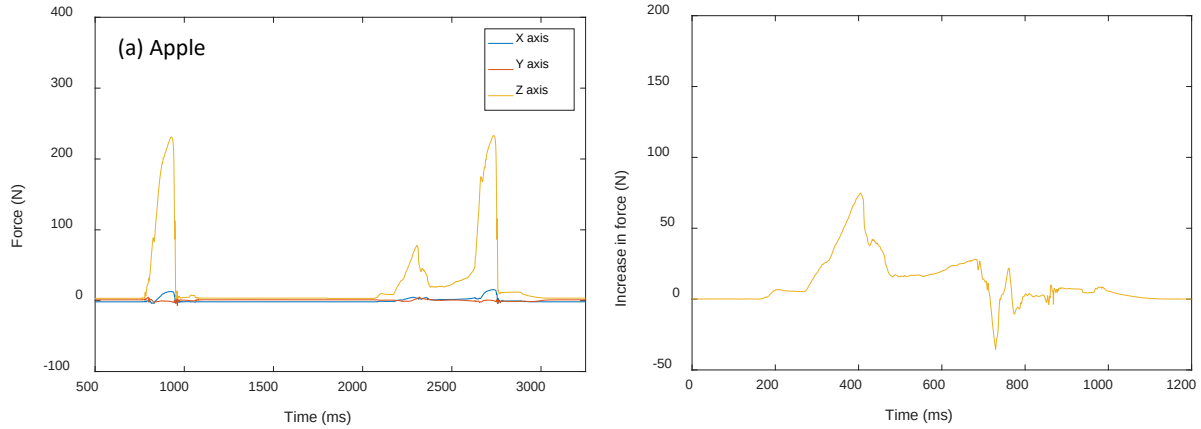
(a) Apple
X axis
Y axis
Z axis
Force (N)
Time (ms)
Increase in force (N)
Time (ms)

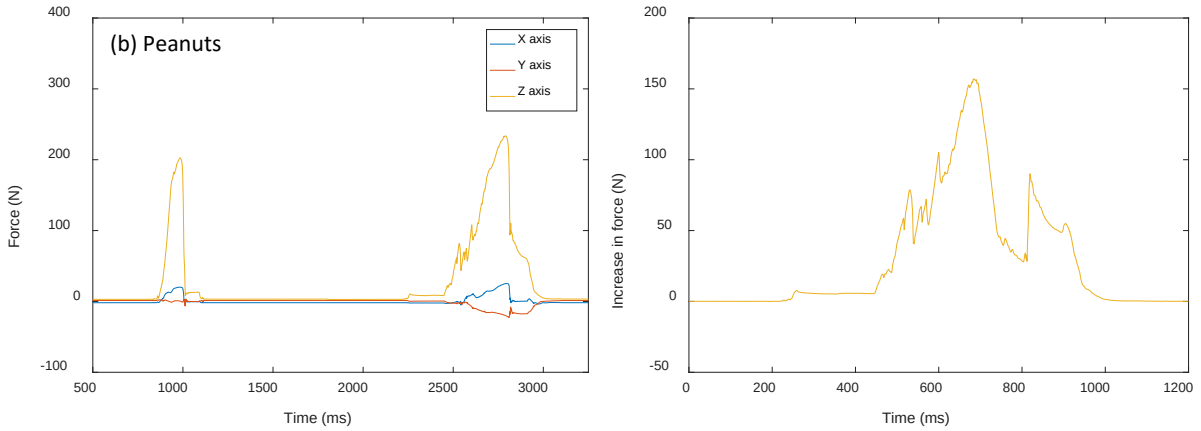
(b) Peanuts
X axis
Y axis
Z axis
Force (N)
Time (ms)
Increase in force (N)
Time (ms)

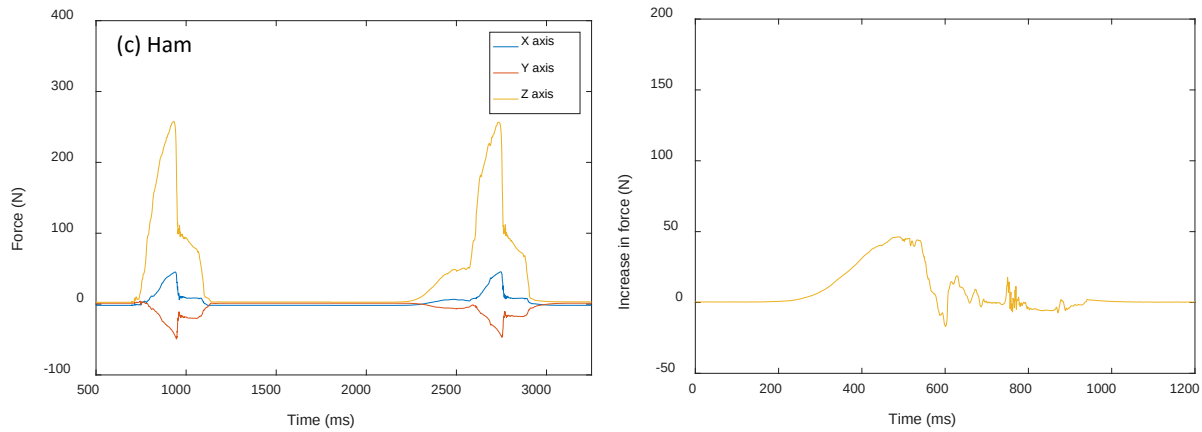
(c) Ham
X axis
Y axis
Z axis
Force (N)
Time (ms)
Increase in force (N)
Time (ms)

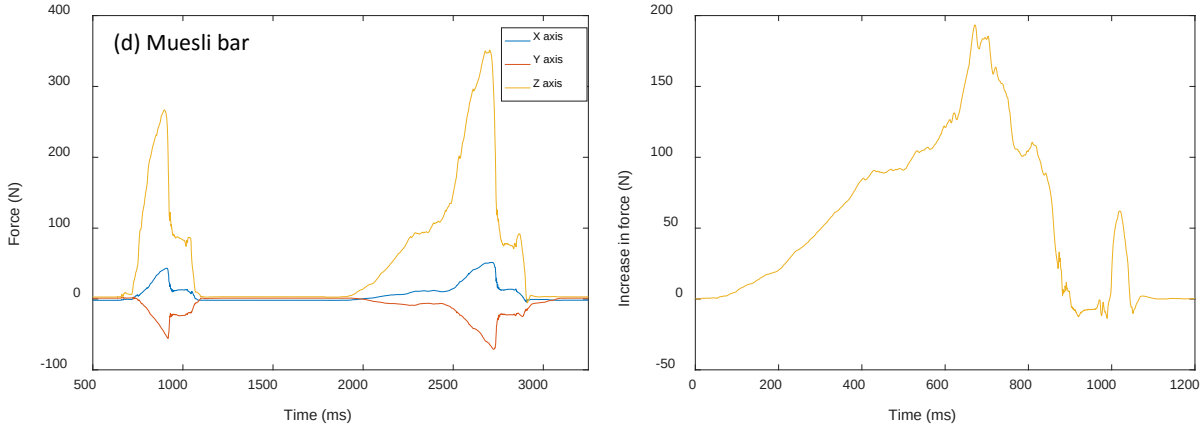
(d) Muesli bar
X axis
Y axis
Z axis
Force (N)
Time (ms)
Increase in force (N)
Time (ms)

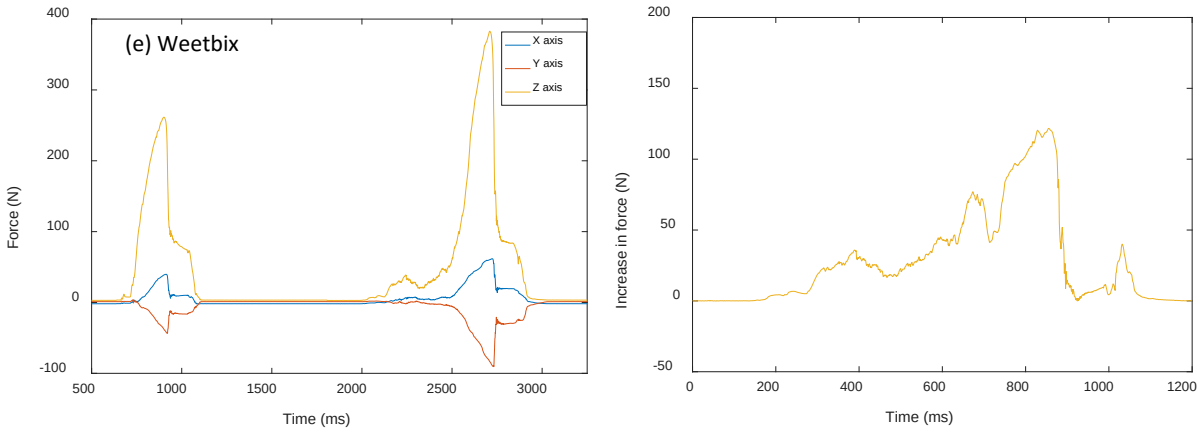


*Figure 7-15: Plots on the left are the typical force deformation plot of the base peak and peak at first chew in the mastication of (a) apple, (b) peanuts, (c) ham, (d) muesli bar, and (e) weetbix. The x, y and z axes are the forces exerted in the sagittal, lateral and vertical directions respectively. Plots on the right are the vertical force deformation plots for first chew (z-axis) after removal of the base peak ($F_{Food} - F_{Base}$).*

Figure 7-16 shows the impulse (i.e. area of the force deformation curve) in the x, y and z directions plotted against the number of chews for each food. In general, the impulse was dependent on the hardness of the bolus. Although the impulse measured in the sagittal plane was the smallest across all foods, the magnitude of the impulse exerted in the sagittal plane (y-axis) was close to those exerted in the lateral plane for apple, peanuts and ham. The forces exerted in the lateral plane were higher for muesli bar and weetbix as more shearing action was applied during chewing in the lateral trajectory. Although ham was chewed in the lateral trajectory, the initial properties of ham was soft, and fibres could be easily torn apart such that the ham did not exert as much force on the occlusal surface in the lateral plane during each chew. Apple and ham boluses had low impulse in the lateral and sagittal (x and y axis respectively) directions. The standard deviations for apple and ham did not change significantly throughout chewing but decreased significantly in the first ten chews for weetbix, muesli bar and peanuts. Weetbix required the highest impulse in the x and y axis at the start, followed by mueslibar, peanuts, then apple and ham. However, weetbix required less impulse than muesli bar and peanuts after five and ten chews respectively. Weetbix experienced a rapid decrease in the x-axis in the first ten chews but did not change much in subsequent chews. The forces measured in the y-axis and z-axis decreased rapidly in the initial chews and continued to decrease at a declining rate up until the end of mastication. This explains the rapid softening in the weetbix in the first few chews which continued to be softened as more XG solution was added. In the initial few chews, mueslibar had the highest impulse in the z-axis followed by weetbix, peanuts, apple and ham. However, as described above for the x and y axis forces, the weetbix softened rapidly as the XG solution was mixed into the bolus, requiring less impulse than peanuts after eight chews and similar impulse as apple and ham after 20 chews.

The median impulse in the x-axis and y-axis were negative after 15 and 22 chews respectively, suggesting that the ham boluses were no longer exerting any forces in the lateral and sagittal directions. The negative values for the x and y axis suggests that during the mastication, the bolus may be squeezed out of the occlusal surface by the teeth in the opposite direction of the upper teeth's set trajectory. Large negative forces were attributed to mechanical error where by the forces were lost when the gear was momentarily stuck during operation, while the small negative forces have been proven to be due to the system having some noise as detailed below.

There is some unexplained variation in the forces measured in the MR because of how the contact surfaces between the upper and lower teeth may shift slightly because of mechanical backlash in the upper teeth. The baseline measurement before the start of each test was used to check that the set parameters for the operation of the robot were providing the correct amount of force during the chewing cycle. Thus, it was essential to determine the variation in these force measurements and their impact on the actual measurements when food is being chewed. Five replicates of five chewing cycles were carried out at the following set parameters: a vertical chewing trajectory (3mm ground link) at a sagittal plane of 15° and at a stage height of 7.45mm. A vertical chewing trajectory at a sagittal plane of 15° should result in little force being measured in the y and x directions respectively, while changing the stage height will allow a large force to be measured in the z direction. The impulse (the area under the force-time curve) for each direction was calculated. Although there was some variation within and between replicates (Table 7-3), the magnitude of the variation was small when compared with the magnitude of the forces measured during the chewing of food. The percentage standard deviation was large for the impulse in the x and y axes, as the forces measured were very small.

*Table 7-3: A summary of the average impulse (N.s) measured for five replicates of five chewing cycles, the standard deviation (SD) and the %SD for each replicate.*

| **X Impulse** | **Replicate 1** | **Replicate 2** | **Replicate 3** | **Replicate 4** | **Replicate 5** |
|---|---|---|---|---|---|
| **Average** | 0.57 | 0.51 | 0.72 | 0.77 | 0.59 |
| **SD** | 0.05 | 0.03 | 0.14 | 0.13 | 0.06 |
| **% SD** | 8.81 | 5.35 | 19.98 | 16.57 | 10.59 |
| **Y Impulse** | **Replicate 1** | **Replicate 2** | **Replicate 3** | **Replicate 4** | **Replicate 5** |
| **Average** | 0.39 | 0.36 | 0.40 | 0.37 | 0.34 |
| **SD** | 0.03 | 0.02 | 0.04 | 0.05 | 0.05 |
| **% SD** | 8.15 | 6.71 | 8.82 | 14.82 | 15.29 |
| **Z Impulse** | **Replicate 1** | **Replicate 2** | **Replicate 3** | **Replicate 4** | **Replicate 5** |
| **Average** | 24.48 | 24.60 | 24.61 | 24.55 | 24.59 |
| **SD** | 0.09 | 0.29 | 0.39 | 0.22 | 0.19 |
| **% SD** | 0.35 | 1.19 | 1.58 | 0.91 | 0.76 |

The force measurements show how the dynamic changes to the bolus may affect the chewing pattern and forces required to breakdown the bolus, which could be used to understand how humans modulate chewing actions for most efficient breakdown of foods as the mastication stage progresses. It would be interesting to determine if foods with similar initial properties and similar bolus properties would have similar patterns in the force profiles in the sagittal, lateral and vertical plane.

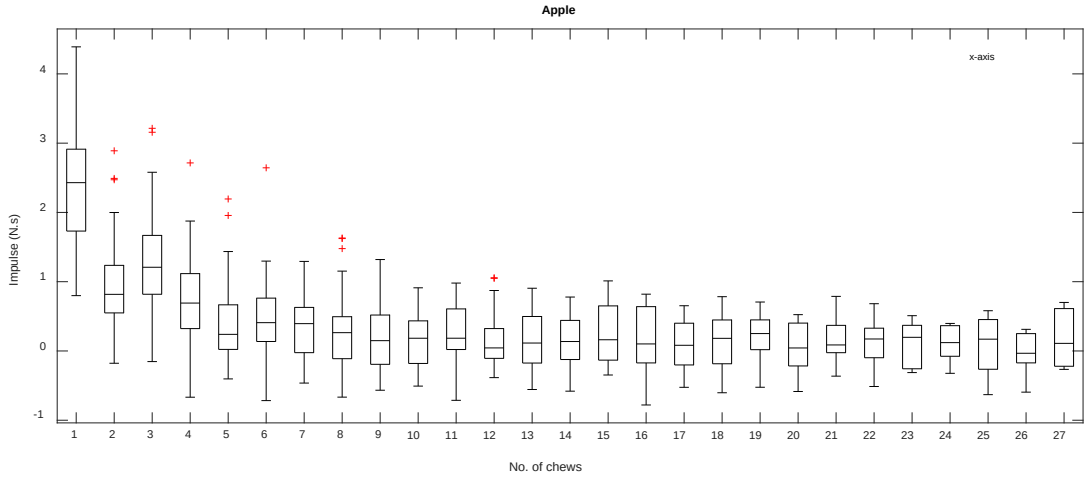


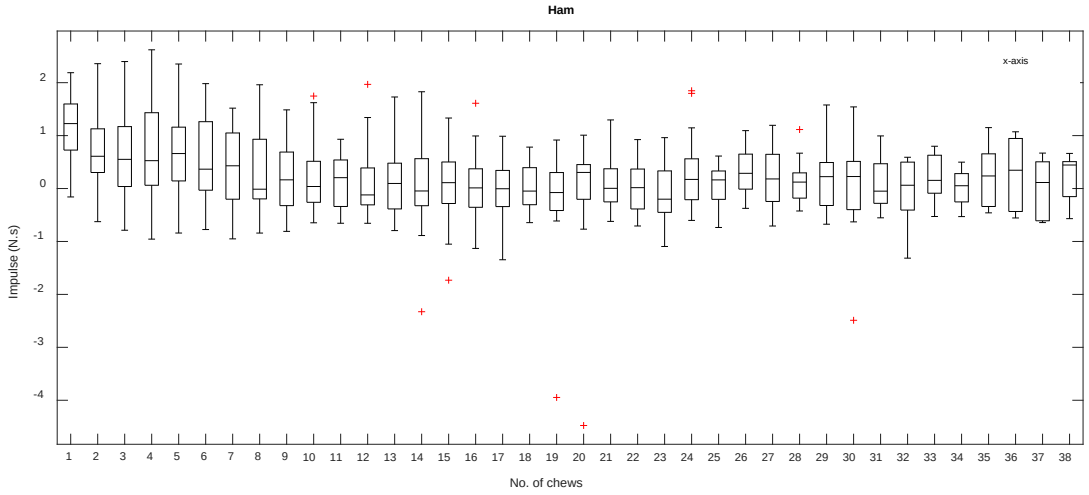


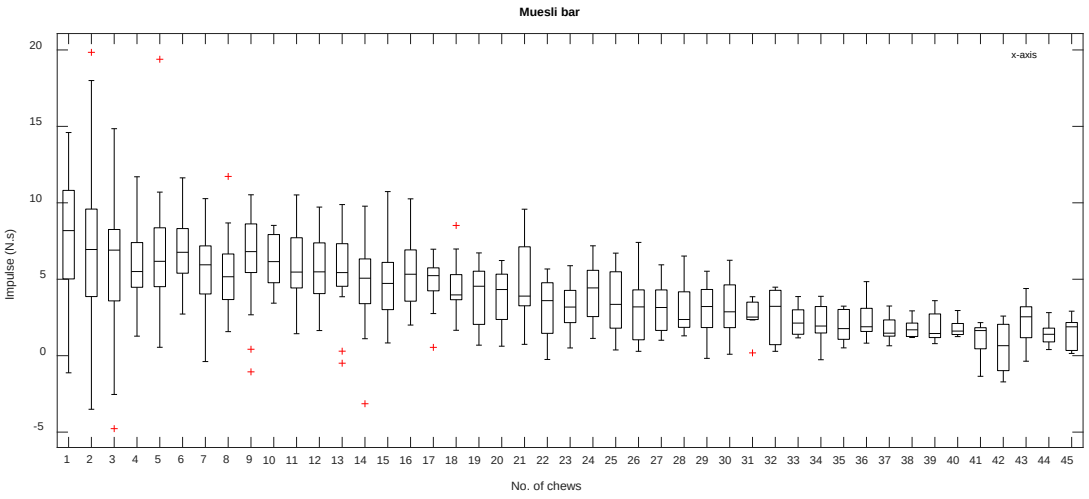

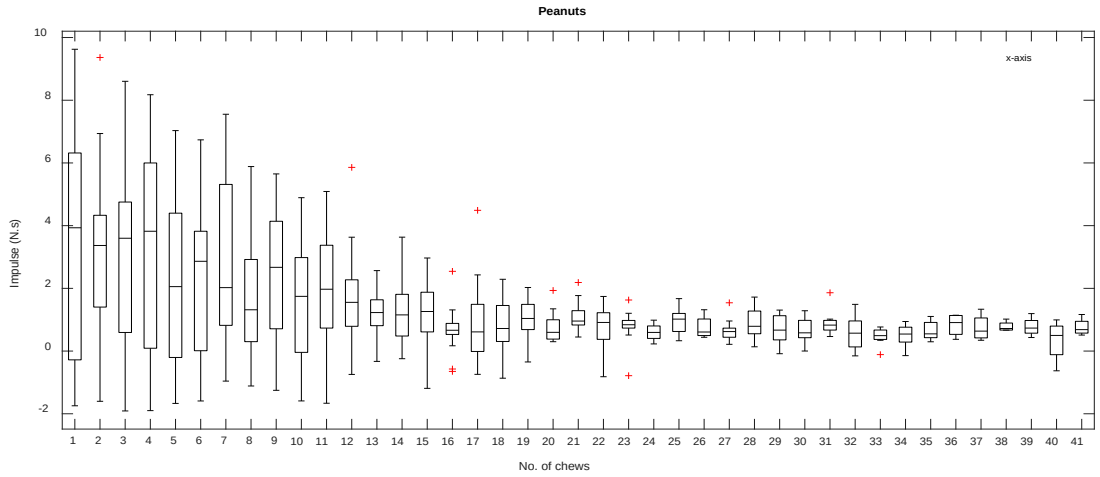
Peanuts
x-axis
Impulse (N.s)
No. of chews

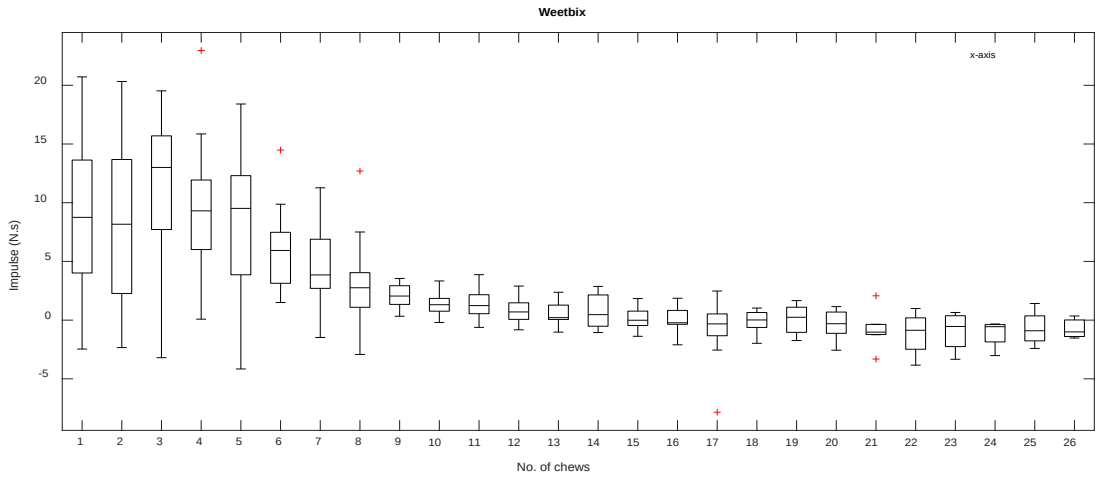
Weetbix
x-axis
Impulse (N.s)
No. of chews

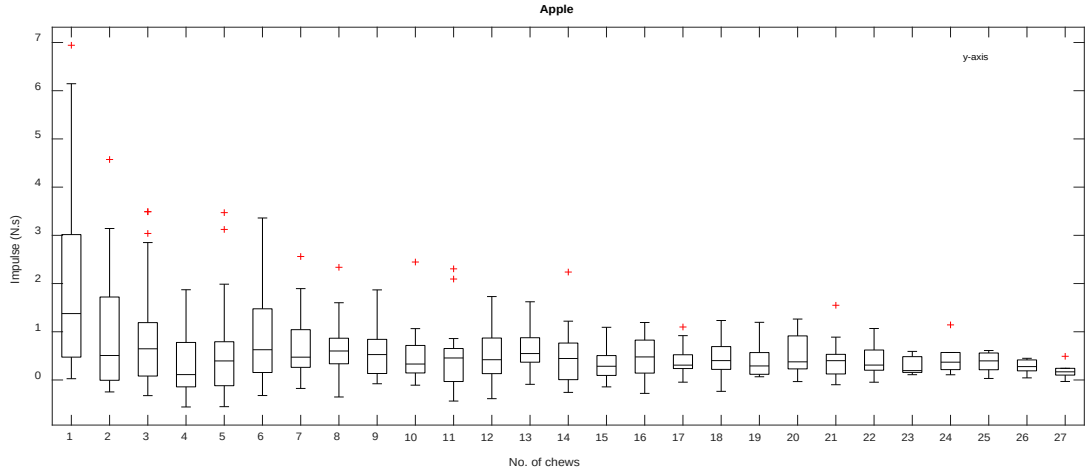
Apple
y-axis
Impulse (N.s)
No. of chews

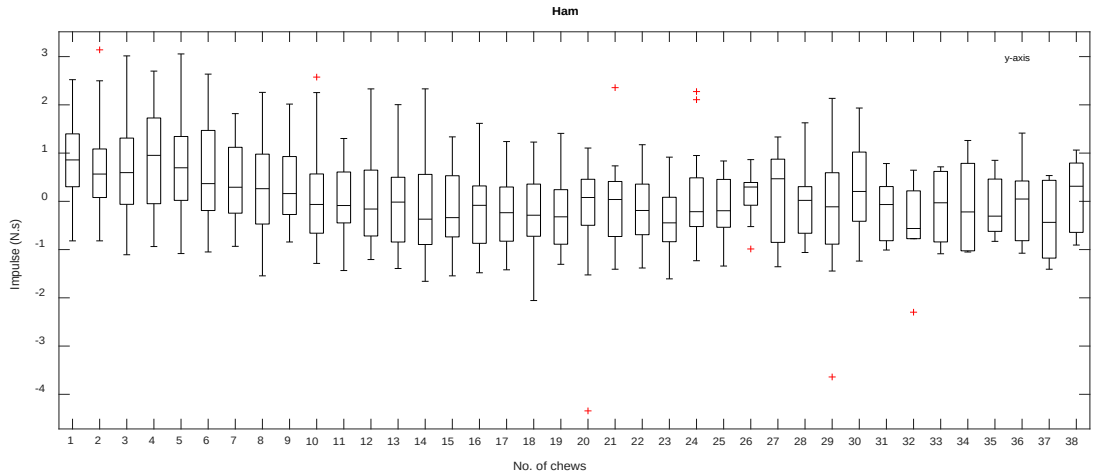
Ham
y-axis
Impulse (N.s)
No. of chews

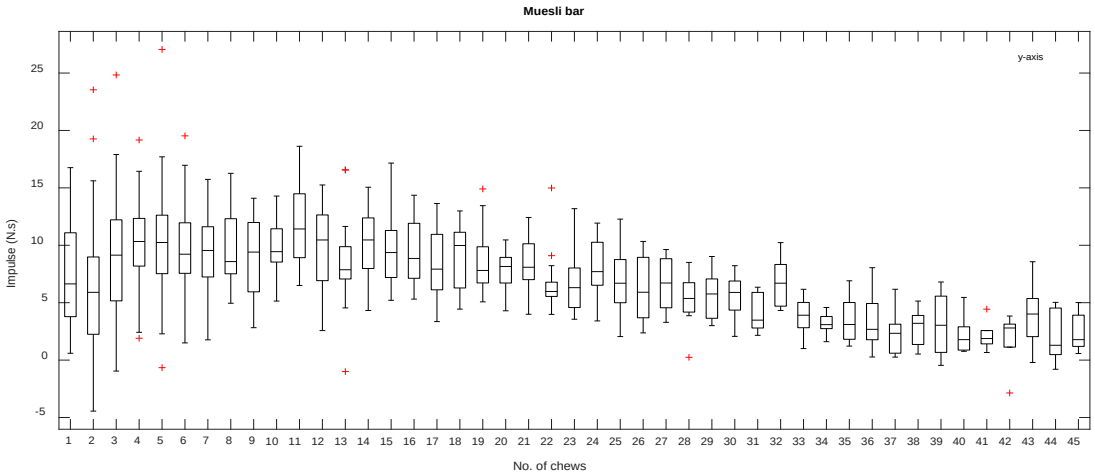
Muesli bar
y-axis
Impulse (N.s)
No. of chews

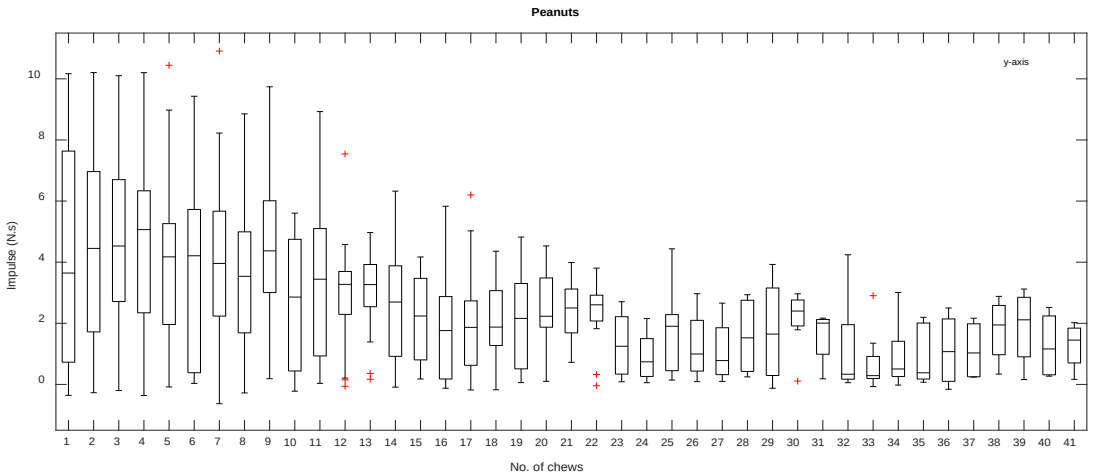
Peanuts
y-axis
Impulse (N.s)
No. of chews

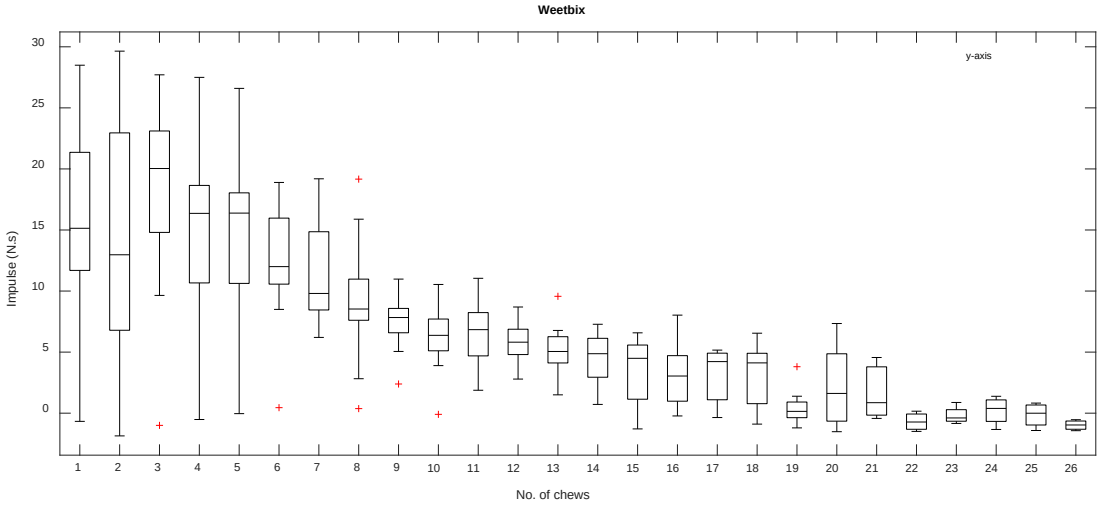
Weetbix
y-axis
Impulse (N.s)
No. of chews

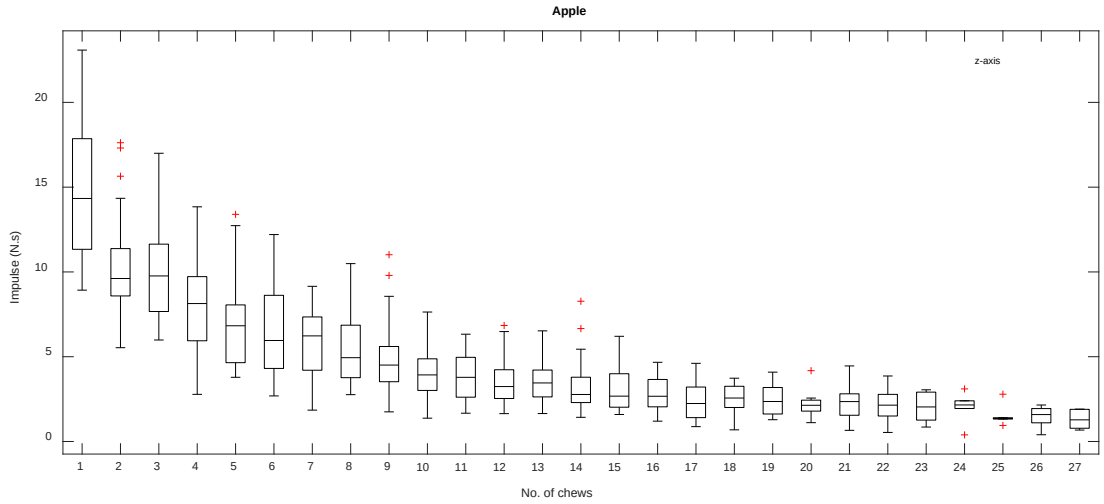
Apple
z-axis
Impulse (N.s)
No. of chews

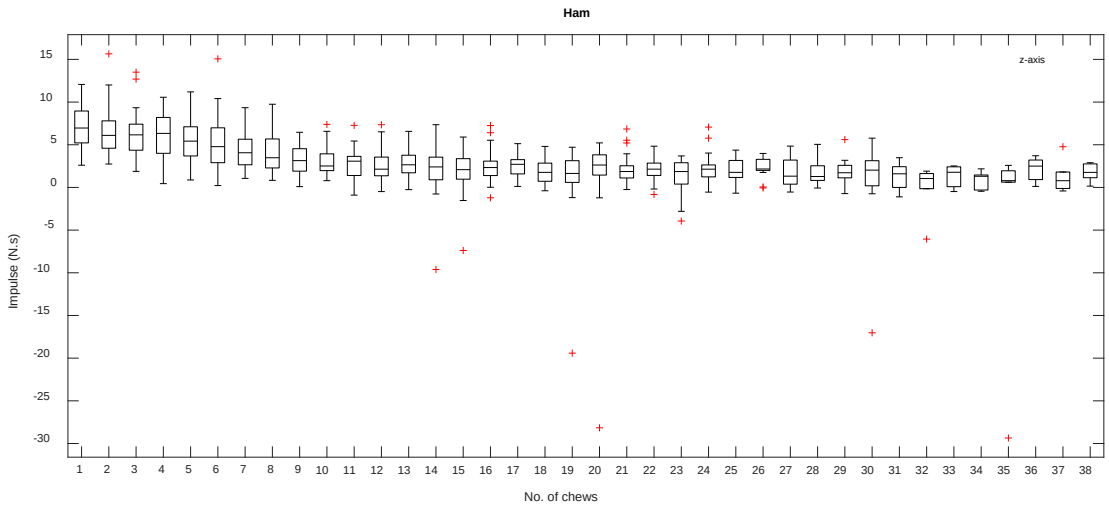
Ham
z-axis
Impulse (N.s)
No. of chews

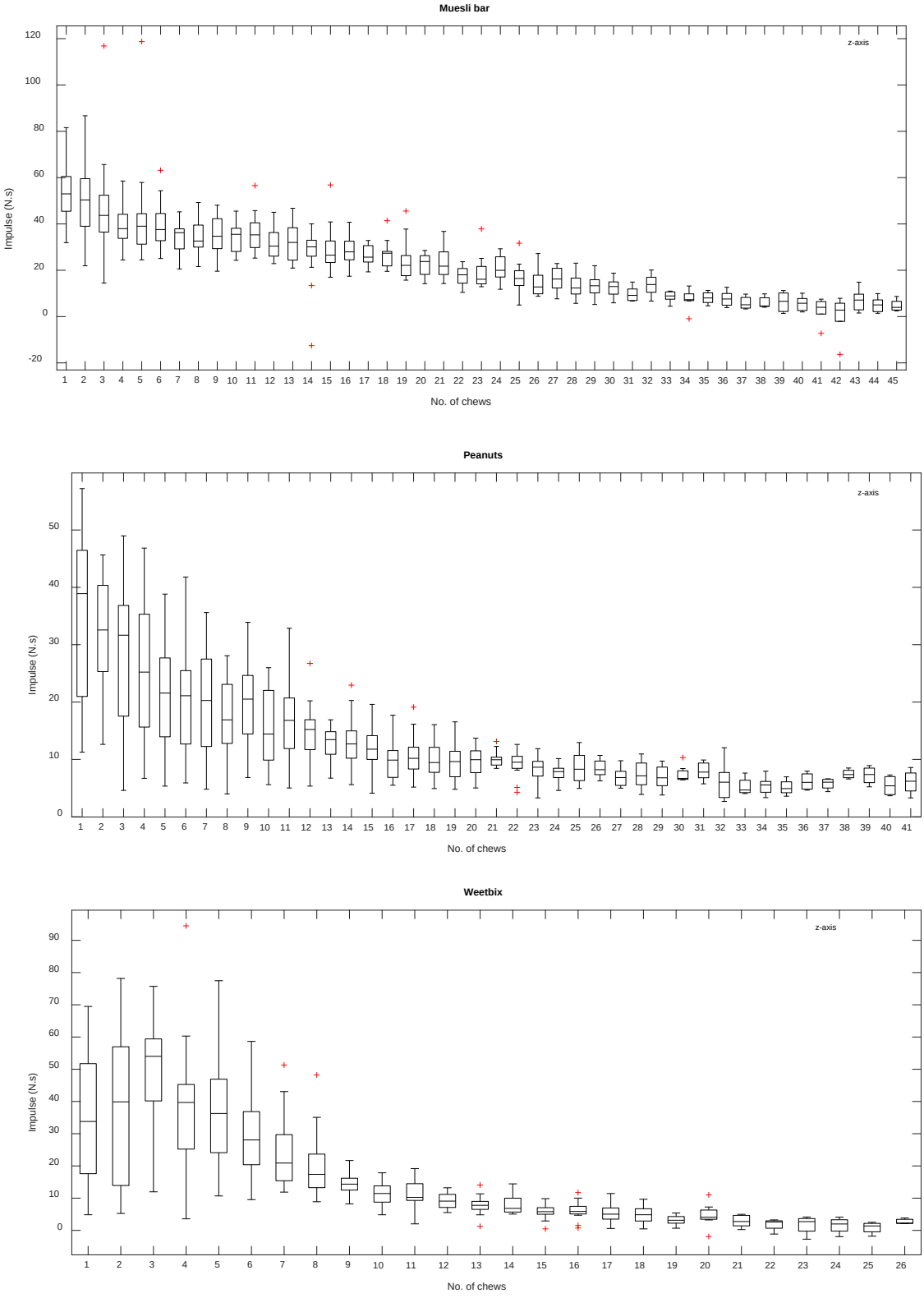


*Figure 7-16: Box plots of the impulse distributions plotted against the number of chews in the three directions (a) x-axis, (b) y-axis, and (c) z-axis. The x, y and z axes are the forces exerted in the sagittal, lateral and vertical directions respectively. The impulse data for all replicates make up the distribution for each chewing cycle. The box represents the 25$^{th}$ percentile, median and 75$^{th}$ percentile of the replicates while the whisker length is 1.5*IQR (inter quartile range) and the red crosses represent the outliers.*

## 7.2.5. Factor Analysis

Factor analysis is based on the assumption that there is high correlation between groups of variables, thus a Pearson correlation analysis was done. Table 7-4 shows the correlation coefficients for all the response measurements from the characterisation tests. For variables that were highly correlated but were measuring similar responses, only one response was selected. For example, only the impulse in the Z-axis of the mastication robot was selected since the impulse in the X and Y axis were linearly related to it. DR/SR ratio was not selected since this variable was calculated from the DR and SR parameters. $MC_{bolus}$ and $SA_{bolus}$ were not selected as these responses were controlled since the amounts of XG solution added were predetermined. Ten variables out of the seventeen were selected for factor analysis and the results are shown in Table 7-5.

Two criterion were used to select the final set of factors for interpretation of the data collected. Based on the scree test criterion, the first four factors qualify as beyond that, the proportion of unique variance in each of the remaining factors would be too high. Although ten factors were generated in the analysis, only the first five factors are shown in *Table 7-5*. As the eigenvalue criterion stipulates that only factors with eigenvalues greater than one are significant, thus only the first three factors were selected. The first factor, F1, is named hardness since the variables with significant loadings describe the force and work measured in the characterisation tests. The second factor, F2, is named swallowability since the deformation and slip resistance are measurements of the swallow properties of a bolus. The third factor, F3, is named homogeneity since energy is high and contrast is small when an image (in this case from the MPP test) has good homogeneity.

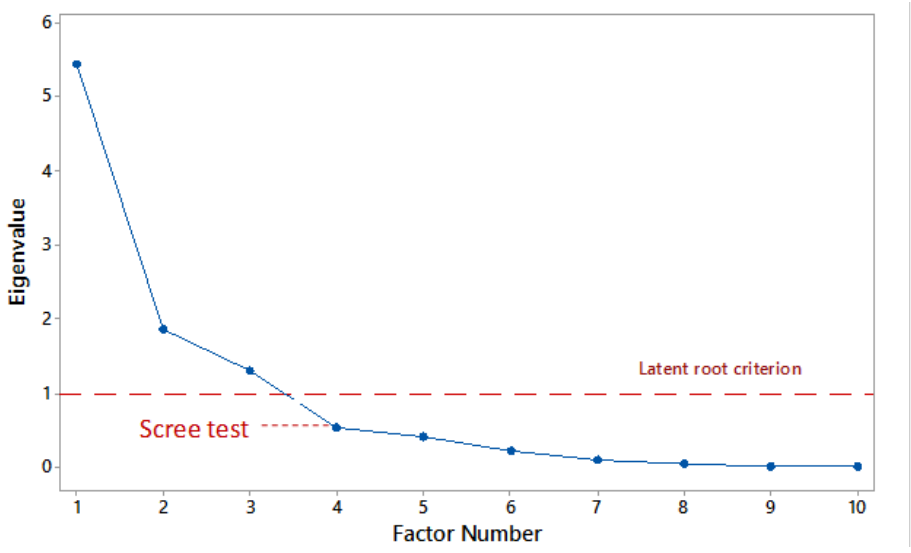


*Figure 7-17: The eigenvalue plot with both the eigenvalue (latent root) criterion and scree test criterion.*

*Table 7-4: Pearson's Correlation coefficients for the variables from the characterization tests.*

| Variable | Impulse (BE) | Hardness (BE) | Cohesiveness (BE) | Adhesiveness (BE) | DR (SET) | SR (SET) | DR/SR Ratio (SET) | $MC_{bolus}$ |
|---|---|---|---|---|---|---|---|---|
| Hardness (BE) | 0.919* | | | | | | | |
| Cohesiveness (BE) | -0.177 | 0.018 | | | | | | |
| Adhesiveness (BE) | 0.113 | 0.008 | 0.080 | | | | | |
| DR (SET) | 0.656* | 0.814* | 0.119 | -0.170 | | | | |
| SR (SET) | 0.543* | 0.744* | 0.123 | -0.301* | 0.959* | | | |
| DR/SR Ratio (SET) | -0.053 | -0.224 | -0.304* | 0.628* | -0.412* | -0.550* | | |
| $MC_{bolus}$ | -0.246 | -0.306* | -0.263* | -0.527* | -0.172 | -0.068 | -0.468* | |
| $SA_{bolus}$ | -0.178 | -0.169 | 0.167 | 0.215 | -0.067 | -0.044 | 0.053 | -0.082 |
| Contrast (MPP) | 0.721* | 0.645* | -0.408* | -0.175 | 0.525* | 0.508* | -0.242 | 0.314* |
| Energy (MPP) | -0.480* | -0.407* | 0.542* | 0.240 | -0.243 | -0.269* | 0.194 | -0.538* |
| Homogeneity (MPP) | -0.570* | -0.477* | 0.528* | 0.219 | -0.319* | -0.325* | 0.208 | -0.503* |
| MF (MPP) | 0.857* | 0.877* | -0.074 | 0.109 | 0.586* | 0.510* | -0.060 | -0.340* |
| X impulse (R) | 0.713* | 0.835* | -0.025 | -0.073 | 0.762* | 0.734* | -0.130 | -0.484* |
| Y impulse (R) | 0.611* | 0.779* | 0.131 | 0.020 | 0.766* | 0.715* | -0.101 | -0.601* |
| Z impulse (R) | 0.778* | 0.866* | -0.005 | 0.088 | 0.710* | 0.621* | -0.009 | -0.543* |
| IQR (MPP) | 0.898* | 0.871* | -0.077 | 0.149 | 0.531* | 0.432* | 0.034 | -0.399* |

| Variables | $SA_{bolus}$ | Contrast (MPP) | Energy (MPP) | Homogeneity (MPP) | MF (MPP) | X impulse (R) | Y impulse (R) | Z impulse (R) |
|---|---|---|---|---|---|---|---|---|
| Contrast (MPP) | -0.194 | | | | | | | |
| Energy (MPP) | 0.286* | -0.823* | | | | | | |
| Homogeneity (MPP) | 0.249* | -0.913* | 0.978* | | | | | |
| MF (MPP) | -0.135 | 0.676* | -0.379* | -0.476* | | | | |
| X impulse (R) | -0.141 | 0.352* | -0.167 | -0.197 | 0.633* | | | |
| Y impulse (R) | -0.088 | 0.185 | 0.045 | 0.009 | 0.586* | 0.953* | | |
| Z impulse (R) | -0.117 | 0.340* | -0.145 | -0.190 | 0.698* | 0.950* | 0.931* | |
| IQR (MPP) | -0.161 | 0.604* | -0.365* | -0.445* | 0.937* | 0.684* | 0.616* | 0.770* |

*Indicates correlations significant at the .05 level.

*Table 7-5: Eigenvalues, proportion of total variance, coefficients and loadings of the first five factors with respect to the measured responses for apple, ham, muesli bar and weetbix boluses.*

| Items | PC axis | | | | |
|---|---|---|---|---|---|
| | F1 | F2 | F3 | F4 | F5 |
| Eigenvalue | 5.453 | 1.864 | 1.311 | 0.534 | 0.418 |
| Proportion | 0.327 | 0.216 | 0.191 | 0.104 | 0.104 |
| Cumulative | 32.7 | 54.3 | 73.4 | 83.8 | 94.2 |

| Variables | Eigen vectors | | | | | | | | | |
|---|---|---|---|---|---|---|---|---|---|---|
| | F1 | | F2 | | F3 | | F4 | | F5 | |
| | Coefficient | Loading | Coefficient | Loading | Coefficient | Loading | Coefficient | Loading | Coefficient | Loading |
| Z impulse | 0.556 | 0.880 | -0.225 | 0.389 | 0.035 | 0.046 | 0.087 | -0.053 | -0.033 | 0.054 |
| Impulse BE | 0.462 | 0.841 | -0.197 | 0.263 | 0.071 | -0.362 | 0.090 | -0.111 | -0.019 | 0.088 |
| Hardness BE | 0.405 | 0.825 | -0.135 | 0.461 | 0.091 | -0.282 | 0.063 | -0.020 | 0.015 | -0.069 |
| Median Force | 0.152 | 0.790 | -0.132 | 0.209 | 0.121 | -0.289 | 0.080 | -0.086 | 0.025 | -0.003 |
| SR/g | -0.338 | 0.338 | 0.803 | 0.897 | 0.077 | -0.155 | -0.155 | 0.191 | 0.135 | -0.085 |
| DR/g | -0.284 | 0.454 | 0.687 | 0.864 | 0.065 | -0.130 | -0.126 | 0.077 | 0.115 | -0.076 |
| Energy | 0.142 | -0.157 | 0.053 | -0.080 | 0.969 | 0.928 | 0.110 | -0.130 | 0.295 | -0.277 |
| Contrast | -0.120 | 0.352 | -0.072 | 0.291 | -0.440 | -0.777 | -0.063 | 0.075 | -0.176 | 0.202 |
| Adhesiveness BE | -0.222 | 0.107 | 0.254 | -0.152 | -0.153 | 0.117 | -1.110 | -0.975 | 0.025 | -0.033 |
| Cohesiveness BE | 0.039 | -0.017 | -0.188 | 0.113 | -0.383 | 0.307 | 0.025 | -0.033 | -1.210 | -0.944 |

MF: median force, SR: slip resistance per gram, DR: deformation resistance per gram. The measurements in which the variables were obtained from is in brackets: MPP- multiple pin penetrometer test, BE-back extrusion test, R-mastication forces from robot, SET- slip extrusion test. Based on a sample size of at least 60, loadings with an absolute value ≥ 0.70 were statistically significant at P=0.05 (Hair et al., 1998).

In Figure 7-18, the average scores for each mastication stage for the four foods are shown with respect to the three factors. Although weetbix and muesli bar had different starting positions for hardness (F1), the boluses had shifted to be in the similar half of the factorial map as the ham and apple boluses as they approached swallow point (Figure 7-18a). As the swallowability (F2) had a higher factor loading on the slip resistance, and weetbix and apple boluses had higher SR than the other foods, thus these two foods had higher scores for F2 at the initial stages of mastication which decreased within 50% of the mastication stage. The F2 score for muesli bar at the initial stages of mastication were lower than expected as SR was low and the variables 'Hardness' and 'z impulse' had negative coefficients which were multiplied to large responses. Ham boluses did not appear to have changed much as the ham was soft and easily deformable as compared to the other foods.

In Figure 7-18b, all boluses had low scores for F3, which described the homogeneity, at the initial stages of mastication. The F3 scores were much higher at swallow point for muesli bar and weetbix boluses as they had maximum energy while apple and ham boluses were more heterogenous. A likely reason is that the gray levels were scaled differently and thus, by the swallow point, the force measured for the muesli bar and weetbix boluses were within the same gray level. Within 30% mastication stage, the weetbix had been completely broken up and thus homogeneity had increased greatly. However, more chews were needed for the addition and mixing of XG solution to further soften the boluses before they approached swallow point. The muesli bar had a rapid decrease in hardness after the initial breakdown of the bar into smaller chunks which was heterogenous in nature. Between 30-40% mastication, individual components had broken up and reformed into a largely cohesive bolus held by the XG solution. This accounted for the huge increase in homogeneity in the muesli bar.

From Figure 7-18a, it is apparent that the factors, hardness (F1) and swallowability (F2) were best in tracking the changes in the bolus properties during the different stages of the mastication. The boluses at the swallow point of the different foods had clustered together which meant that the hardness and swallowability properties became similar as the boluses approached swallow point. Figure 7-19 shows the change in hardness (F1) for the four foods as the stage of mastication progressed. The factor scores tend towards a similar end point for all the foods as the mastication stage progressed, suggesting that hardness is an important factor in determining the swallow point of food.

(a)

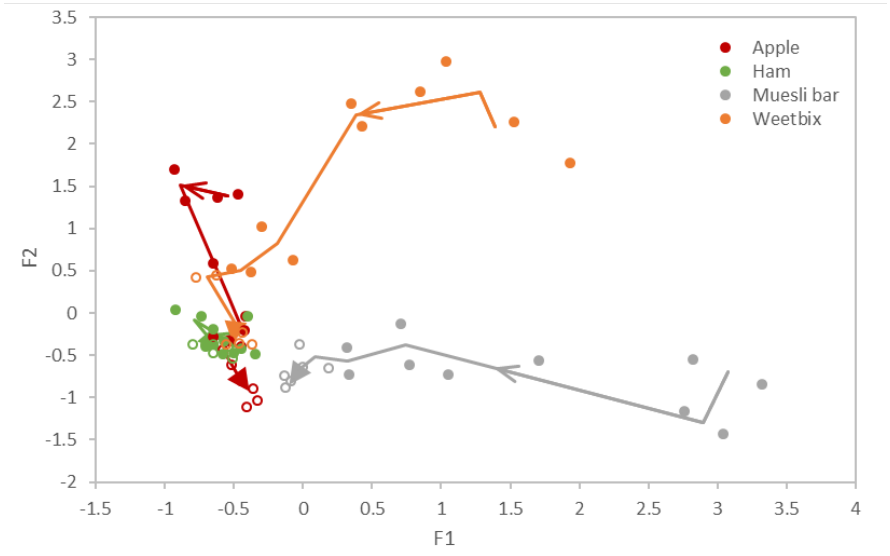


(b)

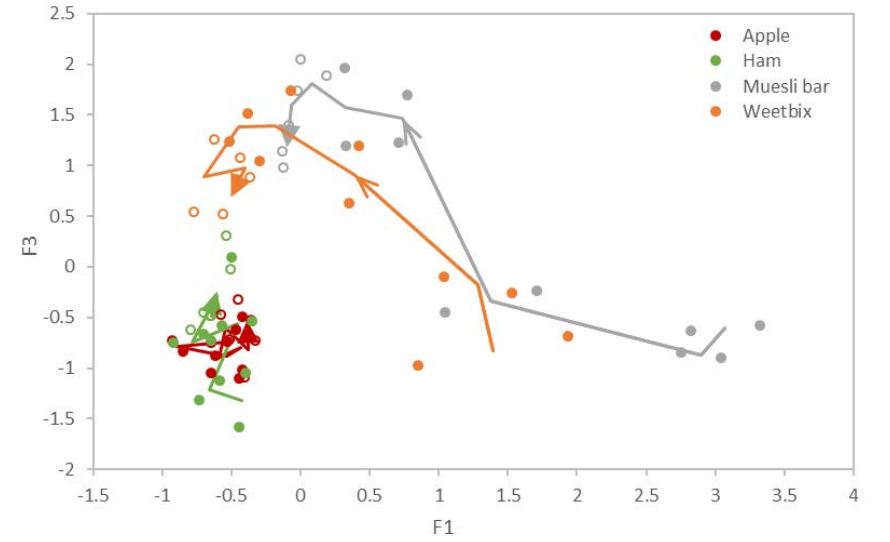


(c)

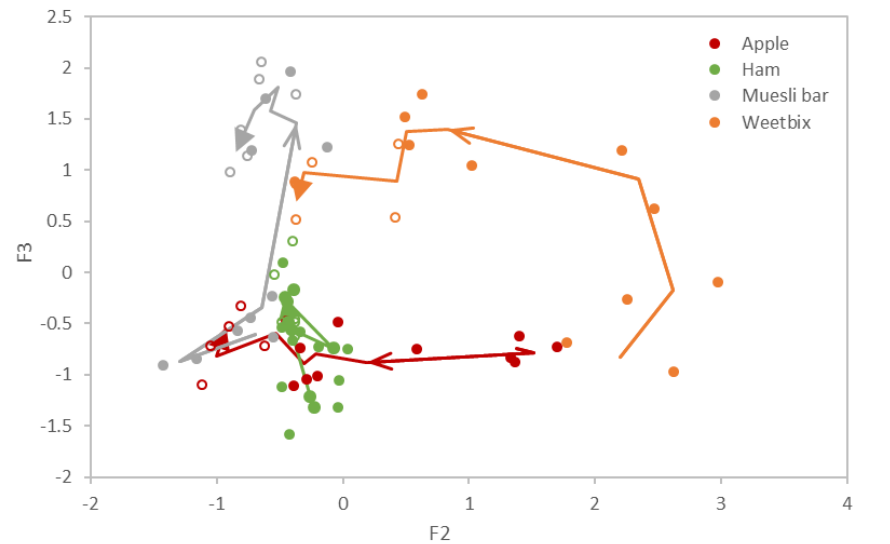


*Figure 7-18: Factorial maps of results collected on duplicate boluses at various stages of the mastication process (filled symbol- 10%, 20%, 30%, 50%, and 75%, hollow symbol- 100%, 125% and 150%). The axis titles F1, F2 and F3 represent hardness, swallowability and homogeneity respectively.*

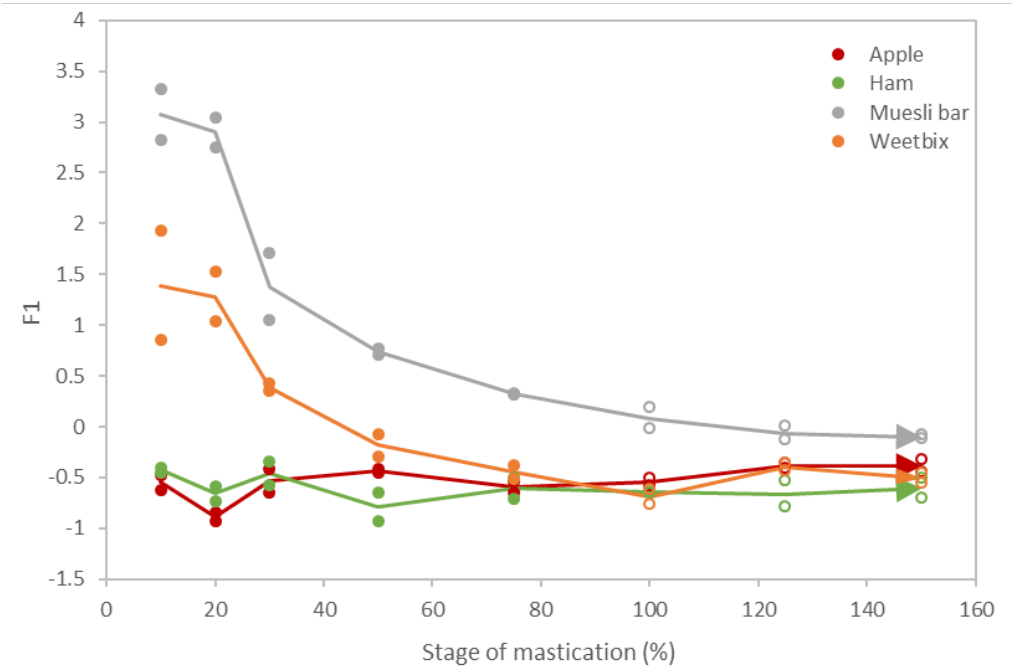


*Figure 7-19: The change in hardness (F1) as the stage of mastication progressed.*

## 7.3. Conclusion

The results of this study show that the mastication robot could be used to replicate a human's chewing trajectories to consistently produce boluses in a controlled trajectory with controlled "simulated saliva" rates throughout the various stages of mastication. In addition, the developed characterisation techniques could be used to track the dynamic changes in the bolus properties for most of the mastication stages from initial chews to the swallow point and beyond that. Through the application of the tests on the different foods, it was discovered that the tensile strength of the SET bags were not high enough for hard foods at 0 and 10% stage of mastication, but the test was otherwise useful in measuring the deformation and slip properties of the boluses at subsequent stages. The disadvantage of the MPPT is that it is not suitable for measuring boluses of hard foods such as nuts as the broken down particles are small enough to be pushed into the surrounding spaces between pins instead of being penetrated by the pins. The results of the back extrusion test for samples without any chews and at early stages of mastication may not be an accurate representation as the test was conducted on the sample at a different orientation from the bolus. Except for ham, the force measurements from the robot decreased with increasing number of chews, and were sensitive enough to detect the small changes in the boluses even after swallow point.

From the SET results, it was shown that the MR could be adjusted to produce boluses with a range of deformation and slip properties, some of which were very similar to the boluses collected from the human subjects. Thus, there is potential for the MR to be used as a tool to produce boluses as an alternative to human subjects, and in a reproducible way. The contour plots of the pressure profiles measured by the MPP gives a good pictorial understanding of the textural changes in the bolus as the mastication progressed. It is thought that as a bolus approaches the swallow point, it becomes more homogenous as the broken down particles gets mixed during bolus formation. The GLCM analysis provides information on the homogeneity, contrast and energy of the bolus based on the pressures measured by the MPP. The 3D forces measured by the force sensor in the MR could be used to explain the differences in breakdown due to forces being exerted on the bolus from different directions which is affected by the chewing trajectory. The factor analysis showed that the properties related to the hardness, swallowability and homogeneity attributes were best at describing the changes in the boluses as they were masticated to swallow point. Energy expended to soften or break down the bolus would result in a decrease in the hardness factor, and this is seen in foods that have high initial hardness properties. For foods that are softer, the swallowability (DR & SR) and homogeneity served to identify the boluses at swallow point better.

# Chapter Eight Conclusions and recommendations for future research

## 8.1. Conclusions

Some of the suggested criterion for a bolus to be ready for swallowing are based on its structure, cohesiveness, and lubrication (Chen, Jianshe & Lolivret, 2011; Loret et al., 2011a; Peyron, Marie-Agnès et al., 2011; Witt & Stokes, 2015; Young et al., 2013; YVEN, CLAUDE et al., 2012). In the safe swallow model proposed by Gray-Stuart (2016), the adhesion, bolus deformability and particle deformation were some of the determinant properties identified for a safe swallow. However, the thresholds for these factors have not been identified. To do so, bolus properties such as the deformability, lubrication need to be quantified. Thus, the aim of this work was to develop novel techniques for the in-vitro study of food breakdown.

The main objectives of this work were:

1. To understand how the MR could be operated to simulate different chewing trajectories possibly employed by humans during mastication and to validate its chewing performance by comparing with human subjects.
2. To develop novel characterisation techniques that may be employed to track the bolus properties throughout different stages of mastication.
3. To develop an experimental methodology that could potentially be used for the in-vitro study of food break down to track the dynamic changes in the bolus properties during mastication and demonstrate its application to different foods.

### 8.1.1. Conclusions for Objective 1

A systematic review of the parameters that could be adjusted in the MR was carried out and these effects on the breakdown rate using peanuts, as a model food, was investigated. Through this preliminary study, it was found that there were indeed differences in breakdown rates between the lateral and vertical trajectories and this could be explained using the breakage and selection functions by Van der Glas et al. (1987). The amount of fragmentation as characterised by the breakage function, *r*, is dependent on the magnitude and direction of forces acting on the food. Higher chewing forces were measured in compressive shear (lateral chewing) as compared to compression (vertical chewing), thus resulting in better breakdown.

Having proved that the MR could be controlled to produce different chewing trajectories and that these trajectories do impact the breakdown rate, the next step was to evaluate if the MR could produce similar breakdown as human subjects since it was built with the goal to be used as an alternative to subjects, to produce boluses in a reproducible way. The MR was validated against human subjects by comparing the chewing efficiency. The validation test was carried out on a non-brittle but fracturable test food, Optosil, and a brittle test food, peanuts. It was found that Optosil was too tough and unsuitable as a test food and the MR was unable to break it down beyond a certain size. Subjects were able to adapt the chewing pattern to break down the Optosil but the MR could not achieve it. Based on the PSD of the peanut boluses, it was concluded that the MR had poorer breakdown capability in comparison to the median human subject. However, this difference in breakdown capability could be mitigated by the reduction of portion size or increased baseline force if the MR was needed to closely replicate a human subject. Since the MR had good reproducibility in bolus preparation and its breakdown capability was comparable to the poorest performing subject, it was concluded that the MR is relevant as a tool to produce boluses for comparative analysis especially for studies investigating the properties of boluses collected from various stages of the mastication process.

### 8.1.2. Conclusions for Objective 2

Although the PSD is one of the factors contributing to bolus formation, it should not be used independently as the determining criterion in triggering a swallow. In addition, the use of PSD is limited to foods that break down into individual particles and not suitable for foods that are pasty or fibrous in nature. Thus, the multiple pin penetrometer (MPP) was developed to characterise the texture by measurement of the spatiotemporal pressure distribution. The MPP was applied to foods of varying homogeneity and hardness, and different data analysis methods were established. The use of an image analysis method, grey level co-occurrence matrix (GLCM), was explored by application to some simple images and the textural features, *contrast*, *energy* and *homogeneity* were used. The method of GLCM analysis to a pressure map of the sample was established and this proved to be an effective method of characterising boluses, by providing statistical textural information about the boluses, in the later chapters.

Other factors related to the rheological properties (such as the lubrication of the bolus through the absorption of saliva) contribute to the triggering of a swallow (Chen, 2012; Peyron et al., 2011). Through a hazard and operability analysis, Gray-Stuart (2016) had identified that bolus deformation and adhesion (slippage of bolus) were two of the determinant properties for safe swallowing. Thus,

the slip extrusion test was developed to measure the deformation and slip properties of boluses. The design and manufacture of the test rig, which was adapted from an extrusion rig (Voisey et al., 1980), and SET bags were designed to mimic geometrical changes a bolus experiences during swallow. The test parameters were established after troubleshooting issues with the noise measurement due to the frictional force between the bag and rollers. The test was evaluated using three model food systems and the results correlated well with the properties of the model foods. It was noted that the SET bag started stretching if the extrusion forces exceeded the tensile strength of the material and thus, this was a limitation especially for the measurement of unchewed solid foods. However, it can be used to investigate the properties of boluses expectorated up to and including the swallow point.

### 8.1.3. Conclusions for objective 3

Having thus developed a series of novel texture characterisation techniques, which enable the tracking of the dynamic changes in the bolus properties across the mastication stage, the next step in this research was to demonstrate the application of these tests to five foods exhibiting different initial properties. This was to show how these techniques could be used in food breakdown studies which includes bolus preparation using the MR, and the developed techniques to characterise these boluses at different stages of mastication. Human subjects were used to establish the bolus characteristics (deformation and slip properties) at various stages of mastication. In addition, the chewing parameters employed by the subjects were determined. To show that the MR could be used to simulate human mastication, this characterisation of boluses was replicated using boluses prepared by the MR. The median subject was selected as an “instrumental” measure that could be compared with the MR. Data on the number of chewing cycles and amount of moisture addition for each food for the median subject were used to establish the parameters for the mastication robot’s set up for the factorial design of experiments. The factors investigated were: (a) chewing trajectory by the MR, (b) the amount of simulated saliva (0.1% XG solution addition) to be added during the chewing cycles in the MR, and (c) baseline force needed for mastication in the MR. The developed models from the factorial study was used to optimize the conditions needed for the MR to achieve boluses with similar deformation and slip properties as the median subject.

The five foods were broken down using the identified parameters, and bolus properties were evaluated at various stages of the mastication process through the application of the slip extrusion test, textural mapping using the multiple pins penetrometer, and the back extrusion test. These novel characterisation techniques could be used to track the dynamic changes in the bolus

properties for most of the mastication stages from initial to the swallow point and beyond that. The deformation and slip properties of the boluses produced by the MR were similar to those collected from human subjects. This showed the MR can be used as a tool to produce boluses as an alternative to human subjects, and in a reproducible way. The factor analysis showed that the properties related to the hardness, swallowability and homogeneity attributes were best at describing the changes in the boluses as they were masticated to swallow point. Thus, as demonstrated through the characterisation of boluses collected at swallow point and establishment of swallow safe thresholds for different foods, there is potential for these factors to be correlated to the sensory perception that triggers a swallow.

In summary, the work done in this research consisted of the implementation of two techniques (the mastication robot and multiple pin penetrometer) that have not been applied in food breakdown characterisation and the development of a new technique (the slip extrusion test). For the first time, a combination of these three different methods was applied to a wide range of foods to characterise the dynamic changes during mastication. In the past, separate techniques were used for different foods such as particle side characterisation for peanuts and warner bratzler for meat etc. Using different measurement methods made it impossible to compare the breakdown characteristics quantitatively between foods. Chapter 7 demonstated that the techniques applied allowed comparison of breakdown characteristics between foods.

## 8.2. Suggestions for future research

The development of these novel techniques allows characterisation of bolus properties to go beyond moisture content and extend to foods that do not form discrete particles (i.e. previously limited to PSD to track breakdown). Rheological measurements have been used to characterise boluses but only at swallow point since measurement is only possible with samples that flow (Loret et al., 2011a).

The 3D force sensor in the MR allows monitoring of the forces changing over time during the mastication process, and it provides a systematic way to break down foods. Improvements could be made to the MR such that it follows the human breakdown better (in terms of force application to the food and trajectory movement) and possibly a tongue system that provides better mixing and automated transport of the bolus to the occlusal surface after each chew cycle. Additionally, there has been much interest in how food structure could impact the disintegration of food and

absorption of nutrients during digestion (Boland et al., 2014). The MR could be used as a tool to produce boluses for studies aimed at relating the food structure at swallow to the subsequent metabolism of the nutrients.

Previously, most of the break down studies were conducted on brittle foods as measuring the particle size distribution seemed to be the only way of quantifying breakdown. However, the MPP can now be used to give a distribution of texture measurement that is somewhat similar to how data is treated for particle size analysis which has been commonly used for brittle foods. For example, the MPP is able to measure textures in pasty and fibrous foods which provide opportunities to study and model meat structure breakdown during mastication. Currently, texture analysis methods such as shearing methods and modified TPA are used, but these methods measure an average force while the MPP measures texture across the plane of the bolus.

Some of the foods at the initial stages of mastication could not be measured using the SET as the SET bag tore during the measurement. Improvements could be made by using a material of higher tensile strength to make the SET bag. The SET measurements could be correlated to perceived sensory properties through the use of dynamic texture perception tests such as qualitative descriptive analysis (QDA), temporal check-all-that-apply (TCATA) and temporal dominance of sensations (TDS) (Devezeaux de Lavergne et al., 2016; Susana & Amparo, 2018). This will provide understanding of the link between the deformation and slip properties of the boluses and the relevant textures perceived by subjects when they approach the swallow point.

In this work, the slip extrusion test to characterise the deformation and slip properties of boluses was successfully developed and applied. However, there is currently still no measure for cohesiveness which has been proposed as one of the key criterion for triggering a swallow in the swallow safe model developed by Gray-Stuart (2016). It has been difficult to find a cohesiveness measurement as the current methods available are not suitable to be applied across a range of foods. Methods to measure cohesiveness or related properties (fluidity) should be developed.

In this work, only boluses at the initial and swallow point were collected from subjects for analysis with the SET. These novel techniques should also be applied to boluses collected from a subject at the various mastication stages, so as to compare the breakdown paths of the food between the MR and human subject. Similarity in both would validate the MR as an alternative tool to simulate

mastication in humans and produce reproducible boluses. The tests should also be applied to characterise bolus property changes during chewing in future human trials.

In addition, the SET should be applied to foods belonging to similar groups, to investigate if their properties change in similar ways, and whether the thresholds for swallow point are similar within a food group. It would also be valuable to define what the swallowing threshold are for a range of different foods. A study on how oral processing behaviour relates with SET results could provide insights on the relationship between bolus properties, risk perception in individuals and the resulting chewing behaviour. For example, does an increase in the level of risk perceived by people influence their eating behaviour resulting in prolonged chewing.

The methodology of using a combination of the techniques developed allows for comparison of the dynamic changes in breakdown properties between foods and this could be extended to study the effects of the chewing behaviour of different population groups on food breakdown. This could be studied by characterising the boluses collected from subjects in different population groups or the MR with adjusted parameters to simulate the chewing behaviour of each population group.

There is still a long way to go to providing understanding of how initial food properties may affect the oral processing behaviour, how oral processing influences the dynamic changes in food properties, and how bolus properties affect perception that a bolus is safe to swallow. The novel techniques established in this work will be useful in future studies that seek to answer some of these questions.

# REFERENCES


Abd-El-Malek, S. (1955). The part played by the tongue in mastication and deglutition. *J Anat, 89*(2), 250-254.

Agrawal, K. R., Lucas, P. W., & Bruce, I. C. (2000). The effects of food fragmentation index on mandibular closing angle in human mastication. *Archives of Oral Biology, 45*(7), 577-584. doi:https://doi.org/10.1016/S0003-9969(00)00019-4

Aguilera, J. M., & Lillford, P. J. E. (2007). *Food materials science: principles and practice*: Springer Science & Business Media.

Al-Battashi, Z., Bronlund, J., & Gupta, G. S. (2015, 11-14 May 2015). *Investigations into force sensor characteristics for food texture measurements.* Paper presented at the 2015 IEEE International Instrumentation and Measurement Technology Conference (I2MTC) Proceedings.

Allen, F. E., J., V. C., Gregory, E., Steve, G., & Caroline, C. (2015). Transforming Structural Breakdown into Sensory Perception of Texture. *Journal of Texture Studies, 46*(3), 152-170. doi:doi:10.1111/jtxs.12105

Anderson, D. J. (1956). Measurement of stress in mastication. I. *J Dent Res, 35*(5), 664-670.

Anderson, K., Throckmorton, G. S., Buschang, P. H., & Hayasaki, H. (2002). The effects of bolus hardness on masticatory kinematics. *J Oral Rehabil, 29*(7), 689-696.

Ash, M. M., & Nelson, S. J. (2003). *Wheeler's Dental Anatomy, Physiology, and Occlusion* (8th ed.). The University of Michigan: W.B. Saunders.

Boehm, M. W., Warren, F. J., Moore, J. E., Baier, S. K., Gidley, M. J., & Stokes, J. R. (2014). Influence of hydration and starch digestion on the transient rheology of an aqueous suspension of comminuted potato snack food. *Food Funct, 5*(11), 2775-2782. doi:10.1039/c4fo00573b

Boland, M., Golding, M., & Singh, H. (2014). *Food Structures, Digestion and Health*: Elsevier Science.

Bourne, M. C. (2002). *Food texture and viscosity : concept and measurement / Malcolm Bourne* (2nd ed.): San Diego, Calif. ; London : Academic.

Brandt, M. A., Skinner, E. Z., & Coleman, J. A. (1963). Texture Profile Method. *Journal of Food Science, 28*(4), 404-409. doi:10.1111/j.1365-2621.1963.tb00218.x

Brenner, T., Hayakawa, F., Ishihara, S., Tanaka, Y., Nakauma, M., Kohyama, K., . . . Nishinari, K. (2014). Linear and Nonlinear Rheology of Mixed Polysaccharide Gels. Pt. II. Extrusion, Compression, Puncture and Extension Tests and Correlation with Sensory Evaluation. *Journal of Texture Studies, 45*(1), 30-46. doi:10.1111/jtxs.12049

Brown, W. E. (1995). Chapter 13 - The use of mastication analysis to examine the dynamics of oral breakdown of food contributing to perceived texture. In A. G. Gaonkar (Ed.), *Characterization of Food* (pp. 309-327). Amsterdam: Elsevier Science B.V.

Brown, W. E., Shearn, M., & MacFie, H. J. H. (1994). Development of a method to investigate differences in chewing behaviour in humans. II. Use of electromyography during chewing to assess chewing behaviour. . *J. Texture Studies*(25), 17-25.

ÇAkir, E., KoÇ, H., Vinyard, C. J., Essick, G., Daubert, C. R., Drake, M., & Foegeding, E. A. (2012). Evaluation Of Texture Changes Due To Compositional Differences Using Oral Processing. *Journal of Texture Studies, 43*(4), 257-267. doi:10.1111/j.1745-4603.2011.00335.x

Chauncey, H. H., Muench, M. E., Kapur, K. K., & Wayler, A. H. (1984). The effect of the loss of teeth on diet and nutrition. *Int Dent J, 34*(2), 98-104.

Chen, J. (2012). Bolus Formation and Swallowing *Food Oral Processing* (pp. 139-156): Wiley-Blackwell.

Chen, J., & Lolivret, L. (2011). The determining role of bolus rheology in triggering a swallowing. *Food Hydrocolloids, 25*(3), 325-332. doi:http://dx.doi.org/10.1016/j.foodhyd.2010.06.010

Cheong, J. N., Foster, K. D., Morgenstern, M. P., Grigor, J. M. V., Bronlund, J. E., Hutchings, S. C., & Hedderley, D. I. (2014). The Application of Temporal Dominance of Sensations (TDS) for Oral

Processing Studies: An Initial Investigation. *Journal of Texture Studies, 45*(6), 409-419. doi:doi:10.1111/jtxs.12091
Cutler, A. N., Morris, E. R., & Taylor, L. J. (1983). Oral Perception Of Viscosity In Fluid Foods And Model Systems. *Journal of Texture Studies, 14*(4), 377-395. doi:10.1111/j.1745-4603.1983.tb00357.x
Dahlberg, B. (1942). The Masticatory Effect. *Acta Med Scand, 139*(Suppl), 1–156.
Darby, R. (2001). *Chemical Engineering Fluid Mechanics, Revised and Expanded*: Taylor & Francis.
Devezeaux de Lavergne, M., Tournier, C., Bertrand, D., Salles, C., van de Velde, F., & Stieger, M. (2016). Dynamic texture perception, oral processing behaviour and bolus properties of emulsion-filled gels with and without contrasting mechanical properties. *Food Hydrocolloids, 52*, 648-660. doi:http://dx.doi.org/10.1016/j.foodhyd.2015.07.022
Devezeaux de Lavergne, M., van de Velde, F., & Stieger, M. (2017). Bolus matters: the influence of food oral breakdown on dynamic texture perception. *Food Funct, 8*(2), 464-480. doi:10.1039/c6fo01005a
Engelen, L., Fontijn-Tekamp, A., & van der Bilt, A. (2005). The influence of product and oral characteristics on swallowing. *Arch Oral Biol, 50*(8), 739-746. doi:10.1016/j.archoralbio.2005.01.004
Filipić, S., & Keros, J. (2002). Dynamic influence of food consistency on the masticatory motion. *Journal of Oral Rehabilitation, 29*(5), 492-496. doi:10.1046/j.1365-2842.2002.00881.x
Fiszman, S., & Tarrega, A. (2018). The dynamics of texture perception of hard solid food: A review of the contribution of the temporal dominance of sensations technique. *J Texture Stud, 49*(2), 202-212. doi:10.1111/jtxs.12273
Flynn, C. S. (2012). *The particle size distribution of solid foods after human mastication.* (Doctor of Philosophy ), Massey University, Auckland, New Zealand. Retrieved from http://mro.massey.ac.nz/xmlui/handle/10179/3906
Flynn, C. S., Foster, K. D., Bronlund, J. E., Lentle, R. G., Jones, J. R., & Morgenstern, M. P. (2011). Identification of multiple compartments present during the mastication of solid food. *Archives of Oral Biology, 56*(4), 345-352. doi:http://dx.doi.org/10.1016/j.archoralbio.2010.10.010
Fontijn-Tekamp, F. A., van der Bilt, A., Abbink, J. H., & Bosman, F. (2004). Swallowing threshold and masticatory performance in dentate adults. *Physiol Behav, 83*(3), 431-436. doi:10.1016/j.physbeh.2004.08.026
Foster, K. D., Woda, A., & Peyron, M. A. (2006). Effect of texture of plastic and elastic model foods on the parameters of mastication. *J Neurophysiol, 95*(6), 3469-3479. doi:10.1152/jn.01003.2005
Frank, F. C., & Lawn, B. R. (1967). Proceedings of the Royal Society of London. Series A, Mathematical and Physical Sciences. *299*(1458), 291-306.
Garcia, J. M., Chambers, E. t., Matta, Z., & Clark, M. (2005). Viscosity measurements of nectar- and honey-thick liquids: product, liquid, and time comparisons. *Dysphagia, 20*(4), 325-335. doi:10.1007/s00455-005-0034-9
Gavião, M. B. D., Engelen, L., & Van Der Bilt, A. (2004). Chewing behavior and salivary secretion. *European Journal of Oral Sciences, 112*(1), 19-24. doi:10.1111/j.0909-8836.2004.00105.x
Gibbs, C. H., Mahan, P. E., Lundeen, H. C., Brehnan, K., Walsh, E. K., Sinkewiz, S. L., & Ginsberg, S. B. (1981). Occlusal forces during chewing—Influences of biting strength and food consistency. *The Journal of Prosthetic Dentistry, 46*(5), 561-567. doi:http://dx.doi.org/10.1016/0022-3913(81)90247-X
Gray-Stuart, E. M. (2016). *Modelling food breakdown and bolus formation during mastication* (Doctor of Philosophy in Bioprocess Engineering), Massey University, Palmerston North, New Zealand
Gray-Stuart, E. M., Jones, J. R., & Bronlund, J. E. (2017). Defining the end-point of mastication: A conceptual model. *Journal of Texture Studies, 48*(5), 345-356. doi:doi:10.1111/jtxs.12253

Gupta, S. (2012). *High Pressure Processing of New Zealand Mussels (Perna canalliicullus).* (Doctor of Philosophy in Chemical and Materials Engineering), The University of Auckland.

Hair, J. F., Tatham, R. L., Anderson, R. E., & Black, W. (1998). *Multivariate Data Analysis (5th Edition)* (5th ed.). New Jersey: Prentice Hall.

Haralick, R. M., Shanmugam, K., & Dinstein, I. (1973). Textural Features for Image Classification. *IEEE Transactions on Systems, Man, and Cybernetics, SMC-3*(6), 610-621. doi:10.1109/TSMC.1973.4309314

Hatch, J. P., Shinkai, R. S. A., Sakai, S., Rugh, J. D., & Paunovich, E. D. (2001). Determinants of masticatory performance in dentate adults. *Archives of Oral Biology, 46*(7), 641-648. doi:http://dx.doi.org/10.1016/S0003-9969(01)00023-1

Hawthornthwaite, D., Ramjan, Y., & Rosenthal, A. (2015). Oral processing of low water content foods – a development to Hutchings and Lillford's breakdown path. *Journal of Texture Studies*, n/a-n/a. doi:10.1111/jtxs.12126

Heath, R. M. (2002). The oral management of food: the bases of oral success and for understanding the sensations that drive us to eat. *Food Quality and Preference, 13*(7–8), 453-461. doi:http://dx.doi.org/10.1016/S0950-3293(02)00106-4

Heath, R. M., & Prinz, J. F. (Eds.). (1999). *Oral processing of foods and the sensory evaluation of texture. In Food Texture: Measurement and Perception.* Gaithersburg, MD: Aspen.

Hiiemae, K., Heath, M. R., Heath, G., Kazazoglu, E., Murray, J., Sapper, D., & Hamblett, K. (1996). Natural bites, food consistency and feeding behaviour in man. *Arch Oral Biol, 41*(2), 175-189.

Hiiemae, M. K., & Palmer, J. B. (1999). Food Transport and Bolus Formation during Complete Feeding Sequences on Foods of Different Initial Consistency. *Dysphagia, 14*(1), 31-42. doi:10.1007/pl00009582

Hutchings, S. C. (2011). *Oral processing of heterogeneous foods* (Doctoral dissertation), Massey University, Palmerston North, New Zealand. Retrieved from http://mro.massey.ac.nz/handle/10179/2653

Hutchings, J. B., & Lillford, P. J. (1988). The Perception Of Food Texture - The Philosophy Of The Breakdown Path. *Journal of Texture Studies, 19*(2), 103-115. doi:10.1111/j.1745-4603.1988.tb00928.x

Hutchings, S. C., Foster, K. D., Bronlund, J. E., Lentle, R. G., Jones, J. R., & Morgenstern, M. P. (2011). Mastication of heterogeneous foods: Peanuts inside two different food matrices. *Food Quality and Preference, 22*(4), 332-339. doi:10.1016/j.foodqual.2010.12.004

Hwang, J., Kim, D.-K., Bae, J. H., Kang, S. H., Seo, K. M., Kim, B. K., & Lee, S. Y. (2012). The Effect of Rheological Properties of Foods on Bolus Characteristics After Mastication. *Annals of Rehabilitation Medicine, 36*(6), 776-784. doi:10.5535/arm.2012.36.6.776

Ishihara, S., Nakauma, M., Funami, T., Odake, S., & Nishinari, K. (2011). Swallowing profiles of food polysaccharide gels in relation to bolus rheology. *Food Hydrocolloids, 25*(5), 1016-1024. doi:http://dx.doi.org/10.1016/j.foodhyd.2010.09.022

Ishijima, T., Koshino, H., Hirai, T., & Takasaki, H. (2004). The relationship between salivary secretion rate and masticatory efficiency. *J Oral Rehabil, 31*(1), 3-6.

Jalabert-Malbos, M.-L., Mishellany-Dutour, A., Woda, A., & Peyron, M.-A. (2007). Particle size distribution in the food bolus after mastication of natural foods. *Food Quality and Preference, 18*(5), 803-812. doi:http://dx.doi.org/10.1016/j.foodqual.2007.01.010

James, B., Young, A., Smith, B., Kim, E., Wilson, A., & Morgenstern, M. P. (2011). Texture changes in bolus to the “point of swallow” - fracture toughness and back extrusion to test start and end points. *Procedia Food Science, 1*(0), 632-639. doi:http://dx.doi.org/10.1016/j.profoo.2011.09.095

Jeltema, M., Beckley, J., & Vahalik, J. (2015). Model for understanding consumer textural food choice. *Food Science & Nutrition, 3*(3), 202-212. doi:10.1002/fsn3.205

Jemt, T., & HedegÅRd, B. (1982). Reproducibility of chewing rhythm and of mandibular displacements during chewing. *J Oral Rehabil, 9*(6), 531-537. doi:10.1111/j.1365-2842.1982.tb01043.x

Jemt, T., Karlsson, S., & Hedega˚rd, B. r. (1979). Mandibular movements of young adults recorded by intraorally placed light-emitting diodes. *The Journal of Prosthetic Dentistry, 42*(6), 669-673. doi:https://doi.org/10.1016/0022-3913(79)90199-9

Kim, E. H.-J., Morgenstern, M. P., Bronlund, J. E., Foster, K. D., & Le Got, A. (2011). *Food breakdown during human mastication – Quantitative characterization.* Paper presented at the 11th International Congress on Engineering and Food, Athens, Greece.

Koç, H., Çakir, E., Vinyard, C. J., Essick, G., Daubert, C. R., Drake, M. A., . . . Foegeding, E. A. (2014). Adaptation of Oral Processing to the Fracture Properties of Soft Solids. *Journal of Texture Studies, 45*(1), 47-61. doi:10.1111/jtxs.12051

Kohyama, K., Hatakeyama, E., Sasaki, T., Azuma, T., & Karita, K. (2004). Effect of sample thickness on bite force studied with a multiple-point sheet sensor. *J Oral Rehabil, 31*(4), 327-334. doi:10.1046/j.1365-2842.2003.01248.x

Kohyama, K., Hatakeyama, E., Sasaki, T., Dan, H., Azuma, T., & Karita, K. (2004). Effects of sample hardness on human chewing force: a model study using silicone rubber. *Archives of Oral Biology, 49*(10), 805-816. doi:http://dx.doi.org/10.1016/j.archoralbio.2004.04.006

Koolstra, J. H., & van Eijden, T. M. G. J. (1999). Three-dimensional dynamical capabilities of the human masticatory muscles. *Journal of Biomechanics, 32*(2), 145-152. doi:http://dx.doi.org/10.1016/S0021-9290(98)00160-2

Lassauzay, C., Peyron, M.-A., Albuisson, E., Dransfield, E., & Woda, A. (2000). Variability of the masticatory process during chewing of elastic model foods. *European Journal of Oral Sciences, 108*(6), 484-492. doi:10.1034/j.1600-0722.2000.00866.x

Le Révérend, B., Saucy, F., Moser, M., & Loret, C. (2016). Adaptation of mastication mechanics and eating behaviour to small differences in food texture. *Physiol Behav, 165*, 136-145. doi:http://dx.doi.org/10.1016/j.physbeh.2016.07.010

Lenfant, F., Loret, C., Pineau, N., Hartmann, C., & Martin, N. (2009). Perception of oral food breakdown. The concept of sensory trajectory. *Appetite, 52*(3), 659-667. doi:https://doi.org/10.1016/j.appet.2009.03.003

Lewis, D. (2006). *A robotic chewing device for food evaluation : a thesis presented in partial fulfilment of the requirements.* (degree of Master of Engineering), Massey University, Palmerston North.

Liedberg, B., & Owall, B. (1991). Masticatory ability in experimentally induced xerostomia. *Dysphagia*(6), 211-213.

Lillford, P. J. (2011). The Importance Of Food Microstructure In Fracture Physics And Texture Perception. *Journal of Texture Studies, 42*(2), 130-136. doi:10.1111/j.1745-4603.2011.00293.x

Loret, C., Walter, M., Pineau, N., Peyron, M. A., Hartmann, C., & Martin, N. (2011). Physical and related sensory properties of a swallowable bolus. *Physiol Behav, 104*(5), 855-864. doi:http://dx.doi.org/10.1016/j.physbeh.2011.05.014

Lucas, P. W. (2004a). The Basic Structure of the Mammalian Mouth *Dental Functional Morphology: How Teeth Work* (pp. 87-132). United Kingdom: Cambridge University Press.

Lucas, P. W. (2004b). How the Mouth Operates *Dental Functional Morphology: How Teeth Work* (pp. 66-67). United Kingdom: Cambridge University Press.

Lucas, P. W. (2004c). Tooth Shape *Dental Functional Morphology: How Teeth Work* (pp. 87-132). United Kingdom: Cambridge University Press.

Lucas, P. W., & Luke, D. A. (1983). Methods for analysing the breakdown of food in human mastication. *Arch Oral Biol, 28*(9), 813-819.

Lucas, P. W., Ow, R. K., Ritchie, G. M., Chew, C. L., & Keng, S. B. (1986). Relationship between jaw movement and food breakdown in human mastication. *J Dent Res, 65*(3), 400-404. doi:10.1177/00220345860650030501

Lucas, P. W., Prinz, J. F., Agrawal, K. R., & Bruce, I. C. (2002). Food physics and oral physiology. *Food Quality and Preference, 13*(4), 203-213. doi:https://doi.org/10.1016/S0950-3293(00)00036-7

Mandel, I. D. (1987). The functions of saliva. *J Dent Res, 66 Spec No*, 623-627.

Mioche, L., Bourdiol, P., Martin, J. F., & Noel, Y. (1999). Variations in human masseter and temporalis muscle activity related to food texture during free and side-imposed mastication. *Arch Oral Biol, 44*(12), 1005-1012.

Mioche, L., Bourdiol, P., & Monier, S. (2003). Chewing behaviour and bolus formation during mastication of meat with different textures. *Arch Oral Biol, 48*(3), 193-200.

Mioche, L., Hiiemae, K. M., & Palmer, J. B. (2002). A postero-anterior videofluorographic study of the intra-oral management of food in man. *Arch Oral Biol, 47*(4), 267-280.

Mishellany-Dutour, A., Peyron, M.-A., Croze, J., François, O., Hartmann, C., Alric, M., & Woda, A. (2011). Comparison of food boluses prepared in vivo and by the AM2 mastication simulator. *Food Quality and Preference, 22*(4), 326-331. doi:http://dx.doi.org/10.1016/j.foodqual.2010.12.003

Mishellany, A., Woda, A., Labas, R., & Peyron, M. A. (2006). The challenge of mastication: preparing a bolus suitable for deglutition. *Dysphagia, 21*(2), 87-94. doi:10.1007/s00455-006-9014-y

Mosca, A. C., & Chen, J. (2017). Food-saliva interactions: Mechanisms and implications. *Trends in Food Science & Technology, 66*, 125-134. doi:https://doi.org/10.1016/j.tifs.2017.06.005

Nakauma, M., Ishihara, S., Funami, T., & Nishinari, K. (2011). Swallowing profiles of food polysaccharide solutions with different flow behaviors. *Food Hydrocolloids, 25*(5), 1165-1173. doi:http://dx.doi.org/10.1016/j.foodhyd.2010.11.003

Ogawa, T., Ogawa, M., & Koyano, K. (2001). Different responses of masticatory movements after alteration of occlusal guidance related to individual movement pattern. *J Oral Rehabil, 28*(9), 830-841.

Okada, A., Honma, M., Nomura, S., & Yamada, Y. (2007). Oral behavior from food intake until terminal swallow. *Physiol Behav, 90*(1), 172-179. doi:http://dx.doi.org/10.1016/j.physbeh.2006.09.032

Olthoff, L. W., Van Der Bilt, A., De Boer, A., & Bosman, F. (1986). Comparison Of Force-Deformation Characteristics Of Artificial And Several Natural Foods For Chewing Experiments. *Journal of Texture Studies, 17*(3), 275-289. doi:10.1111/j.1745-4603.1986.tb00553.x

Olthoff, L. W., Vanderbilt, A., Bosman, F., & Kleizen, H. H. (1984). Distribution Of Particle Sizes In Food Comminuted By Human Mastication. *Archives of Oral Biology, 29*(11), 899-903. doi:10.1016/0003-9969(84)90089-x

Pangborn, R. M., & Lundgren, B. (1977). Salivary secretion in response to mastication of crisp bread. *J Texture Stud*(8), 463-472.

Panouillé, M., Saint-Eve, A., Déléris, I., Le Bleis, F., & Souchon, I. (2014). Oral processing and bolus properties drive the dynamics of salty and texture perceptions of bread. *Food Research International, 62*(0), 238-246. doi:http://dx.doi.org/10.1016/j.foodres.2014.02.031

Panouillé, M., Saint-Eve, A., & Souchon, I. (2016). Instrumental methods for bolus characterization during oral processing to understand food perceptions. *Current Opinion in Food Science, 9*, 42-49. doi:http://dx.doi.org/10.1016/j.cofs.2016.05.002

Pereira, L. J., Duarte Gaviao, M. B., & Van Der Bilt, A. (2006). Influence of oral characteristics and food products on masticatory function. *Acta Odontol Scand, 64*(4), 193-201. doi:10.1080/00016350600703459

Peyron, M.-A., Gierczynski, I., Hartmann, C., Loret, C., Dardevet, D., Martin, N., & Woda, A. (2011). Role of Physical Bolus Properties as Sensory Inputs in the Trigger of Swallowing. *PLoS ONE, 6*(6), e21167. doi:10.1371/journal.pone.0021167

Peyron, M. A., Lassauzay, C., & Woda, A. (2002). Effects of increased hardness on jaw movement and muscle activity during chewing of visco-elastic model foods. *Exp Brain Res, 142*(1), 41-51. doi:10.1007/s00221-001-0916-5

Peyron, M. A., Mishellany, A., & Woda, A. (2004). Particle size distribution of food boluses after mastication of six natural foods. *J Dent Res, 83*(7), 578-582. doi:10.1177/154405910408300713

Pineau, N., Cordelle, S., & Schlich, P. (2003, July 20–24). *Temporal Dominance of Sensations: A new technique to record several sensory attributes simultaneously over time.* Paper presented at the 5th Pangborn symposium.

Prinz, J., F., & Lucas, P. W. (1997). An Optimization Model for Mastication and Swallowing in Mammals. *Proceedings: Biological Sciences, 264*(1389), 1715-1721. doi:10.2307/51106

Pröschel, P., & Hofmann, M. (1988). Frontal chewing patterns of the incisor point and their dependence on resistance of food and type of occlusion. *The Journal of Prosthetic Dentistry, 59*(5), 617-624. doi:https://doi.org/10.1016/0022-3913(88)90082-0

Rodrigues, S. A., Young, A. K., James, B. J., & Morgenstern, M. P. (2014). Structural Changes Within a Biscuit Bolus During Mastication. *Journal of Texture Studies, 45*(2), 89-96. doi:10.1111/jtxs.12058

Rosenthal, A. J., & Share, C. (2014). Temporal Dominance of Sensations of peanuts and peanut products in relation to Hutchings and Lillford's "breakdown path". *Food Quality and Preference, 32*, 311-316. doi:https://doi.org/10.1016/j.foodqual.2013.09.004

Saint-Eve, A., Panouillé, M., Capitaine, C., Déléris, I., & Souchon, I. (2015). Dynamic aspects of texture perception during cheese consumption and relationship with bolus properties. *Food Hydrocolloids, 46*, 144-152. doi:https://doi.org/10.1016/j.foodhyd.2014.12.015

Shiozawa, K., & Kohyama, K. (2011). Effects of Addition of Water on Masticatory Behavior and the Mechanical Properties of the Food Bolus. *Journal of Oral Biosciences, 53*(2), 148-157. doi:http://dx.doi.org/10.1016/S1349-0079(11)80018-6

Sierpinska, T., Golebiewska, M., & Lapuc, M. (2008). The effect of mastication on occlusal parameters in healthy volunteers. *Adv Med Sci, 53*(2), 316-320. doi:10.2478/v10039-008-0049-1

Slagter, A. P., van der Glas, H. W., Bosman, F., & Olthoff, L. W. (1992). Force-deformation properties of artificial and natural foods for testing chewing efficiency. *The Journal of Prosthetic Dentistry, 68*(5), 790-799. doi:http://dx.doi.org/10.1016/0022-3913(92)90204-N

Sun, C. (2012). *Modelling and compliance control of a linkage chewing robot and its application in food evaluation* (Doctoral dissertation), Massey University, Albany, New Zealand. Retrieved from http://mro.massey.ac.nz/handle/10179/3966

Sun, C., Xu, W. L., Bronlund, J. E., & Morgenstern, M. P. (2014). Dynamics and Compliance Control of a Linkage Robot for Food Chewing. *IEEE Transactions on Industrial Electronics, 61*, 377-386.

Szczesniak, A. S. (1963). Classification of Textural Characteristics. *Journal of Food Science, 28*(4), 385-389. doi:10.1111/j.1365-2621.1963.tb00215.x

Szczesniak, A. S. (1971). Consumer Awareness Of Texture And Of Other Food Attributes, II. *Journal of Texture Studies, 2*(2), 196-206. doi:10.1111/j.1745-4603.1971.tb00581.x

Szczesniak, A. S., Brandt, M. A., & Friedman, H. H. (1963). Development of Standard Rating Scales for Mechanical Parameters of Texture and Correlation Between the Objective and the Sensory Methods of Texture Evaluation. *Journal of Food Science, 28*(4), 397-403. doi:10.1111/j.1365-2621.1963.tb00217.x

Szczesniak, A. S., & Kahn, E. L. (1971). Consumer Awareness Of And Attitudes To Food Texture. *Journal of Texture Studies, 2*(3), 280-295. doi:10.1111/j.1745-4603.1971.tb01005.x

Takahashi, T., Hayakawa, F., Kumagai, M., Akiyama, Y., & Kohyama, K. (2009). Relations among mechanical properties, human bite parameters, and ease of chewing of solid foods with various textures. *Journal of Food Engineering, 95*(3), 400-409. doi:http://dx.doi.org/10.1016/j.jfoodeng.2009.05.023

Texture Technologies.Abd-El-Malek, S. (1955). The part played by the tongue in mastication and deglutition. *J Anat, 89*(2), 250-254.
Aguilera, J. M., & Lillford, P. J. E. (2007). *Food materials science: principles and practice*: Springer Science & Business Media.
Al-Battashi, Z., Bronlund, J., & Gupta, G. S. (2015, 11-14 May 2015). *Investigations into force sensor characteristics for food texture measurements.* Paper presented at the 2015 IEEE International Instrumentation and Measurement Technology Conference (I2MTC) Proceedings.
Allen, F. E., J., V. C., Gregory, E., et al. (2015). Transforming Structural Breakdown into Sensory Perception of Texture. *Journal of Texture Studies, 46*(3), 152-170. doi: doi:10.1111/jtxs.12105
Anderson, D. J. (1956). Measurement of stress in mastication. I. *J Dent Res, 35*(5), 664-670.
Anderson, K., Throckmorton, G. S., Buschang, P. H., et al. (2002). The effects of bolus hardness on masticatory kinematics. *J Oral Rehabil, 29*(7), 689-696.
Ares, G., Jaeger, S. R., Antúnez, L., et al. (2015). Comparison of TCATA and TDS for dynamic sensory characterization of food products. *Food Research International, 78*, 148-158. doi: https://doi.org/10.1016/j.foodres.2015.10.023
Ash, M. M., & Nelson, S. J. (2003). *Wheeler's Dental Anatomy, Physiology, and Occlusion* (8th ed.). The University of Michigan: W.B. Saunders.
Boehm, M. W., Warren, F. J., Moore, J. E., et al. (2014). Influence of hydration and starch digestion on the transient rheology of an aqueous suspension of comminuted potato snack food. *Food Funct, 5*(11), 2775-2782. doi: 10.1039/c4fo00573b
Bourne, M. (2002). *Food Texture and Viscosity: Concept and Measurement*: Elsevier Science.
Bourne, M. C. (2002). *Food texture and viscosity : concept and measurement / Malcolm Bourne* (2nd ed.): San Diego, Calif. ; London : Academic.
Brandt, M. A., Skinner, E. Z., & Coleman, J. A. (1963). Texture Profile Method. *Journal of Food Science, 28*(4), 404-409. doi: 10.1111/j.1365-2621.1963.tb00218.x
Brenner, T., Hayakawa, F., Ishihara, S., et al. (2014). Linear and Nonlinear Rheology of Mixed Polysaccharide Gels. Pt. II. Extrusion, Compression, Puncture and Extension Tests and Correlation with Sensory Evaluation. *Journal of Texture Studies, 45*(1), 30-46. doi: 10.1111/jtxs.12049
Brown, W. E. (1995). Chapter 13 - The use of mastication analysis to examine the dynamics of oral breakdown of food contributing to perceived texture. In A. G. Gaonkar (Ed.), *Characterization of Food* (pp. 309-327). Amsterdam: Elsevier Science B.V.
Brown, W. E., Shearn, M., & MacFie, H. J. H. (1994). Development of a method to investigate differences in chewing behaviour in humans. II. Use of electromyography during chewing to assess chewing behaviour. . *J. Texture Studies*(25), 17-25.
ÇAkir, E., KoÇ, H., Vinyard, C. J., et al. (2012). EVALUATION OF TEXTURE CHANGES DUE TO COMPOSITIONAL DIFFERENCES USING ORAL PROCESSING. *Journal of Texture Studies, 43*(4), 257-267. doi: 10.1111/j.1745-4603.2011.00335.x
Chauncey, H. H., Muench, M. E., Kapur, K. K., et al. (1984). The effect of the loss of teeth on diet and nutrition. *Int Dent J, 34*(2), 98-104.
Chen, J. (2012). Bolus Formation and Swallowing *Food Oral Processing* (pp. 139-156): Wiley-Blackwell.
Chen, J., Khandelwal, N., Liu, Z., et al. (2013). Influences of food hardness on the particle size distribution of food boluses. *Arch Oral Biol, 58*(3), 293-298. doi: 10.1016/j.archoralbio.2012.10.014
Chen, J., & Lolivret, L. (2011). The determining role of bolus rheology in triggering a swallowing. *Food Hydrocolloids, 25*(3), 325-332. doi: http://dx.doi.org/10.1016/j.foodhyd.2010.06.010

Cheong, J. N., Foster, K. D., Morgenstern, M. P., et al. (2014). The Application of Temporal Dominance of Sensations (TDS) for Oral Processing Studies: An Initial Investigation. *Journal of Texture Studies, 45*(6), 409-419. doi: doi:10.1111/jtxs.12091

Cutler, A. N., Morris, E. R., & Taylor, L. J. (1983). ORAL PERCEPTION OF VISCOSITY IN FLUID FOODS AND MODEL SYSTEMS. *Journal of Texture Studies, 14*(4), 377-395. doi: 10.1111/j.1745-4603.1983.tb00357.x

Dahlberg, B. (1942). The Masticatory Effect. *Acta Med Scand, 139*(Suppl), 1–156.

Darby, R. (2001). *Chemical Engineering Fluid Mechanics, Revised and Expanded*: Taylor & Francis.

Devezeaux de Lavergne, M., Tournier, C., Bertrand, D., et al. (2016). Dynamic texture perception, oral processing behaviour and bolus properties of emulsion-filled gels with and without contrasting mechanical properties. *Food Hydrocolloids, 52*, 648-660. doi: http://dx.doi.org/10.1016/j.foodhyd.2015.07.022

Devezeaux de Lavergne, M., van de Velde, F., & Stieger, M. (2017). Bolus matters: the influence of food oral breakdown on dynamic texture perception. *Food Funct, 8*(2), 464-480. doi: 10.1039/c6fo01005a

Devezeaux de Lavergne, M. S. M., Delft, J. M. v., Velde, F. v. d., et al. (2015). Dynamic texture perception and oral processing of semi-solid food gels: Part 1: Comparison between QDA, progressive profiling and TDS. *Food Hydrocolloids, 43*, 207-217.

Engelen, L., Fontijn-Tekamp, A., & van der Bilt, A. (2005). The influence of product and oral characteristics on swallowing. *Arch Oral Biol, 50*(8), 739-746. doi: 10.1016/j.archoralbio.2005.01.004

Filipić, S., & Keros, J. (2002). Dynamic influence of food consistency on the masticatory motion. *Journal of Oral Rehabilitation, 29*(5), 492-496. doi: 10.1046/j.1365-2842.2002.00881.x

Fiszman, S., & Tarrega, A. (2018). The dynamics of texture perception of hard solid food: A review of the contribution of the temporal dominance of sensations technique. *J Texture Stud, 49*(2), 202-212. doi: 10.1111/jtxs.12273

Flynn, C. S. (2012). *The particle size distribution of solid foods after human mastication.* (Doctor of Philosophy ), Massey University, Auckland, New Zealand. Retrieved from http://mro.massey.ac.nz/xmlui/handle/10179/3906

Flynn, C. S., Foster, K. D., Bronlund, J. E., et al. (2011). Identification of multiple compartments present during the mastication of solid food. *Archives of Oral Biology, 56*(4), 345-352. doi: http://dx.doi.org/10.1016/j.archoralbio.2010.10.010

Fontijn-Tekamp, F. A., van der Bilt, A., Abbink, J. H., et al. (2004). Swallowing threshold and masticatory performance in dentate adults. *Physiol Behav, 83*(3), 431-436. doi: 10.1016/j.physbeh.2004.08.026

Foster, K. D., Woda, A., & Peyron, M. A. (2006). Effect of texture of plastic and elastic model foods on the parameters of mastication. *J Neurophysiol, 95*(6), 3469-3479. doi: 10.1152/jn.01003.2005

Frank, F. C., & Lawn, B. R. (1967). Proceedings of the Royal Society of London. Series A, Mathematical and Physical Sciences. *299*(1458), 291-306.

Gao, J., Wong, J. X., Lim, J. C.-S., et al. (2015). Influence of bread structure on human oral processing. *Journal of Food Engineering, 167*, 147-155. doi: https://doi.org/10.1016/j.jfoodeng.2015.07.022

Garcia, J. M., Chambers, E. t., Matta, Z., et al. (2005). Viscosity measurements of nectar- and honey-thick liquids: product, liquid, and time comparisons. *Dysphagia, 20*(4), 325-335. doi: 10.1007/s00455-005-0034-9

Gavião, M. B. D., Engelen, L., & Van Der Bilt, A. (2004). Chewing behavior and salivary secretion. *European Journal of Oral Sciences, 112*(1), 19-24. doi: 10.1111/j.0909-8836.2004.00105.x

Gibbs, C. H., Mahan, P. E., Lundeen, H. C., et al. (1981). Occlusal forces during chewing—Influences of biting strength and food consistency. *The Journal of Prosthetic Dentistry, 46*(5), 561-567. doi: http://dx.doi.org/10.1016/0022-3913(81)90247-X

Gray-Stuart, E. M. (2016). *Modelling food breakdown and bolus formation during mastication* (Doctor of Philosophy in Bioprocess Engineering), Massey University, Palmerston North, New Zealand

Gupta, S. (2012). *High Pressure Processing of New Zealand Mussels (Perna canalliicullus).* (Doctor of Philosophy in Chemical and Materials Engineering), The University of Auckland.

Hair, J. F., Tatham, R. L., Anderson, R. E., et al. (1998). *Multivariate Data Analysis (5th Edition)* (5th ed.). New Jersey: Prentice Hall.

Haralick, R. M., Shanmugam, K., & Dinstein, I. (1973). Textural Features for Image Classification. *IEEE Transactions on Systems, Man, and Cybernetics, SMC-3*(6), 610-621. doi: 10.1109/TSMC.1973.4309314

Hatch, J. P., Shinkai, R. S. A., Sakai, S., et al. (2001). Determinants of masticatory performance in dentate adults. *Archives of Oral Biology, 46*(7), 641-648. doi: http://dx.doi.org/10.1016/S0003-9969(01)00023-1

Heath, R. M. (2002). The oral management of food: the bases of oral success and for understanding the sensations that drive us to eat. *Food Quality and Preference, 13*(7–8), 453-461. doi: http://dx.doi.org/10.1016/S0950-3293(02)00106-4

Heath, R. M., & Prinz, J. F. (Eds.). (1999). *Oral processing of foods and the sensory evaluation of texture. In Food Texture: Measurement and Perception.* Gaithersburg, MD: Aspen.

Hiiemae, K., Heath, M. R., Heath, G., et al. (1996). Natural bites, food consistency and feeding behaviour in man. *Arch Oral Biol, 41*(2), 175-189.

Hiiemae, M. K., & Palmer, J. B. (1999). Food Transport and Bolus Formation during Complete Feeding Sequences on Foods of Different Initial Consistency. *Dysphagia, 14*(1), 31-42. doi: 10.1007/pl00009582

Hutchings, J. B., & Lillford, P. J. (1988). THE PERCEPTION OF FOOD TEXTURE - THE PHILOSOPHY OF THE BREAKDOWN PATH. *Journal of Texture Studies, 19*(2), 103-115. doi: 10.1111/j.1745-4603.1988.tb00928.x

Hutchings, S. C. (2011). *Oral processing of heterogeneous foods* (Doctoral dissertation), Massey University, Palmerston North, New Zealand. Retrieved from http://mro.massey.ac.nz/handle/10179/2653

Hutchings, S. C., Foster, K. D., Bronlund, J. E., et al. (2011). Mastication of heterogeneous foods: Peanuts inside two different food matrices. *Food Quality and Preference, 22*(4), 332-339. doi: 10.1016/j.foodqual.2010.12.004

Hutchings, S. C., Foster, K. D., Bronlund, J. E., et al. (2012). Particle breakdown dynamics of heterogeneous foods during mastication: Peanuts embedded inside different food matrices. *Journal of Food Engineering, 109*(4), 736-744. doi: https://doi.org/10.1016/j.jfoodeng.2011.11.011

Hwang, J., Kim, D.-K., Bae, J. H., et al. (2012). The Effect of Rheological Properties of Foods on Bolus Characteristics After Mastication. *Annals of Rehabilitation Medicine, 36*(6), 776-784. doi: 10.5535/arm.2012.36.6.776

Ishihara, S., Nakauma, M., Funami, T., et al. (2011). Swallowing profiles of food polysaccharide gels in relation to bolus rheology. *Food Hydrocolloids, 25*(5), 1016-1024. doi: http://dx.doi.org/10.1016/j.foodhyd.2010.09.022

Ishijima, T., Koshino, H., Hirai, T., et al. (2004). The relationship between salivary secretion rate and masticatory efficiency. *J Oral Rehabil, 31*(1), 3-6.

Jalabert-Malbos, M.-L., Mishellany-Dutour, A., Woda, A., et al. (2007). Particle size distribution in the food bolus after mastication of natural foods. *Food Quality and Preference, 18*(5), 803-812. doi: https://doi.org/10.1016/j.foodqual.2007.01.010

James, B., Young, A., Smith, B., et al. (2011a). Texture changes in bolus to the "point of swallow" - Fracture toughness and back extrusion to test start and end points. *Procedia Food Science, 1*, 632–639. doi: 10.1016/j.profoo.2011.09.095

James, B., Young, A., Smith, B., et al. (2011b). Texture changes in bolus to the “point of swallow” - fracture toughness and back extrusion to test start and end points. *Procedia Food Science, 1*(0), 632-639. doi: http://dx.doi.org/10.1016/j.profoo.2011.09.095
Jeltema, M., Beckley, J., & Vahalik, J. (2015). Model for understanding consumer textural food choice. *Food Science & Nutrition, 3*(3), 202-212. doi: 10.1002/fsn3.205
Jemt, T., & HedegÅRd, B. (1982). Reproducibility of chewing rhythm and of mandibular displacements during chewing. *J Oral Rehabil, 9*(6), 531-537. doi: 10.1111/j.1365-2842.1982.tb01043.x
Jemt, T., Karlsson, S., & Hedega˚rd, B. r. (1979). Mandibular movements of young adults recorded by intraorally placed light-emitting diodes. *The Journal of Prosthetic Dentistry, 42*(6), 669-673. doi: https://doi.org/10.1016/0022-3913(79)90199-9
Khamnei, S., Zamanlu, M., Shakouri, S. K., et al. (2016). Mastication Patterns in Humans: Gender Differences. *Neurophysiology, 48*(5), 375-379. doi: 10.1007/s11062-017-9612-3
Kim, E. H.-J., Morgenstern, M. P., Bronlund, J. E., et al. (2011). *Food breakdown during human mastication – Quantitative characterization.* Paper presented at the 11th International Congress on Engineering and Food, Athens, Greece.
Koç, H., Çakir, E., Vinyard, C. J., et al. (2014). Adaptation of Oral Processing to the Fracture Properties of Soft Solids. *Journal of Texture Studies, 45*(1), 47-61. doi: 10.1111/jtxs.12051
Kohyama, K., Hatakeyama, E., Sasaki, T., et al. (2004). Effect of sample thickness on bite force studied with a multiple-point sheet sensor. *J Oral Rehabil, 31*(4), 327-334. doi: 10.1046/j.1365-2842.2003.01248.x
Kohyama, K., Hatakeyama, E., Sasaki, T., et al. (2004). Effects of sample hardness on human chewing force: a model study using silicone rubber. *Archives of Oral Biology, 49*(10), 805-816. doi: http://dx.doi.org/10.1016/j.archoralbio.2004.04.006
Koolstra, J. H., & van Eijden, T. M. G. J. (1999). Three-dimensional dynamical capabilities of the human masticatory muscles. *Journal of Biomechanics, 32*(2), 145-152. doi: http://dx.doi.org/10.1016/S0021-9290(98)00160-2
Lassauzay, C., Peyron, M.-A., Albuisson, E., et al. (2000). Variability of the masticatory process during chewing of elastic model foods. *European Journal of Oral Sciences, 108*(6), 484-492. doi: 10.1034/j.1600-0722.2000.00866.x
Lassauzay, C., Peyron, M. A., Albuisson, E., et al. (2000). Variability of the masticatory process during chewing of elastic model foods. *Eur J Oral Sci, 108*(6), 484-492.
Lenfant, F., Loret, C., Pineau, N., et al. (2009). Perception of oral food breakdown. The concept of sensory trajectory. *Appetite, 52*(3), 659-667. doi: https://doi.org/10.1016/j.appet.2009.03.003
Lewis, D. (2006). *A robotic chewing device for food evaluation : a thesis presented in partial fulfilment of the requirements.* (degree of Master of Engineering), Massey University, Palmerston North.
Lewis, D. (2006). *A robotic chewing device for food evaluation.* (Master of Engineering Thesis), Massey University, New Zealand.
Liedberg, B., & Owall, B. (1991). Masticatory ability in experimentally induced xerostomia. *Dysphagia*(6), 211-213.
Lillford, P. J. (2011). The Importance Of Food Microstructure In Fracture Physics And Texture Perception. *Journal of Texture Studies, 42*(2), 130-136. doi: 10.1111/j.1745-4603.2011.00293.x
Loret, C., Walter, M., Pineau, N., et al. (2011a). Physical and related sensory properties of a swallowable bolus. *Physiol Behav, 104*(5), 855-864. doi: 10.1016/j.physbeh.2011.05.014
Loret, C., Walter, M., Pineau, N., et al. (2011b). Physical and related sensory properties of a swallowable bolus. *Physiol Behav, 104*(5), 855-864. doi: https://doi.org/10.1016/j.physbeh.2011.05.014

Lucas, P. W. (2004a). The Basic Structure of the Mammalian Mouth *Dental Functional Morphology: How Teeth Work* (pp. 87-132). United Kingdom: Cambridge University Press.
Lucas, P. W. (2004b). How the Mouth Operates *Dental Functional Morphology: How Teeth Work* (pp. 66-67). United Kingdom: Cambridge University Press.
Lucas, P. W. (2004c). Tooth Shape *Dental Functional Morphology: How Teeth Work* (pp. 87-132). United Kingdom: Cambridge University Press.
Lucas, P. W., & Luke, D. A. (1983). Methods for analysing the breakdown of food in human mastication. *Arch Oral Biol, 28*(9), 813-819.
Lucas, P. W., Ow, R. K., Ritchie, G. M., et al. (1986). Relationship between jaw movement and food breakdown in human mastication. *J Dent Res, 65*(3), 400-404. doi: 10.1177/00220345860650030501
Lucas, P. W., Prinz, J. F., Agrawal, K. R., et al. (2002). Food physics and oral physiology. *Food Quality and Preference, 13*(4), 203-213. doi: https://doi.org/10.1016/S0950-3293(00)00036-7
Mandel, I. D. (1987). The functions of saliva. *J Dent Res, 66 Spec No*, 623-627.
Medicis, S., & Hiiemae, K. (1998). *Natural bite sizes for common foods.* Paper presented at the Journal of Dental Research.
Mioche, L., Bourdiol, P., & Monier, S. (2003). Chewing behaviour and bolus formation during mastication of meat with different textures. *Arch Oral Biol, 48*(3), 193-200.
Mioche, L., Bourdiol, P., Monier, S., et al. (2002). The relationship between chewing activity and food bolus properties obtained from different meat textures. *Food Quality and Preference, 13*(7), 583-588. doi: https://doi.org/10.1016/S0950-3293(02)00056-3
Mioche, L., Hiiemae, K. M., & Palmer, J. B. (2002). A postero-anterior videofluorographic study of the intra-oral management of food in man. *Arch Oral Biol, 47*(4), 267-280.
Mishellany-Dutour, A., Peyron, M.-A., Croze, J., et al. (2011). Comparison of food boluses prepared in vivo and by the AM2 mastication simulator. *Food Quality and Preference, 22*(4), 326-331. doi: http://dx.doi.org/10.1016/j.foodqual.2010.12.003
Mishellany, A., Woda, A., Labas, R., et al. (2006). The challenge of mastication: preparing a bolus suitable for deglutition. *Dysphagia, 21*(2), 87-94. doi: 10.1007/s00455-006-9014-y
Monique, A., Sylvain, D., Lionel, B., et al. (2007). France Patent No. FR2921185A1.
Mosca, A. C., & Chen, J. (2017). Food-saliva interactions: Mechanisms and implications. *Trends in Food Science & Technology, 66*, 125-134. doi: https://doi.org/10.1016/j.tifs.2017.06.005
Nakauma, M., Ishihara, S., Funami, T., et al. (2011). Swallowing profiles of food polysaccharide solutions with different flow behaviors. *Food Hydrocolloids, 25*(5), 1165-1173. doi: http://dx.doi.org/10.1016/j.foodhyd.2010.11.003
Ogawa, T., Ogawa, M., & Koyano, K. (2001). Different responses of masticatory movements after alteration of occlusal guidance related to individual movement pattern. *J Oral Rehabil, 28*(9), 830-841.
Okada, A., Honma, M., Nomura, S., et al. (2007). Oral behavior from food intake until terminal swallow. *Physiol Behav, 90*(1), 172-179. doi: http://dx.doi.org/10.1016/j.physbeh.2006.09.032
Olthoff, L. W., Van Der Bilt, A., De Boer, A., et al. (1986). Comparison Of Force-Deformation Characteristics Of Artificial And Several Natural Foods For Chewing Experiments. *Journal of Texture Studies, 17*(3), 275-289. doi: 10.1111/j.1745-4603.1986.tb00553.x
Olthoff, L. W., Vanderbilt, A., Bosman, F., et al. (1984). DISTRIBUTION OF PARTICLE SIZES IN FOOD COMMINUTED BY HUMAN MASTICATION. *Archives of Oral Biology, 29*(11), 899-903. doi: 10.1016/0003-9969(84)90089-x
Palinkas, M., Nassar, M. S. P., Cecílio, F. A., et al. (2010). Age and gender influence on maximal bite force and masticatory muscles thickness. *Archives of Oral Biology, 55*(10), 797-802. doi: https://doi.org/10.1016/j.archoralbio.2010.06.016
Pangborn, R. M., & Lundgren, B. (1977). Salivary secretion in response to mastication of crisp bread. *J Texture Stud*(8), 463-472.

Panouillé, M., Saint-Eve, A., Déléris, I., et al. (2014). Oral processing and bolus properties drive the dynamics of salty and texture perceptions of bread. *Food Research International, 62*(0), 238-246. doi: http://dx.doi.org/10.1016/j.foodres.2014.02.031

Panouillé, M., Saint-Eve, A., & Souchon, I. (2016). Instrumental methods for bolus characterization during oral processing to understand food perceptions. *Current Opinion in Food Science, 9*, 42-49. doi: http://dx.doi.org/10.1016/j.cofs.2016.05.002

Pereira, L. J., Duarte Gaviao, M. B., & Van Der Bilt, A. (2006). Influence of oral characteristics and food products on masticatory function. *Acta Odontol Scand, 64*(4), 193-201. doi: 10.1080/00016350600703459

Peyron, M.-A., & Gierczynski, I. (2009, 15-18 June). *Use of texture profile analysis (TPA) test for a rheological characterisation of food bolus collected in the course of mastication.* Paper presented at the Proceedings of 5th International Symposium on Food Rheology and Structure, Zurich, Switzerland.

Peyron, M.-A., Gierczynski, I., Hartmann, C., et al. (2011). Role of Physical Bolus Properties as Sensory Inputs in the Trigger of Swallowing. *PLOS ONE, 6*(6), e21167. doi: 10.1371/journal.pone.0021167

Peyron, M. A., Lassauzay, C., & Woda, A. (2002). Effects of increased hardness on jaw movement and muscle activity during chewing of visco-elastic model foods. *Exp Brain Res, 142*(1), 41-51. doi: 10.1007/s00221-001-0916-5

Peyron, M. A., Mishellany, A., & Woda, A. (2004). Particle size distribution of food boluses after mastication of six natural foods. *J Dent Res, 83*(7), 578-582. doi: 10.1177/154405910408300713

Pineau, N., Cordelle, S., & Schlich, P. (2003, July 20–24). *Temporal Dominance of Sensations: A new technique to record several sensory attributes simultaneously over time.* Paper presented at the 5th Pangborn symposium.

Prinz, J., F., & Lucas, P. W. (1997). An Optimization Model for Mastication and Swallowing in Mammals. *Proceedings: Biological Sciences, 264*(1389), 1715-1721. doi: 10.2307/51106

Pröschel, P., & Hofmann, M. (1988). Frontal chewing patterns of the incisor point and their dependence on resistance of food and type of occlusion. *The Journal of Prosthetic Dentistry, 59*(5), 617-624. doi: https://doi.org/10.1016/0022-3913(88)90082-0

Rodrigues, S. A., Young, A. K., James, B. J., et al. (2014). Structural Changes Within a Biscuit Bolus During Mastication. *Journal of Texture Studies, 45*(2), 89-96. doi: 10.1111/jtxs.12058

Rosenthal, A. J., & Share, C. (2014). Temporal Dominance of Sensations of peanuts and peanut products in relation to Hutchings and Lillford's "breakdown path". *Food Quality and Preference, 32*, 311-316. doi: https://doi.org/10.1016/j.foodqual.2013.09.004

Saint-Eve, A., Panouillé, M., Capitaine, C., et al. (2015). Dynamic aspects of texture perception during cheese consumption and relationship with bolus properties. *Food Hydrocolloids, 46*, 144-152. doi: https://doi.org/10.1016/j.foodhyd.2014.12.015

Salles, C., Tarrega, A., Mielle, P., et al. (2007). Development of a chewing simulator for food breakdown and the analysis of in vitro flavor compound release in a mouth environment. *Journal of Food Engineering, 82*(2), 189-198. doi: https://doi.org/10.1016/j.jfoodeng.2007.02.008

Sharma, M., & Duizer, L. (2019). Characterizing the Dynamic Textural Properties of Hydrocolloids in Pureed Foods-A Comparison Between TDS and TCATA. *Foods, 8*(6). doi: 10.3390/foods8060184

Shiozawa, K., & Kohyama, K. (2011). Effects of Addition of Water on Masticatory Behavior and the Mechanical Properties of the Food Bolus. *Journal of Oral Biosciences, 53*(2), 148-157. doi: http://dx.doi.org/10.1016/S1349-0079(11)80018-6

Sierpinska, T., Golebiewska, M., & Lapuc, M. (2008). The effect of mastication on occlusal parameters in healthy volunteers. *Adv Med Sci, 53*(2), 316-320. doi: 10.2478/v10039-008-0049-1

Slagter, A. P., van der Glas, H. W., Bosman, F., et al. (1992). Force-deformation properties of artificial and natural foods for testing chewing efficiency. *The Journal of Prosthetic Dentistry, 68*(5), 790-799. doi: http://dx.doi.org/10.1016/0022-3913(92)90204-N

Smewing, J. (2015). Texture Analysis in Action: the Multiple Puncture Probe. Retrieved from https://textureanalysisprofessionals.blogspot.com/2015/05/texture-analysis-in-action-multiple.html

The squeeze test for tubes and packets. (2014). *Texture Technologies*. Retrieved from http://texturetechnologies.com/blog/the-squeeze-test-for-tubes-and-packets/

Sun, C. (2012a). *Modelling and compliance control of a linkage chewing robot and its application in food evaluation* (Doctoral dissertation), Massey University, Albany, New Zealand. Retrieved from http://mro.massey.ac.nz/handle/10179/3966

Sun, C. (2012b). *Modelling and compliance control of a linkage chewing robot and its application in food evaluation : a thesis presented in partial fulfilment of the requirements for the degree of Doctor of Philosophy in Engineering at Massey University, Albany, New Zealand.* (Doctor of Philosopy (Ph.D.) Doctoral), Massey University. Retrieved from http://hdl.handle.net/10179/3966

Sun, C., Xu, W. L., Bronlund, J. E., et al. (2014). Dynamics and Compliance Control of a Linkage Robot for Food Chewing. *IEEE Transactions on Industrial Electronics, 61*(1), 377-386. doi: 10.1109/TIE.2013.2251732

Sun, C., Xu, W. L., Bronlund, J. E., et al. (2014). Dynamics and Compliance Control of a Linkage Robot for Food Chewing. *IEEE Transactions on Industrial Electronics, 61*, 377-386.

Szczesniak, A. S. (1963). Classification of Textural Characteristicsa. *Journal of Food Science, 28*(4), 385-389. doi: 10.1111/j.1365-2621.1963.tb00215.x

Szczesniak, A. S. (1971). CONSUMER AWARENESS OF TEXTURE AND OF OTHER FOOD ATTRIBUTES, II. *Journal of Texture Studies, 2*(2), 196-206. doi: 10.1111/j.1745-4603.1971.tb00581.x

Szczesniak, A. S., Brandt, M. A., & Friedman, H. H. (1963). Development of Standard Rating Scales for Mechanical Parameters of Texture and Correlation Between the Objective and the Sensory Methods of Texture Evaluation. *Journal of Food Science, 28*(4), 397-403. doi: 10.1111/j.1365-2621.1963.tb00217.x

Szczesniak, A. S., & Kahn, E. L. (1971). CONSUMER AWARENESS OF AND ATTITUDES TO FOOD TEXTURE. *Journal of Texture Studies, 2*(3), 280-295. doi: 10.1111/j.1745-4603.1971.tb01005.x

Takahashi, T., Hayakawa, F., Kumagai, M., et al. (2009). Relations among mechanical properties, human bite parameters, and ease of chewing of solid foods with various textures. *Journal of Food Engineering, 95*(3), 400-409. doi: http://dx.doi.org/10.1016/j.jfoodeng.2009.05.023

Takanobu, H., Ohtsuki, K., Takanishi, A., et al. (2003, 20-24 July 2003). *Jaw training robot and its clinical results.* Paper presented at the Proceedings 2003 IEEE/ASME International Conference on Advanced Intelligent Mechatronics (AIM 2003).

van den Braber, W., van der Glas, H. W., van der Bilt, A., et al. (2001). Chewing efficiency of pre-orthognathic surgery patients: selection and breakage of food particles. *Eur J Oral Sci, 109*(5), 306-311.

van der Bilt, A., & Abbink, J. H. (2017). The influence of food consistency on chewing rate and muscular work. *Archives of Oral Biology, 83*, 105-110. doi: https://doi.org/10.1016/j.archoralbio.2017.07.011

van der Bilt, A., Abbink, J. H., Mowlana, F., et al. (1993). A comparison between data analysis methods concerning particle size distributions obtained by mastication in man. *Archives of Oral Biology, 38*(2), 163-167. doi: http://dx.doi.org/10.1016/0003-9969(93)90202-W

Van der Bilt, A., Olthoff, L. W., Van der Glas, H. W., et al. (1987). A Mathematial Description of the Comminution of Food During Mastication in Man. *Archs oral Biol., 32*(8), 579-586.

Van der Bilt, A., Van Der Glas, H. W., & Bosman, F. (1992). A Computer Simulation of the Influence of Selection and Breakage of Food on the Chewing Efficiency of Human Mastication. *J Dent Res, 71*(3), 458-465. doi: doi:10.1177/00220345920710030701

Van der Bilt, A., Van der Glas, H. W., Olthoff, L. W., et al. (1991). The effect of particle size reduction on the jaw gape in human mastication. *J Dent Res, 70*(5), 931-937. doi: 10.1177/00220345910700051301

Van der Glas, H. W., Al-Ibrahim, A., & Lyons, M. F. (2012). A STABLE ARTIFICIAL TEST FOOD SUITABLE FOR LABELING TO QUANTIFY SELECTION AND BREAKAGE IN SUBJECTS WITH IMPAIRED CHEWING ABILITY. *Journal of Texture Studies, 43*(4), 287-298. doi: 10.1111/j.1745-4603.2011.00344.x

Van der Glas, H. W., Van der Bilt, A., Olthoff, L. W., et al. (1987). Measurement of selection changes and breakage functions during chewing in man. *J Dent Res, 66*(10), 1547-1550.

Voisey, P. W., Kloek, M., Summers, K., et al. (1980). A Method For Testing The Ease Of Extrusion Of Icing Marketed In Plastic Tubes. *Journal of Texture Studies, 10*(4), 435-448. doi: 10.1111/j.1745-4603.1980.tb00869.x

Watt, D. M. (1976). Monitoring Mastication. *J Dent Res*(4), 271-278.

Wilkinson, C., Dijksterhuis, G. B., & Minekus, M. (2000). From food structure to texture. *Trends in Food Science & Technology, 11*(12), 442-450. doi: http://dx.doi.org/10.1016/S0924-2244(01)00033-4

Wilson, A., Luck, P., Woods, C., et al. (2016). Comparison of jaw tracking by single video camera with 3D electromagnetic system. *Journal of Food Engineering, 190*, 22-33. doi: https://doi.org/10.1016/j.jfoodeng.2016.06.008

Wilson, A. W., I.; Motoi, L.; Kim, E.; Morgenstern, M. (2013, 10–12 April 2013). *Video analysis of chewing patterns.* Paper presented at the In Proceedings of the F. Bioact. Process. Qual. & Nutr.

Witt, T., & Stokes, J. R. (2015). Physics of food structure breakdown and bolus formation during oral processing of hard and soft solids. *Current Opinion in Food Science, 3*, 110-117. doi: https://doi.org/10.1016/j.cofs.2015.06.011

Woda, A., Foster, K., Mishellany, A., et al. (2006). Adaptation of healthy mastication to factors pertaining to the individual or to the food. *Physiol Behav, 89*(1), 28-35. doi: 10.1016/j.physbeh.2006.02.013

Woda, A., Mishellany-Dutour, A., Batier, L., et al. (2010). Development and validation of a mastication simulator. *Journal of biomechanics, 43*, 1667-1673. doi: 10.1016/j.jbiomech.2010.03.002

Xu, W. L., Lewis, D., Bronlund, J. E., et al. (2008). Mechanism, design and motion control of a linkage chewing device for food evaluation. *Mechanism and Machine Theory, 43*(3), 376-389. doi: https://doi.org/10.1016/j.mechmachtheory.2007.03.004

Young, A. K., Cheong, J. N., Hedderley, D. I., et al. (2013). Understanding the Link between Bolus Properties and Perceived Texture. *Journal of Texture Studies, 44*(5), 376-386. doi: doi:10.1111/jtxs.12025

Youssef, R. E., Throckmorton, G. S., Ellis, E., 3rd, et al. (1997). Comparison of habitual masticatory patterns in men and women using a custom computer program. *J Prosthet Dent, 78*(2), 179-186. doi: 10.1016/s0022-3913(97)70123-9

Yven, C., Culioli, J., & Mioche, L. (2005). Meat bolus properties in relation with meat texture and chewing context. *Meat Sci, 70*(2), 365-371. doi: 10.1016/j.meatsci.2005.02.002

YVEN, C., PATARIN, J., MAGNIN, A., et al. (2012). CONSEQUENCES OF INDIVIDUAL CHEWING STRATEGIES ON BOLUS RHEOLOGICAL PROPERTIES AT THE SWALLOWING THRESHOLD. *Journal of Texture Studies, 43*(4), 309-318. doi: 10.1111/j.1745-4603.2011.00340.x

van den Braber, W., van der Glas, H. W., van der Bilt, A., & Bosman, F. (2001). Chewing efficiency of pre-orthognathic surgery patients: selection and breakage of food particles. *Eur J Oral Sci, 109*(5), 306-311.

van der Bilt, A., & Abbink, J. H. (2017). The influence of food consistency on chewing rate and muscular work. *Archives of Oral Biology, 83*, 105-110. doi:https://doi.org/10.1016/j.archoralbio.2017.07.011

van der Bilt, A., Abbink, J. H., Mowlana, F., & Heath, M. R. (1993). A comparison between data analysis methods concerning particle size distributions obtained by mastication in man. *Archives of Oral Biology, 38*(2), 163-167. doi:http://dx.doi.org/10.1016/0003-9969(93)90202-W

Van der Bilt, A., Olthoff, L. W., Van der Glas, H. W., Van der Weelen, K., & Bosman, F. (1987). A Mathematial Description of the Comminution of Food During Mastication in Man. *Archs oral Biol., 32*(8), 579-586.

Van der Bilt, A., Van Der Glas, H. W., & Bosman, F. (1992). A Computer Simulation of the Influence of Selection and Breakage of Food on the Chewing Efficiency of Human Mastication. *J Dent Res, 71*(3), 458-465. doi:doi:10.1177/00220345920710030701

Van der Bilt, A., Van der Glas, H. W., Olthoff, L. W., & Bosman, F. (1991). The effect of particle size reduction on the jaw gape in human mastication. *J Dent Res, 70*(5), 931-937. doi:10.1177/00220345910700051301

Van der Glas, H. W., Al-Ibrahim, A., & Lyons, M. F. (2012). A Stable Artificial Test Food Suitable For Labeling To Quantify Selection And Breakage In Subjects With Impaired Chewing Ability. *Journal of Texture Studies, 43*(4), 287-298. doi:10.1111/j.1745-4603.2011.00344.x

Van der Glas, H. W., Van der Bilt, A., Olthoff, L. W., & Bosman, F. (1987). Measurement of selection changes and breakage functions during chewing in man. *J Dent Res, 66*(10), 1547-1550.

Voisey, P. W., Kloek, M., Summers, K., & Gillette, M. (1980). A Method For Testing The Ease Of Extrusion Of Icing Marketed In Plastic Tubes. *Journal of Texture Studies, 10*(4), 435-448. doi:10.1111/j.1745-4603.1980.tb00869.x

Watt, D. M. (1976). Monitoring Mastication. *J Dent Res*(4), 271-278.

Wilkinson, C., Dijksterhuis, G. B., & Minekus, M. (2000). From food structure to texture. *Trends in Food Science & Technology, 11*(12), 442-450. doi:http://dx.doi.org/10.1016/S0924-2244(01)00033-4

Wilson, A., Luck, P., Woods, C., Foegeding, E. A., & Morgenstern, M. (2016). Comparison of jaw tracking by single video camera with 3D electromagnetic system. *Journal of Food Engineering, 190*, 22-33. doi:https://doi.org/10.1016/j.jfoodeng.2016.06.008

Wilson, A. W., I.; Motoi, L.; Kim, E.; Morgenstern, M. (2013, 10–12 April 2013). *Video analysis of chewing patterns.* Paper presented at the In Proceedings of the F. Bioact. Process. Qual. & Nutr.

Witt, T., & Stokes, J. R. (2015). Physics of food structure breakdown and bolus formation during oral processing of hard and soft solids. *Current Opinion in Food Science, 3*, 110-117. doi:https://doi.org/10.1016/j.cofs.2015.06.011

, A., Foster, K., Mishellany, A., & Peyron, M. A. (2006). Adaptation of healthy mastication to factors pertaining to the individual or to the food. *Physiol Behav, 89*(1), 28-35. doi:10.1016/j.physbeh.2006.02.013

Xu, W. L., Lewis, D., Bronlund, J. E., & Morgenstern, M. P. (2008). Mechanism, design and motion control of a linkage chewing device for food evaluation. *Mechanism and Machine Theory, 43*(3), 376-389. doi:http://dx.doi.org/10.1016/j.mechmachtheory.2007.03.004

Young, A. K., Cheong, J. N., Hedderley, D. I., Morgenstern, M. P., & James, B. J. (2013). Understanding the Link between Bolus Properties and Perceived Texture. *Journal of Texture Studies, 44*(5), 376-386. doi:doi:10.1111/jtxs.12025

Yven, C., Culioli, J., & Mioche, L. (2005). Meat bolus properties in relation with meat texture and chewing context. *Meat Sci, 70*(2), 365-371. doi:10.1016/j.meatsci.2005.02.002

Yven, C., Patarin, J., Magnin, A., LabourÉ, H., Repoux, M., Guichard, E., & Feron, G. (2012). CONSEQUENCES OF INDIVIDUAL CHEWING STRATEGIES ON BOLUS RHEOLOGICAL

PROPERTIES AT THE SWALLOWING THRESHOLD. *Journal of Texture Studies, 43*(4), 309-318. doi:10.1111/j.1745-4603.2011.00340.x

# APPENDIX A

## *Measuring the particle size breakdown of a dental testing food*

**Primary questionnaire**

Thank you for expressing interest in this study. Prior to your participation, please answer the following questions.

1. Is your age between than 18 and 50?
   Y N
2. Do you have 8 post canine teeth?
   Y N
3. Do you experience any pain/discomfort while chewing?
   Y N
4. Have you suffered any serious jaw injuries in the past?
   Y N
5. Do you currently wear tooth braces?
   Y N
6. Do you have a problem with dry mouth or salivary flow?
   Y N
7. Do you wear dentures?
   Y N
8. Do you currently take any medication that might affect saliva flow, such as oxybutynin or amitriptyline?
   Y N
9. Do you have a disorder of the mouth?
   Y N
10. Do you currently have any significant problems with tooth decay or gum disease?
    Y N
11. Have you noticed any tooth grinding or excessive tooth clenching while chewing?
    Y N
12. Are you aware of any other health problems that may inhibit your ability to take part in this study or put your health at risk in any way?
    Y N
13. Do you suffer from any blood borne infectious disease?
    Y N

If you are able to answer YES to Q1 and Q2 and NO to all other questions above, you are invited to come and look at the laboratory where the experiments will take place and discuss the project and the role of a participant in more detail.

MASSEY UNIVERSITY
COLLEGE OF SCIENCES
TE WĀHANGA PŪTAIAO

# *Particle size reduction of a dental test food "Optosil"*

## INFORMATION SHEET

Hello,

My name is Grace Ng; I am a PhD student in the School of Engineering and Advanced Technology. I would like to invite you to participate in a chewing study.

In this study, data on the breakdown of a test food widely used for dental studies will be collected from human subjects. This will be used to calibrate a novel mastication simulator developed at Massey in collaboration with Plant and Food Research.

**Participant Involvement**

The trials will involve you chewing on Optosil particles; the samples will consist of a specific number and size of particles prepared by the researcher. The samples will be served to you and you will be required to chew for different number of chewing cycles before expectorating the particles. The expectorated particles will be collected and analysed by the researcher. Image recording will be done throughout the chewing process so that jaw movement can be analysed.

Before participating in the chewing experiments, you will be required to complete a screening questionnaire. Selection will be based on your age, dental, and health status. Please note that if you volunteer and are screened out it is not an indication that there is any issue with your dental health.

If you are selected, you will be compensated for your time at $15 for an hour session. Payment will be in the form of supermarket vouchers. You will initially be required for only one session but may be asked to participate in a follow up session. Session times are very flexible and can be arranged to meet your schedule.

Data collected will be used as the basis for calibration of the mastication simulator. To protect your privacy, all of your data will be placed under a code so that you will not be identified in any publications, and a summary of the findings will be posted to you after data analysis and writing up.

You are under no obligation to accept this invitation. If you decide to participate, you have the right to:

- decline to answer any particular question;
- withdraw from the study at anytime
- ask any questions about the study at any time during participation;
- provide information on the understanding that your name will not be used unless you give permission to the researcher;
- be given access to a summary of the project findings when it is concluded.

If you are interested in taking part, or have any further questions about the project, please do not hesitate to contact the researcher listed below. Your interest will be greatly appreciated. A screening questionnaire will be given to see if you're eligible to take part.

**Project Contact**

Grace Ng
06 350 9099 ext 85570
G.C.F.Ng@massey.ac.nz

Professor John Bronlund
06 356 9099 ext 84140
J.E.Bronlund@massey.ac.nz

**MUHEC APPLICATIONS**

**Committee Approval Statement**

"This project has been evaluated by peer review and judged to be low risk. Consequently, it has not been reviewed by one of the University's Human Ethics Committees. The researcher(s) named above are responsible for the ethical conduct of this research.

If you have any concerns about the conduct of this research that you wish to raise with someone other than the researcher(s), please contact Professor John O'Neill, Director, Research Ethics, telephone 06 350 5249, email: humanethics@massey.ac.nz".

MASSEY UNIVERSITY
COLLEGE OF SCIENCES
TE WĀHANGA PŪTAIAO

# *Particle size reduction of a dental test food "optosil"*

## PARTICIPANT CONSENT FORM - INDIVIDUAL

I have read the Information Sheet and have had the details of the study explained to me. My questions have been answered to my satisfaction, and I understand that I may ask further questions at any time.

I agree to participate in this study under the conditions set out in the Information Sheet.

**Signature:** ..... **Date:** .....

**Full Name - printed** .....

# APPENDIX B

MASSEY UNIVERSITY
COLLEGE OF SCIENCES
TE WĀHANGA PŪTAIAO

## *Measuring the physical properties of ready-to-swallow food boluses*

### INFORMATION SHEET

Hello,

My name is Grace Ng; I am a PhD student in the School of Engineering and Advanced Technology. I would like to invite you to participate in a chewing study.

In this study, physical properties will be measured for food boluses collected from human subjects. This data will be used to validate a novel mastication simulator developed at Massey in collaboration with Plant and Food Research.

**Participant Involvement**

The trials will involve you chewing on natural portion sizes of 5 foods and expectorate the bolus when they feel it is ready for swallow. The foods to be used are commercially purchased Weet-Bix Bites, muesli bar, apple, peanuts and ham. At least 8 replicates will be required for each food. Up to two sessions per subject with duration of up to 1 hour each will be required. Subjects will expectorate boluses into prepared containers, and the samples will be either; 1) immediately weighed and dried to obtain the moisture content of the bolus or 2) analysed using a novel slip extrusion test which measures the force needed to change shape and flow. Image recording will be done throughout the chewing process so that jaw movement can be analysed.

Before participating in the chewing experiments, you will be required to complete a screening questionnaire. Selection will be based on your age, dental, and health status. Please note that if you volunteer and are screened out it is not an indication that there is any issue with your dental health.

If you are selected, you will be compensated for your time at $15 for an hour session. Payment will be in the form of supermarket vouchers. You will initially be required for only one session but may be asked to participate in a follow up session. Session times are very flexible and can be arranged to meet your schedule.

Data collected will be used to validate the mastication simulator. To protect your privacy, all of your data will be placed under a code so that you will not be identified in any publications, and a summary of the findings will be posted to you after data analysis and writing up.

You are under no obligation to accept this invitation. If you decide to participate, you have the right to:

- decline to answer any particular question;
- withdraw from the study at anytime
- ask any questions about the study at any time during participation;
- provide information on the understanding that your name will not be used unless you give permission to the researcher;
- be given access to a summary of the project findings when it is concluded.

If you are interested in taking part, or have any further questions about the project, please do not hesitate to contact the researcher listed below. Your interest will be greatly appreciated. A screening questionnaire will be given to see if you're eligible to take part.

**Project Contact**

Grace Ng
06 350 9099 ext 85570
G.C.F.Ng@massey.ac.nz

Professor John Bronlund
06 356 9099 ext 84140
J.E.Bronlund@massey.ac.nz

**MUHEC APPLICATIONS**

**Committee Approval Statement**
"This project has been evaluated by peer review and judged to be low risk. Consequently, it has not been reviewed by one of the University's Human Ethics Committees. The researcher(s) named above are responsible for the ethical conduct of this research.

If you have any concerns about the conduct of this research that you wish to raise with someone other than the researcher(s), please contact Professor John O'Neill, Director, Research Ethics, telephone 06 350 5249, email: humanethics@massey.ac.nz".

MASSEY UNIVERSITY
COLLEGE OF SCIENCES
TE WĀHANGA PŪTAIAO

# *Measuring the physical properties of ready-to-swallow food boluses*

## PARTICIPANT CONSENT FORM - INDIVIDUAL

I have read the Information Sheet and have had the details of the study explained to me. My questions have been answered to my satisfaction, and I understand that I may ask further questions at any time.

I agree to participate in this study under the conditions set out in the Information Sheet.

**Signature:** ..... **Date:** .....

**Full Name - printed** .....

# APPENDIX C

*Table C-1: Moisture content of the five foods.*

| Food | MC (g/g dry wt) |
|---|---|
| Apple | 6.61 ± 0.76 |
| Ham | 3.34 ± 0.01 |
| Muesli bar | 0.13 ± 0.01 |
| Peanuts | 0.03 ± 0.00 |
| Weetbix | 0.11 ± 0.00 |

*Table C-2: Moisture content of the boluses of the five foods collected from the MR in chapter 7.*

| Food | Mastication stage (%) | No. of chews | Bolus MC (g/g dry wt) |
|---|---|---|---|
| Apple | 150 | 27 | 7.74 |
| Apple | 150 | 27 | 7.39 |
| Apple | 125 | 22 | 9.56 |
| Apple | 125 | 22 | 6.89 |
| Apple | 100 | 18 | 7.89 |
| Apple | 100 | 18 | 9.38 |
| Apple | 75 | 13 | 9.45 |
| Apple | 75 | 13 | 8.00 |
| Apple | 50 | 9 | 7.30 |
| Apple | 50 | 9 | 8.51 |
| Apple | 30 | 5 | 7.72 |
| Apple | 30 | 5 | 9.79 |
| Apple | 20 | 3 | 10.44 |
| Apple | 20 | 3 | 8.64 |
| Ham | 150 | 38 | 4.57 |
| Ham | 150 | 38 | 4.29 |
| Ham | 125 | 31 | 4.40 |
| Ham | 125 | 31 | 4.20 |
| Ham | 100 | 25 | 4.16 |
| Ham | 100 | 25 | 3.99 |
| Ham | 75 | 18 | 3.54 |
| Ham | 75 | 18 | 3.90 |
| Ham | 50 | 13 | 4.39 |
| Ham | 50 | 13 | 4.26 |
| Ham | 30 | 8 | 3.71 |
| Ham | 30 | 8 | 4.10 |
| Ham | 20 | 5 | 3.60 |
| Ham | 20 | 5 | 4.12 |
| Ham | 10 | 2 | 3.56 |
| Ham | 10 | 2 | 3.37 |
| Ham | 0 | 0 | 3.06 |
| Ham | 0 | 0 | 3.27 |

| | | | |
|---|---|---|---|
| Muesli bar | 150 | 45 | 0.79 |
| Muesli bar | 150 | 45 | 0.80 |
| Muesli bar | 125 | 37 | 0.71 |
| Muesli bar | 125 | 37 | 0.71 |
| Muesli bar | 100 | 30 | 0.61 |
| Muesli bar | 100 | 30 | 0.61 |
| Muesli bar | 75 | 22 | 0.50 |
| Muesli bar | 75 | 22 | 0.52 |
| Muesli bar | 50 | 15 | 0.44 |
| Muesli bar | 50 | 15 | 0.44 |
| Muesli bar | 30 | 9 | 0.35 |
| Muesli bar | 30 | 9 | 0.34 |
| Muesli bar | 20 | 6 | 0.32 |
| Muesli bar | 20 | 6 | 0.31 |
| Muesli bar | 10 | 3 | 0.27 |
| Muesli bar | 10 | 3 | 0.29 |
| Peanuts | 150 | 41 | 1.02 |
| Peanuts | 150 | 41 | 1.03 |
| Peanuts | 125 | 34 | 0.87 |
| Peanuts | 125 | 34 | 0.87 |
| Peanuts | 100 | 27 | 0.75 |
| Peanuts | 100 | 27 | 0.73 |
| Peanuts | 75 | 20 | 0.61 |
| Peanuts | 75 | 20 | 0.62 |
| Peanuts | 50 | 13 | 0.49 |
| Peanuts | 50 | 13 | 0.48 |
| Peanuts | 30 | 8 | 0.36 |
| Peanuts | 30 | 8 | 0.37 |
| Peanuts | 20 | 5 | 0.31 |
| Peanuts | 20 | 5 | 0.31 |
| Peanuts | 10 | 2 | 0.23 |
| Peanuts | 10 | 2 | 0.24 |

# APPENDIX D

**The matlab code for the GLCM analysis**

```
%retrieve csv file exported from the Chameleon TVR software
[InputFile Pathname]=uigetfile('*.csv');
filename=fullfile(Pathname,InputFile);
data = csvread(filename,2,0);
[pathstr,name,ext] = fileparts(filename);

%find min value at last zero before test starts
[maxtest, locmax]=max(max(data(:,end-1023:end),[],2));
TotalArea=data(:,end-1024);
[maxArea, locMaxArea]=max(TotalArea);
AreaZero=find(TotalArea==0);
ZeroPoint=find(AreaZero<locMaxArea,1,'last');
MeanBack=min(data(1:ZeroPoint,end-1023:end));
Background=reshape(MeanBack,32,32);

%find max pressure for each pin        Or      %find pressure for each pin at maximum area
elements=data(:,end-1023:end);                  elements=data(locMaxArea,end-1023:end);
M=max(elements);                                A=reshape(elements,32,32);
A=reshape(M,32,32);

% Subtract noise
A2=A-Background;

%only plot area with pins
B=A2(11:19,9:20);  %WB(9x12pins)       Or
B=A2(11:19,8:21);  %MB(9x14pins)       Or
B=A2(11:19,8:20);  %Apple(9x13pins)    Or
B=A2(8:21,8:21);   %Ham(14x14pins)     Or

%convert data from pressure to force
Force=pi*1^2*(B);

%parameters for GLCM analysis
offsets = [0 1; -1 1;-1 0;-1 -1];

%Graylimits set were based on the average max and min force measured for each food [H(0 1) or
MB(0 4) or WB(0 5) or Apple(0 0.7) or ], values in red are changed according to the food
[glcms, SI] = graycomatrix(Force,'Offset',offsets,'Symmetric', true,'NumLevels',9,'GrayLimits',[0 1]);

%apply graycoprops function to obtain textural information (contrast, energy and homogeneity)
info4=graycoprops(glcms);
T4 = struct2table(info4);
```